

**SYNTHESIS AND APPLICATIONS OF ALKYL AND ARYL VINYL SULFIDES
AND SIDEARM-SUBSTITUTED BISOXAZOLINES**

by

Paul Bichler

B.Sc., The University of Alberta, 2005

A THESIS SUBMITTED IN PARTIAL FULFILLMENT OF
THE REQUIREMENTS FOR THE DEGREE OF

DOCTOR OF PHILOSOPHY

in

THE FACULTY OF GRADUATE STUDIES
(Chemistry)

THE UNIVERSITY OF BRITISH COLUMBIA
(Vancouver)

August 2012

© Paul Bichler, 2012

Abstract

The presence of sulfur in numerous blockbuster drugs, natural products and other medicinally active molecules necessitates the development of efficient methods for the synthesis of carbon-sulfur bonds. Transition metal approaches towards the construction of C-S bonds have largely aided in the synthesis of aryl thioethers and related functionalities. However, few examples of catalytic processes demonstrate a tolerance for less reactive aliphatic thiols, leading to a widespread belief of an incompatibility of these substrates in catalytic C-S bond formation.

To this end, our group has demonstrated the first examples of rhodium-catalyzed alkyne hydrothiolation processes for the synthesis of alkyl vinyl sulfides. The work detailed in this thesis encompasses the use of Wilkinson's catalyst in alkyne hydrothiolation for the selective formation of *E*-linear alkyl and aryl vinyl sulfides. The substrate scope of this process is quite general, tolerating a variety of useful functional groups capable of undergoing further elaboration. Interestingly, alkyne substrates with adjacent heteroatoms undergo a reversal of regioselectivity, often favouring the branched regioisomer relative to the expected *E*-linear vinyl sulfide. The use of our catalytic alkyne hydrothiolation methodology was applied to the synthesis of a promising cancer chemotherapeutic agent, ON 01910.Na, which shows broad-spectrum activity towards a large number of cancer cell lines.

Additionally, the reactivity of aryl and vinyl sulfides was evaluated within the context of vinylogous thioesters capable of undergoing electrocyclizations. The development of a Sonogashira cross-coupling thio-Michael addition sequence allowed for the synthesis of a variety of heteroaromatic substituted vinylogous thioesters. The treatment of these substrates with excess triflic acid proved optimal in facilitating cyclization to thiaindanone-type products, a motif found in molecules with application towards the treatment of neurologic diseases. The observation of interesting skeletal rearrangements suggests a competition between the expected Nazarov cyclization and an intramolecular Friedel-Crafts acylation.

Lastly, a series of sidearm-substituted bisoxazolines were synthesized and a preliminary investigation of their coordination chemistry is reported. The application of these complexes towards a variety of asymmetric transformations, including the Nazarov cyclization, is currently ongoing.

Preface

Chapter 2 incorporates elements of a review published in Topics in Organometallic Chemistry, as part of a special edition encompassing research towards the formation of C-X bonds, where X is representative of a halogen or heteroatom. I wrote the original draft in its entirety and assisted Dr. Jennifer Love in editing the manuscript prior to submission. Bichler, P.; Love, J.A. *Top. Organomet. Chem.* **2010**, *31*, 39-64.

Chapter 3 is based on work conducted with Dr. Shiva Shoai in the laboratory of Dr. Jennifer Love. I assisted in optimizing the reaction conditions, including solvent choice, temperature and in assessing the compatibility of substrates involving more nucleophilic thiols. Additionally, I synthesized and characterized several of the alkyl vinyl sulfides reported. The discussion of any vinyl sulfides prepared by Dr. Shiva Shoai is clearly indicated in the relevant sections of this thesis. The manuscript was written by Dr. Shiva Shoai in conjunction with Dr. Jennifer Love and published in Organometallics, a journal affiliated with the American Chemical Society. Shoai, S.; Bichler, P.; Kang, B.; Buckley, H.; Love, J. A. *Organometallics* **2007**, *26*, 5778-5781.

Chapter 5 was published within a special edition of Inorganica Chimica Acta dedicated to the memory of Dr. Swiatoslaw Trofimenko. I wrote the original draft in its entirety and assisted Dr. Jennifer Love in editing the manuscript prior to submission. I synthesized all the compounds reported with the exception of two substrates, which were prepared by Mr. Alex Sun. The compounds prepared by Alex Sun are clearly indicated in the relevant sections of this thesis. Dr. Brian Patrick, the departmental expert in crystallography, conducted the acquisition and analysis of all solid-state structural data obtained by X-ray crystallography. Bichler, P.; Sun, A. D.; Patrick, B. O.; Love, J. A. *Inorg. Chim. Acta.* **2009**, *362*, 4546-4552.

Table of Contents

Abstract.....	ii
Preface.....	iii
Table of Contents	iv
List of Tables	vii
List of Figures.....	viii
List of Abbreviations	x
Acknowledgements	xvi
Dedication	xvii
Chapter 1 The Revelance of Studying Organosulfur Compounds.....	1
1.1 Medicinal Chemistry of Organosulfur Compounds.....	2
1.1.1 Early Sulfonamides	3
1.1.2 Discovery of Penicillin	3
1.1.3 Sulfonamide Resistance and Mechanism of Action.....	4
1.1.4 Penicillin Mode of Action	5
1.1.5 Second Generation Sulfur Containing Antibiotics	6
1.1.6 Summary of Sulfur Containing Antibiotics.....	9
1.2 Sulfur Containing Peptidomimetics.....	9
1.2.1 Peptidomimetics Containing Sulfur-Based Michael-Acceptors.....	11
1.2.2 Mechanism of Action for Vinyl Sulfone Peptidomimetics	13
1.2.3 Summary of Biologically Active Michael-Acceptors	14
1.3 Sulfur in Organic Synthesis	16
1.3.1 Named Reactions Involving Organosulfur Compounds.....	16
1.3.2 Organosulfur Compounds in Natural Product Synthesis	20
1.4 Summary.....	26
Chapter 2 Transition Metal Catalyzed Synthesis of Carbon-Sulfur Bonds.....	28
2.1 Cross-Coupling Approaches to C-S Bond Formation	29
2.1.1 Historical Precedent for Copper-Mediated Carbon-Element Bond Formation.....	30
2.1.2 Copper-Catalyzed Carbon-Sulfur Bond Formation.....	30

2.2	Palladium-Catalyzed Carbon-Sulfur Bond Formation	33
2.2.1	Historical Context for Palladium-Catalyzed <i>S</i> -Arylations	34
2.2.2	Mechanistic Considerations for Palladium-Catalyzed <i>S</i> -Arylations	34
2.2.3	Optimization of Palladium-Catalyzed <i>S</i> -Arylations	35
2.2.4	Synthesis of Biologically Active Molecules Utilizing <i>S</i> -Arylation	37
2.2.5	Synthesis of Vinyl Sulfides via Palladium- and Copper-Catalyzed Cross Coupling Reactions.....	38
2.3	Alkyne Hydrothiolation in the Synthesis of Vinyl Sulfides	40
2.3.1	Alkyne Hydrothiolation with Group 10 Transition Metals	40
2.3.2	Alkyne Hydrothiolation with Group 9 Transition Metals	44
2.3.3	Mechanistic Comparison of Group 9 and 10 Metals in Alkyne Hydrothiolation	48
2.3.4	Sulfur-Element Bond Activation and Applications to Alkyne Addition Reactions.....	50
2.4	Summary: Transition Metal Approaches to Carbon-Sulfur Bond Formation	52

Chapter 3 Towards a General Method for the Hydrothiolation of Alkynes with Alkyl

Thiols.....	55	
3.1	Establishing Precedent: Solvent and Reactivity Studies.....	56
3.2	Evaluation of Substrate Scope (<i>in-situ</i> Experiments)	59
3.3	Evaluation of Substrate Scope (Preparative Reactions)	63
3.3.1	Limitations of Alkyne Hydrothiolation with Alkyl Thiols	66
3.4	Summary of Alkyne Hydrothiolation with Alkyl Thiols.....	66
3.5	Evaluation of Substrate Scope (Arene Thiols)	67
3.5.1	Limitations of Alkyne Hydrothiolation (Arene Thiols)	69
3.5.2	Summary Arene Thiol Substrate Scope	70
3.6	Alkyne Hydrothiolation for the Synthesis of Biologically Active Compounds	70
3.6.1	Propargyl Amine Substrates in Alkyne Hydrothiolation.....	71
3.6.2	Alkyne Hydrothiolation as a Strategy Towards the Synthesis of ON 01910.Na	77
3.7	Conclusions.....	80
3.8	Experimental.....	81
3.8.1	General Procedures.....	81
3.8.2	Materials and Methods	81
3.8.3	General Experimental Procedure for Hydrothiolation	82
3.8.4	Analytical Data for Hydrothiolation Products.....	83

Chapter 4 Applications of Alkyne Hydrothiolation.....	95
4.1 Divinyl Ketones and the Nazarov Cyclization	96
4.1.1 Substituent Effects on the Reactivity of Dienones	97
4.1.2 Cascade Processes Involving the Nazarov Cyclization.....	101
4.2 Vinyl Sulfide Containing Divinyl Ketones.....	103
4.2.1 Hydrothiolation Approach to Divinyl Ketones (Substrate Design)	105
4.2.2 Synthesis of 84 and Optimization of Conditions for the Nazarov Cyclization	107
4.2.3 Analysis of Sulfide Substitution on the Nazarov Cyclization	120
4.2.4 Investigation of 3-Substituted Thiophene Dienones	124
4.2.5 Investigation of Benzothiophene Containing Dienones	129
4.2.6 Investigation of Other Heteroaromatic Substituted Dienones.....	133
4.3 Conclusions.....	139
4.4 Experimental.....	142
4.4.1 General Procedures.....	142
4.4.2 Materials and Methods	142
4.4.3 General Experimental Procedures	143
4.4.4 Analytical Data for Dienones and Cyclopentanones.....	144
Chapter 5 Development of Novel Scorpionate-Type Proligands.....	158
5.1 Catalytic Asymmetric Nazarov Cyclizations and Olefin Aziridinations.....	158
5.2 Synthesis of Sidearm-Substituted Bisoxazolines.....	161
5.3 Coordination Chemistry of Sidearm-Substituted Bisoxazolines	164
5.4 Conclusions.....	168
5.5 Experimental.....	170
5.5.1 General Procedures.....	170
5.5.2 Materials and Methods	171
5.5.3 Analytical Data.....	172
Chapter 6 Conclusions and Future Work	182
6.1 Conclusions.....	182
6.2 Future Work.....	184
References.....	188
Appendix A : X-ray Data for Chapter Five.....	199

List of Tables

Table 3.1 Solvent Optimization	57
Table 3.2 <i>In-Situ</i> Analysis of Cyclopentylthiol and Phenylacetylene.....	59
Table 3.3 <i>In-Situ</i> Analysis of Substrate Scope.....	62
Table 3.4 Substrate Scope (Preparative)	65
Table 3.5 Aryl Thiol Substrate Scope	68
Table 3.6 Hydrothiolation of Propargyl Amines 45-47 with Thiophenol.....	74
Table 3.7 Hydrothiolation of Propargyl Amines 45-47 with Benzyl Mercaptan.....	75
Table 3.8 Hydrothiolation of Propargyl Amines 46-47 at Higher Temperature.....	76
Table 3.9 Attempted Synthesis of ON 01910.Na Vinyl Sulfide	79
Table 4.1 Reactivity of 84 with Various Lewis Acids (Initial Screening).....	109
Table 4.2 Reactivity of 84 with Triflic Acid (TfOH).....	111
Table 4.3 Reactivity of (84) with Triflic Acid (TfOH) Under Microwave Irradiation.....	118
Table 4.4 Final Screening of Conditions for Cyclization of 84	119
Table 4.5 Synthesis of Sulfur-Substituted Dienones.....	121
Table 4.6 Nazarov Cyclizations of Sulfur-Substituted Dienones	122
Table 4.7 Nazarov Cyclizations of Dienone (102).....	135
Table A.1 Selected Crystallographic Parameters for Compounds 128-130	201

List of Figures

Figure 1.1 Example of Sulfur Containing Aroma Compounds	1
Figure 1.2 Naturally Occurring Sulfur Odourants	2
Figure 1.3 Early Sulfonamide Drugs	3
Figure 1.4 Selected Penicillins.....	4
Figure 1.5 PABA, Sulfanilamide and Folic Acid	4
Figure 1.6 DHPS Mediated Synthesis of Dihydropteroic Acid.....	5
Figure 1.7 Abbreviated Structure of Peptidoglycan.....	6
Figure 1.8 Carbapenem and Cephalosporin Families and Select Examples.....	7
Figure 1.9 Three Generations of Cephalosporin Antibiotics	7
Figure 1.10 Mechanism of β -Lactam Opening and Expulsion of Pyridine	8
Figure 1.11 Common β -Lactamase Inhibitors Used in Combination Therapies	8
Figure 1.12 Cephalosporin Peptidomimetic.....	10
Figure 1.13 MK-0822, A Highly Selective Cathepsin K Inhibitor	12
Figure 1.14 Select Examples of Irreversible Cysteine Protease Inhibitors.....	12
Figure 1.15 Binding Domains of K777 and Mechanism of Inhibition	13
Figure 1.16 Comparison of Inverse-Secondary Inactivation Rates for P1' Analogues	14
Figure 1.17 Biologically Active Michael-Acceptors	15
Figure 1.18 Organosulfur Containing Blockbuster Drugs	26
Figure 2.1 Medicinally Relevant Arylthioethers.....	30
Figure 2.2 Common Ligand Additives in Copper-Catalyzed <i>S</i> -Arylations	32
Figure 2.3 Dependence of Ligand Bite-Angle on Rate of Reductive Elimination	35
Figure 2.4 Proligands in Palladium-Catalyzed <i>S</i> -Arylations	36
Figure 2.5 Pyrazolylborate Ligands Tested in Alkyne Hydrothiolation with Alkyl Thiols ..	47
Figure 2.6 <i>N,N</i> and <i>P,N</i> -Ligands in Alkyne Hydrothiolation with Group 9 Metals	48
Figure 2.7 Biologically Active <i>E</i> -Vinyl Sulfones.....	53
Figure 3.1 Thiol and Alkyne Substrates Examined	60
Figure 3.2 Challenging Substrates in Alkyne Hydrothiolation with Wilkinson's Catalyst...	66
Figure 3.3 Challenging Arene Thiol Substrates in Catalytic Alkyne Hydrothiolation	70
Figure 3.4 Propargyl Amine Substrates Examined in Alkyne Hydrothiolation	72

Figure 4.1 Possible Conformations for Substituted Divinyl Ketones.....	101
Figure 4.2 Chemoselectivity for Cross-Conjugated Ynones	105
Figure 4.3 ¹ H NMR Chemical Shift Values for 2 and 3-Substituted Thiaindanes	113
Figure 4.4 ¹ H NMR Spectra of the Cyclopentanones Obtained with DCE or CH ₃ CN.....	114
Figure 4.5 ¹ H NMR Spectra of Dienone (92) Before and After Cyclization.....	123
Figure 4.6 Crude ¹ H NMR Analysis for the Synthesis of Cyclopentanone 98	126
Figure 4.7 Product Comparison for the Cyclization of 3 and 2-Substituted Dienones.....	127
Figure 4.8 Similarity of Products Obtained by Cyclization of Dienone (98) and (84).....	128
Figure 4.9 ¹ H- ¹ H Correlation Spectrum (COSY) for Dienone (99) Contaminant.....	131
Figure 4.10 Comparison of Dienone 105 to 99	136
Figure 4.11 Reaction Coordinate Diagram for Cyclization of Vinylogous Thioesters	140
Figure 4.12 Reactivity of Various Heteroaromatic Vinylogous Thioesters.....	141
Figure 5.1 Proligands for Asymmetric Aziridination	160
Figure 5.2 Design of Sidearm-Substituted Bisoxazoline Proligands.....	161
Figure 5.3 κ^2 and κ^3 Binding Modes.....	165
Figure 5.4 Solid-State Structural Representation for Complex 127	166
Figure 5.5 ORTEP for Complex 128	167
Figure 5.6 ORTEP for Complex 129	167
Figure 5.7 ORTEP for Complex (130).....	168
Figure A.1 Original ORTEP for Complex (128)	199
Figure A.2 Original ORTEP for Complex (129)	200
Figure A.3 Original ORTEP for Complex (130)	200

List of Abbreviations

2-D	Two Dimensional
Å	Angstrom
α	<i>Alpha</i>
AB q	Second-Order Quartet
AB t	Second Order Triplet
Ac	Acetyl
acac	Acetylacetonate
Ac ₂ O	Acetic Anhydride
Ala	Alanine
APCI	Atmospheric Pressure Chemical Ionization
API	Active Pharmaceutical Ingredient
app. d	Apparent Doublet
app. t	Apparent Triplet
APT	Attached Proton Test
Ar	Aryl
ASE	Aromatic Stabilization Energy
β	<i>Beta</i>
BARF	[3,5-Bis(trifluoromethyl)phenyl]-borate
bim	Bis(1-methylimidazol-2-yl)methane
Bn	Benzyl
Boc	<i>tert</i> -Butoxycarbonyl
Boc ₂ O	Di- <i>tert</i> -Butyl Dicarboxylate
Bp*	Dihydrobis(3,5-dimethylpyrazolyl)-borate
bpm	Bis(pyrazol-1-yl)methane
BPS	<i>tert</i> -Butyldiphenylsilane
br	Broad Signal
Bz	Benzoyl
Calcd.	Calculated
Cbz	Carboxylbenzyl
COSY	¹ H- ¹ H Correlated Spectroscopy

Cy	Cyclohexyl
Cys	Cysteine
δ	<i>Delta</i>
d	Doublet
DAP	Diaminopimelic acid
DBU	1,8-Diazabicyclo[5.4.0]undec-7-ene
DCM	Dichloromethane
dd	Doublet of Doublets
ddd	Doublet of Doublet of Doublets
DHPPP	7,8-Dihydro-6-Hydroxymethylpterin Phosphate
DHPS	Dihydropteroate Synthase
DIPEA	<i>N,N</i> -Diisopropylethyl Amine
DiPPF	1,1'-Bis(diisopropylphosphino)ferrocene
DMAD	Dimethyl Acetylenedicarboxylate
DMF	Dimethylformamide
DMAP	<i>para</i> -Dimethylaminopyridine
DME	Dimethoxyethane
DPEphos	Oxydi-2,1-phenylene)bis(diphenylphosphine)
DPPBz	1,2-Bis(diphenylphosphino)benzene
DPPE	1,2-Bis(diphenylphosphino)ethane
DPPF	1,1'-Bis(diphenylphosphino)ferrocene
dr	Disastereomeric Ratio
dt	Doublet of Triplets
<i>E</i>	Entgegen
E ⁺	Electrophile
E1cB	Unimolecular Elimination by Conjugate Base
EDG	Electron Donating Group
<i>ee</i>	Enantiomeric Excess
EI	Electron Impact
EPP	<i>N</i> -Ethylpiperidine
Eq.	Equation

Equiv.	Equivalents
ESI	Electrospray Ionization
esp	$\alpha,\alpha,\alpha',\alpha'$ -Tetramethyl-1,3-benzenedipropionic acid
Et	Ethyl
Et ₂ O	Diethyl Ether
EtOH	Ethanol
EtOAc	Ethyl Acetate
EWG	Electron Withdrawing Group
γ	Gamma
Glu	Glutamic Acid
h	Hour
HFIP	Hexafluoroisopropanol
His	Histidine
HMBC	Heteronuclear Multiple-Bond Correlation Spectroscopy
HMPA	Hexamethylphosphoramide
HPLC	High Pressure Liquid Chromatography
HRMS	High Resolution Mass Spectrometry
HSQC	Heteronuclear Single-Quantum Correlation Spectroscopy
Hz	Hertz, s ⁻¹
<i>i</i> -PrOH	<i>iso</i> -Propanol
ImP	1-Methyl-2-[(2-(diphenylphosphino)ethyl]imidazole
Ipent	Diisopentylphenylimidazolium
<i>J</i>	Coupling Constant
Josiphos	(<i>R</i>)-1-[(<i>S_p</i>)-2-(<i>Di-tert</i> -butylphosphino)ferrocenyl]ethylbis(2-methylphenyl)phosphine
κ	Kappa
kcal	kilocalories
KHMDS	Potassium Hexamethyldisilazide
KO <i>t</i> -Bu	Potassium <i>tert</i> -Butoxide
LA	Lewis Acid
LDA	Lithium Diisopropylamide

LiHMDS	Lithium Hexamethyldisilazide
Li <i>Oi</i> -Pr	Lithium <i>iso</i> -Propoxide
M	Molarity
m	Multiplet
<i>m</i> -	<i>meta</i> -Substitution
<i>m</i> -CPBA	<i>meta</i> -Chloroperbenzoic Acid
m/z	Mass to Charge Ratio (Mass Spectrometry)
Me	Methyl
MeOH	Methanol
MeSal	3-Methylsalicylate
mg	Milligram
MHz	Megahertz
min.	Minutes
mL	millilitre
ML _n	Transition Metal Complex
mmol	Milimole
MOM	Methoxymethyl
M.S.	Molecular Sieves
MTM	Methylthiomethyl
<i>n</i> -Bu	<i>n</i> -Butyl (linear)
Na <i>Ot</i> -Bu	Sodium <i>tert</i> -Butoxide
NHC	<i>N</i> -Heterocyclic Carbene
NMP	<i>N</i> -Methyl-2-pyrrolidone
NMR	Nuclear Magnetic Resonance
NOESY	Nuclear Overhauser Effect Spectroscopy
<i>o</i> -	<i>ortho</i> -Substitution
<i>o</i> -Tol	<i>ortho</i> -Toluene
ORTEP	Oakridge Thermal Elipsoid Plot
OTf	Trifluoromethanesulfonate (Triflate)
<i>p</i> -	<i>Para</i> -Substitution
<i>p. Falciparum</i>	<i>Plasmodium Falciparum</i>

P ₂ -Et	1-Ethyl-2,2,4,4,4-pentakis(dimethylamino)-2Λ ⁵ -catenadi(phosphazene)
P1-site	Position of a Peptide, Counted from the Position of Cleavage
<i>p</i> -TsCl	<i>para</i> -Toluenesulfonyl Chloride
<i>p</i> -TsOH	<i>para</i> -Toluenesulfonic Acid
PABA	<i>para</i> -Aminobenzoic Acid
PBP	Penicillin Binding Protein
Pd ₂ dba ₃	Tris(Dibenzylideneacetone)dipalladium(0)
PG _x	Protecting Group
Ph	Phenyl
PLK	Polo-like Kinase
ppm	Parts Per Million
PyP	1-(2-Diphenylphosphino)ethylpyrazole
q	Quartet
R, R', R''	Organic Group
RE	Resonance Energy
rt	Room Temperature
RX	Alkylating Agent
s	Singlet
s ⁻¹ M ⁻¹	Inverse Second by Inverse Molarity
SAR	Structure Activity Relationship
t	Triplet
<i>t</i> -Bu	<i>tert</i> -Butyl (branched)
<i>t</i> -BuLi	<i>tert</i> -Butyllithium
<i>t</i> -BuOH	<i>tert</i> -Butanol
TBAF	Tetra- <i>n</i> -butylammonium Fluoride
TBS	<i>tert</i> -Butyldimethylsilyl
TBSOTf	<i>tert</i> -Butyldimethylsilyl Trifluoromethanesulfonates
Temp.	Temperature
td	Triplet of Doublets
TFA	Trifluoroacetic Acid

TFAA	Trifluoroacetic Anhydride
TfOH	Trifluoromethanesulfonic Acid (Triflic Acid)
Tf ₂ O	Trifluoromethanesulfonic Anhydride (Triflic Anhydride)
THF	Tetrahydrofuran
TIPS	Triisopropylsilane
TLC	Thin Layer Chromatography
TMB	1,3,5-Trimethoxybenzene
TMS	Trimethylsilane
TMSOTf	Trimethylsilyl Trifluoromethanesulfonate
(+/-)-Tol-BINAP	Racemic 2,2'-bis(di- <i>p</i> -tolylphosphino)-1,1'-binaphthyl
Tp	Hydrotris(pyrazolyl)-borate
Tp*	Hydrotris(3,5-dimethylpyrazolyl)-borate
Tp ^{Ph}	Hydrotris(3-phenylpyrazolyl)-borate
Tp ^{Ph, Me}	Hydrotris(3,5-phenylmethylpyrazolyl)-borate
Ts	<i>para</i> -Toluenesulfonyl
TsOH	<i>para</i> -Toluenesulfonic Acid
UV	Ultraviolet
W	Watts
X	Halogen or Heteroatom
Xantphos	4,5-Bis(Diphenylphosphino)-9,9-dimethylxanthene
Y	Heteroatom
Z	Zusammen
(+)	Dextrorotatory
(-)	Levorotatory
(+/-)	Racemic
°C	Degrees Celsius
Δν	Difference in Chemical Shift (Hz)
π-bond	pi-bond
μm	Micrometer
μL	Microlitre
μW	Microwave

Acknowledgements

I would like to thank professor Dr. Jennifer A. Love for her support and guidance throughout my doctoral studies. I am forever indebted to Dr. Love for allowing me to pursue projects of my own devise, and for her trust in assigning me talented undergraduate students to assist me along the way. To this end, I would like to thank Jeffrey Bird, Owen Scadeng, Shabnam Yazdi and Kanghee Park for their contributions in the lab, and for adapting to my unique vernacular during their studies. I would also like to thank all the past and present graduate students within the Love lab for their support. In particular, I would like to thank Alex Dauth, Lauren Keyes and Dr. Shiva Shoai for their friendship and for discussions regarding chemistry and future directions. I also wish to thank my committee members: Dr. Glenn Sammis, Dr. Peter Legzdins and especially Dr. Martin Tanner for helping edit my thesis. Additionally, I am continually grateful for the training and supervision I received from my undergraduate research supervisor (Dr. Rik Tykwinski) who has helped me during my studies here at UBC. I also owe gratitude to the support staff in UBC chemistry including Dr. Yun Ling for mass spectrometric analysis, Dr. Brian Patrick for X-ray crystallography and Dr. Maria Ezhova for NMR spectroscopy training.

Of course, I am also indebted to my family for emotional and financial support throughout the years. I would also like to thank my peers, especially Dr. David Leitch, Dr. Julien Dugal-Tessier and Jason Wickenden for all the inspiring discussions of synthetic and organometallic chemistry. Lastly, I would like to thank my partner Ashlee Jollymore, for her love and support through the hard times in graduate school, and for bearing with me during the preparation of this thesis.

Dedicated to my family, friends and AJJ

Chapter 1 The Relevance of Studying Organosulfur Compounds

The synthetic utility of sulfur containing molecules is often undermined by negative stereotypes concerning the handling of these reagents. Typically this relates to the offensive odours of this class of compounds, and the common misconception that sulfur “poisons” transition metal catalysts. These preconceptions of sulfur are often misguided given the prevalence of organosulfur compounds in the perfume and fragrance industries, as principle aroma compounds present in several food products, and the presence of thiolate ligands in the active sites of several iron and copper based metalloenzymes.¹⁻⁴ Depicted in Figure 1.1 are select examples of organosulfur compounds that are commercially available food additives, or formed during food preparation. Grapefruit mercaptan (**1**) and kahweofuran (**2**) represent commercially available organosulfur compounds that occur naturally and are responsible for the aroma of grapefruit and roasted coffee respectively. The cysteine derivative (**3**) represents a volatile sulfide characteristic of Sauvignon white wine, and compound **4** is released during the preparation of roast beef, and typically referred to as the pleasant “meaty” smell that sulfur compounds can sometimes possess.^{2,3}

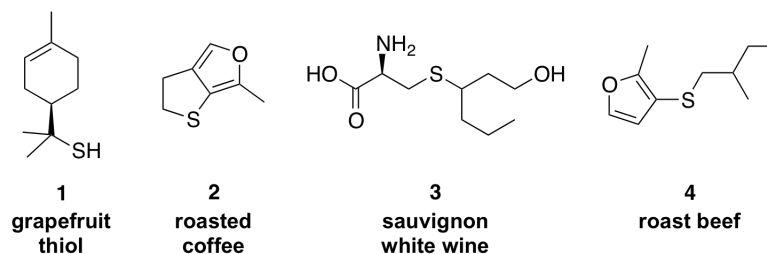


Figure 1.1 Example of Sulfur Containing Aroma Compounds

Of course, these pleasantries are often overshadowed by the more offensive aromas produced by compounds **5-11**, which run the gamut of smells associated with onion and garlic, to the characteristic urine smell upon digestion of asparagus.⁵⁻⁷ These small molecules demonstrate that structurally homologous organosulfur compounds (such as **3**, **5**, and **6**) can elicit a wide variety of responses from olfactory receptors. More importantly, this demonstrates that small molecule compounds containing thiols, sulfides, and the more oxidized derivatives (e.g., sulfoxides and sulfones) can give rise to a number of biological responses. For this reason, organosulfur compounds have found extensive use as medicines,

most notably for the treatment of bacterial infections. Furthermore, oxidized derivatives, such as vinyl substituted sulfones, are beginning to demonstrate considerable use in the inhibition of parasitic proteases responsible for neglected illnesses such as Chagas disease and malaria.⁸⁻¹⁸

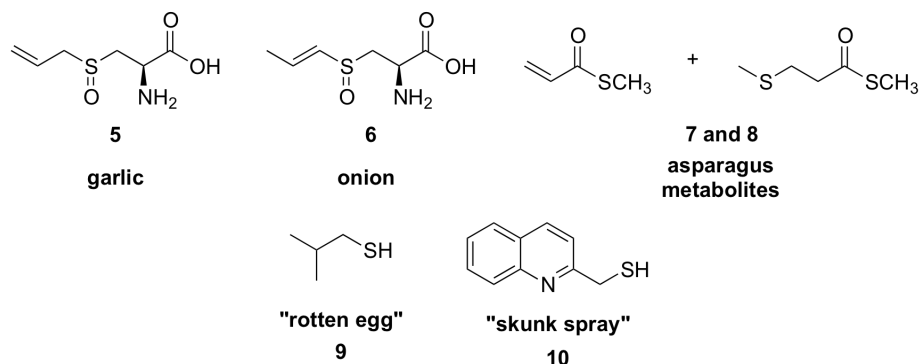


Figure 1.2 Naturally Occurring Sulfur Odourants

This chapter serves to illustrate the importance of organosulfur compounds in medicinal and synthetic chemistry. This will involve a discussion of historically relevant organosulfur molecules encompassing early sulfonamide, penicillin and carbapenem antibiotics. The evolution of vinyl sulfone based peptidomimetics as promising new therapies for the treatment of cancer and neglected illnesses including malaria and Chagas disease will be discussed as well. Lastly, select synthetic transformations that exploit the unique reactivity of organosulfur compounds will be highlighted in conjunction with relevant examples involving the synthesis of complex natural products.

1.1 Medicinal Chemistry of Organosulfur Compounds

Organosulfur compounds are widespread in medicinal chemistry, and the emergence of these compounds can be traced back to studies involving anti-bacterial agents following the First World War. It is speculated that the discovery of both the penicillin and sulfonamide classes of antibiotics was largely inspired by the participation of Alexander Fleming and Gerhard Johannes Paul Domagk in the British and German militaries. This research was largely driven by the use of cresol and other antiseptics for the treatment of war related injuries. This was largely unsuccessful in preventing the onset of bacterial infections, thus necessitating the development of more effective antibiotic medications.¹⁹

1.1.1 Early Sulfonamides

The development of the first aryl sulfonamide antibacterial was accomplished at Bayer, where Domagk tested a variety of synthetic azo dyes in the treatment of streptococcal infections. The most potent of these compounds tested was the red azo dye, later named Prontosil. Related research by French chemists identified Rubiazol as a similarly effective antibacterial compound. More importantly this same group of scientists discovered that the reduced form of the azo dye was also an effective antibacterial agent leading to the discovery of sulfanilamide. The identification of this simplified form of Prontosil allowed for the synthesis of a diverse library of compounds for the treatment of bacterial infections, thus establishing the sulfonamide as an important functionality in drug design. The prevalence of the sulfonamide functionality in medicinally active molecules led to the collective designation of these compounds as sulfa-drugs.

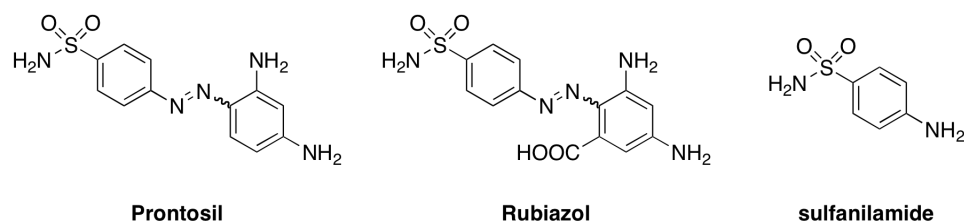


Figure 1.3 Early Sulfonamide Drugs

1.1.2 Discovery of Penicillin

A similar breakthrough in medicinal chemistry was accomplished with the discovery of penicillin by Alexander Fleming, who observed the growth of a fungus within a Petri dish containing staphylococci. This fungus appeared to be destroying neighboring bacterial cells, and Fleming later began using the filtrate from similar fungal growths in the treatment of various infections. This spurred an enormous amount of research between the British and American governments in order to develop scalable synthetic and fermentation processes for the production of the various penicillins (Figure 1.4). At the core of these molecules is the strained β -lactam fused to the sulfur containing thiazolidine ring. The marked instability of these functionalities deterred scientists from fully investigating the potential of the penicillins as chemotherapeutic treatments for bacterial infections.¹⁹ Despite the efforts of some of the most prominent figures in organic chemistry, a successful total synthesis of one of these molecules was not reported until almost a decade following the Second World War. This was

largely made possible by the structural elucidation of penicillin G by Professor Dorothy Crowfoot-Hodgkin at Oxford University. As with many synthetic endeavours, the synthesis of penicillin V rested upon the invention of a new synthetic technology, which involved the construction of amide bonds under neutral conditions. This was in relation to the long recognized instability of the β -lactam functionality to acid hydrolysis. The results of this effort represent the invention of *N,N'*-dicyclohexylcarbodiimide.

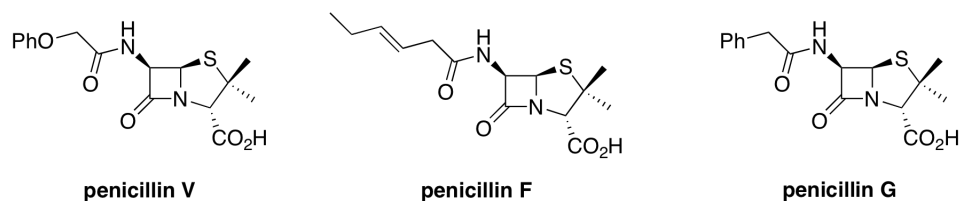


Figure 1.4 Selected Penicillins

The discovery of the sulfonamide family of antibiotics and the penicillins established the reputation of organosulfur compounds as possessing valuable biological activity in the treatment of bacterial infections. However, the continued clinical use of these medications inevitably led to the development of bacterial resistance towards this class of antibiotics. This necessitated the discovery and synthesis of compounds with similar broad-spectrum applicability in order to effectively treat patients with resistant strains.

1.1.3 Sulfonamide Resistance and Mechanism of Action

The primary mechanism that underlies the bacteriostatic nature of sulfonamides is the inhibition of the enzyme dihydropteroate synthase (DHPS). The sulfonamides typically act as antagonists towards DHPS, preventing the recognition of *p*-aminobenzoic acid (PABA) and thus arresting the production of folic acid and halting bacterial growth.

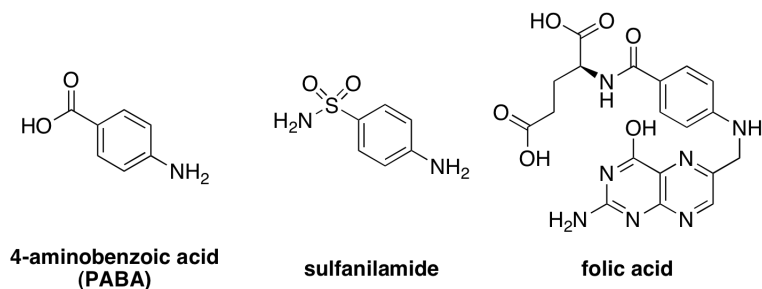


Figure 1.5 PABA, Sulfanilamide and Folic Acid

wall. The mechanism for which peptidoglycan synthesis is interrupted relates to the ability of β -lactam antibiotics to geometrically mimic the D-Ala-D-Ala peptide bond present in the peptidoglycan. This residue is substituted with a diaminopimelic acid (DAP) unit, from a neighbouring peptidoglycan strand, thus generating the necessary cross-linkage. This in turn influences the balance between peptidoglycan degrading and synthesizing enzymes, where inhibition of the latter will cause the degradation to become dominant. This can eventually lead to the destruction of the cell wall, or the weakening of the peptidoglycan cross-links, which can lead to rupture under high osmotic pressures.^{22, 23}

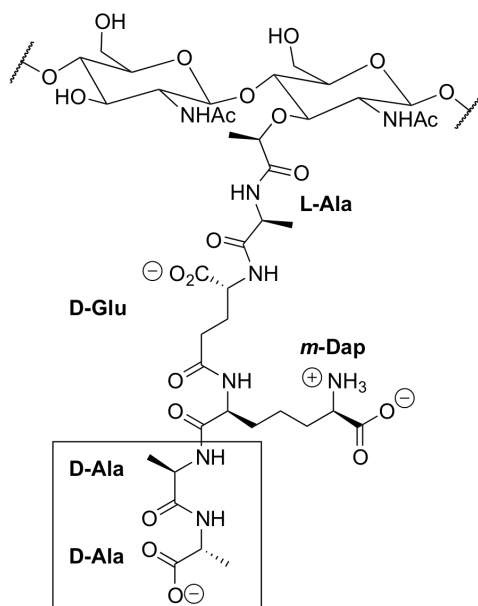


Figure 1.7 Abbreviated Structure of Peptidoglycan

1.1.5 Second Generation Sulfur Containing Antibiotics

The development of resistance towards sulfonamide and β -lactam antibiotics led to the development of novel therapies that combat the evolution of destructive β -lactamase enzymes, or improve substrate binding. This led to the development of second-generation antibiotics consisting of the carbapenem, cephalosporin, and β -lactamase inhibitors that serve to enhance the effectiveness of antibiotic medications. The most recognizable members of these families to organic chemists are thienamycin and cephalosporin C, as these molecules represent landmarks in chemical synthesis conducted by Merck Sharp and Dohme (Rahway) and R.B. Woodward, respectively.^{24, 25}

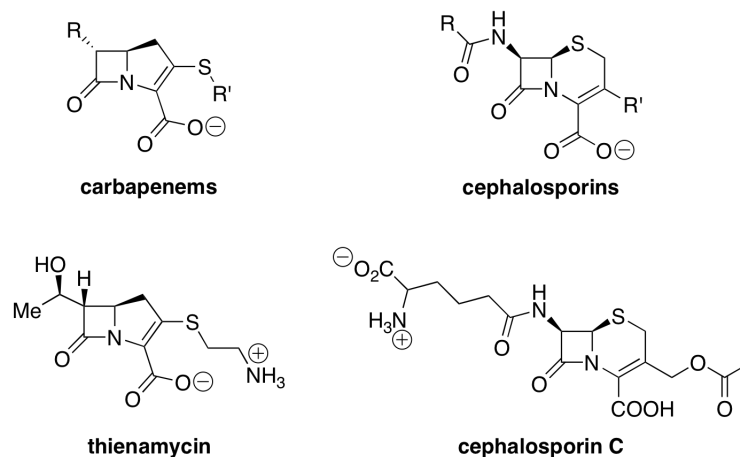


Figure 1.8 Carbapenem and Cephalosporin Families and Select Examples

The carbapenem and cephalosporin antibiotics both contain the pharmacophoric β -lactam moiety and thus have similar biological activity to the structurally homologous penicillins. These compounds were an initial victory in battling bacterial resistance; however, bacteria eventually overcame the structural novelty of these classes of antibiotics. This was accomplished either through the further evolution of β -lactamase enzymes or in the penicillin binding proteins that these compounds target. The continued development of this class of antibiotics is represented in the three generations of cephalosporin related drugs marketed by GlaxoSmithKline (Figure 1.9).²⁶

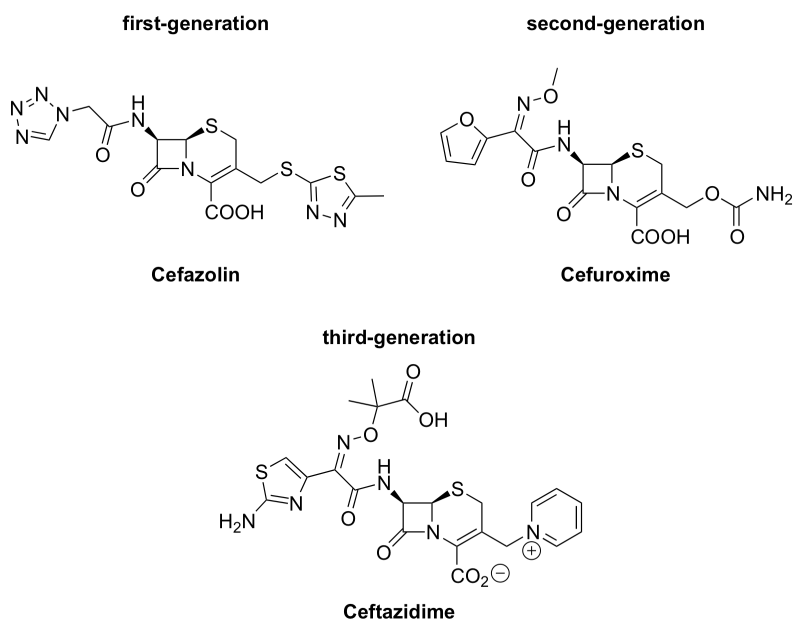


Figure 1.9 Three Generations of Cephalosporin Antibiotics

The general mechanism associated with this class of antibiotic involves the formation of an acyl enzyme complex via the addition of a nucleophilic amino acid residue present within the enzymatic active site. This can lead to expulsion of the R' side chain characteristic of the cephalosporins. As may be expected with structures such as ceftazidime, the R' group may improve solubility at the cost of increased toxicity, as this compound has been noted to produce unacceptable levels of pyridine at physiological temperature.²⁷

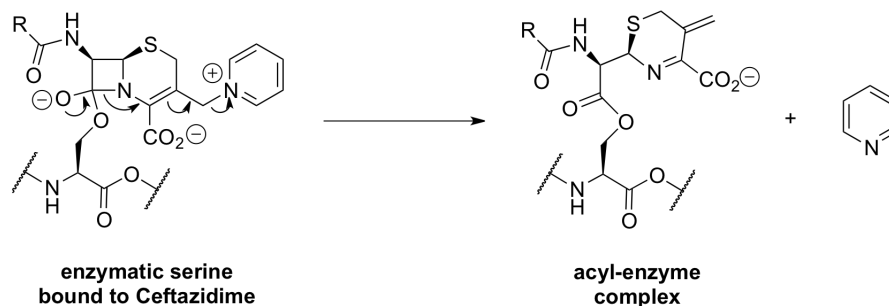


Figure 1.10 Mechanism of β -Lactam Opening and Expulsion of Pyridine

As a means of balancing the susceptibility of the penicillin, carbapenem, and cephalosporin antibiotics towards β -lactamase enzymes, these medications may be prescribed along with an inhibitor for these enzymes. These inhibitors are designed to react preferentially with the β -lactamase enzyme, allowing the antibiotic to reach its target unscathed. As a result, the β -lactamase inhibitors bear significant structural similarity to the antibiotic, but contain a more oxidized variant of the thiazolidine, where the sulfide is replaced by the corresponding sulfone. This likely enhances the formation of the acyl enzyme complex by further decreasing the already diminished C-N double bond character of the β -lactam amide. The two typical β -lactamase inhibitors prescribed are sulbactam and tazobactam (Figure 1.11).

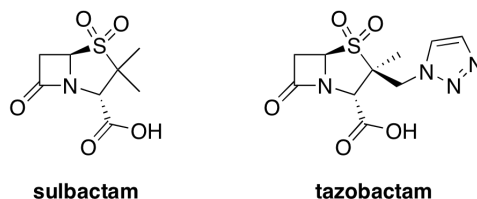


Figure 1.11 Common β -Lactamase Inhibitors Used in Combination Therapies

1.1.6 Summary of Sulfur Containing Antibiotics

As discussed in the preceding sections, organosulfur compounds are ubiquitous in medicinal chemistry, especially in therapies for the treatment of bacterial infections. Considerable effort has been devoted to the continued synthesis of these organosulfur compounds, particularly the cephalosporin antibiotics. However, the advances made in identifying medicinal targets stemming from this family of molecules are always marred by the eventual development of bacterial resistance. This has led to the implementation of β -lactamase inhibitors, used in combination therapies, as a means of preventing the degradation of the active pharmaceutical ingredient.²⁸ The pharmacophore typically associated with these drug molecules is the β -lactam nucleus, which is common among all molecules discussed thus far, with the exception of the early sulfa-drugs (Section 1.1.1). This likely suggests that a description of the role of sulfur in these drug molecules is largely conformational in nature, where the five and six-membered sulfur containing rings play a significant role in orienting the β -lactam within the enzyme active site.

The following section will discuss organosulfur compounds where the sulfur containing functionality is directly involved in the mechanism of action. This specifically relates to vinyl sulfone peptidomimetics, which act as irreversible Michael-acceptors with applications towards the inhibition of various cysteine proteases. These compounds represent promising new therapies for the treatment of neglected illnesses, including parasitic infections.

1.2 Sulfur Containing Peptidomimetics

As mentioned in Section 1.1.4, β -lactam antibiotics can mimic the D-Ala-D-Ala peptide bond present in peptidoglycan, thus interfering with the enzymes responsible for cross-linking individual peptidoglycan units. This will often lead to errors in the generation and repair of bacterial cell walls, and an imbalance of peptidoglycan synthesis and degradation enzymes, eventually culminating in cell rupture.²² The development of novel cephalosporins that contain peptide fragments characteristic of peptidoglycan synthesizing enzymes represents a new strategy to combating resistance to typical therapies involving this class of molecules. The successful synthesis of one such cephalosporin, and its incubation with *Streptomyces sp.* strain R61, led to the isolation of a covalently bound inhibitor-enzyme

complex. In the figure below, the red substituent represents the portion of the cephalosporin (12) that mimics the D-Ala-D-Ala peptide bond. This group eventually becomes bound to a serine residue present within the active site of a penicillin binding protein. The portion of the molecules highlighted in blue are thought to help mimic the diaminopimelic acid residue from a neighbouring peptidoglycan unit. This residue is typically responsible for the generation of the peptide cross-linkage necessary for cell wall synthesis. By binding the inhibitor to a PBP, the investigators were able to use crystallography in identifying key residues in the enzyme active site that interact with the acyl-enzyme complex during cell wall synthesis. The solid state crystallographic data obtained for this complex provides critical information regarding the final step of bacterial cell wall synthesis and will inevitably aid in the design of novel antibiotic compounds.²⁹

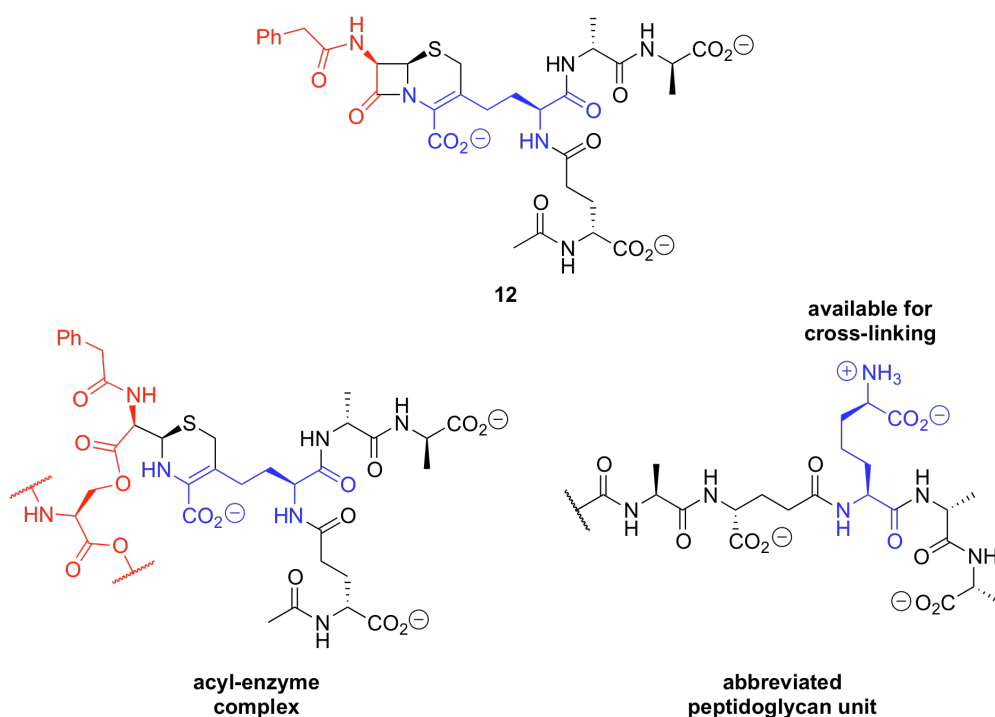


Figure 1.12 Cephalosporin Peptidomimetic

The success of the example discussed above represents a popular field of drug design, where structural and biological properties associated with endogenous molecules, like peptides, are mimicked within a small molecule. These so called peptidomimetics represent attractive therapies in comparison to the clinical use of naturally occurring peptides. This relates to the rapid excretion, poor selectivity, and rapid proteolysis in serum and the

gastrointestinal tract, which effectively make natural peptides less bioavailable. These shortcomings are at least partially overcome by the use of peptidomimetics, where medicinal chemistry efforts can aid in creating a therapeutic agent with greater resistance to the aforementioned degradation pathways.³⁰ One area where peptidomimetics have found considerable use is in the inhibition of cysteine proteases, enzymes commonly linked to several illnesses and parasitic infections. Some of the most successful inhibitors of this class of enzymes take advantage of the tendency for the cysteine sulfur to engage in Michael-addition with an appropriate electrophilic acceptor. The application of various electrophiles, including the vinyl sulfone Michael-acceptors, towards cysteine protease inhibition is discussed in the following section.

1.2.1 Peptidomimetics Containing Sulfur-Based Michael-Acceptors

The over expression of cysteine protease enzymes has been linked to several major illnesses including cancer, arthritis, osteoporosis, and cardiovascular diseases.³¹ Additionally, several parasites are known to accumulate nutrients or invade healthy cells based upon the availability of cysteine proteases.³² This has attracted considerable interest from academia and pharmaceutical based medicinal chemistry groups, as inhibition of parasitic or endogenous cysteine proteases may yield valuable therapeutic effects. Research into this field has yielded several promising drug candidates for the aforementioned infectious and metastatic diseases. A common feature of these drug molecules is an electrophilic group capable of provoking the cysteine residue of the parent protease into engaging in nucleophilic attack. This process can be either reversible or irreversible depending on the strength of the electrophile and the composite atoms.

To this end, Merck Frosst developed a series of cysteine protease inhibitors that contain an electrophilic cyano moiety capable of undergoing reversible nucleophilic addition with the cathepsin family of human proteases (Figure 1.13). In particular, these compounds are highly selective for cathepsin K, a lysosomal cysteine protease that is abundant in cells responsible for bone degradation during bone repair processes. Interestingly, the cyano group does not undergo *in-vitro* hydrolysis and subsequent proteolysis, even under the relatively acidic conditions characteristic of lysosomal proteases.^{33, 34}

endemic in Latin American countries. Structurally analogous compounds to K777, such as K11017, also demonstrate excellent inhibition profiles with organisms such as *P. Falciparum*, the parasite responsible for one of the most lethal forms of malaria.³⁵ The broad spectrum activity of the vinyl sulfones towards multiple parasitic cysteine proteases relates to the structural homology of several proteases. For example, falcipain the cysteine protease characteristic of *P. Falciparum*, and cruzain (from *Trypanosoma cruzi*) both belong to the papain family and have a high degree of similarity within the enzyme active site.⁹

1.2.2 Mechanism of Action for Vinyl Sulfone Peptidomimetics

The high degree of selectivity characteristic of the vinyl sulfone peptidomimetics is often attributed to the mild electrophilicity of the β -carbon and the manner in which the compound docks within the enzyme active site. In particular, cysteine residues within the papain-type proteases appear to have a greatly enhanced acidity relative to similar thiols, such as 3-mercaptopropionate. This increase in acidity is attributed to a stabilizing interaction with a neighbouring histidine residue. The greater degree of ionization of the cysteine sulfur to the corresponding thiolate, and the presence of the protonated histidine represents an ideal environment for the activation of a Michael-acceptor (Figure 1.15).

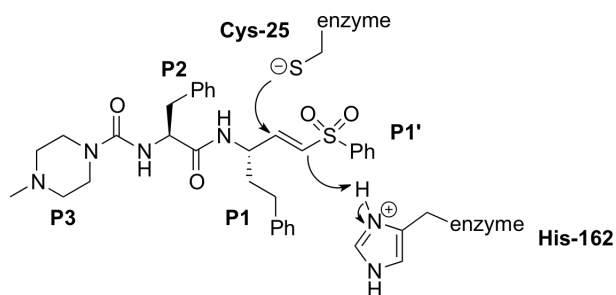


Figure 1.15 Binding Domains of K777 and Mechanism of Inhibition

Indeed, the protonated histidine is shown by crystallography to be in close contact with the sulfone oxygen atoms, activating the olefin towards nucleophilic attack by the cysteine sulfur.^{13, 36} The sulfone moiety is said to lie within the P1' of the papain family of cysteine proteases, and based upon solid state structural data, shows possible hydrogen bonds with the proximal histidine-162 and tryptophan-184 residues, while cysteine-25 is bound to the β -carbon. The P1' portion of K777 is quite tolerant to derivation and a series of sulfonate

esters, sulfonamides, and varying aryl and alkyl sulfones have been synthesized as part of a structure activity relationship (SAR) study. Of these modifications, replacement of the phenyl ring of the vinyl sulfone with an aryl ether markedly increases the second-order inactivation rate of the cruzain cysteine protease. This is believed to be a consequence of the aryl ether functionality exerting an inductive effect upon the vinyl sulfone; thereby increasing the electrophilicity of the β -carbon. This is a result of the poor π -donation between oxygen and sulfur due to the disparate size of the atoms.³⁷ In general, elongation of the sulfone P1' substituent by one atom appears to have a favourable effect on inactivation of the cysteine protease and is believed to relate to the parent structure only partially occupying the P1' domain (Figure 1.16).¹² The further homologated alkyl sulfone showed a decrease in activity relative to the benzylsulfone derivative demonstrating that larger analogues possess a less desirable fit within the enzyme active site. Additionally, the ethyl substituted sulfonate ester is less active than the parent derivative, which is consistent with the general behaviour of these compounds as indiscriminate alkylating agents similar to the popular methylating agent dimethylsulfate.

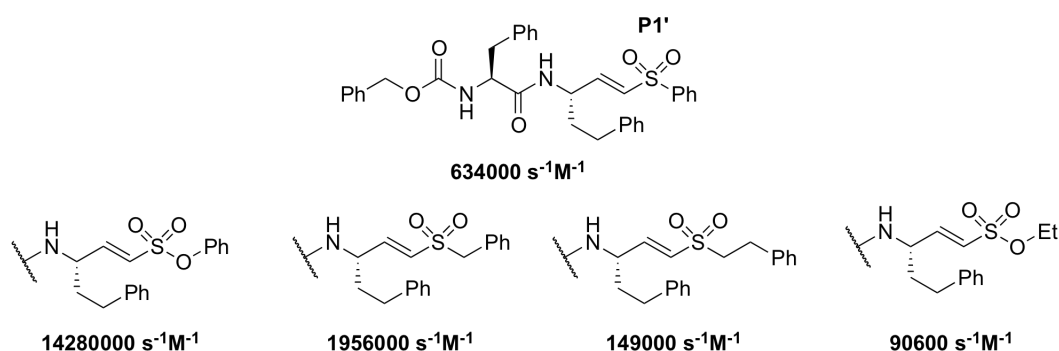


Figure 1.16 Comparison of Inverse-Secondary Inactivation Rates for P1' Analogues

1.2.3 Summary of Biologically Active Michael-Acceptors

The ability of vinyl sulfone and similar peptidomimetics to inhibit a diverse array of parasitic and endogenous cysteine proteases is continuing to attract attention of medicinal chemists both in academia and industry. However, these functionalities are not limited to the inhibition of proteases, but also show promising inhibition of polo-like kinases (PLK), which are involved in regulating cellular division. In particular, Onconova Pharmaceuticals is investigating the use of vinyl sulfones as anti-cancer medications, where ON 01910.Na is in

phase I and II clinical trials as treatments for human B-cell lymphocytic leukemia and several solid tumor malignancies (Figure 1.17).

Interest in expanding upon current motifs involving vinyl sulfone peptidomimetics has yielded novel falcipain-2 inhibitors, incorporating benzo[1,4]diazepin-2-one's as β -turn mimics. These compounds serve as a foundation for additional SAR studies for the development of anti-malarial medications, as many peptidomimetics suffer from premature degradation of the constituent peptide bonds. Lastly, simple divinyl sulfones have shown potent antiviral properties; however, as one may predict, these structures are often unselective and possess high cytotoxicity due to competitive Michael-addition of endogenous nucleophiles such as glutathione.³⁸⁻⁴²

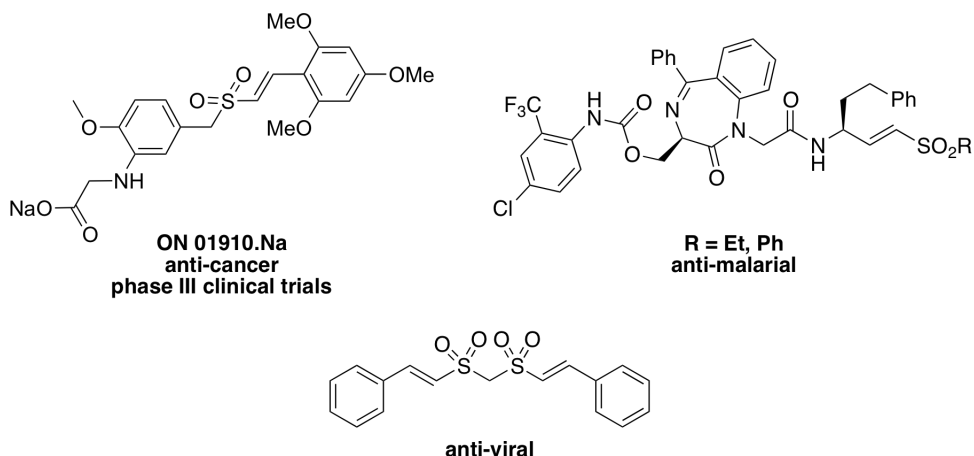


Figure 1.17 Biologically Active Michael-Acceptors

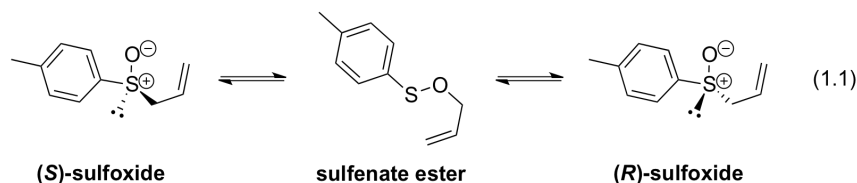
Given the diverse array of biological activities, and the emergence of parasitic resistance towards current therapies, peptidomimetic vinyl sulfones show promise as novel chemotherapeutics. Importantly, these medicines may aid in the treatment of neglected illnesses such as malaria, African sleeping sickness, Chagas disease, and many more. Additionally, the anti-cancer and anti-viral properties of these analogous compounds further demonstrate the importance in developing methods for the synthesis of these valuable synthetic intermediates.

1.3 Sulfur in Organic Synthesis

The importance of organosulfur compounds in synthetic chemistry extends well beyond target-oriented synthesis of biologically active non-natural products such as those mentioned in the sections above. Rather, sulfur-containing molecules find considerable use in natural product synthesis based upon the ability of these molecules to undergo a variety of useful synthetic transformations for the synthesis of carbon-carbon bonds. The diverse reactivity characteristic of these molecules is largely due to the different oxidation states of sulfur and the facile synthesis of these derivatives in the presence of other oxygen-sensitive functional groups. The presence of these compounds in relevant synthetic methodologies will be discussed in the following sections, as well as examples of their use in natural product synthesis.

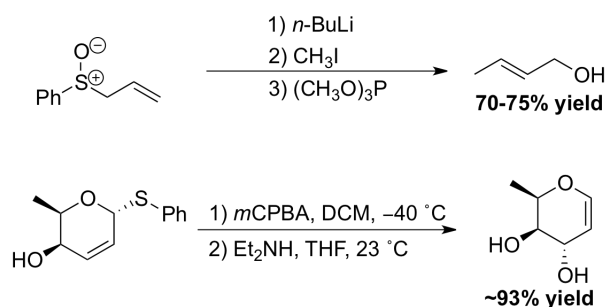
1.3.1 Named Reactions Involving Organosulfur Compounds

The value of organosulfur compounds as intermediates in complex molecule synthesis has led to the development of several named transformations. These popular organic reactions predominately rely on the use of oxidized derivatives of sulfides, including the sulfoxide and sulfone. One of the most widely used transformations involving the sulfoxide functional group is the Mislow-Evans [2,3]-sigmatropic rearrangement. Additionally, the generation of sulfur stabilized carbocations via the Pummerer rearrangement represents a useful strategy for the formation of carbon-carbon, or carbon-heteroatom bonds. Both of these transformations use the latent nucleophilicity of the sulfoxide oxygen, either in the addition to an adjacent π -system, or in reacting with hard acylating agents. Conversely, the sulfone functional group allows for the generation of stabilized α -carbanions, characteristic of both the Julia olefination and the Ramberg-Bäcklund rearrangement.



It was first observed that optically pure allylic sulfoxides could racemize at appreciable rates at relatively low temperatures, typically ranging from 50 to 70 °C (Eq. 1.1).

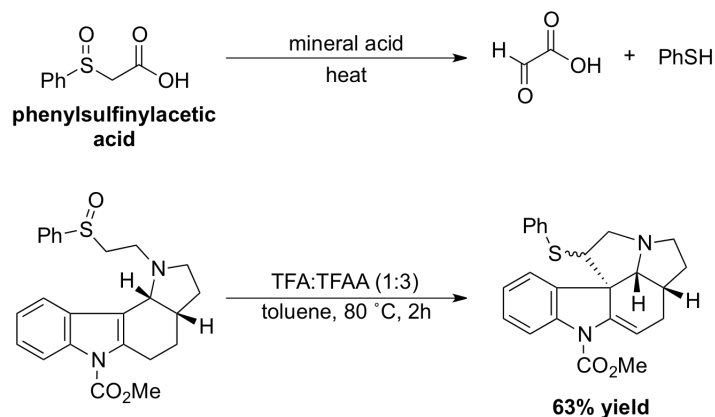
This is much lower than the typical temperatures required for the pyramidal inversion of sulfoxides, which ranges from 190-220 °C.⁴³ The conversion of the sulfoxide to the intermediate sulfenate ester was determined to occur in a synchronous fashion, and did not involve initial fragmentation recombination pathway. Only later did Evans report the synthetic utility of this transformation by intercepting the intermediate sulfenate ester with an appropriate nucleophilic scavenger, or thiophile. The sequence below demonstrates the use of trimethyl phosphite as a reagent capable of converting the intermediate sulfenate ester to the corresponding allylic alcohol; however, secondary amines such as diethylamine are also capable of this interconversion (Scheme 1.1). Of particular significance is the regioselectivity of the transformation, where the *E*-linear olefin is isolated in high yield, further supporting the synchronous nature of this sigmatropic rearrangement. Furthermore, the rearrangement occurs suprafacially, allowing for the generation of allylic alcohols with retention of configuration based upon the original asymmetric center. This is useful, as it allows for the synthesis of diastereomeric sulfoxides, which upon rearrangement provide a single diastereomeric species, as demonstrated below.⁴⁴



Scheme 1.1

The Pummerer rearrangement represents another useful transformation of the sulfoxide functionality, allowing for additional bond formation processes, or as a synthetic handle for the strategic introduction of an aldehyde. The discovery of this reaction occurred when phenylsulfinylacetic acid was heated in the presence of mineral acids, yielding both thiophenol and glyoxylic acid.^{45, 46} This reaction proved general and represents an *in-situ* hydrolysis of the thionium ion generated upon elimination of the sulfoxide oxygen, either following acylation or as mediated by the addition of Brønsted acids. The thionium ion is also a useful electrophile for the formation of carbon-carbon, or carbon-heteroatom bonds,

dependent on the availability of suitable nucleophiles for the interception of this reactive intermediate. The examples in Scheme 1.2 demonstrate these processes, where the thionium ion generated is capable of undergoing Friedel-Craft type alkylations with electron rich aromatic nuclei, such as the indole shown.⁴⁵⁻⁴⁷

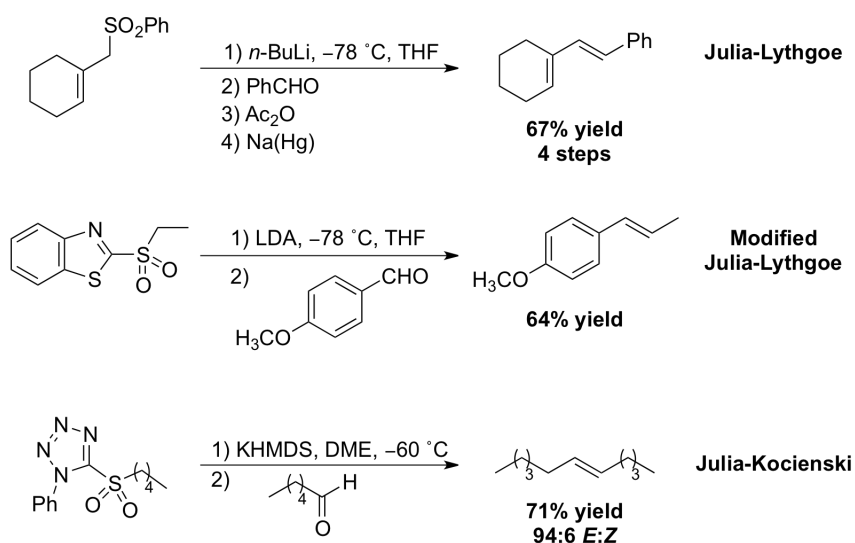


Scheme 1.2

The reactivity of the sulfone functional group is distinct from that of the sulfoxide, where the formation of α -carbanions is normally followed by either a condensation with an aldehyde or alkylating agent. The Julia-Lythgoe olefination and the Ramberg-Bäcklund rearrangement allow for the transformation of sulfones to olefins with high regioselectivity for the *E*-linear isomer, dependent on the conditions employed. The mechanisms by which these processes operate are quite distinct, where the Ramberg-Bäcklund rearrangement allows for strategic ring contraction, generating 1,2-disubstituted alkenes embedded within a variety of large or small ring systems. The contraction of the ring containing the sulfone occurs through chelotropic extrusion of sulfur dioxide from an episulfone intermediate.

The Julia-Lythgoe olefination, and modifications thereof, are amongst the most reliable methods for the synthesis of *E*-1,2-disubstituted olefins. The original methodology, developed by Marc Julia, is rather cumbersome, and requires the use of harsh reducing conditions involving treatment of the β -acyloxysulfone with sodium amalgam in order to facilitate elimination to the corresponding olefin.⁴⁸ Sylvestre Julia later modified this by replacing the aryl sulfone with a heteroaryl sulfone, such as the benzothiazole derivative shown in Scheme 1.3.⁴⁹ This procedure typically works best with substrates that yield a conjugated olefin, providing high selectivity for the *E*-linear olefin and reasonable synthetic

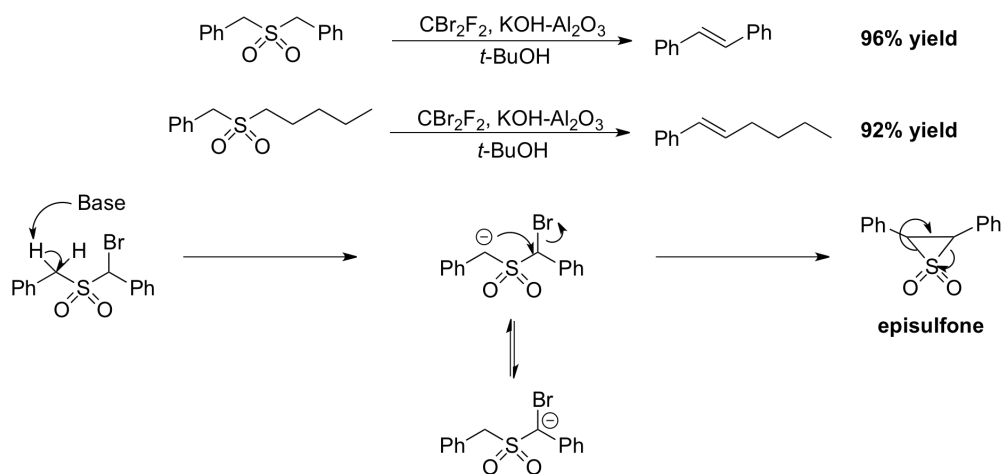
yield. Similarly, the Julia-Kocienski olefination, which utilizes the phenyltetrazole-substituted sulfones, helps circumvent the tendency for the analogous benzothiazole derivatives to undergo self-condensation, even at low temperatures.⁵⁰ This methodology also tolerates simple aliphatic sulfones and aldehydes, thus extending the scope beyond substrates that possess conjugation. Lastly, the Julia-Kocienski olefination is sensitive to the nature of the cation, where the selectivity follows the trend $K^+ > Na^+ > Li^+$; however, larger cations tend to give reduced yields of the desired olefin. Additionally, highly coordinating solvents such as dimethoxyethane (DME), and additives, such as hexamethylphosphoramide (HMPA), influence the selectivity in favour of the *E*-linear isomer. As a compromise, lithium hexamethyldisilazide (LiHMDS) may be used in conjunction with an additive such as HMPA to ensure high selectivity for *E*-linear olefins without significantly lowering reaction efficiency.⁵⁰



Scheme 1.3

Lastly, the Ramberg-Bäcklund rearrangement represents another strategic method for the introduction of *E*-linear olefins from easily prepared sulfone starting materials. This process is especially useful for the synthesis of strained ring systems that possess either an *E* or *Z* alkene dependent on the size of the ring. The use of CBr₂F₂ is superior to CCl₄ as a halogen source, as the latter may lead to the formation of cyclopropane byproducts as a result of carbene formation and reaction with the incipient olefin. Additionally, the use of KOH-Al₂O₃ has proven superior to pulverized KOH due to the enhanced surface area and

activating effect of the heterogenous support. This procedure also helps suppress dihalogenation of the sulfone allowing for previously difficult dialkyl sulfones substrates to rearrange readily to the corresponding alkene in high yield (Scheme 1.4).⁵¹

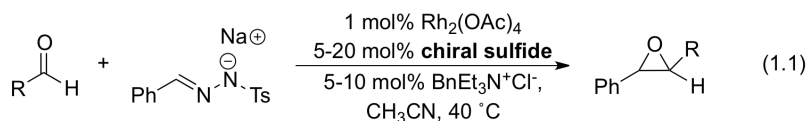


Scheme 1.4

The examples discussed above do not serve as an exhaustive review of synthetic transformations involving organosulfur compounds. Instead, the examples are selected based upon their prevalence in natural product synthesis, the inevitable goal in the development of methodologies for carbon-carbon and carbon-heteroatom bond formation. The following sections illustrate relevant examples of natural product syntheses where organosulfur compounds are part of key steps in reaching the target molecule.

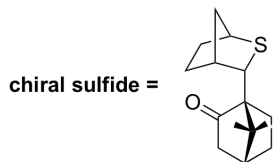
1.3.2 Organosulfur Compounds in Natural Product Synthesis

The utility of organosulfur compounds is certainly not restricted to the sulfoxide and sulfone functional groups discussed in the previous section. Rather, simple sulfides are known to readily form stable ylides with applications in asymmetric epoxidation and aziridination reactions. The process shown in Eq 1.1 is analogous to the Corey-Chaykovsky epoxidation and cyclopropanation methodologies, with the exception that this method is catalytic with respect to the sulfide, and enantioselective based on the camphor-derived auxiliary. This methodology affords the corresponding epoxides with high trans selectivity and enantiomeric excess, and is also extendable to the use of imines in the generation of the corresponding aziridines.⁵²⁻⁵⁵

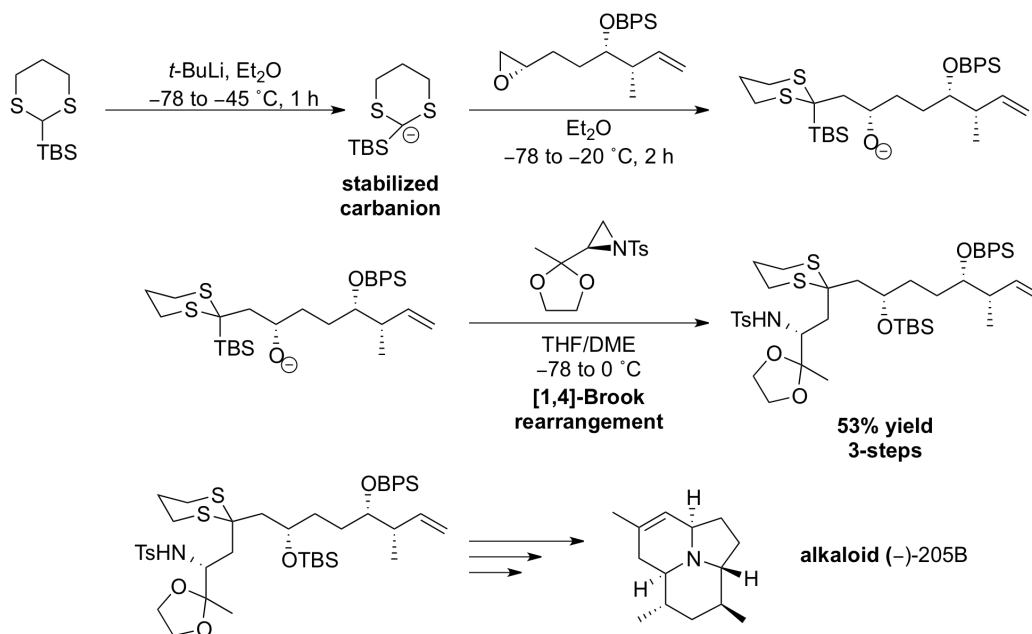


R = Ph, *p*-ClPh, *p*-NO₂Ph, *p*-MeOPh, *p*-MePh, Cy

58-84% yield
90-94% ee



Furthermore, the umpolung reactivity of dithianes serves as another example of the synthetic utility of sulfides, and represents a class of intermediates that serve as acyl anion equivalents, where treatment with an appropriate base generates a stabilized carbanion. Upon trapping of these carbanions with a suitable electrophile, the dithiane may be hydrolyzed to the corresponding unsymmetrical ketone. This strategy has been popularized in the synthesis of natural products by combining the deprotonation of the dithiane with anionic rearrangements, allowing for remote functionalization and so-called anion relay processes.

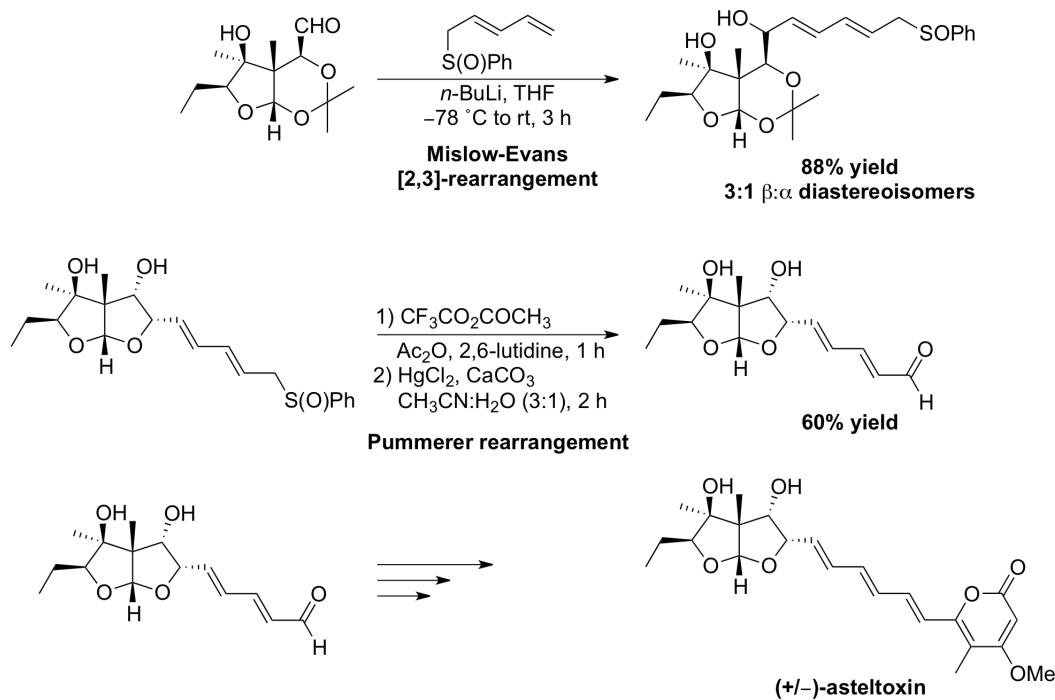


Scheme 1.5

This process is exemplified in Scheme 1.5, where the addition of the stabilized carbanion to the epoxide electrophile subsequently initiates a [1,4]-Brook rearrangement, effectively regenerating a sulfur stabilized carbanion. This intermediate is then analogously

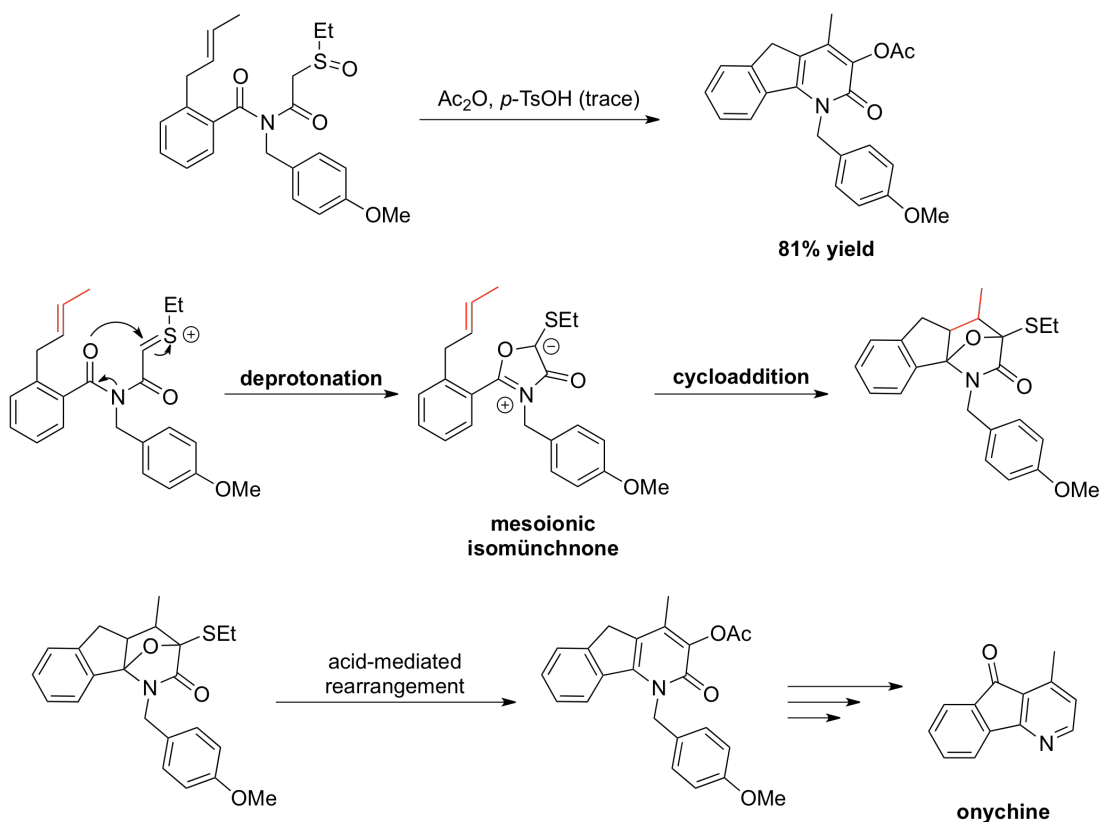
intercepted by the aziridine electrophile, generating an advanced intermediate en route to the natural product, alkaloid (-)-205B.⁵⁶

The racemic synthesis of asteltoxin by Schreiber represents a hallmark in organic synthesis and truly showcases the diverse reactivity of organosulfur compounds. This exploits both the enolate-like reactivity of sulfoxides, a [2,3]-sigmatropic rearrangement characteristic of allylic sulfoxides, and the generation of a thionium electrophile by way of the Pummerer rearrangement. This sequence was strategically employed by initially condensing the dienyl sulfoxide shown in Scheme 1.6, which at room temperature underwent a double allylic transposition, known as the Mislow-Evans rearrangement. Typically, this yields a 1,3 transposition of an allylic sulfoxide for an allylic alcohol, when the reaction is conducted in the presence of a phosphine based thiophile, i.e. POMe_3 . However, as this rearrangement occurs through conjugation of the diene, the resulting product is the original sulfoxide, where this group is now present at the opposite terminus of the conjugated double bonds. As shown in Scheme 1.6, this rearrangement typically occurs with complete selectivity for the *E*-linear olefin. The ability of sulfoxides to act as aldehyde surrogates is demonstrated through the strategic application of the Pummerer rearrangement shown in scheme 1.6. This is known to proceed through the electrophilic thionium ion, which upon aqueous hydrolysis eliminates thiophenol, thus generating the carbonyl compound shown. This intermediate was then only two steps removed from asteltoxin.⁵⁷



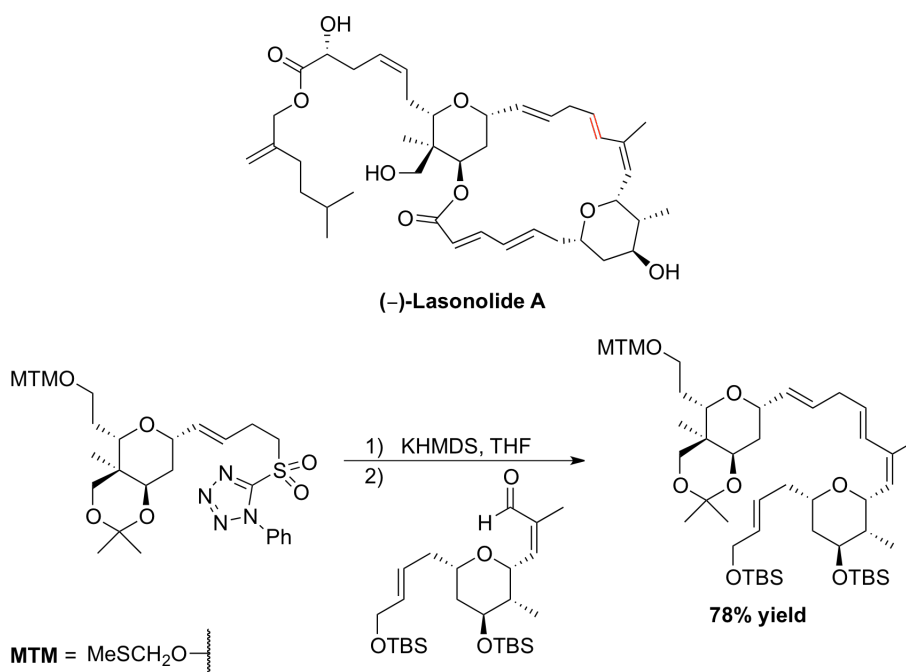
Scheme 1.6

Furthermore, the synthetic utility of the Pummerer rearrangement is not restricted to the transformation of sulfoxides to the corresponding aldehyde, but may serve as a reactive intermediate for the initiation of cascade bond formation sequences. Scheme 1.7 demonstrates one such example, where intramolecular interception of the resultant thionium ion with the adjacent amide generates a mesoionic isomünchnone. This process is represented in Scheme 1.7, where the *in-situ* generated isomünchnone, undergoes a [3+2] cycloaddition with the pendant olefin; thereby, generating the corresponding cycloaddition product. Upon acid-mediated ring opening of the bridging ether, the corresponding pyridinone is formed, which was eventually transformed into the natural product onychine (Scheme 1.7).⁵⁸



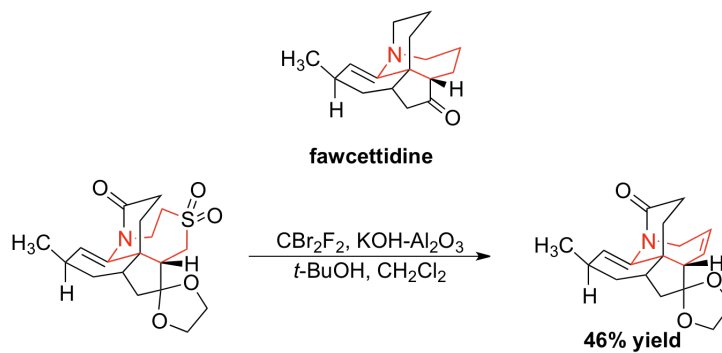
Scheme 1.7

The further oxidized sulfone reacts much like the dithiane and sulfoxide intermediates, where the functionality is also capable of stabilizing adjacent carbanions. The consequent condensation of these sulfone stabilized carbanions with carbonyl electrophiles represents the popular olefination methodology developed by Marc Julia. This technology finds considerable use in the synthesis of marine macrolides, where the union of advanced synthetic intermediates is typically accomplished by applying this olefination methodology. The example shown involves the synthesis of the marine macrolide lasonolide, which possesses potent antitumor properties towards A-549 human lung cancer carcinoma and Panc-1 human pancreatic carcinoma cells. The Julia-Kocienski reaction was successfully applied in the union of the two tetrahydropyran, providing the indicated *E*-linear alkene with complete regioselectivity.⁵⁹



Scheme 1.8

Similarly, the Ramberg-Bäcklund rearrangement serves as another method for the installation of *E*-linear alkenes; however, this occurs with concomitant ring-contraction based upon chelotropic extrusion of sulfur dioxide. Despite the failure of other methods for the synthesis of the indicated seven-membered ring, the strategic application of the Ramberg-Bäcklund proved successful in the synthesis of the alkaloid fawcettidine.⁶⁰



Scheme 1.9

1.4 Summary

The preceding sections should demonstrate the immense value of organosulfur compounds, from their use as common fragrances and food additives, to their presence in countless molecules of interest to synthetic and medicinal chemists alike. In fact, some of the most successful drugs marketed in the last two decades include either the sulfonamide or sulfide functionalities (Figure 1.18).^{61,62}

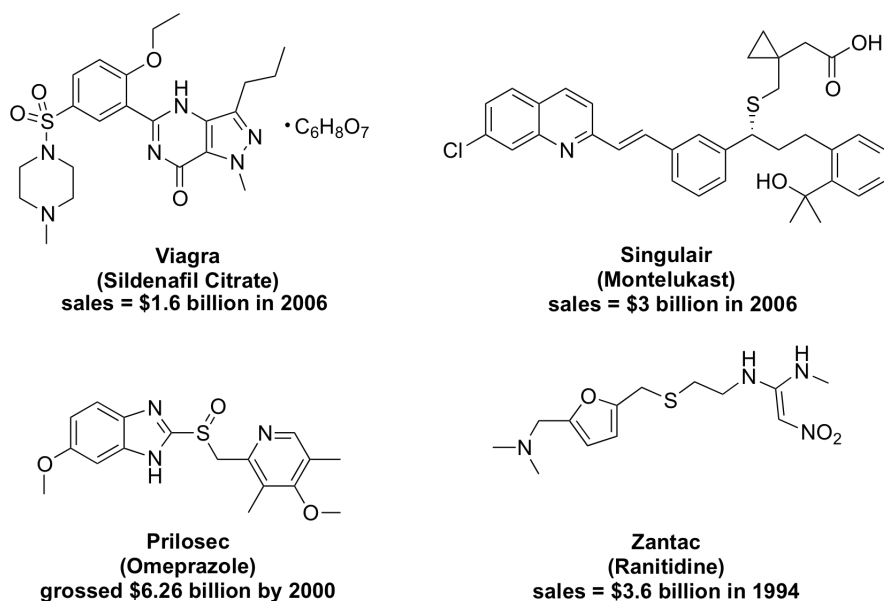


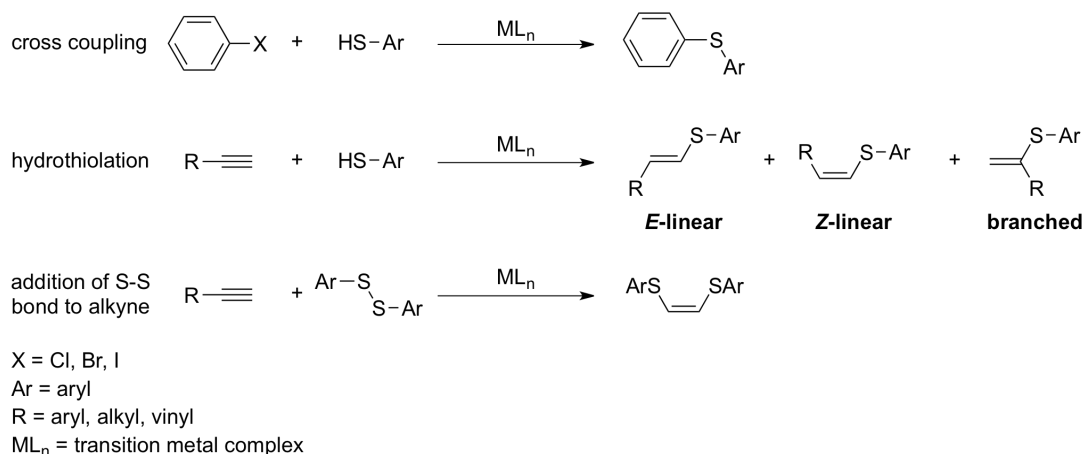
Figure 1.18 Organosulfur Containing Blockbuster Drugs

Given the widespread applicability of these molecules new methods for the development of carbon-sulfur bonds is necessary. In particular, the development of general methods for the synthesis of vinyl sulfides is especially necessary given the applicability of the corresponding sulfones towards treating neglected illnesses such as Chagas disease, African sleeping sickness, and malaria. Chapter 2 will begin with a discussion of the methods currently available for the synthesis of vinyl sulfides and will demonstrate our initial contributions to the field of rhodium (I) catalyzed alkyne hydrothiolation. Chapter 3 involves a discussion of our current efforts towards the development of a catalytic alkyne hydrothiolation methodology utilizing Wilkinson's catalyst ($RhCl(PPh_3)_3$). In chapter 4, the focus will center on the extension of alkyne hydrothiolation towards Nazarov-type 4π -electrocyclizations for the synthesis of polycyclic ring systems. Chapter 5 will discuss the synthesis of novel scorpionate-type proligands, originally developed for the asymmetric

aziridination of olefins, which may find use in the processes discussed in chapter 4. Lastly, chapter 6 will discuss conclusions and future work made possible based on the studies illustrated in the preceding chapters.

Chapter 2 Transition Metal Catalyzed Synthesis of Carbon-Sulfur Bonds

The use of organometallic reagents in the catalytic formation of C-S bonds remains scarce compared to methods to form C-O and C-N bonds. Nevertheless, despite the oft-cited belief that sulfur poisons metal catalysts, methods for the construction of C-S bonds are becoming increasingly prevalent in the literature. Indeed, the use of metal catalysts, including gold, copper, rhodium and palladium, represent widely employed synthetic strategies for the installation of C-S bonds. A common synthetic strategy involves palladium- and copper-catalyzed cross-coupling reactions of thiolate nucleophiles with aryl and vinyl electrophiles. Other examples of transition metal catalyzed processes for C-S bond formation includes hydrothiolation, in which both C-S and C-H bonds are formed in one transformation and dithiolation, in which two C-S bonds are formed (Scheme 2.1). These two approaches account for the majority of available methods for the synthesis of C-S bonds. Moreover, the functional group compatibility of these processes continues to increase, which has led to applications of metal-mediated C-S bond formation in complex molecule synthesis.⁶³⁻⁶⁹



Scheme 2.1

Despite the demonstrated utility of these methods, there is continued pressure to develop more efficient methods that rapidly generate molecular complexity. As such, a summary of recent advances is warranted. This chapter will focus on two general strategies for C-S bond formation – cross coupling and hydrothiolation. The reader is directed to a series of reviews that discuss a broad array of transition metals capable of catalyzing C-S

bond formation.⁷⁰⁻⁷⁹ In particular, the following sections detail catalytic C-S bond formation with transition metals from groups 9, 10 and 11. Furthermore, the application of these methodologies towards the synthesis of biologically active natural and non-natural products is discussed.

2.1 Cross-Coupling Approaches to C-S Bond Formation

The use of late transition metal complexes in catalytic cross-coupling reactions represents a popular strategy for the synthesis of carbon-sulfur bonds. This typically involves the use of sp^2 hybridized carbon electrophiles (e.g., aryl or vinyl boronic acids), and arene thiolate nucleophiles; however, the developments of methods capable of tolerating alkyl thiols are beginning to emerge in the literature. This is important, as numerous medicinal targets contain vinyl or aryl substituted alkyl thioethers. Additionally, nucleophilic aryl substitution processes for the synthesis of these functionalities often require forcing conditions, necessitating the development of mild catalytic protocols. The efforts described in the following sections represent key advances in the development of mild and effective methods for the formation of carbon-sulfur bonds. This discussion will focus on the use of copper and palladium complexes as catalysts for cross-coupling processes, as these metals represent the most popular choices in effecting this transformation.

As discussed in chapter 1, the development of cross-coupling technologies for the formation of carbon-sulfur bonds is critical in facilitating the discovery and synthesis of biologically active compounds. To this end, cross-coupling methodologies aided in the discovery of the low nanomolar serotonin reuptake inhibitor Lu AA21004 and in the multikilogram synthesis of PF-04191834 (Figure 2.1). These compounds may prove crucial towards the treatment of mood and anxiety disorders, as well as the management of symptoms related to asthma and chronic obstructive pulmonary disease, respectively. The synthesis of Lu AA21004 and PF-04191834 will be discussed in Section 2.2.4.

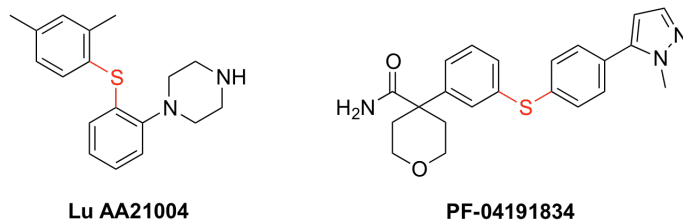
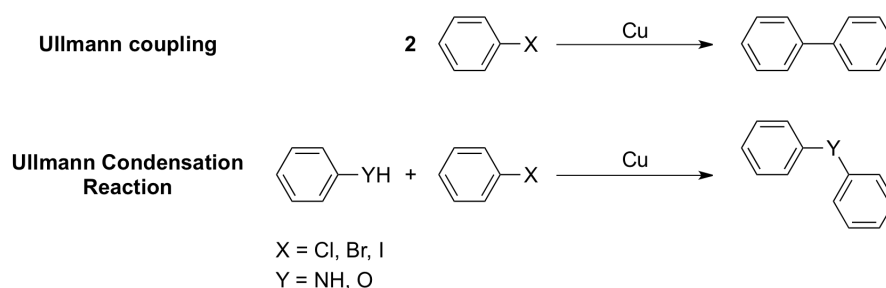


Figure 2.1 Medicinally Relevant Arylthioethers

2.1.1 Historical Precedent for Copper-Mediated Carbon-Element Bond Formation

One of the earliest examples of a coupling reaction dates back to 1901, when Ullmann demonstrated the propensity of aryl halides to undergo dimerization in the presence of copper metal.⁸⁰ In the current literature, this is typically referred to as a homocoupled product, which represents the most common byproduct formed during the coupling of two chemically distinct aryl halides. Ullmann later demonstrated the ability of anilines and phenols to undergo a similar transformation, now described as the Ullmann condensation (Scheme 2.2). The original versions of these coupling reactions typically required temperatures in excess of 200 °C and stoichiometric quantities of copper metal or an equivalent salt.^{81, 82} Amendments to this protocol involved an extensive screen of additives, ligands, coupling partners, temperatures, and solvents for the development of a general and mild procedure for copper-catalyzed cross-couplings.

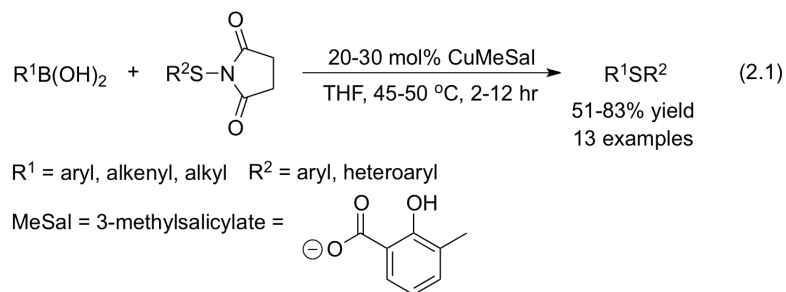


Scheme 2.2

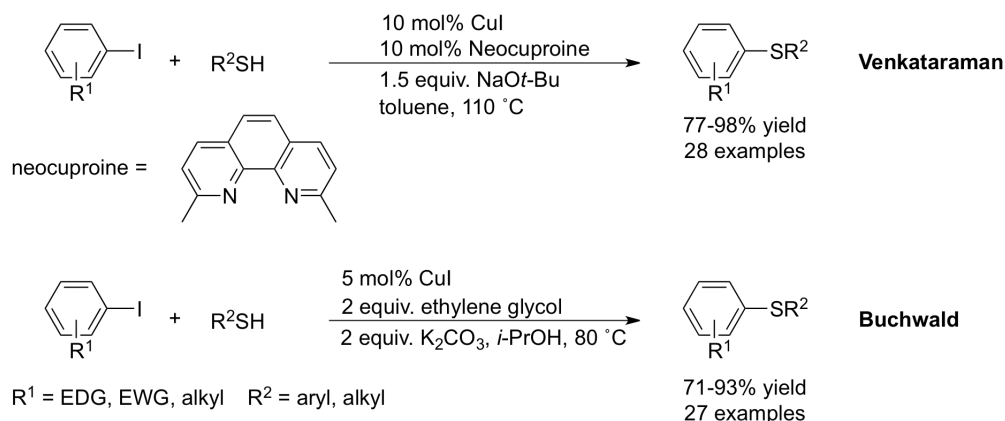
2.1.2 Copper-Catalyzed Carbon-Sulfur Bond Formation

Recent efforts have focused on supplementing tertiary amine bases with an appropriate additive, as well as exploring ligands capable of better solubilizing the copper precatalysts. These modifications have largely been evaluated within the context of aryl ether and aryl amine synthesis; however, this section will focus on methods that allow the use of aryl and alkyl thiols, as these reagents are most relevant to this thesis.

A necessary consideration when investigating cross-coupling reactions involving thiols is their tendency to form disulfides in the presence of copper (II) salts. One method for avoiding this oxidation is shown in Eq. 2.1, where thioimides are used in place of the free thiol in the presence of copper (I) complexes. The authors propose that this process is initiated upon oxidative addition of the copper (I) 3-methylsalicylate complex to the thioimide. This generates a presumed copper (III) thiolate which avoids the need for a tertiary amine base.⁸³ This method proved general for a variety of boronic acid and thioimide substrates, yielding the corresponding thioethers in good to excellent yields. Additionally, sub-stoichiometric amounts of the copper-catalyst were possible in this system within temperature ranges only slightly above ambient.



During this time, the groups of Buchwald and Venkataraman independently published similar procedures detailing the catalytic cross-coupling of aryl and alkyl thiols with aryl iodides mediated by copper (I) precatalysts.^{84, 85} The report by Venkataraman represents one of the first methods capable of tolerating alkyl thiols in such cross-coupling reactions. However, butyl and cyclohexylmercaptan were the only substrates reported to be effective in this transformation. Similarly, Buchwald described a method capable of tolerating aliphatic thiols, extending the substrate scope to include benzylmercaptan and 6-mercaptohexanol. These accounts utilize previously established reagent combinations, stemming from the two groups expertise in effecting carbon-nitrogen and carbon-oxygen bond formation.



Scheme 2.3

The subtle differences in the respective procedures illustrate the variance that may be encountered when extending methods developed for separate heteroatom cross-couplings to that of *S*-arylation. For instance, both methods in Scheme 2.3 use the same Cu (I) precatalyst but utilize separate combinations of ligand, base, temperature and solvent. This suggests that both methods rely more on solubilizing the *in-situ* generated Cu (I) catalyst. It is likely that this depends heavily on the aforementioned parameters, and may vary significantly from one procedure to another. The figure below lists several ligands that appear to accelerate copper-catalyzed *S*-arylations. Given the difficulty in mechanistic analysis of copper systems, the exact nature of this acceleration is often unknown. It is often suggested that this effect is a consequence of a reduction in aggregation of the catalytically active copper species in solution.⁸⁶⁻⁹⁹

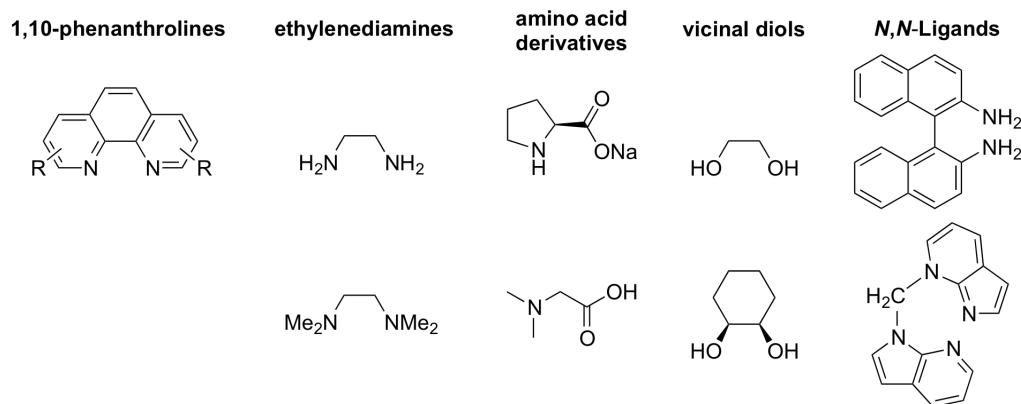
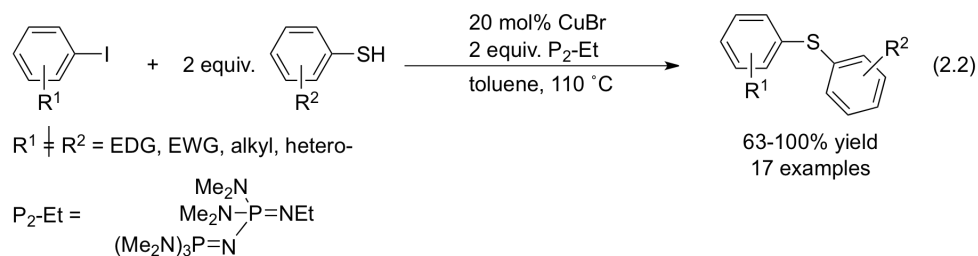


Figure 2.2 Common Ligand Additives in Copper-Catalyzed *S*-Arylations

The methods described by Venkataraman and Buchwald both improved upon an earlier report by Paloma, which described a series of *S*-arylations that utilized Schwesinger's phosphazene bases in order to generate "naked" thiolate ions. Paloma's report was one of the first examples where sterically encumbered arene thiols, such as 2-methylthiophenol and other *ortho*-disubstituted thiophenols, could be used (Eq. 2.2).¹⁰⁰ The disadvantage was that the procedure relied on relatively expensive phosphazene bases. However, the use of these bases did impart a high degree of chemoselectivity in regards to substrates like 4-hydroxythiophenol, where competitive *O*-arylation did not occur. This is likely due to the substantial difference in acidity of the S-H bond relative to the O-H, thus preferentially affording the thiolate ion and yielding *S*-arylation chemoselectively.



The use of copper salts in place of noble metals represents an attractive advantage for arylation strategies for the industrial preparation of biologically active molecules. However, these reactions are mechanistically less well understood in comparison to the analogous palladium systems. Additionally, the lower catalyst loadings observed for palladium-catalyzed aryations may lead to an overall reduction in waste; thereby, reducing costs. The following section will briefly discuss relevant palladium based systems for *S*-arylation.

2.3 Palladium-Catalyzed Carbon-Sulfur Bond Formation

The ease in studying palladium systems spectroscopically has allowed for more detailed mechanistic analyses, relative to copper systems. This is attributable to the well-behaved redox chemistry of various palladium complexes. Indeed, Hartwig has published an extensive survey of palladium (II) thiolate complexes with varying electronics, sterics, bidentate phosphine ligands, and covalently bound carbon-based ligands (aryl, vinyl, alkynyl, and alkyl). The information gained through these investigations led to the development of highly active palladium complexes for *S*-arylation, capable of catalysis at loadings in the

parts-per-million range.^{66, 79, 101-105, 105-108} A brief discussion of initial studies regarding palladium-catalyzed *S*-arylations will follow, in order to better illustrate the amendments made possible through mechanistic studies.

2.3.1 Historical Context for Palladium-Catalyzed *S*-Arylations

The first report of palladium-catalyzed *S*-arylation was made by the group of Migita in Japan in 1978.¹⁰⁹ This method described the use of palladium tetrakis(triphenyl)phosphine (Pd(PPh₃)₄) in catalyst loadings as low as 1 mol% in refluxing alcoholic solvents. The base used in this system was generated by the addition of sodium metal to the alcohol solvent, thus forming the corresponding sodium alkoxide. This method relied heavily on the more reactive aryl iodides and bromides, as reduced yields were observed with aryl chloride substrates. The authors also noted that alkyl thiols were tolerated under these conditions, and in competition experiments reacted approximately nine times faster than arene thiols. This illustrates the greater nucleophilicity of alkyl thiolates.¹¹⁰

2.3.2 Mechanistic Considerations for Palladium-Catalyzed *S*-Arylations

Hartwig's pioneering work in carbon-carbon and carbon-heteroatom bond formation through reductive elimination aided in the discovery of highly effective palladium complexes for *S*-arylation. The key findings of these studies demonstrated that reductive elimination of carbon-sulfur bonds occurred from a four-coordinate palladium (II) intermediate possessing electron rich bidentate phosphines. In most cases, an excess of PPh₃ was added to trap the palladium (0) intermediates generated upon reductive elimination. The concentration of this added phosphine had little effect on the overall rate of reductive elimination but may affect other steps of the catalytic cycle. Additionally, changing the ligand backbone had little effect on the rate of reductive elimination. However, bidentate phosphines possessing large bite-angles dramatically accelerated this process (Figure 2.3). This feature in particular inspired the development of Josiphos and other bidentate phosphines discussed in the subsequent section.

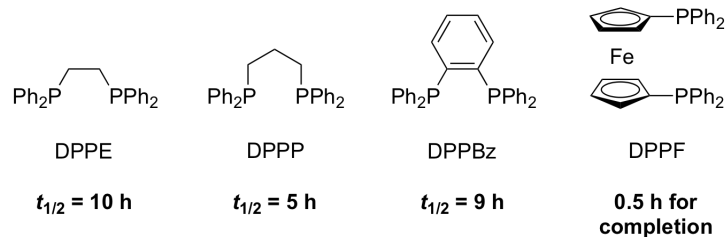


Figure 2.3 Dependence of Ligand Bite-Angle on Rate of Reductive Elimination

2.3.3 Optimization of Palladium-Catalyzed *S*-Arylations

Since the initial examples reported by Migita and Hartwig, later accounts have attempted to reduce the severity of the reaction conditions. This has primarily involved reducing the temperature of the reaction and the quantity of the added base. This is largely necessary due to the competitive reactivity of various functional groups with nucleophilic bases, often limiting the substrate scope with respect to the aryl halides employed. This is inherent with functionalities such as cyano-, carboxymethyl-, and enolizable ketones or aldehydes. These functional groups may undergo base-mediated hydrolysis, transesterification, and competitive enolate condensation processes, respectively. Typically, these moieties remain inert with the use of mild carbonate bases (Cs_2CO_3 , K_2CO_3). Greater yields are often obtained with stronger alkoxide bases (NaOt-Bu , KOt-Bu); however, this often leads to the aforementioned side reactions with more functionalized aryl halides. In some cases, the choice of strongly chelating, sterically encumbered bisphosphine or *N*-heterocyclic carbene (NHC) prolignands may lower the overall temperature of the process. Unfortunately, this is often accompanied by an increase in catalyst loading, in order to achieve similar conversions observed at higher temperatures. The figure below illustrates several popular prolignands for use in palladium-catalyzed *S*-arylations.^{101, 103-106, 109-138}

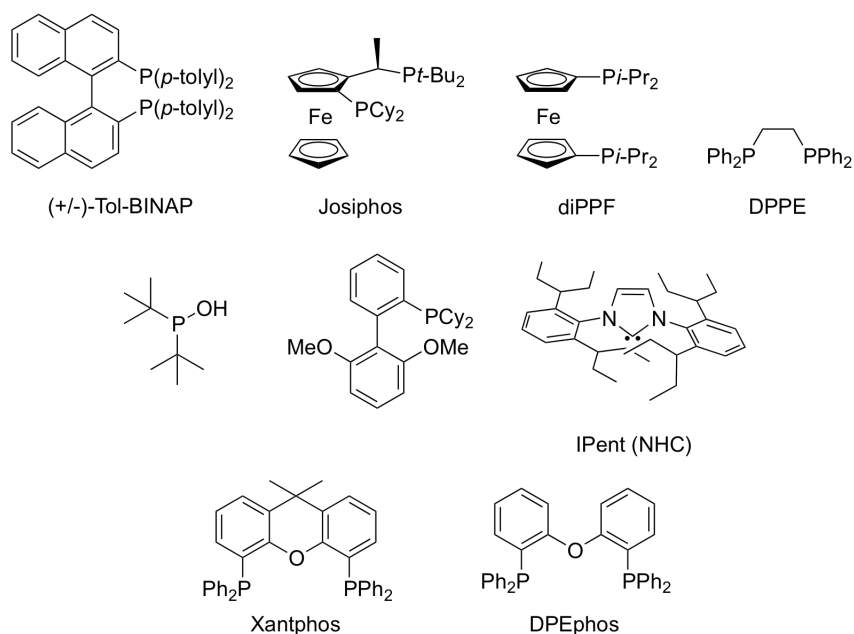


Figure 2.4 Prolignands in Palladium-Catalyzed *S*-Arylations

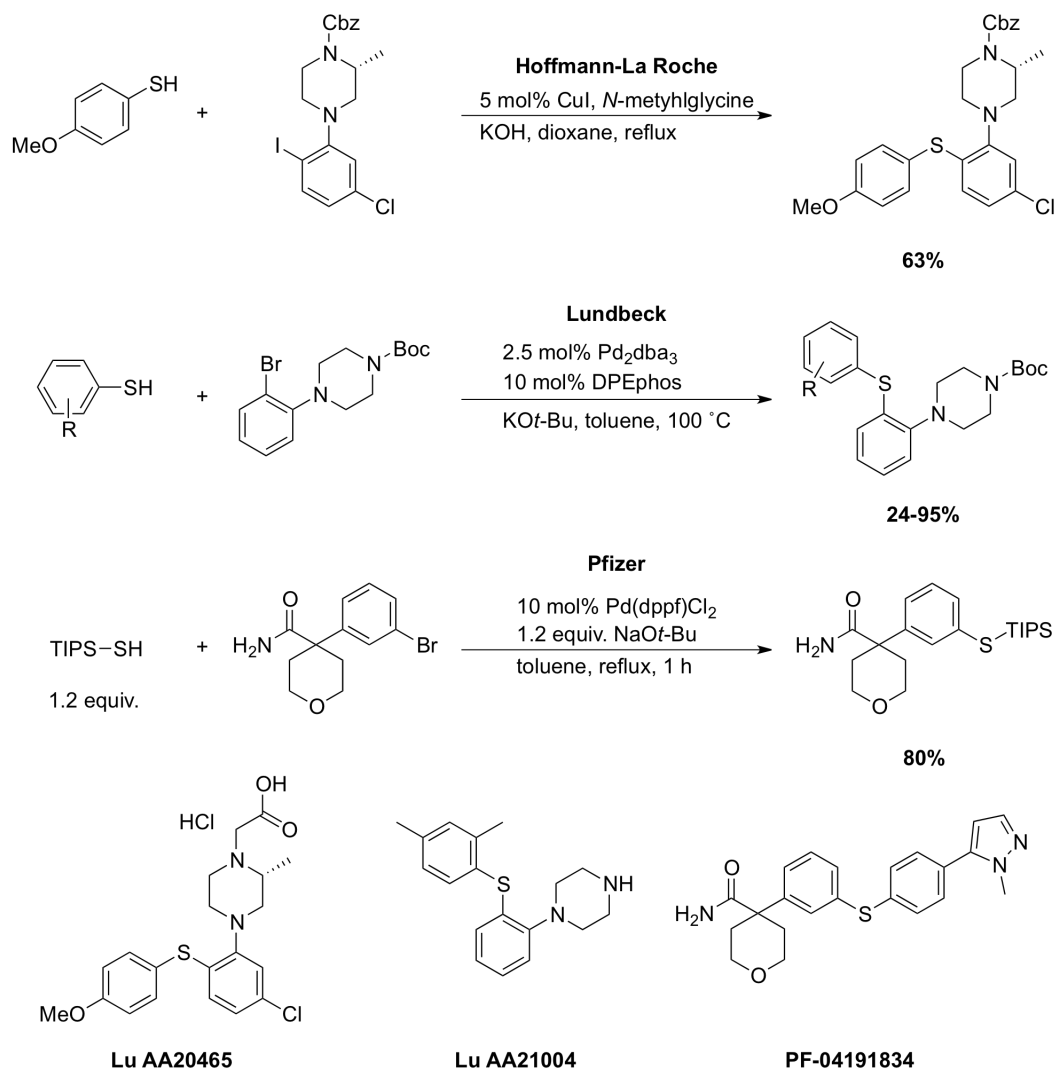
Of the prolignands depicted in Figure 2.4, palladium complexes generated *in-situ* with Josiphos are capable of catalyzing *S*-arylations with precatalyst loadings as low as 0.005%.^{66, 79, 107, 108} This system is quite robust and tolerant of aryl tosylates and chlorides as electrophilic partners with an innumerable amount of aryl and alkyl thiol nucleophiles. This process provides excellent yields of the corresponding thioethers with reaction times often less than 12 hours, which can often be lowered further by increasing the precatalyst loading. The temperature of the process is still high (110 °C) and is inversely proportional to the precatalyst loading, and the nature of the aryl halide employed. Remarkably, ambient temperature is often suitable for aryl iodides, with little impact on reaction time and yield.

Palladium-catalyzed *S*-arylations with the IPent (isopentyl) NHC prolignand (Figure 2.4) also tolerate reduced temperatures at the expense of longer reaction times. However, this process permits several difficult thioetherifications, using sterically hindered aryl and alkyl thiols, as well as sterically shielded aryl bromides and chlorides. Intriguingly, this process requires the addition of sub-stoichiometric quantities of $LiO\text{-}i\text{-Pr}$ in addition to an excess of base ($KO\text{-}t\text{-Bu}$). This additive is presumed to aid in reduction of the palladium (II) species, and often requires pre-mixing at higher temperature to activate the organometallic species to oxidative addition with the aryl halide. The use of $(n\text{-Bu})_2Mg$ and morpholine was also

attempted, but LiOi-Pr was found to be most practical given the sensitivity of dialkylmagnesium compounds, and the possibility of competitive *N*-arylation with 2° nitrogen bases.¹³⁹

2.3.4 Synthesis of Biologically Active Molecules Utilizing *S*-Arylation

The development of methodologies towards *S*-arylation represents a process of critical importance for the discovery of medicinally active molecules. Furthermore, this technique often finds use in process chemistry, in the kilogram synthesis of active pharmaceutical ingredients (APIs). The scheme below illustrates a number of examples, including the Ullmann-type condensation utilized by scientists at Hoffmann-La Roche for the synthesis of Lu AA20465, a molecule of interest for the treatment of schizophrenia.⁸⁹ Similarly, a medicinal chemistry group demonstrated the use of palladium DPEphos complexes in the synthesis of numerous *S*-arylated piperazines with application towards the treatment of mood and affective disorders.¹⁴⁰ Lastly, chemists at Pfizer developed an improved process by which the anti-asthma therapeutic PF-04191834 could be synthesized on multikilogram scale involving two consecutive palladium based couplings with relatively high catalyst loading. This was necessary in order to minimize exposure of the API to the reaction conditions, as extended reaction times proved to yield symmetrical sulfides that complicated the purification of PF-04191834.¹⁴¹

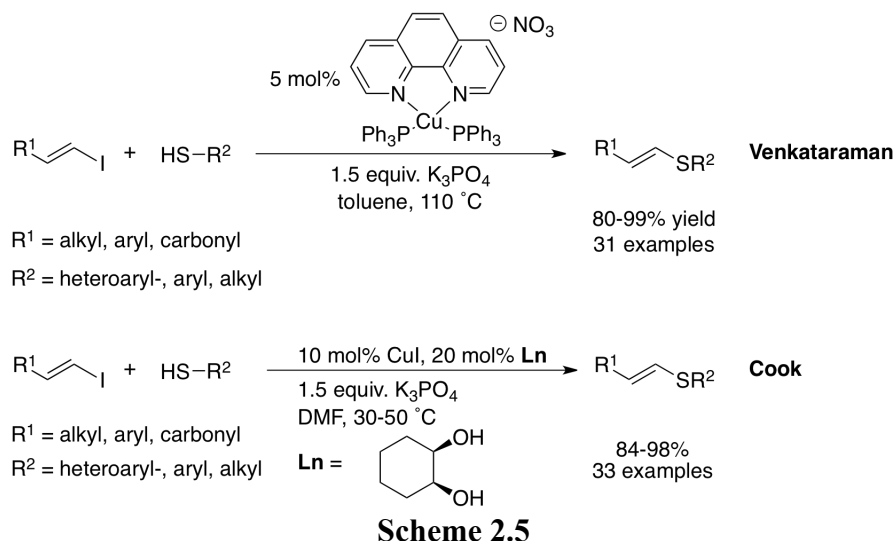


Scheme 2.4

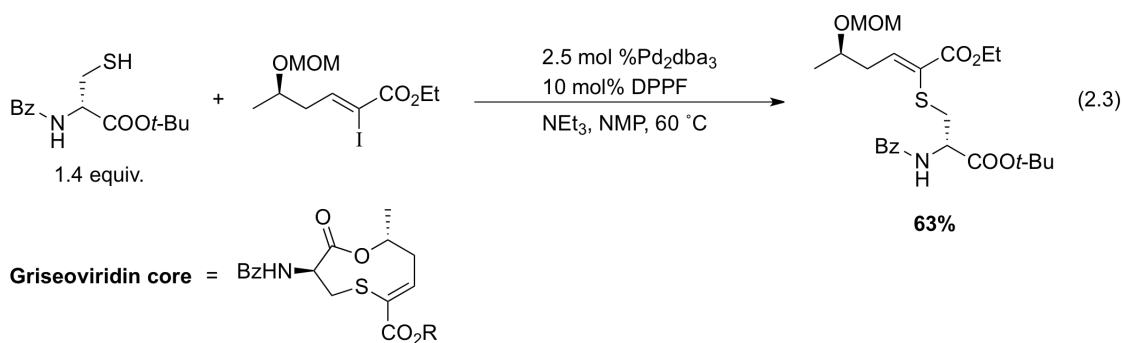
2.3.5 Synthesis of Vinyl Sulfides via Palladium- and Copper-Catalyzed Cross-Coupling Reactions

Similar to the copper and palladium processes for *S*-arylation, the analogous addition of thiolate nucleophiles to vinyl halides represents a strategy for the synthesis of vinyl sulfides. This process is applicable to aryl and alkyl thiols, drawing extensively from the optimized conditions for *S*-arylation. Of these processes, the use of copper (I) catalysts demonstrates much higher functional group compatibility and substrate scope than those of the corresponding palladium systems. This is in direct contrast to the *S*-arylation techniques discussed in the previous sections, where palladium complexes significantly outperform

analogous copper systems. The scheme below summarizes two mild and efficient copper-catalyzed methods for *S*-vinylation of a variety of heteroaryl-, aryl, and alkyl thiolates.^{85,94}



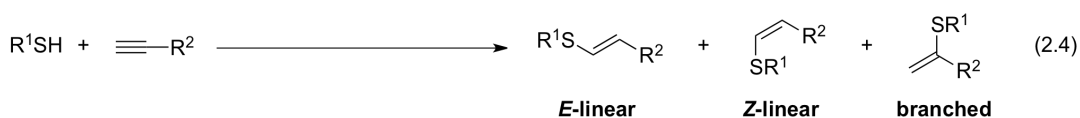
While palladium-catalyzed approaches to *S*-vinylation do exist, the substrate scope reported in the procedures detailed above (Scheme 2.5) is far more extensive.^{69, 111, 113, 115, 117, 127, 129, 135} However, an interesting application of *S*-vinylation towards the synthesis of the nine-membered core of the antibiotic Griseoviridin hinged upon a critical palladium-catalyzed cross-coupling. This example demonstrates the synthetic potential of *S*-vinylation towards the synthesis of complex natural products, and the functionalities tolerated in such an endeavour (Eq. 2.3).⁶⁸



The cross-coupling approach to vinyl sulfides suffers in part due to the availability of the requisite vinyl iodides. This is typically plagued by the use of non-atom economical processes involving chromium or phosphorus ylides, which generate potentially hazardous waste. This necessitates a separate approach to the atom economical formation of these synthetically versatile vinyl sulfides, which is discussed in the following section.

2.4 Alkyne Hydrothiolation in the Synthesis of Vinyl Sulfides

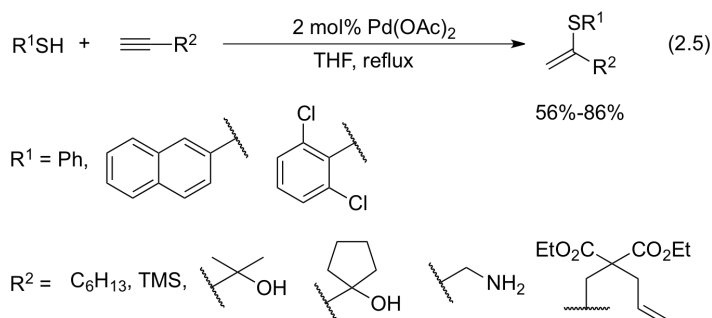
Alkyne hydrothiolation is formally represented by the insertion of a sulfur-hydrogen bond across the alkyne π -system, generating a new carbon-sulfur and carbon-hydrogen bond. This addition can result in the production of several distinct regioisomers, where the ratio of these compounds depends heavily on the nature of the sulfur reagent and the catalyst employed. Prior to our involvement in catalytic alkyne hydrothiolation with group 9 transition metals, aliphatic thiols were found to be unreactive. The formation of the *E*-linear isomer is typically favoured with arene thiols and complexes of rhodium and iridium, and the use of supramolecular catalysts such as β -cyclodextrin.¹⁴²⁻¹⁴⁷ The *Z*-linear isomer is often the result of uncatalyzed background processes, such as the nucleophilic addition of thiyl radicals or thiolate ions to the alkyne π -system.¹⁴⁷⁻¹⁶⁰ Lastly, the branched regioisomer is typically favoured with the use of group 10 transition metal complexes. The *E*- and *Z*-linear olefins, are collectively referred to as the anti-Markovnikov products, whereas the branched isomer is referred to as the Markovnikov adduct. The following sections will describe approaches towards the synthesis of vinyl sulfides involving the use of transition metals, highlighting in particular the influence of the metal complex on selectivity and the functional group tolerance of existing methods. This chapter concludes with our approach towards alkyne hydrothiolation, including the successes and failures of this process.



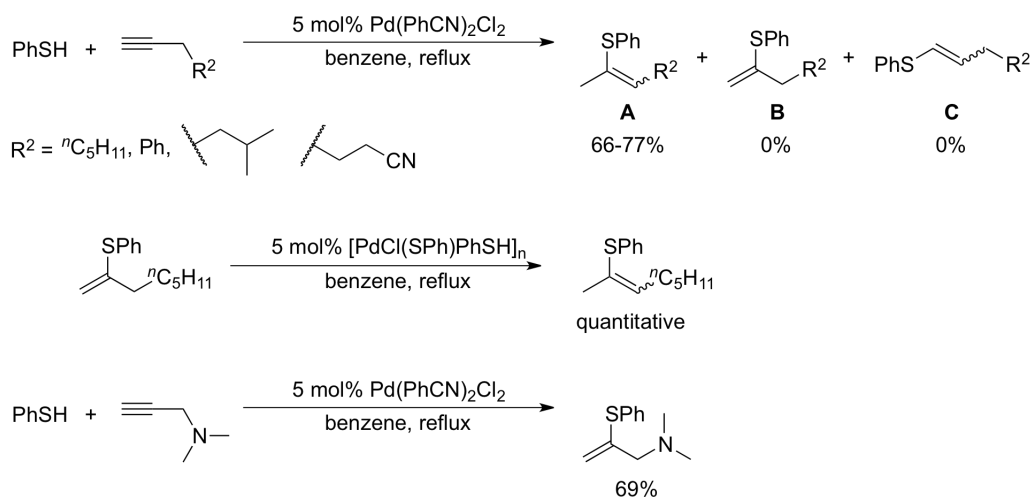
2.4.1 Alkyne Hydrothiolation with Group 10 Transition Metals

Since the first reported example of group 10 catalyzed alkyne hydrothiolation in 1992 by Ogawa and coworkers, several studies involving the use of group 10 metals complexes have appeared in the literature. The consistent trend for the use of these metal salts is the selectivity for the branched regioisomer, and the tolerance of a range of aliphatic and aryl alkynes. The thiol scope was limited to three examples, where an evaluation of functional group tolerance, or the reactivity of aliphatic thiols was notably absent (Eq. 2.5). The authors reported that *p*-substitution had a drastic effect on the selectivity of the process, where *p*-hydroxy- and *p*-chlorothiophenol yielded products similar to the addition of disulfides to

alkynes. This may occur via the formation of a dimeric palladium thiolate complex, where insertion of the alkyne into a Pd-S bond may be followed by subsequent C-S reductive elimination. Typically, turnover is accomplished by protonolysis of the vinyl sulfide with remaining thiol, or acetic acid generated through ligand substitution. Additionally, the use of *p*-methylthiophenol and *p*-methoxythiophenol proved unreactive in the optimized conditions, yielding small amounts of products and unreacted starting material.¹⁶¹



As the palladium (II) acetate catalyzed hydrothiolation of alkynes selectively yielded the branched regioisomer, later reports were targeted towards the synthesis of the linear isomers. Interestingly, the use of Pd(PhCN)₂Cl₂ in alkyne hydrothiolation with terminal alkynes generated trisubstituted vinyl sulfides (**A**), presumably by isomerization of the branched regioisomer (**B**). This hypothesis was supported by the formation of isomerized products when an authentic sample of the branched vinyl sulfide was added to a solution of [Pd(SPh)(PhSH)]_n. This complex was synthesized by treatment of Pd(PhCN)₂Cl₂ with two equivalents of thiophenol, and is believed to be the active catalyst in this reaction. This process is advantageous as the use of internal alkynes is avoided in synthesizing the corresponding trisubstituted vinyl sulfides (**A**). Typically, internal alkynes represent challenging substrates in catalytic hydrothiolation, often requiring more forcing conditions. Surprisingly, the use of *N,N*-dimethylpropargylamine resulted in the selective formation of the branched regioisomer (**B**), with little to no observed double bond isomerization. This suggests that the *in-situ* generated catalyst may be inhibited by the presence of a basic amine, and undergoes isomerization much slower than the other alkynes examined. This report represents an efficient method for the synthesis of internal vinyl sulfides (**A**); however, in all cases, the isomerized product forms as an equimolar ratio of *E* and *Z* isomers (Scheme 2.6).¹⁴⁵



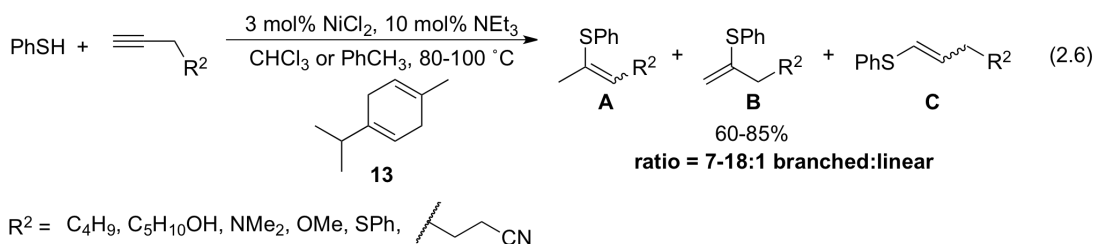
Scheme 2.6

Despite the rather limited scope in regard to the thiol substrates employed in these reports, further studies by this group simply expanded this method towards the use of carbonylative conditions.¹⁶² However, this study did successfully employ both *p*-methylthiophenol and *p*-fluorothiophenol in addition to benzene thiol, suggesting the carbonylative sequence is less sensitive to *p*-substitution than the regular alkyne hydrothiolation process.¹⁶¹ The thioformylation was also tolerant of dodecane thiol, although this gave the poorest yield.

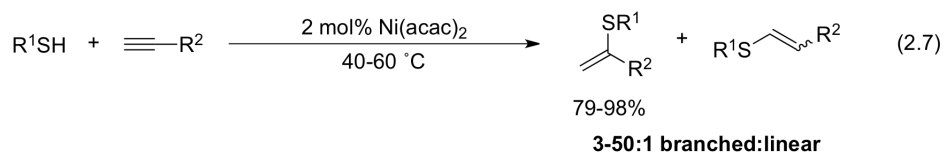
Similar to the work of Ogawa, related methods for alkyne hydrothiolation using various nickel precatalysts generally provide selective formation of the Markovnikov or branched vinyl sulfide, but are again limited in scope with respect to the thiols employed. Initial work demonstrated the competence of $\text{Ni(PPh}_2\text{Me)}_4$ in conjunction with catalytic amounts of $\text{Ph}_2\text{P(O)OH}$, catalyzing the addition of thiophenol to 1-octyne in high yield and selectivity. This result was largely driven by the investigation of related nickel precatalysts for the catalytic synthesis of alkenylphosphonates, through a related addition of the P-H bond across the π -system of various alkynes.¹⁶³

Subsequent to this report, NiCl_2 was found to be an efficient precatalyst for the addition of thiophenol to a variety of terminal and internal alkynes.¹⁶⁴ Critical to the success of this method was the addition of a catalytic amount of NEt_3 , which proved to greatly enhance the selectivity of the Markovnikov adduct (**B**) relative to the isomerized vinyl sulfide (**A**). This observation is consistent with the selectivity obtained in the hydrothiolation

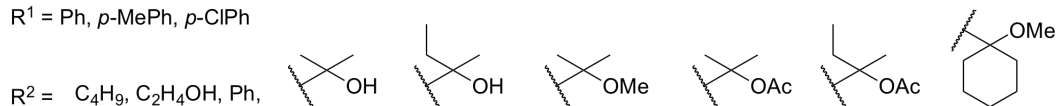
of *N,N*-dimethylpropargylamine with Pd(PhCN)₂Cl₂, where no isomerization was observed following formation of the branched vinyl sulfide (Scheme 2.6). This is likely due to the inhibition of a metal-catalyzed isomerization process by ligation of the active catalyst with the propargyl nitrogen, or by NEt₃. Similarly, the effect of phosphine ligands was shown to dramatically alter the selectivity of the process. In particular, phosphite ligands (P(OPh)₃) provided the linear olefins (**C**) almost exclusively. In the absence of the radical inhibitor γ -terpinene (**13**) the Markovnikov selectivity drops dramatically, as the vigorous conditions allow for the facile generation of thiyl radicals (Eq. 2.6).



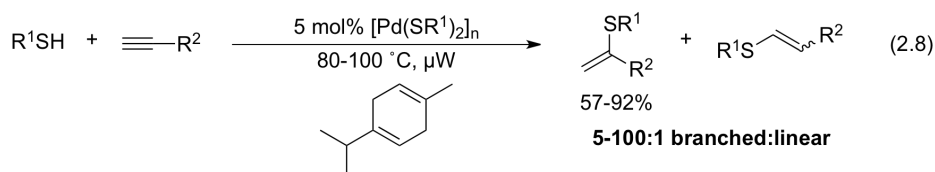
A consistent observation in the studies discussed thus far is the formation of an insoluble brown precipitate, indicating the formation of a polymeric species likely consistent of bridging thiolate ligands [Ni(SAr)₂]_n or [Pd(SAr)₂]_n. Evidence for the formation of this type of polymer has only been roughly deduced through elemental analysis, where structural data has been precluded due to issues in solubility. However, the polymeric network of various nickel and palladium complexes has been imaged using techniques such as scanning electron microscopy, revealing a range of particle sizes varying from 0.5-8.5 μm . The utilization of these polymeric species in alkyne hydrothiolation has led to the development of a highly practical nickel based system, where the heterogeneous catalyst is generated by treatment of Ni(acac)₂ with an aryl thiol. This system is tolerant of a range of propargyl substituted alkynes, can be run under solvent free conditions with temperatures slightly above ambient, and is scalable to produce up to 50 grams of branched vinyl sulfide. Reaction times are considerably shorter for the solvent free system, where alkyne is typically consumed within 15 minutes to 3.5 hours. Similar to previous reports the aryl thiol scope was limited to three examples (Eq. 2.7).



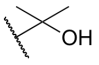
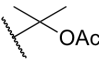
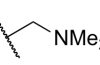
R¹ = Ph, *p*-MePh, *p*-ClPh



Likewise, alkyl thiols such as cyclohexylmercaptan and benzylmercaptan were tolerated in alkyne hydrothiolation with heterogeneous palladium-catalysts. The heterogeneous catalyst was synthesized by treating Pd(OAc)₂ with the alkyl thiol, and was active in alkyne hydrothiolation for a similar array of propargyl substituted alkyne (Eq 2.8).^{165, 166}



R¹ = Cy, Bn

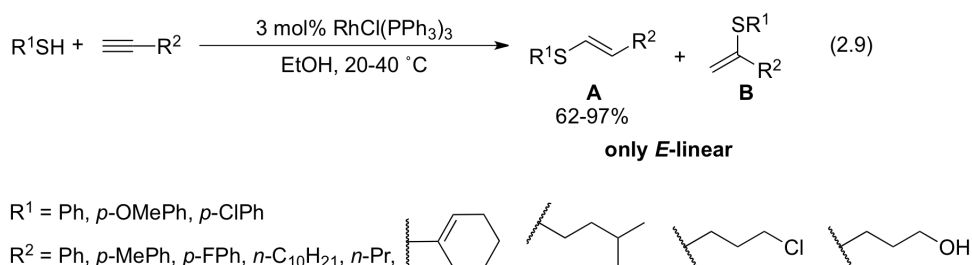
R² = C₄H₉, Ph, , , 

These studies represent important advances in the practical synthesis of branched vinyl sulfides; additionally, the limitations in regards to thiol scope demonstrate the need for more thorough investigations of the tolerance of these systems towards aryl and aliphatic thiols. The following section describes applications of group 9 metals towards this goal, including our report of the first general synthesis of alkyl vinyl sulfides, which is also the first successful use of alkyl thiols in alkyne hydrothiolation.

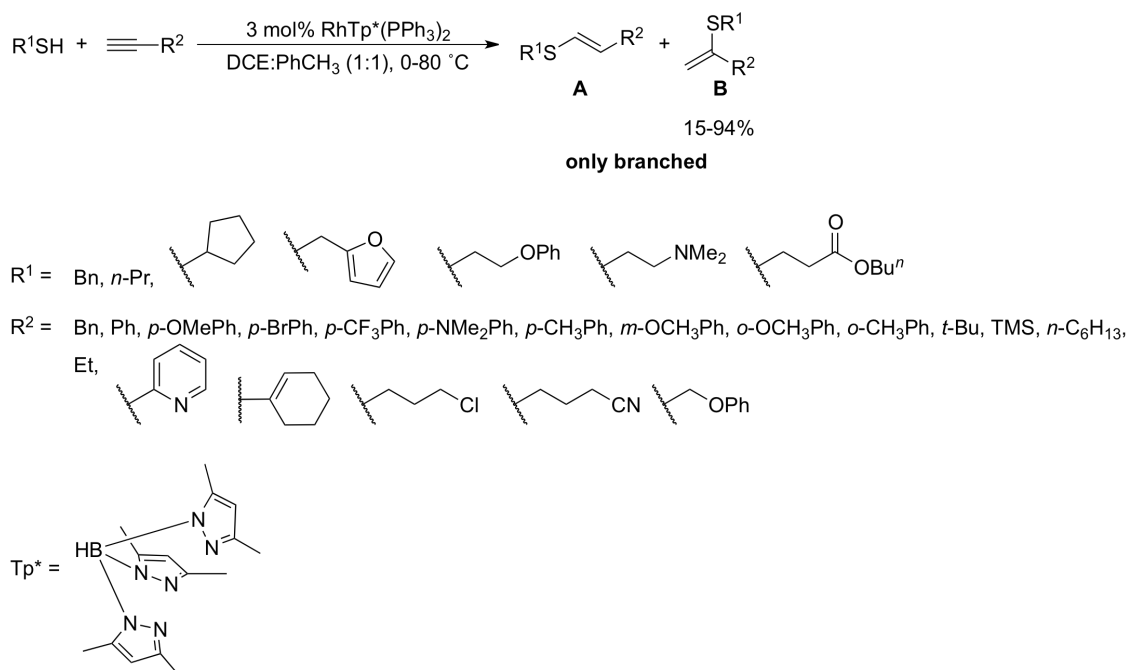
2.4.2 Alkyne Hydrothiolation with Group 9 Transition Metals

Compared to the volume of work encompassing the use of group 10 metals in alkyne hydrothiolation¹⁶³⁻²¹⁰, the use of cobalt, rhodium, and iridium is relatively scarce in comparison.^{142-146, 162, 211-215} One of the first examples of a group 9 metal-catalyzed process for the synthesis of organosulfur compounds was reported by Ogawa's group and involved the thioformylation of alkynes using RhHCO(PPh₃)₃.¹⁶² This seminal report was later followed by the publication of RhCl(PPh₃)₃ as an effective catalyst in the hydrothiolation of terminal

and internal alkynes.¹⁴⁵ This study was one of the first to demonstrate the complementary selectivity of group 9 metals relative to group 10, as the *E*-linear vinyl sulfide was the favoured regioisomer with RhCl(PPh₃)₃. Formation of this product is sometimes attributed to a non-catalytic background reaction involving thiyl radical addition to alkynes. However, when the catalytic reaction was conducted in the presence of a radical inhibitor, the formation of the *E*-linear vinyl sulfide was still evident, suggesting that this is not a consequence of a radical background reaction. Additionally, the lack of reactivity evident in the absence of RhCl(PPh₃)₃ supports the necessity of the transition metal in catalyzing the reaction. Interestingly, the use of more basic and bulkier phosphine additives such as P(*n*-Bu)₃ and P(*o*-tol)₃ helped increase the overall yield of the process. However, this markedly reduced the selectivity for the *E*-linear isomer (**A**), forming the branched vinyl sulfide (**B**) in appreciable quantities. The use of aromatic solvents provided mixtures of the *E*-linear (**A**) and branched (**B**) vinyl sulfides, only slightly favouring **A**. This selectivity was increased with the use of PhCF₃ as solvent, which is similar in polarity to common halogenated solvents. To this end, the selectivity for the *E*-linear isomer (**A**) appeared unaffected with the use of dichloromethane and 1,2-Dichloroethane, providing similar quantities of the branched vinyl sulfide (**B**). The use of acetonitrile and *N,N*-dimethylformamide drastically reduced the overall yield of the reaction, and appeared to facilitate the decomposition of the branched regioisomer (**B**). The optimized solvent for alkyne hydrothiolation with Wilkinson's catalyst proved to be ethanol, providing the *E*-linear isomer (**A**) exclusively at room temperature. At higher temperatures (40 °C), the selectivity appeared unaffected. Similar to the scope reported for palladium- and nickel-catalyzed hydrothiolation processes, only three thiols were examined during the course of this investigation, where aliphatic thiols proved inert to the optimized conditions (Eq. 2.9). For simplicity the alkyne substrate in Eq. 2.9 is drawn as terminal; however, internal alkynes are also tolerated.



Following this report, our group demonstrated the first example of a transition metal catalyzed alkyne hydrothiolation capable of tolerating alkyl thiols. This utilized a highly reactive rhodium (I) bisphosphine complex involving the popular scorpionate ligand, hydrotris(3,5-dimethylpyrazolyl)borate or Tp*. Given the precedent for the use of similar complexes in alkane C-H bond activation, we believed that similar reactions would occur with less reactive aliphatic thiols.²¹⁶ Interestingly, this rhodium (I) complex gave selectivity opposite to that of RhCl(PPh₃)₃, yielding the branched regioisomer (**B**) exclusively for a variety of alkyl thiols and alkynes. This is in agreement with the observation made by Ogawa, where bulkier ligands gave rise to an increase in the formation of the branched vinyl sulfide (**B**); however, the exact mechanistic nature behind this switch in regioselectivity is unknown. Notably, this work represented the first time that aliphatic thiols could be used in catalytic alkyne hydrothiolation – an important point if this strategy were to be applicable to a number of the drug candidates discussed in Chapter 1. The substrate scope of this process was later expanded to encompass a large number of alkynes with good functional group tolerance (Scheme 2.7).^{144, 215} For simplicity, the alkyne in Scheme 2.7 is drawn as terminal; however, internal alkynes are also possible.



Scheme 2.7

A later report from our group evaluated the effect of pyrazolyl substitution and ligand denticity on the selectivity of rhodium (I) pyrazolylborate complexes in alkyne hydrothiolation (Figure 2.5). This study revealed that a fine balance existed between the aforementioned parameters. In general, the greatest selectivity and yields were accomplished with bulky tridentate ligands such as Tp^* , Tp^{Ph} , and $\text{Tp}^{\text{Ph,Me}}$. This may be attributed to the stabilization of the intermediate following oxidation addition to the S-H bond of the thiol. Alternatively, bulky ligands may prevent the formation of potentially inactive dimeric or oligomeric thiolate complexes (Figure 2.5). In addition, Bp^* demonstrated greater efficiency and selectivity over the unsubstituted trispyrazolylborate proligand (Tp).²¹³

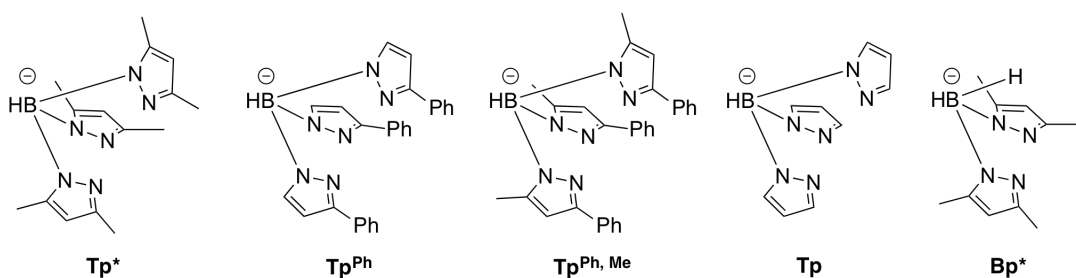


Figure 2.5 Pyrazolylborate Ligands Tested in Alkyne Hydrothiolation with Alkyl Thiols

Messerle and coworkers published a series of rhodium and iridium carbonyl complexes involving bidentate N,N and N,P -ligands, and tested their efficiency in catalytic alkyne hydrothiolation.^{142, 143} In general, cationic iridium complexes containing the pyrazole-phosphine ligand (PyP) demonstrated greater catalytic activity relative to the analogous imidazole-phosphine ligand (ImP). The hydrothiolation of phenylacetylene with thiophenol in the presence of a cationic iridium PyP complex provided a mixture of linear isomers favouring the E -linear (9:1 $E:Z$). This gave excellent yields of the E -linear vinyl sulfide with catalyst loadings as low as 1 mol%. Unfortunately, this result was not extendable to other alkyne substrates, where lower selectivity for the linear isomers was observed. Additionally, markedly increased reaction times and temperatures were necessary for similar conversions to those obtained for phenylacetylene. Lastly, the analogous rhodium complexes generally provided lower selectivity and longer reaction times relative to the iridium complexes studied.

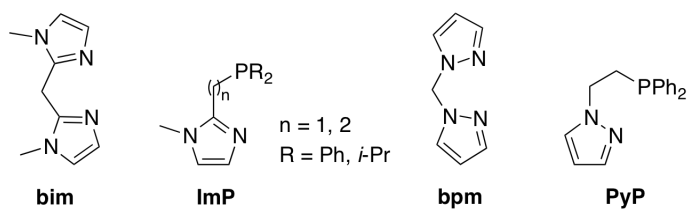
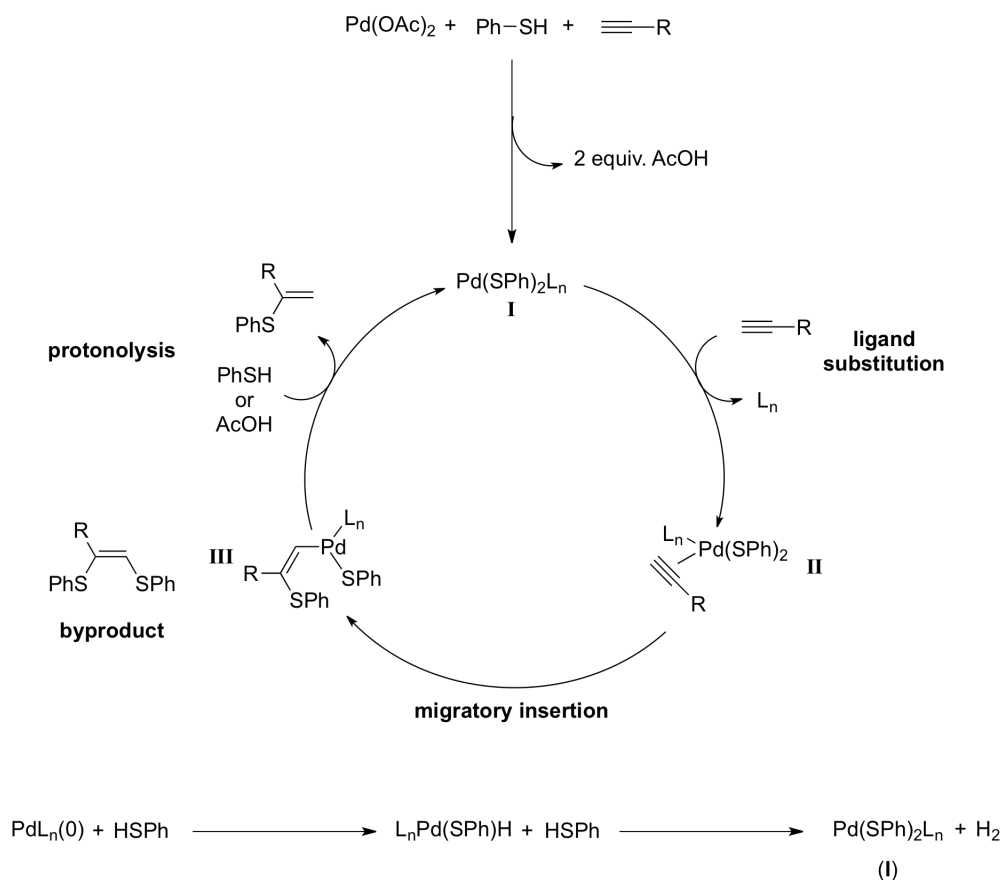


Figure 2.6 *N,N* and *P,N*-Ligands in Alkyne Hydrothiolation with Group 9 Metals

2.4.3 Mechanistic Comparison of Group 9 and 10 Metals in Alkyne Hydrothiolation

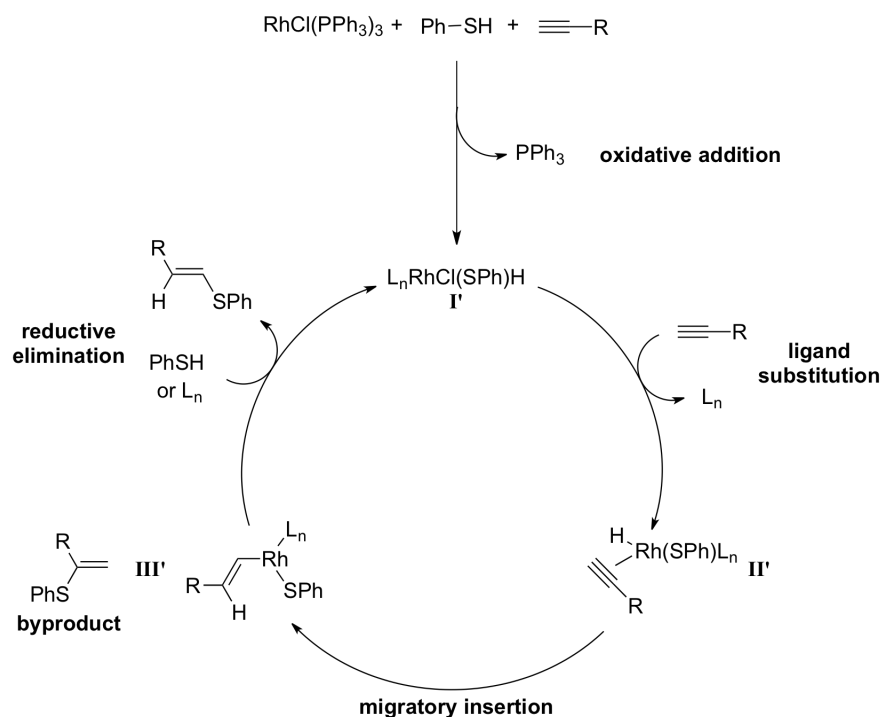
The contradictory regioselectivity afforded by Wilkinson's catalyst and group 10 transition metals warrants a brief discussion of the proposed mechanisms regarding their use in alkyne hydrothiolation. The current hypothesis regarding the mechanism of alkyne hydrothiolation with palladium and nickel precatalysts involve processes that differ from traditional redox cycles.^{75, 145, 161, 163, 165, 166, 168, 184, 185, 197, 207, 209} This typically involves the generation of an active palladium or nickel (II) thiolate complex based upon substitution of the initial ligands present. This may result in the precipitation of oligomeric complexes, which have been shown to serve as heterogenous catalysts in solvent-free alkyne hydrothiolation.^{165, 166} The next step involves coordination of the alkyne, followed by migratory insertion into the metal-sulfur bond (**II** to **III**). This particular process has been shown to occur stoichiometrically with palladium (II) thiolates and dimethylacetylenedicarboxylate (DMAD). Solid-state structural data obtained in this investigation indicated a new complex involving cis-insertion of the alkyne into the metal-sulfur bond.¹⁸⁴ This process was then followed by a simple protonolysis; thereby, regenerating the active thiolate complex, and releasing the corresponding branched vinyl sulfide. A typical byproduct of this reaction involves the reductive elimination of a carbon-sulfur bond from complex **III**. This generates a *Z*-linear trisubstituted olefin containing two thiophenol molecules (Scheme 2.8). This forms a palladium or nickel (0) species that re-enters the catalytic cycle upon oxidative addition with the free thiol. This metal thiolate species can react with free thiol, producing molecular hydrogen and the catalytically active dithiolate complex (**I**).¹⁶⁴



Scheme 2.8

Conversely, the use of group 9 metals in alkyne hydrothiolation is believed to involve a more traditional rhodium (I) to rhodium (III) redox cycle consisting of oxidative addition, migratory insertion, and reductive elimination.^{145, 211, 212} Ogawa and coworkers conducted stoichiometric reactions involving the addition of thiophenol to $\text{RhCl}(\text{PPh}_3)_3$, leading to the formation of a complex consistent with **I'**. This was supported by NMR spectroscopic evidence indicating the formation of a rhodium-hydride. This is believed to initiate the catalytic cycle and is subsequently followed by the coordination of alkyne to form complex **II'**. The bound alkyne can then insert into a Rh-H bond to generate complex **III'**, which upon reductive elimination yields the *E*-linear vinyl sulfide.¹⁴⁵ To this end, Ogawa provided preliminary evidence for preferential insertion of the alkyne into the Rh-H bond, as the hydridic resonance associated with complex **II'** disappeared over time, following the addition of alkyne to complex **I'**. This was indicated by the formation of vinylic resonances, suggesting the formation of a species consistent with complex **III'**. The formation of the *E*-

linear vinyl sulfide was then accompanied by the addition of a second equivalent of thiophenol, which presumably occurred by C-S reductive elimination.¹⁴⁵ We believe a mechanism similar to that in Scheme 2.9 is operable for catalytic alkyne hydrothiolation with $\text{RhTp}^*(\text{PPh}_3)_2$. However, consistent with selectivities observed for group 10 metals, complex **II'** may undergo preferential insertion into the Rh-S bond followed by C-H reductive elimination (Scheme 2.9). This would effectively generate the branched regioisomer, rather than the expected *E*-linear vinyl sulfide.¹⁴⁴ Detailed studies with $\text{RhTp}^*(\text{PPh}_3)_2$ are underway.

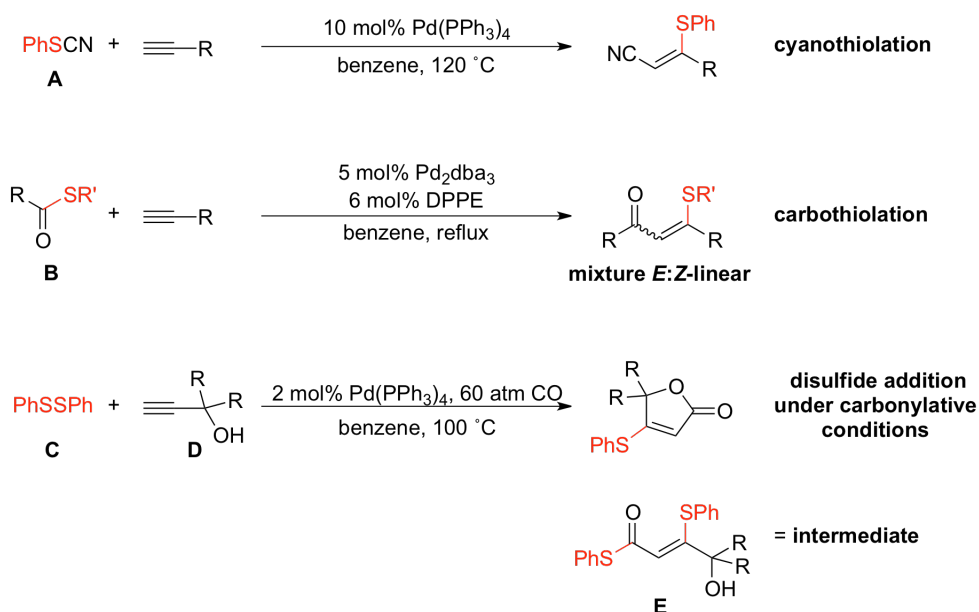


Scheme 2.9

2.4.4 Sulfur-Element Bond Activation and Applications to Alkyne Addition Reactions

As discussed in the preceding sections, alkyne hydrothiolation represents the formal addition of a sulfur-hydrogen bond across an alkyne π -system. Given the mechanistic details outlined above, several groups have attempted to extend alkyne hydrothiolation to include various weak sulfur-element bonds, where oxidative addition and migratory insertion provides more functionalized olefin products. These methods include cyanothiolation (**A**), carbothiolation (**B**), carbonylative hydrothiolation, and the activation and insertion of disulfides to alkynes (**C**). These methods typically require the use of Pd(0) complexes, as the

initiation of the catalytic cycle requires oxidative addition into the sulfur-element bond. To this end, the use of arylthiocyanates (**A**) provided excellent yield and regioselectivity when reacted with a variety of alkynes. The use of more easily accessible alkylthiocyanates proved ineffective under these optimized conditions.^{189, 192, 195} Similarly, the use of thioesters (**B**) in catalytic alkyne addition reactions provides products analogous to those obtained under carbonylative conditions. This helps avoid the use of relatively high pressures of carbon monoxide (Scheme 2.10).^{162, 177, 179, 190, 198, 199, 199, 200, 202-204, 211, 217} Interestingly, it was observed that the formation of unsaturated lactones occurred when diphenyl disulfide (**C**) was reacted with propargyl alcohols (**D**) in the presence of palladium tetrakis(triphenylphosphine) and carbon monoxide. The success of this reaction is dependent upon the isomerization of the intermediate vinylogous dithiocarbonate (**E**), which was shown to be dependent on the presence of Pd(PPh₃)₄. The exact nature of this isomerization process is unknown, but speculated to involve the formation of a reactive ketene species. This is then followed by intramolecular coordination of the propargyl oxygen and C-O reductive elimination to form the corresponding lactone (Scheme 2.10).¹⁷⁷



Scheme 2.10

2.5 Summary: Transition Metal Approaches to Carbon-Sulfur Bond Formation

As discussed in chapter 1, sulfur finds a place in myriad privileged structures that convey biological activity with promise as chemotherapeutics for a variety of ailments. As a consequence, the development of methods capable of reliably and efficiently synthesizing carbon-sulfur bonds is increasing in demand. Two such processes that allow for the catalytic formation of C-S bonds include transition metal cross-coupling reactions, and the hydrothiolation of alkynes as discussed in the preceding sections. Of these reactions, cross-couplings are particularly reliable for the synthesis of various aryl and heteroaryl sulfides. Therefore, cross-couplings are prominent in medicinal chemistry for the identification and synthesis of lead molecules. This method has also been exploited in process chemistry routes towards the multikilogram synthesis of active pharmaceutical ingredients.¹⁴¹

Conversely, the transition metal catalyzed synthesis of vinyl sulfides and their corresponding oxidized derivatives (sulfoxide and sulfone) remains relatively unexplored. These functionalities are beginning to demonstrate considerable applicability in the development of peptidomimetic-based chemotherapies. This class of molecules is finding considerable use for the development of effective treatments for neglected diseases such as malaria, Chagas disease, and African sleeping sickness (Section 1.2). Additionally, vinyl sulfides and their oxidized derivatives are excellent substrates for several processes including the additive Pummerer rearrangement, Povarov-type cycloadditions [3+2], and [4+2]-cycloadditions, the Pauson-Khand reaction, and numerous other synthetic transformations.²¹⁸⁻
²²² These synthetically useful reactions serve to readily introduce molecular complexity and find continual application within natural product synthesis.

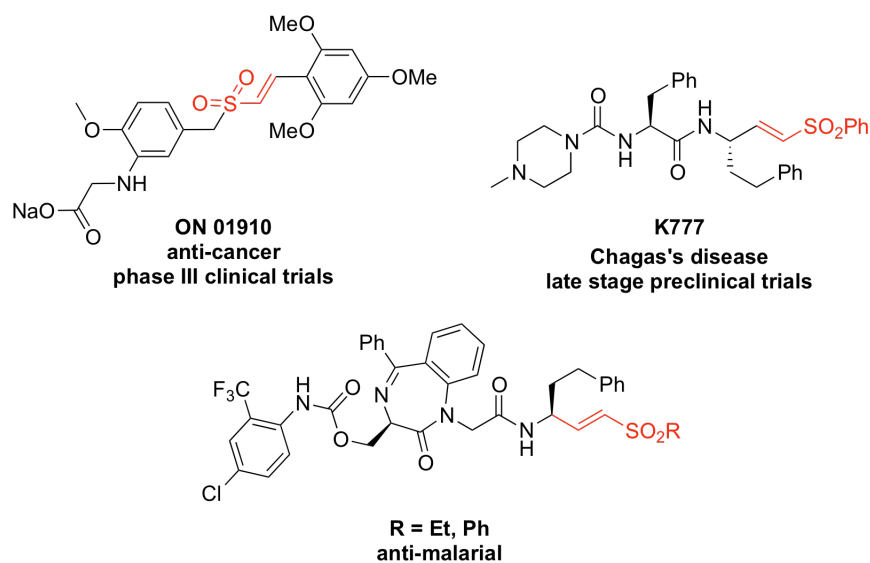


Figure 2.7 Biologically Active *E*-Vinyl Sulfones

Despite the widespread utility of vinyl sulfides in medicinal and natural product chemistry, the synthesis of these intermediates is relatively limited. Cross-coupling approaches to these molecules rely on the stereoselective synthesis of requisite vinyl iodides, which often results in the production of toxic chromium waste products. To this end, alkyne hydrothiolation represents an attractive method for the formation of vinyl sulfides. Literature reports typically evaluate substrate scope in relation to alkynes, often ignoring the scope relative to thiols. Likewise, procedures for the hydrothiolation of alkynes that display tolerance of less reactive alkyl thiols are scarce in the literature. This is not unwarranted, as ample precedent exists for the incompatibility of alkyl thiols in procedures optimized for the use of aryl thiols in alkyne hydrothiolation.^{145, 162, 189, 198, 211} These reports often unintentionally perpetuate the stereotype that alkyl thiols are inert in catalytic alkyne hydrothiolation, thus preventing the pursuit and development of general methods towards this transformation. The next chapter will involve a discussion of our progress towards the development of a general method for alkyne hydrothiolation tolerant of alkyl thiols, and the extension of this method towards the synthesis of molecules of medicinal interest.²²³ Furthermore, an evaluation of the functional group tolerance of various aryl thiols in our alkyne hydrothiolation with Wilkinson's catalyst will be presented, given the literature focus on alkyne scope. This study revealed an interesting dependence on propargyl substituents in dictating the regioselectivity of alkyne hydrothiolation with aryl and alkyl thiols. This has particular application in the

synthesis of cysteine protease inhibitors, such as K777, and efforts towards this synthesis will be discussed as well.

Chapter 3 Towards a General Method for the Hydrothiolation of Alkynes with Alkyl Thiols

During our investigation of $\text{RhTp}^*(\text{PPh}_3)_2$ as a catalyst for alkyne hydrothiolation with aliphatic thiols, we became interested in reevaluating whether similar reactivity could be observed for Wilkinson's catalyst. Prior to this, Ogawa reported that alkyl thiols were incompatible in alkyne hydrothiolation with Wilkinson's catalyst. However, details concerning the exact reaction conditions were not specified, leading us to assume that the optimized conditions developed for aryl thiols were simply extended to aliphatic thiols. The successful use of $\text{RhCl}(\text{PPh}_3)_3$ in alkyne hydrothiolation is advantageous, given the commercial availability of this complex. Additionally, if Wilkinson's catalyst affords the *E*-linear vinyl sulfide with aliphatic thiols, this would prove complementary to the branched regioselectivity observed for $\text{RhTp}^*(\text{PPh}_3)_2$. As the *Z*-linear isomer is often associated with radical and nucleophilic addition of thiols to alkynes, regioselective access to all regioisomers via alkyne hydrothiolation would become possible, just by varying the reaction conditions. This is advantageous in extending these methods towards the synthesis of bioactive molecules, as well as regioisomeric analogues, which would contribute to structure-activity-relationship studies.

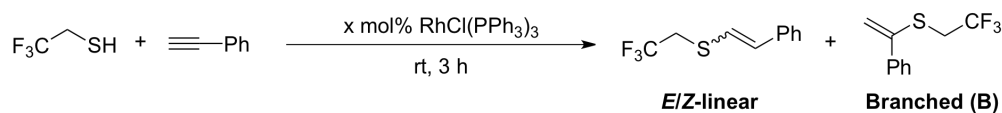
In order to assess whether Wilkinson's catalyst could effectively catalyze alkyne hydrothiolation with aliphatic thiols, we chose to evaluate two separate model systems. In one system, we elected to test 2,2,2-trifluoroethanethiol as a substrate given the similarity to thiophenol (the prototypical substrate in alkyne hydrothiolation) in terms of S-H bond acidity. Furthermore, in order to determine whether the conditions analyzed for 2,2,2-trifluoroethanethiol were extendable to other aliphatic thiols, we also chose to investigate cyclopentylthiol. This would assess whether the greater nucleophilicity of cyclopentylthiol imparted any observable changes in catalytic activity or regioselectivity. The choice of phenylacetylene as the alkyne partner allows for relative ease in assessing the regioselectivity of the process, as this substrate will not undergo any subsequent double bond isomerization. In the majority of cases, the regioisomers are easily distinguished by ^1H NMR spectroscopy, based upon analysis of the corresponding coupling constants. The 3J value characteristic of an *E*-linear vinyl sulfide is typically greater than 15 Hz whereas that of the *Z*-linear isomer is

approximately 10-11 Hz. Conversely, the branched regioisomer possesses a small 1J coupling constant of 1-2 Hz, which is often undetectable in the ^1H NMR spectrum.

3.1 Establishing Precedent: Solvent and Reactivity Studies

Initial studies towards the development of an alkyne hydrothiolation methodology with Wilkinson's catalyst commenced with the evaluation of two aliphatic thiol substrates. This work was done in conjunction with Dr. Shiva Shoai, who investigated the reactivity of 2,2,2-trifluoroethanethiol with phenylacetylene.²²⁴ Similarly, I explored the reactivity of cyclopentylthiol, a more nucleophilic aliphatic thiol, under analogous conditions. These efforts were targeted towards assessing the selectivity and efficiency of these thiol substrates in alkyne hydrothiolation with Wilkinson's catalyst, with the goal of optimizing the reaction conditions.

To this end, Table 3.1 contains information regarding the influence of solvent on the reactivity of 2,2,2-trifluoroethanethiol with phenylacetylene, in the presence of 3 mol% Wilkinson's catalyst. The use of ethanol as solvent in entries 1 and 2 reflects the optimized conditions developed by Ogawa for thiophenol in alkyne hydrothiolation with Wilkinson's catalyst.¹⁴⁵ This solvent appeared to be compatible with 2,2,2-trifluoroethanethiol, leading to a mixture of the *E* and *Z*-linear vinyl sulfides. However, identical reactivity was observed in the absence of catalyst, suggesting that the vinyl sulfides form as a consequence of an uncatalyzed background reaction (entry 2). The use of aromatic solvent led to the selective formation of the *E*-linear vinyl sulfide, where benzene provided a superior yield relative to toluene (entries 3 and 4). Aliphatic solvents proved ineffective, likely due to the poor solubility of Wilkinson's catalyst in non-polar solvents. The use of ethereal and halogenated solvents evidently gave rise to the best selectivity for the *E*-linear vinyl sulfide. The greater selectivity observed for tetrahydrofuran (THF) relative to 1,2-Dichloroethane (DCE) was small in comparison to the largely diminished yield for this solvent. As the solubility of Wilkinson's catalyst is considerably greater in halogenated solvents, we elected to use DCE in the evaluation of the substrate scope for this process.

Table 3.1 Solvent Optimization

Entry ^{a,b}	Catalyst Loading (mol%)	Solvent	Isolated Yield (%)	<i>E</i> : <i>Z</i> : <i>B</i> ^c
1	3	EtOH	50	1.4:1:0
2	0	EtOH	50	1.4:1:0
3	3	toluene	70	5:0:1
4	3	benzene	85	5:0:1
5	3	hexanes	<10	2:0:1
6	3	THF	51	10:0:1
7	3	DCE	90	9:0:1
8	0	DCE	0	n/a

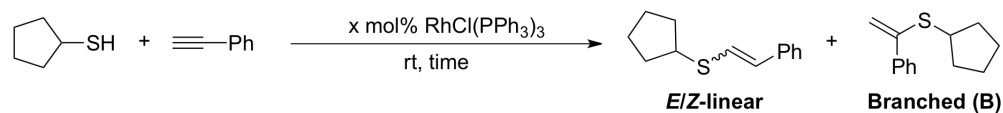
^a Reaction conditions: 0.3 mmol phenylacetylene (0.17 M), 0.33 mmol trifluoroethanethiol, 0.009 mmol RhCl(PPh₃)₃. ^b Solvent optimization conducted by Dr. Shiva Shoai. ^c Determined by ¹H NMR spectroscopy.

As DCE is often used as a solvent in catalysis, its role may be more significant than simply solubilizing the precatalyst. In fact, DCE has been observed to coordinate cationic iridium complexes in a bidentate fashion, and has been implicated in stabilizing reactive intermediates.^{225, 226} DCE has also been implicated in facilitating ligand dissociation with select *N*-heterocyclic carbene complexes. This was speculated to occur by ligand dissociation accompanied by irreversible alkylation of the carbene ligand through consecutive displacement reactions.²²⁷ Lastly, the combination of Wilkinson's catalyst and dichloromethane (DCM) has been shown to be an effective catalyst for the alkylation of thiols in the presence of triethylamine. No reactivity was observed for this reaction in the absence of RhCl(PPh₃)₃.²²⁸ Interestingly, we did not see the formation of products consistent with thiol alkylation in the reactions studied, even though DCE was an effective electrophile in the aforementioned report.

As mentioned earlier, we wished to quickly ascertain whether the conditions above would be extendable to other aliphatic thiols prior to a more comprehensive investigation of substrate scope. Thus, using the optimal conditions found by Dr. Shiva Shoai, we were now poised to investigate the reactivity of cyclopentylthiol with phenylacetylene in the presence

of varying amounts of Wilkinson's catalyst, in CDCl_3 and C_6D_6 . This choice reflects the solvents that provided optimum yield in Table 3.1 (entries 4 and 7), where CDCl_3 is comparable to DCE in solubilizing Wilkinson's catalyst and is much less expensive than deuterated-DCE.

As indicated in Table 3.2, use of more nucleophilic substrates like cyclopentyl thiol is tolerated with Wilkinson's catalyst, with optimum efficiency in halogenated solvents. However, unlike the reaction of 2,2,2-trifluoroethanethiol with phenylacetylene, the above transformation appears to show considerable amounts of a byproduct resembling the dimer of phenylacetylene, which is known to form under rhodium (I) catalysis.^{229, 230} This result is not surprising as the rhodium-sulfur bond would be predicted to be stronger with cyclopentylthiol relative to 2,2,2-trifluoroethane thiol. The stronger bond may slow reductive elimination or a separate step critical to the catalytic cycle proposed by Ogawa (Scheme 2.9), leading to competitive alkyne dimerization. Consequently, the alkyne dimer may inflate the observed ^1H NMR conversion, given the dependence on the limiting reagent in the formation of this byproduct. Nonetheless, we were pleased to have preliminary data demonstrating for the first time the feasibility of alkyne hydrothiolation with alkyl thiols.

Table 3.2 *In-Situ* Analysis of Cyclopentylthiol and Phenylacetylene

Entry ^a	Catalyst Loading (mol%)	Solvent	Time (h)	Conversion (%) ^b	E:Z:B ^b
1	3	CDCl ₃	1	60	5:0:1
2	3	CDCl ₃	2	72	5:0:1
3	3	CDCl ₃	6	86	5:0:1
4	3	CDCl ₃	22	>95	5:0:1
5	3	C ₆ D ₆	1	39	2:0:1
6	3	C ₆ D ₆	2	46	1:0:1
7	3	C ₆ D ₆	19	66	1:0:1
8	5	C ₆ D ₆	1	38	1.2:0:1
9	5	C ₆ D ₆	2	42	1.2:0:1
10	5	C ₆ D ₆	19	55	1.2:0:1

^a Reaction conditions: 0.15 mmol alkyne (0.15 M), 0.17 mmol thiol, 0.0045 mmol RhCl(PPh₃)₃.

^b Determined by ¹H NMR spectroscopy, based on integration of vinyl sulfide and terminal alkyne resonances.



3.2 Evaluation of Substrate Scope (*in-situ* Experiments)

Given the compatibility of 2,2,2-trifluoroethanethiol and cyclopentylthiol in alkyne hydrothiolation, we elected to further explore the limits of this transformation with the combination of several aliphatic thiols with both aliphatic and aryl alkynes (Figure 3.1). The evaluation of substrate scope, as well as the optimization discussed above, was done in conjunction with Dr. Shiva Shoai in the laboratory of Dr. Jennifer Love.

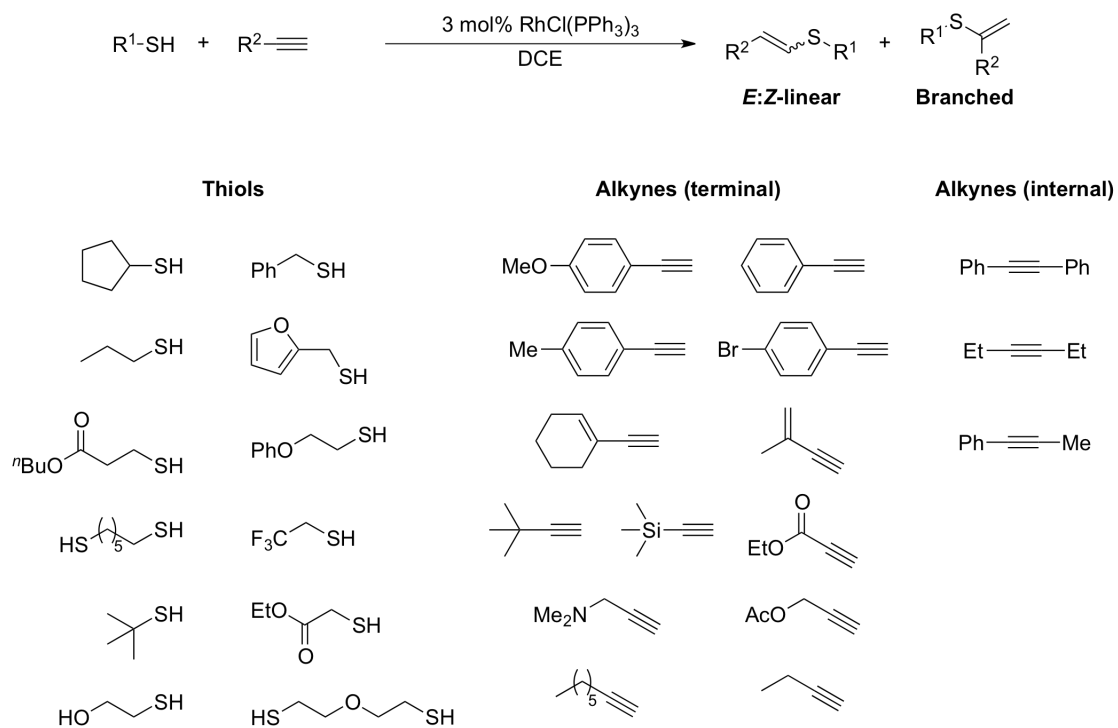


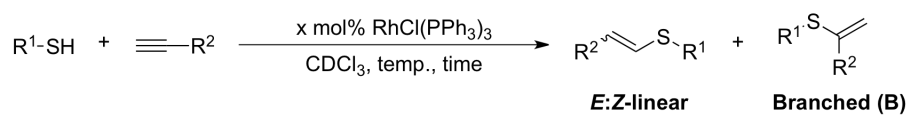
Figure 3.1 Thiol and Alkyne Substrates Examined

Having established the ability of cyclopentylthiol and phenylacetylene to undergo catalytic alkyne hydrothiolation, we selected the reaction of cyclopentylthiol with 1-ethynylcyclohexene, which is structurally similar to phenylacetylene (entry 1 and 2, Table 3.3). This transformation appeared quite selective for the corresponding *E*-linear vinyl sulfide; however, the reaction did not reach completion at room temperature. Additionally, the formation of a new byproduct was present, which did not appear to be consistent with alkyne dimerization. The selectivity of this process did not significantly change at higher temperatures (65 °C), although the yield appeared to decrease slightly. A comparable yield was obtained when the reaction of cyclopentylthiol and 1-ethynylcyclohexene was conducted in refluxing *d*⁸-toluene (58%, 24 hours). Consistent with the optimization data, the use of hydrocarbon solvents led to a reduction in selectivity, providing a 2:1 ratio of the *E*-linear and branched regioisomer. Interestingly, it appeared that the branched vinyl sulfide slowly decomposed at higher temperature, generating a similar byproduct as observed in entries 1 and 2 in Table 3.3. Given the influence of temperature on the decomposition of the branched regioisomer we speculate that this may be the result of a Diels-Alder cycloaddition process, where unreacted alkyne may serve as the dienophile in this reaction. The isolation of this

byproduct, or the *E*-linear vinyl sulfide was complicated by an apparent instability to column chromatography. The use of triethylamine-washed silica or neutral alumina proved ineffective in separating the two compounds and often led to the formation of additional byproducts, thus complicating the interpretation of spectral data.

Undeterred, we chose to investigate other aliphatic thiols in conjunction with 1-ethynylcyclohexene, as the corresponding sulfur substituted 1,3-dienes may prove useful in Diels-Alder cycloadditions. Gratifyingly, treatment of 1-ethynylcyclohexene with benzylmercaptan resulted in the highly selective formation of the *E*-linear vinyl sulfide at room temperature over a period of 24 hours (entry 3). Alternatively, the reaction of 1-propanethiol is considerably slower, requiring higher temperatures relative to benzylmercaptan. Additionally, a byproduct similar to that observed for the reaction of cyclopentylthiol with 1-ethynylcyclohexene was evident. The greater reactivity of benzylmercaptan relative to cyclopentyl and propane thiol is consistent with literature observations. This relates to the greater catalytic activity observed for less nucleophilic thiols when reacted with structurally similar alkynes.¹⁶⁵

Table 3.3 *In-Situ* Analysis of Substrate Scope



Entry ^a	R ¹	R ²	mol %	Temp. (°C)	Time (h)	<i>in-situ</i> Yield (%) ^b	Selectivity ^c (<i>E:Z:B</i>)
1			3	rt	30	64	only <i>E</i> ^d
2			10	40	24	56	only <i>E</i> ^d
3			3	rt	24	85	17:0:1
4			3	65	24	42	only <i>E</i> ^d
5			3	rt	20	90	19:0:1 ^e
6			3	rt	24	65	3:0:1
7			3	rt	24	84	4:0:1
8			3	65	24	57	3:0:1
9			3	rt	24	72	7:0:1
10			3	rt	24 to 168	< 5	n/a
11			3	rt	72	19	only <i>E</i>
12			3	65	24	30	only <i>E</i> ^f
13			3	rt	24	> 95	only <i>E</i> ^f

^a Reaction conditions: 0.15 mmol alkyne (0.15 M), 0.17 mmol thiol, 0.0045 mmol RhCl(PPh₃)₃, 1,3,5-trimethoxybenzene (TMB).

^b Yield determined by ratio of vinyl sulfide resonance and TMB aryl C-H. ^c Determined by ¹H NMR. ^d Unidentified byproduct present. ^e Experiment conducted by Dr. Shiva Shoai. ^f 10 equivalents of alkyne used.

Of the alkyl thiols examined in Table 3.3, benzylmercaptan demonstrated the most promising reactivity at room temperature. This often provided excellent regioselectivity for the *E*-linear vinyl sulfide with good to excellent yield. The reaction with 4-

ethynylbromobenzene represents an exception, but may be a consequence of competitive insertion of Wilkinson's catalyst within the weak carbon-bromine bond (entry 6). Consumption of starting material during the reaction of 4-ethynylbromobenzene with benzylmercaptan seemed to be disproportionate to the formation of the corresponding *E*-linear and branched vinyl sulfides. This supports our assumption that Wilkinson's catalyst may competitively insert into the carbon-bromine bond of 4-ethynylbromobenzene. The use of furfuryl mercaptan in place of benzylmercaptan also provided good regioselectivity and yield in the hydrothiolation of phenylacetylene (entry 9). However, no appreciable conversion was evident over several days when furfuryl mercaptan was reacted with propargyl acetate (entry 10). This lack of reactivity may be a result of coordination of the acetate group to Wilkinson's catalyst. Consequently, this coordination may inhibit catalytic processes such as migratory insertion or oxidative addition of the complex to the sulfur-hydrogen bond. This is consistent with previous results concerning the reactivity of propargyl ethers in alkyne hydrothiolation with $\text{RhTp}^*(\text{PPh}_3)_2$ as catalyst.²¹⁵ The use of bulky aliphatic alkynes also demonstrated reduced rates of reaction, requiring higher temperatures and concentrations to achieve reasonable yields (entries 12 and 13). The increased bulk of these alkynes did appear to reinforce the formation of the *E*-linear vinyl sulfide, where this was the sole product evident in entries 12 and 13.

These *in-situ* experiments suggest that optimal reactivity is observed for the reaction of more activated alkyl thiols, such as benzylmercaptan, and conjugated alkynes such as substituted phenylacetylenes and 1-ethynylcyclohexene. Decreased reactivity is observed for the treatment of unfunctionalized alkyl thiols such as 1-propanethiol and cyclopentylthiol, and aliphatic alkynes like *tert*-butylacetylene and ethynyltrimethylsilane. With this information in mind we set out to evaluate the ease in isolating the vinyl sulfide products present in Table 3.3.

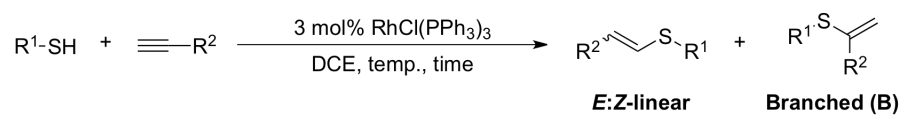
3.3 Evaluation of Substrate Scope (Preparative Reactions)

Preparative scale reactions for the synthesis of a variety of *E*-linear alkyl vinyl sulfides are illustrated in Table 3.4. In general, larger scale reactions provided similar selectivity and yields to those done *in-situ*. Furthermore, the selectivity appeared relatively unaffected at higher temperature, where reactions run at room temperature were simply lower

yielding (entries 1, 2, 5, and 6). The use of butyl 3-mercaptopropionate (entry 11) is of particular interest as this substrate would likely be incompatible with cross-coupling procedures that require stoichiometric amounts of base. This relates to the positioning of the sulfur at the β -carbon relative to the ester moiety, which may cause vinyl sulfide **23** to be highly susceptible to base-mediated elimination.

The reaction of 2-phenoxyethanethiol with propargyl acetate was selected given the presence of chelating functionalities on either substrate (entry 14). This was evaluated based upon the *in-situ* reaction of furfuryl mercaptan and propargyl acetate, where no vinyl sulfide was observed over an extended period of time (Table 3.3, entry 10). The use of 2-phenoxyethane thiol appeared to yield more of vinyl sulfide **26**; however, unreacted starting materials represented the majority of the isolated mixture. Interestingly, the branched regioisomer appeared to be the principle vinyl sulfide formed, suggesting that propargyl heteroatoms may influence the rate and selectivity of this process. Lastly, Dr. Shoai demonstrated that alkyne hydrothiolation reactions involving 2,2,2-trifluoroethanethiol gave competitive yields of vinyl sulfides **16**, **19**, and **25** with markedly reduced reaction times (entries 3, 7, and 13). This provides support for an inverse relationship between thiol nucleophilicity and catalytic activity, where non-nucleophilic thiols represent ideal substrates.

Table 3.4 Substrate Scope (Preparative)

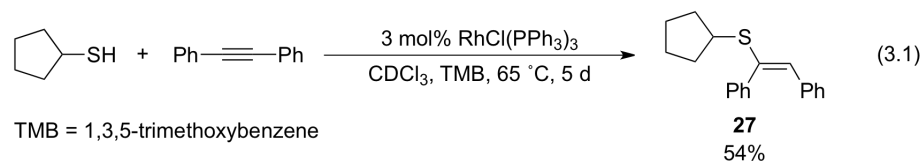


Entry	R ¹	R ²	Vinyl Sulfide	Temp. (°C)	Time (h)	Yield (%)	Selectivity ^a (E:Z:B)
1			15	rt	24	67	only E
2			15	80	24	95	only E
3			16	rt	1	46 ^{b,c}	6:0:1
4			17	rt	24	20	only E ^d
5			18	rt	16	89	10:0:1
6			18	65	24	95	5:0:1
7			19	rt	1	90 ^c	only E
8			20	65	24	89	4:0:1
9			21	65	24	82	4:0:1
10			22	65	24	96	8:0:1
11			23	rt	24	72	8:0:1
12			24	rt	24	67	only E ^{e,f}
13			25	rt	2	65	only E ^c
14			26	65	24	n/a	predominately branched ^g

^a Determined by ¹H NMR. ^b *In-situ* yield. ^c Experiment conducted by Dr. Shiva Shoai. ^d 1.1 equivalents of alkyne used. ^e Small amount of mono-hydrothiolation product formed. ^f 10 equivalents of alkyne used ^g Mainly unreacted starting material.

In addition to the terminal alkynes evaluated, internal alkynes are also tolerated under the optimized conditions. In particular, the reaction of diphenylacetylene with

cyclopentylthiol yielded the vinyl sulfide (**27**) in 54% yield after 5 days (Eq. 3.1). The use of 3-hexyne in place of diphenylacetylene proved less effective in alkyne hydrothiolation, where minimal conversion was observed under similar conditions.



3.3.1 Limitations of Alkyne Hydrothiolation with Alkyl Thiols

The conditions optimized for the hydrothiolation of alkynes with aliphatic thiols proved tolerant of a variety of useful functionalities. Importantly, our methodology for catalytic alkyne hydrothiolation constitutes the first general approach towards the synthesis of alkyl vinyl sulfides. However, a noticeable lack of reactivity was observed for select substrate combinations (Figure 3.2). In particular, thiols containing proximal heteroatoms capable of chelating the active catalyst often proved inert to the optimized conditions. Additionally, the use of aliphatic alkynes typically gave poor yields and lower selectivity for the *E*-linear vinyl sulfide. The use of propargyl acetate was ineffective as an alkyne substrate, where only small amounts of the branched vinyl sulfide (**26**) were formed when this compound was treated with 2-phenoxyethanethiol. This suggests that the presence of heteroatoms near the alkyne terminus may influence regioselectivity in alkyne hydrothiolation with Wilkinson's catalyst. Lastly, the use of ynoates in alkyne hydrothiolation appeared to undergo substantial background reactions involving conjugate addition of the thiol, yielding a complex mixture of regioisomers.

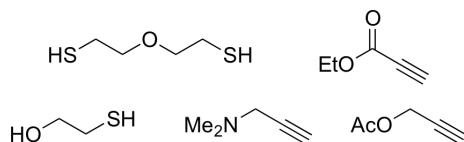


Figure 3.2 Challenging Substrates in Alkyne Hydrothiolation with Wilkinson's Catalyst

3.4 Summary of Alkyne Hydrothiolation with Alkyl Thiols

Our decision to investigate whether aliphatic thiols are tolerated in alkyne hydrothiolation with rhodium (I) precatalysts, stemmed largely from the success encountered with RhTp*(PPh₃)₂.¹⁴⁴ Given the literature precedent suggesting the incompatibility of

Wilkinson's catalyst in alkyne hydrothiolation with alkyl thiols, we were pleasantly surprised to observe the tolerance of these substrates in our optimized system. The ability of our hydrothiolation methodology to tolerate aliphatic thiols likely represents the result of substrate choice rather than the reaction conditions examined. The use of cyclohexanethiol as a substrate in Ogawa's optimized conditions reflects the group's history in developing palladium- and platinum-catalyzed thiocarbonylations.^{145, 162, 189, 199, 231} This particular thiol demonstrated the greatest reactivity, which may explain the choice in evaluating this substrate in alkyne hydrothiolation with Wilkinson's catalyst. Conversely, our discovery that more functionalized thiols are compatible with Wilkinson's catalyst may reflect a dependence of catalytic activity on the nucleophilicity of the thiol. In particular, the ability of 2,2,2-trifluoroethane thiol to engage in catalytic alkyne hydrothiolation with similar efficiency as observed for arene thiols, suggests that the nucleophilicity of the thiol may certainly be relevant to the observed catalytic activity. With this in mind, and given that results had previously been reported for only three aryl thiols, we decided to evaluate the substrate scope relative to arene thiols in alkyne hydrothiolation with Wilkinson's catalyst.

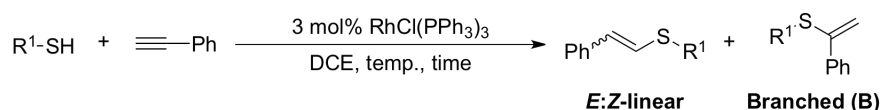
3.5 Evaluation of Substrate Scope (Arene Thiols)

Given the similarity in pKa of 2,2,2-trifluoroethane thiol to thiophenols, we decided to investigate the reactivity of a variety of aryl thiols in alkyne hydrothiolation with Wilkinson's catalyst. We anticipated that the lower nucleophilicity of aryl thiols would allow for similar yields and reaction times with phenylacetylene as that obtained for 2,2,2-trifluoroethane thiol. For consistency, the reactions of aryl thiols were run at room temperature (where possible), for a duration of 1 hour. This would enable us to assess the relative reactivity of the arene thiol to 2,2,2-trifluoroethane thiol. The reaction of a series of *para*-substituted thiophenols with phenylacetylene under the optimized conditions determined for alkyne hydrothiolation with aliphatic thiols is illustrated in Table 3.5 below.

As predicted, the reaction of thiophenol with phenylacetylene proceeded with similar efficiency as the analogous reaction with 2,2,2-trifluoroethane thiol, providing the *E*-linear vinyl sulfide (**28**) with excellent selectivity (entries 1 and 2). Furthermore, the ability of Wilkinson's catalyst to tolerate a range of *p*-substituents in alkyne hydrothiolation stands in contrast to reports describing the use of Pd(OAc)₂.¹⁶¹ The greater tolerance of rhodium (I)

systems towards *p*-substitution of the arene thiol is consistent with Ogawa's later report. However, only 4-methylbenzenethiol and 4-chlorothiophenol were tested in addition to thiophenol. Furthermore, it appears that the use of DCE as solvent drastically lowers the reaction time relative to that observed for ethanol (20 hours). This is likely the consequence of the greater solubility of Wilkinson's catalyst in halogenated solvents compared to alcohols.¹⁴⁵

Table 3.5 Aryl Thiol Substrate Scope



Entry	R ¹	Vinyl Sulfide	Temp. (°C)	Time (h)	Isolated Yield (%) ^a	Selectivity (<i>E</i> : <i>Z</i> :B) ^b
1		19	rt	1	90	only <i>E</i> ^c
2		28	rt	1	93	20:0:1
3		29	rt	1	79	only <i>E</i>
4		30	rt	1	72	10:1:0
5		31	rt	1	90	only <i>E</i>
6		32	rt	1	75	10:1:0
7		33	rt	1	50	only <i>E</i> ^d
8		34	rt	1	98	only <i>E</i>
9		35	rt	1	95	only <i>E</i>
10		36	rt	1	94	33:0:1
11		37	rt	24	95	14:0:1
12		38	80	24	91	3:0:1

^a Average over several runs. ^b Determined by integration of relevant vinyl signals. ^c Experiment conducted by Dr. Shiva Shoai. ^d Potentially contaminated with disulfide or sulfoxide of **33**.

The use of electron withdrawing groups is tolerated under these conditions, typically affording the corresponding *E*-linear vinyl sulfide in good yield and regioselectivity. The reduction in yield observed for thiophenols containing strong inductively withdrawing groups in the *para*-position, such as entries 3 and 4, may be a function of metal-sulfur back bonding with the rhodium (III) intermediate. The strength of this interaction may be heavily influenced by the relative location of the phosphine ligands, where a *trans* relationship would likely give rise to a greater degree of back bonding. This may slow processes such as alkyne coordination, or insertion into the rhodium-sulfur bond, which may also explain the high selectivity for the linear regioisomers for these substrates. The presence of the *Z*-linear regioisomer (entries 4 and 6) is attributed to a radical background reaction. The observation of the *Z*-linear isomer is more prevalent with the use of arene thiols, presumably due to the lower homolytic S-H bond energy of aryl (79.1 kcal for PhSH) relative to alkyl thiols (86.1 kcal for PhCH₂SH).^{232, 233} The radical background reaction can largely be prevented by wrapping the round bottom with aluminum foil prior to the addition of the thiol.

The use of electron donating groups (entries 8-12) was well tolerated in this system, where aryl ethers and free phenols were acceptable substrates (entry 9 versus 11). Additionally, use of 4-aminothiophenol and 4-mercaptophenol represent chemoselective functionalizations of the sulfur-hydrogen bond relative to the nitrogen or oxygen-hydrogen bonds. However, these reactions did require extended reaction times, suggesting that the presence of these unprotected functionalities may lead to competitive coordination events. This may slow the oxidative addition of Wilkinson's catalyst to the S-H bond, or prevent the subsequent coordination of phenylacetylene. The reduced selectivity for the *E*-linear vinyl sulfide (**38**) in entry 12 is likely the consequence of the higher temperature employed, where room temperature led to much lower conversion.

3.5.1 Limitations of Alkyne Hydrothiolation (Arene Thiols)

The presence of alkyl and aryl sulfones in several medicinally active compounds illustrates the need for the convenient synthesis of vinyl sulfide precursors. The tolerance of our alkyne hydrothiolation methodology for a multitude of aliphatic and aryl thiols with sensitive functionalities will allow for further studies towards the synthesis of biologically active compounds and analogues thereof. As heteroaromatic species such as pyrimidines and

imidazoles are commonly found in molecules of therapeutic value, we were interested in testing the limits of the arene thiol scope with the substrates depicted in Figure 3.3. Unfortunately, these thiols proved inert to the optimized conditions for alkyne hydrothiolation. Additionally, the use of higher catalyst loadings and elevated temperatures failed to improve the efficiency of these reactions. This is likely due to the lower solubility of these substrates in DCE and the large number of Lewis basic groups which may interfere with the active catalyst in solution.

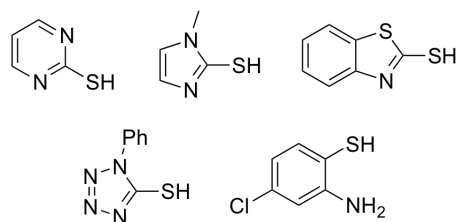


Figure 3.3 Challenging Arene Thiol Substrates in Catalytic Alkyne Hydrothiolation

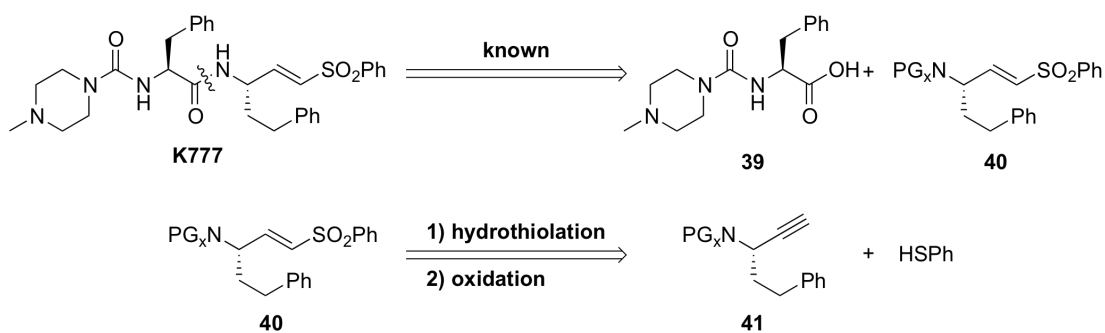
3.5.2 Summary Arene Thiol Substrate Scope

The results included in Table 3.5 demonstrate how our optimized conditions for the use of alkyl thiols in alkyne hydrothiolation are readily extendable to the use of arene thiols with a variety of *para*-substituents. In general, it appears that *para*-substitution has little effect on the rate of hydrothiolation, except in the presence of functional groups capable of binding to Wilkinson's catalyst. This is in contrast to our initial hypothesis that thiol nucleophilicity may correlate with the observed catalytic activity in alkyne hydrothiolation. Consequently, Matthew Wathier, a second year PhD student in the laboratory of Jennifer Love, is currently conducting more quantitative kinetic investigations in order to assess the effect of *para*-substituents on the rate of alkyne hydrothiolation with arene thiols. The preliminary results of these studies demonstrate no clear relationships between *para*-substitution and the observed rate of hydrothiolation. Further mechanistic studies will ideally aid in the development of second-generation rhodium catalysts that will be capable of incorporating the thiol substrates shown in Figures 3.2 and 3.3 in alkyne hydrothiolation.

3.6 Alkyne Hydrothiolation for the Synthesis of Biologically Active Compounds

The ability of our optimized conditions to tolerate a range of aliphatic and arene thiols in alkyne hydrothiolation encouraged us to explore the utility of this methodology in the

synthesis of biologically active compounds. In particular, we were interested in an alkyne hydrothiolation, oxidation sequence for the synthesis of *E*-linear vinyl sulfones present in compounds such as K777. This is demonstrated in Scheme 3.1, where interception of the known intermediates could be accomplished upon oxidation of the vinyl sulfide synthesized through alkyne hydrothiolation. This would likely require the use of one or two protecting groups on the propargyl amine, in order to avoid unproductive coordination of the nitrogen to Wilkinson's catalyst. This substrate combination has thus far proven resistant to our optimized conditions with alkyl thiols (Section 3.3.1). Additionally, the presence of an oxygen-protecting group in the propargyl position appears to affect both reactivity and selectivity of these substrates in alkyne hydrothiolation (Table 3.3, entry 10, page 62). Given the incompatibility that this substrate combination may possess, we decided to evaluate the use of a series of propargyl amines in alkyne hydrothiolation with thiophenol and benzyl mercaptan.



Scheme 3.1

3.6.1 Propargyl Amine Substrates in Alkyne Hydrothiolation

The use of alkynes with oxygen and nitrogen groups in the propargyl position are well represented in group 10 metal-catalyzed alkyne hydrothiolation.^{145, 161, 164-166, 168, 169, 186, 187, 194, 234} Furthermore, the use of unprotected propargyl amine in the zirconium-catalyzed hydrothiolation of alkynes led to a surprising rate enhancement, suggesting an active role of the proximal nitrogen during the catalytic cycle. Additionally, the selectivity of this process was largely dependent on the zirconium precatalyst employed, suggesting that the nitrogen may also play a role in dictating regioselectivity.²³⁵ Given the tolerance of these substrates with transition metal precatalysts from groups 4 and 10, it is surprising that few examples

exist for rhodium (I) catalyzed processes. Ogawa demonstrated the successful use of 4-pentyn-1-ol in rhodium (I) catalyzed hydrothiolation and hydrothioformylation; however, the oxygen is three atoms removed from the reactive alkyne terminus.^{145, 162} The use of propargyl alcohol was largely unsuccessful with *N,N* and *P,N*-complexes of rhodium and iridium. This appeared to yield very little of the corresponding vinyl sulfide, despite the use of extended reaction times and higher temperatures.^{142, 143}

Given the information above, it appears that the use of propargyl amine or alcohol substrates in catalytic alkyne hydrothiolation with RhTp*(PPh₃)₂ and group 10 metal complexes may reflect a “matched” scenario. This is meant to suggest that both the substrate and the active catalyst mutually reinforce reactivity and regioselectivity. In order to assess reactivity of these substrates in alkyne hydrothiolation with Wilkinson’s catalyst, we elected to evaluate the propargyl amine compounds below. This selection is based upon the varying electronic nature expected for the tertiary amine (**42**) and the carbamates **43** and **44**.

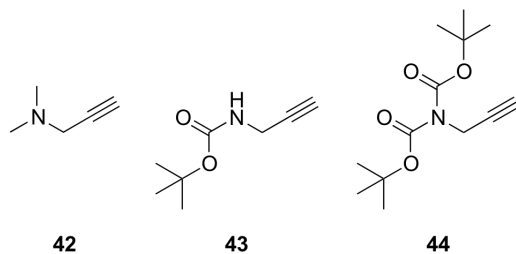
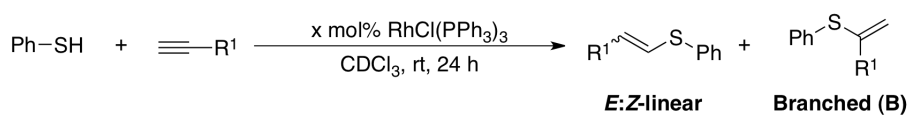


Figure 3.4 Propargyl Amine Substrates Examined in Alkyne Hydrothiolation

The Boc-protected propargyl amines **43** and **44** were synthesized according to a literature procedure detailing the formation of the diprotected adduct (**44**). Conveniently, this process provided both the mono (**43**) and diprotected (**44**) propargyl amines that could be separated chromatographically.²³⁶ With these compounds in hand, we sought to test their efficiency in alkyne hydrothiolation at a variety of temperatures and catalyst loadings with both thiophenol and benzyl mercaptan.

The room temperature reaction of thiophenol with propargyl amine **44** formed very little product at catalyst loadings of 3 and 5 mol%. At 10 mol% the reaction proceeded smoothly, and provided a 1.6:1 mixture of the *E*-linear and branched regioisomers (Table 3.6, entry 3). On preparative scale, it was found that lower catalyst loadings were employable at temperatures of 80 °C, giving similar selectivity and yield of vinyl sulfide **45** compared to the

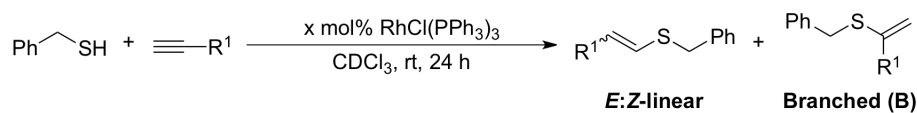
use of 10 mol% $\text{RhCl}(\text{PPh}_3)_3$. The formation of the branched regioisomer with catalytic amounts of $\text{RhCl}(\text{PPh}_3)_3$ was unexpected, given the high regioselectivity for the *E*-linear isomer as demonstrated in Tables 3.4 and 3.5. This suggests that the carbamate oxygens may serve to direct the regioselectivity of this process, as the *tert*-butoxycarbonyl protecting groups should render the nitrogen lone-pair unavailable for chelation. The use of propargyl amine (**43**) with thiophenol proved to be less reactive than the diprotected version, likely reflecting the ability for this substrate to competitively bind to Wilkinson's catalyst. At 10 mol% catalyst loading the yield of the reaction improved to 12%, providing an equimolar mixture of the *E*-linear and branched regioisomers (Table 3.6, entry 6). The selectivity of this process was slightly lower than that of the corresponding diprotected analogue (**44**); however, this may simply be a consequence of experimental error. The use of the tertiary amine (**42**) in this process proved unreactive at room temperature, providing small amounts of the corresponding vinyl sulfide. Interestingly, this appeared to yield the branched regioisomer exclusively, suggesting that the propargyl amine may serve to direct the selectivity of this process. The lack of reactivity for this process may be attributable to an acid-base process between the basic tertiary amine and thiophenol. This may lead to the formation of various catalytically inactive thiolate complexes, or may prevent the formation of a rhodium-hydride species necessary for insertion to the alkyne.

Table 3.6 Hydrothiolation of Propargyl Amines 42-44 with Thiophenol

Entry	R ¹	Vinyl Sulfide	Catalyst Loading (mol%)	Selectivity ^a	<i>In-Situ</i> Yield (%) ^b
1	Boc ₂ N-CH ₂ -CH ₂ -CH ₂ -	45	3	N/A	<5
2	Boc ₂ N-CH ₂ -CH ₂ -CH ₂ -	45	5	N/A	<5
3	Boc ₂ N-CH ₂ -CH ₂ -CH ₂ -	45	10	1.6:1 E:B	>95 (95) ^{c,d}
4	BocHN-CH ₂ -CH ₂ -CH ₂ -	46	3	N/A	<5
5	BocHN-CH ₂ -CH ₂ -CH ₂ -	46	5	N/A	<5
6	BocHN-CH ₂ -CH ₂ -CH ₂ -	46	10	1.2:1 E:B	12
7	Me ₂ N-CH ₂ -CH ₂ -CH ₂ -	47	3	100% B	6
8	Me ₂ N-CH ₂ -CH ₂ -CH ₂ -	47	5	100% B	9
9	Me ₂ N-CH ₂ -CH ₂ -CH ₂ -	47	10	100% B	7

^a Determined by integration of the relevant vinyl signals. ^b Yield determined by ratio of vinyl sulfide resonance and aryl C-H of 1,3,5-trimethoxybenzene. ^c Isolated yield (%). ^d Conditions: 3 mol% RhCl(PPh₃)₃, DCE, 80 °C, 24 h.

We next investigated the reactivity of benzyl mercaptan with propargyl amines **42-44** in order to assess the selectivity and reactivity of aliphatic thiols relative to thiophenol. The room temperature reaction of benzyl mercaptan with propargyl amines **42-44** appeared to yield none of the desired vinyl sulfides **48-50**. This is consistent with the general lack of reactivity characteristic of aliphatic thiols with less activated alkynes, such as the propargyl derivatives examined. However, when benzyl mercaptan was mixed with propargyl amine **42** a small amount of vinyl sulfide **50** was produced with exclusive selectivity for the branched regioisomer. The conditions used for entry 8 were repeated on larger scale, with an extended stir period of 36 hours, giving the branched vinyl sulfide in 47% isolated yield (Table 3.7).

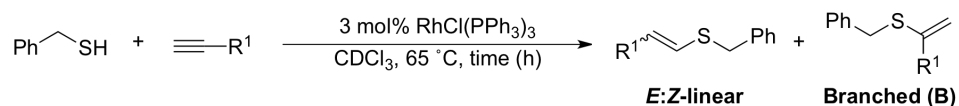
Table 3.7 Hydrothiolation of Propargyl Amines 42-44 with Benzyl Mercaptan

Entry	R ¹	Vinyl Sulfide	Catalyst Loading (%)	Selectivity ^a	<i>In-Situ</i> Yield (%) ^b
1	Boc ₂ N-CH ₂ -CH ₂ -CH ₂ -R ¹	48	3	N/A	<5
2	Boc ₂ N-CH ₂ -CH ₂ -CH ₂ -R ¹	48	5	N/A	<5
3	Boc ₂ N-CH ₂ -CH ₂ -CH ₂ -R ¹	48	10	N/A	<5
4	BocHN-CH ₂ -CH ₂ -CH ₂ -R ¹	49	3	N/A	<5
5	BocHN-CH ₂ -CH ₂ -CH ₂ -R ¹	49	5	N/A	<5
6	BocHN-CH ₂ -CH ₂ -CH ₂ -R ¹	49	10	N/A	<5
7	Me ₂ N-CH ₂ -CH ₂ -CH ₂ -R ¹	50	3	100% B	5
8	Me ₂ N-CH ₂ -CH ₂ -CH ₂ -R ¹	50	5	100% B	5 (47) ^{c,d}
9	Me ₂ N-CH ₂ -CH ₂ -CH ₂ -R ¹	50	10	100% B	18

^a Determined by integration of the relevant vinyl signals. ^b Yield determined by ratio of vinyl sulfide resonance and aryl C-H of 1,3,5-trimethoxybenzene. ^c Isolated yield (%).

^d Conditions: 5 mol% RhCl(PPh₃)₃, rt, DCE, 36 h.

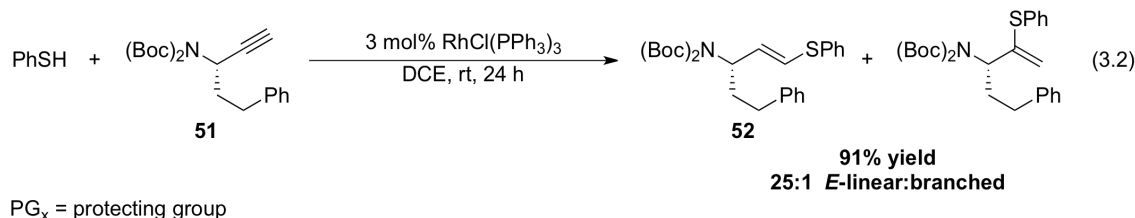
In order to better assess the reactivity and selectivity of benzyl mercaptan with propargyl amines **42-44** we investigated entries 1 and 3 from Table 3.7 at higher temperatures. This yielded small amounts of the vinyl sulfides, where the use of the diprotected substrate (**44**) demonstrated the best selectivity for the *E*-linear isomer (**48**, entry 2, Table 3.8). This is in agreement with the results obtained for thiophenol, where diprotection of the propargyl amine seems necessary to achieve partial selectivity for the *E*-linear regioisomer. Interestingly, when **43** was heated in the presence of benzyl mercaptan it appeared that the branched regioisomer slowly decomposed over time (entry 3 versus entry 4, Table 3.8). This is consistent with the use of propargyl alcohol in related rhodium- and iridium-catalyzed alkyne hydrothiolation reactions reported by Field and Burling.^{142, 143} In these reports, the branched regioisomer appeared to undergo subsequent double bond migration, eventually yielding the corresponding aldehyde.

Table 3.8 Hydrothiolation of Propargyl Amines 43-44 at Higher Temperature

Entry	R ¹	Vinyl Sulfide	Time	Selectivity ^a	<i>In-Situ</i> Yield (%) ^b
1	Boc ₂ N-CH ₂ -CH ₂ -CH ₂ -R ¹	48	1	2:1 <i>E</i> : <i>B</i>	5
2	Boc ₂ N-CH ₂ -CH ₂ -CH ₂ -R ¹	48	24	2:1 <i>E</i> : <i>B</i>	9
3	BocHN-CH ₂ -CH ₂ -CH ₂ -R ¹	49	1	1:1.3 <i>E</i> : <i>B</i>	21
4	BocHN-CH ₂ -CH ₂ -CH ₂ -R ¹	49	24	only <i>E</i>	10 ^c

^a Determined by integration of the relevant vinyl signals. ^b Yield determined by ratio of vinyl sulfide resonance and aryl C-H of 1,3,5-trimethoxybenzene. ^c Reduction in yield reflects decomposition of the branched regioisomer.

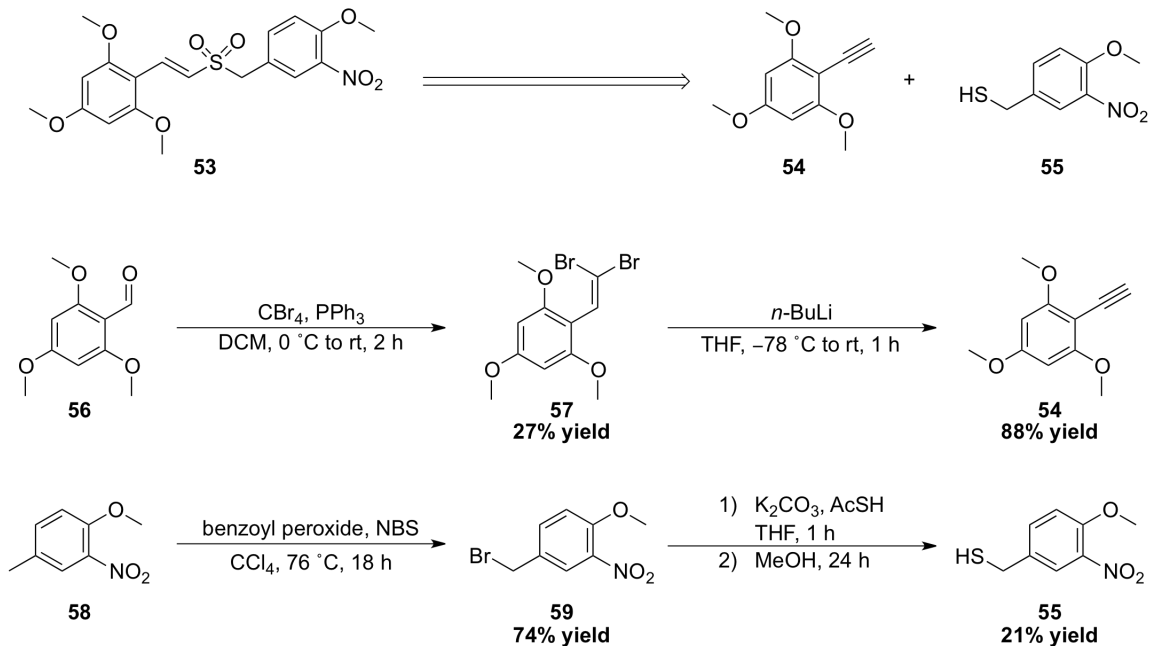
The results depicted in Tables 3.6 to 3.8 demonstrate that the presence of a propargyl heteroatom clearly impact the regioselectivity of alkyne hydrothiolation with Wilkinson's catalyst. As the substrates in these studies represent propargyl amines derived from glycine, it seems reasonable that this methodology could be extended to the synthesis of peptidomimetic vinyl sulfones. Ideally, the use of sterically hindered substrates may inhibit the formation of the branched regioisomer. Erica Kiemele, a colleague working towards the synthesis of K777, demonstrated that the diprotected propargyl amine substrate (**51**) reacted efficiently with thiophenol (Eq. 3.2). This resulted in a 25:1 ratio of regioisomers favouring the *E*-linear vinyl sulfide **52**, suggesting that α -substitution does sterically shield the formation of the Markovnikov adduct. The selective formation of the *E*-linear vinyl sulfide below constitutes a formal synthesis, where progress towards a completed synthesis of K777 and analogues thereof is currently underway. Given the substrate scope depicted in Table 3.6, the use of alkyne hydrothiolation towards the synthesis of K777 should prove readily amenable to the synthesis of analogues. The following section will discuss preliminary results towards a separate medically active vinyl sulfone, ON 01910.Na, which possesses anti-cancer properties.



3.6.2 Alkyne Hydrothiolation as a Strategy Towards the Synthesis of ON 01910.Na

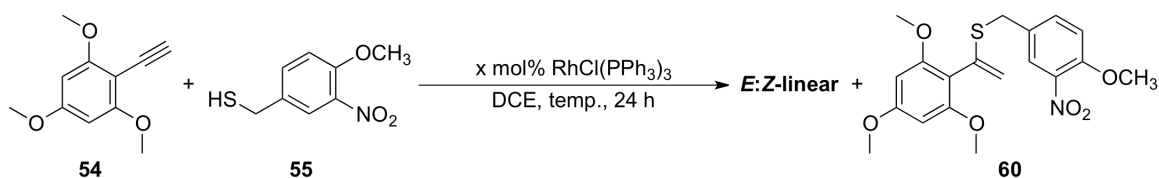
Given the applicability of alkyne hydrothiolation towards the synthesis of K777, we thought a similar sequence could be used in synthesizing ON 01910.Na. This would intercept the known intermediate vinyl sulfone **53**, which can be elaborated to ON 01910.Na in three known steps. We envisioned that this intermediate **53** could be synthesized through the hydrothiolation of 2,4,6-trimethoxyphenylacetylene (**54**) with thiol **55** derived from 4-methoxy-3-nitrotoluene (**58**, Scheme 3.2).

To this end, 2,4,6-trimethoxyphenylacetylene (**54**) was synthesized from 2,4,6-trimethoxybenzaldehyde (**56**) using the Corey-Fuchs homologation procedure, giving the desired alkyne in 24% overall yield. Similarly, the thiol (**55**) was synthesized by radical bromination of 4-methoxy-3-nitrotoluene (**58**) with a combination of benzoylperoxide and *N*-bromosuccinimide in refluxing carbon tetrachloride. Following this, the benzylic bromide (**59**) was displaced with the *in-situ* generated potassium salt of thioacetic acid. The intermediate thioester was then hydrolyzed by adding methanol to the mixture, as a one-pot synthesis of thiol **55** (Scheme 3.2). With these substrates in hand we set out to determine their compatibility in catalytic alkyne hydrothiolation with Wilkinson's catalyst.



Scheme 3.2

It was anticipated that these substrates would successfully undergo hydrothiolation as the combination of benzyl mercaptan with a variety of aryl and aliphatic alkynes was tolerated under our optimized conditions. When thiol **55** was treated with **54** in the presence of Wilkinson's catalyst, it appeared that the optimized conditions for hydrothiolation proved ineffective, predominately yielding the starting alkyne and thiol (entry 1, Table 3.9). At higher temperature greater reactivity was observed, yielding a complex mixture of compounds with what appeared to be the vinyl sulfide **60**. At 5 mol% catalyst loading and ambient temperature the reaction was no more effective than 3 mol% (entry 3). A reasonable amount of vinyl sulfide was obtained when the reaction flask was charged with an additional 3 mol% of catalyst, following 1 hour of mixing. However, the ¹H NMR spectrum is consistent with the formation of the branched regioisomer and not the desired *E*-linear vinyl sulfide. This result was surprising given the steric bulk imparted by the *ortho*-substituents of alkyne **54**, suggesting that these functionalities may serve some role in directing regioselectivity.

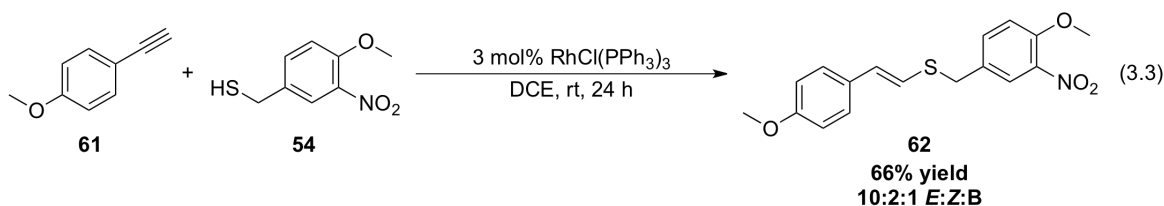
Table 3.9 Attempted Synthesis of ON 01910.Na Vinyl Sulfide

Entry	Catalyst Loading (%)	Temp. (°C)	Recovered Alkyne (%) ^a	Isolated Yield (%)	Selectivity (E:Z:B) ^b
1	3	rt	87	N/A	N/A
2	3	80	72	8	complex mixture
3	5	rt	87	N/A	N/A
4	6 ^c	rt	75	15 (60) ^d	100% B ^e

^a Determined after column chromatography. ^b Determined by integration of the relevant vinyl signals.

^c An additional 3 mol% $\text{RhCl}(\text{PPh}_3)_3$ was added by cannula after 1 hour. ^d Based on recovered starting material (BRSM). ^e Impurities present.

In an attempt to verify whether the *ortho*-substituents of alkyne **54** may influence regioselectivity, we attempted to use mono-substituted ethynylanisoles in alkyne hydrothiolation with thiol **55**. Of the substrates employed, only 4-ethynylanisole (**61**) demonstrated appreciable reactivity, providing a 10:2:1 mixture of the regioisomers favouring the *E*-linear vinyl sulfide **62** (Eq. 3.3). The greater selectivity observed for this particular alkyne suggests that the *ortho*-substituents in alkyne **54** may indeed reinforce the formation of the branched regioisomer similar to the aforementioned propargyl amines. The use of bulkier rhodium phosphine complexes may help prevent coordination of the *ortho*-substituents, allowing for the selective synthesis of the *E*-linear isomer.



3.7 Conclusions

The work detailed in this chapter demonstrates the development of a general method for alkyne hydrothiolation that incorporates a variety of alkyl and arene thiols. Previous reports concerning alkyne hydrothiolation have largely explored the substrate scope relative to alkynes, and neglect to explore the functional group tolerance with respect to thiol. Our results involving the use of Wilkinson's catalyst in alkyne hydrothiolation appears to tolerate a variety of alkyl thiols, despite the literature precedent to the contrary.¹⁴⁵ This process generates the *E*-linear regioisomer in high selectivity with good to excellent yields.¹⁴⁶

Given the presence of *E*-linear vinyl sulfones in a variety of biologically active molecules, we sought to test our methodology in the synthesis of two such examples, including K777 and ON 01910.Na. To this end, we have found that heteroatoms proximal to the alkyne influence the regioselectivity of alkyne hydrothiolation in favour of the branched vinyl sulfide. We hypothesized that the use of *tert*-butoxycarbonyl protecting groups (Boc) would correspondingly lower the contribution of the propargyl nitrogen in coordinating the active catalyst in solution. Indeed, the directing group effect can be reversed in circumstances involving Boc-protected propargyl amines. Additionally, the use of propargyl amines derived from α -amino acids (**51**) appear to be more selective for the desired *E*-linear vinyl sulfide. This likely reflects a balance between the electronic influence of the propargyl nitrogen, and the steric influence of the α -substituent. The use of higher catalyst loadings is still necessary in order to achieve adequate reactivity, demonstrating the need for further catalyst development. Similarly, our initial approach to ON 01910.Na proved ineffective in synthesizing the desired *E*-linear vinyl sulfide, where selectivity for the branched regioisomer was obtained. Ideally, mechanistic studies of this process will aid in the rational development of more active catalysts for alkyne hydrothiolation with alkyl and arene thiols.

Given the widespread use of vinyl sulfides and their oxidized derivatives in synthetic and medicinal chemistry, we elected to further explore the reactivity of these useful synthetic intermediates. Chapter 4 will involve a discussion of our efforts towards extending alkyne hydrothiolation in the synthesis of divinyl ketones capable of undergoing the Nazarov cyclization.

3.8 Experimental

3.8.1 General Procedures

Manipulation of organometallic compounds was performed using standard Schlenk techniques under an atmosphere of dry nitrogen or in a nitrogen-filled Vacuum Atmospheres drybox ($O_2 < 2$ ppm). NMR spectra were recorded on Bruker Avance 300 or Bruker Avance 400 spectrometers. 1H , ^{13}C and ^{19}F NMR spectra are reported in parts per million and were referenced to residual solvent: $CDCl_3 = 7.26$ 1H NMR, 77.0 for ^{13}C NMR, for $CD_2Cl_2 = 5.32$ 1H NMR, 53.8 for ^{13}C NMR, for $CD_3CN = 1.94$ 1H NMR, 118.26 for ^{13}C NMR. Coupling constant values were extracted assuming first-order coupling. The multiplicities are abbreviated as follows: s = singlet, d = doublet, t = triplet, q = quartet, m = multiplet, br = broad signal, dd = doublet of doublets, dt = doublet of triplets, td = triplet of doublets, AB q = second order quartet, app. t = apparent triplet. The chemical shift value for second order quartets (AB q) were reported based upon the solution to the equation $(1-3) = (2-4) = [(\Delta\nu)^2 + J^2]^{1/2}$ where J = coupling constant (Hz) and $\Delta\nu$ = chemical shift difference (Hz) = unknown value and (1-3) or (2-4) represents left to right numbering of the individual peaks related to the multiplet (Hz). The value for $\Delta\nu$ was then subtracted or added to the middle of the coupling pattern and converted to ppm based upon the spectrometer frequency. Values for the integration of peaks in the 1H NMR spectrum of compounds containing a mixture of vinyl sulfides are referenced to the vinyl resonances of the *E*-linear regioisomer. All spectra were obtained at 25 °C. Mass spectra were recorded on a Kratos MS-50 mass spectrometer.

3.8.2 Materials and Methods

Hexanes, benzene, diethyl ether, THF and toluene were dried by passage through solvent purification columns.²³⁷ 1,2-Dichloroethane and $CDCl_3$ were distilled over P_2O_5 and degassed prior to use. Unless specifically mentioned, all organic reagents were obtained from commercial sources and used without further purification. The *in-situ* reactions were conducted with an appropriate amount of 1,3,5-Trimethoxybenzene, which was sublimed prior to use. Transition metal reagents such as $RhCl(PPh_3)_3$ were purchased from Strem Chemicals and taken directly into an inert atmosphere glovebox without further purification. Compounds **16**, **19**, **25** were prepared by Dr. Shiva Shoai.²²⁴

3.8.3 General Experimental Procedure for Hydrothiolation

In-Situ Reactions (Monitored by NMR)

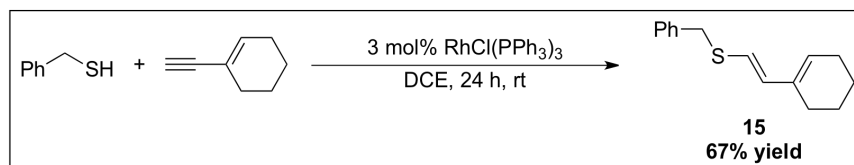
In an inert atmosphere glovebox, RhCl(PPh₃)₃ (4.5 mg, 0.0048 mmol, 3 mol%) and 1,3,5-Trimethoxybenzene (8.7 mg, 0.052 mmol, 0.33 equiv.) were dissolved and transferred to a screw cap NMR tube in approximately 500 μ L of CDCl₃. To this was added thiol (0.17 mmol, 1.1 equiv.) and alkyne (0.15 mmol, 0.15 M) in an additional 500 μ L of CDCl₃. The NMR tube was then removed from the glovebox and the progress of the reaction monitored by ¹H NMR. Integration of the vinylic resonances corresponding to the vinyl sulfide product in comparison to the value obtained for the aryl C-H of 1,3,5-Trimethoxybenzene allowed for the determination of the *in-situ* yield. If higher than ambient temperatures were necessary, the mixture was heated in a mineral oil bath. In some cases, standard solutions of Wilkinson's catalyst and 1,3,5-Trimethoxybenzene in CDCl₃ were prepared in order to accurately deliver the aforementioned quantities to an NMR tube.

Preparative Scale Reactions

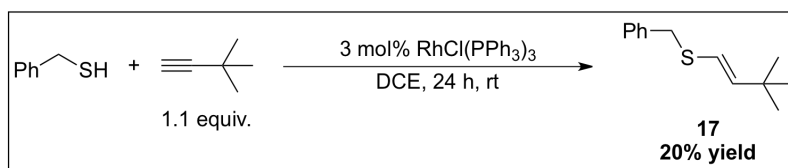
In an inert atmosphere glovebox, RhCl(PPh₃)₃ (18.4 mg, 0.0198 mmol, 3 mol%) was added directly to a round bottom flask equipped with a magnetic stir bar. The flask was sealed with a serum cap and removed from the glovebox, attached to a schlenk line, and held under a continuous flow of N₂. To this was added 3 mL of 1,2-Dichloroethane and the round bottom wrapped in aluminum foil in order to suppress any radical background reactions. Following this, thiol (0.724 mmol, 1.1 equiv.) and alkyne (0.655 mmol, 0.2 M) were added sequentially, which is often accompanied by a change from a red to orange solution. The mixture was then vigorously stirred for the required time and monitored by thin layer chromatography (TLC), visualizing with either UV irradiation or use of a *p*-anisaldehyde stain. In situations that required elevated temperatures, the round bottom flask would be submerged within a heated mineral oil bath. Following completion of the stir period, or completion of the reaction as monitored by TLC, the solution was concentrated and passed through a silica gel plug with an eluent consisting of hexanes and ethyl acetate. In many cases involving arene thiols, the filtrate collected following chromatography was washed with saturated Na₂CO₃ or 0.5 M NaOH, and the aqueous layer extracted three times with 10

mL of dichloromethane. This typically afforded clean material, if not, column chromatography was used to further purify the crude compounds.

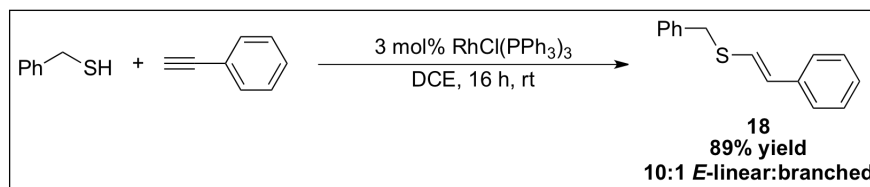
3.8.4 Analytical Data for Hydrothiolation Products



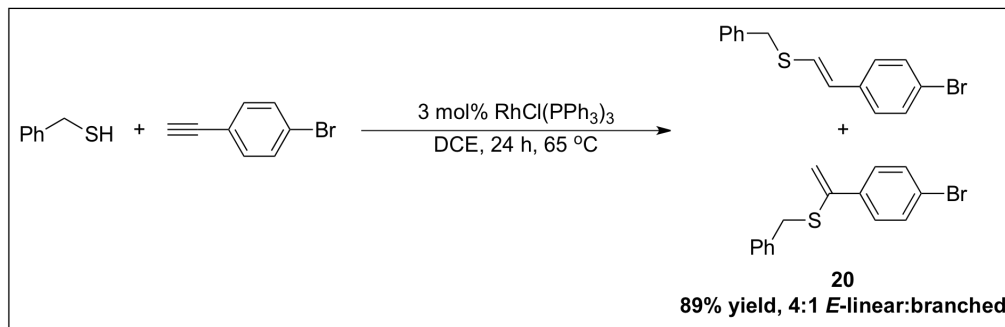
Vinyl sulfide **15**, exclusively the *E*-linear isomer. ^1H NMR (CDCl_3 , 300 MHz, δ 7.26): δ 7.34 – 7.31 (m, 5H), 6.24 (d, 1H, $J = 15.4$ Hz), 6.02 (d, 1H, $J = 15.4$ Hz), 3.92 (s, 2H), 2.11 – 2.06 (m, 4H), 1.70 – 1.54 (m, 5H). $^{13}\text{C}\{^1\text{H}\}$ NMR (CDCl_3 , 75 MHz, δ 77.0) δ 137.8, 135.1, 133.3, 128.8, 128.5, 128.1, 127.1, 119.3, 37.7, 25.8, 24.5, 22.5. HRMS (EI) m/z calcd for $\text{C}_{15}\text{H}_{18}\text{S}$: 230.1129; found: 230.1129.



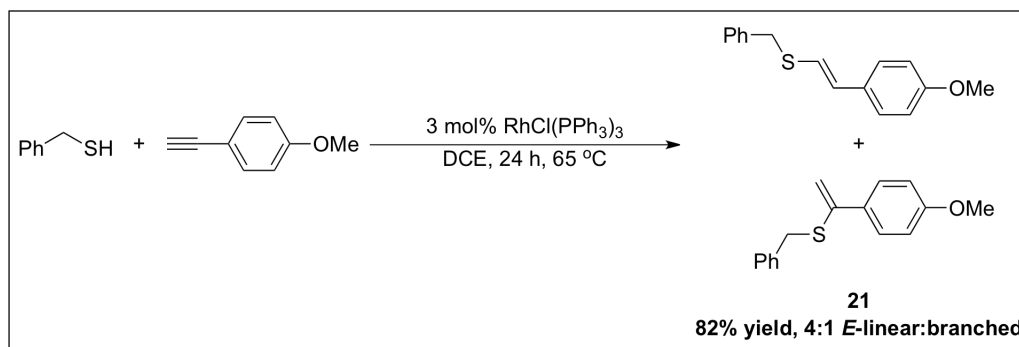
Vinyl sulfide **17**, exclusively the *E*-linear isomer. ^1H NMR (CDCl_3 , 300 MHz, δ 7.26): δ 7.32 (m, 5H), 5.86 (d, 1H, $J = 15.3$ Hz), 5.72 (d, 1H, $J = 15.3$ Hz), 3.86 (s, 2H), 1.00 (s, 9H). Known compound.²³⁸



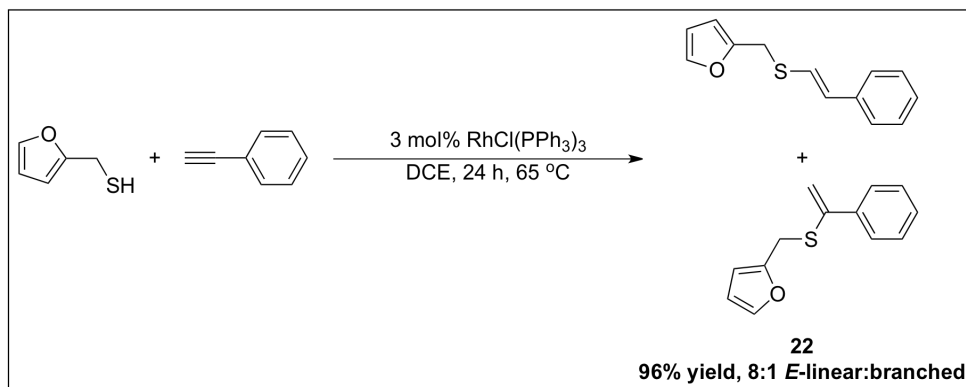
Vinyl Sulfide **18**, 10:1 mixture of *E*-linear:branched. ^1H NMR (CDCl_3 , 300 MHz, δ 7.26): δ 7.40 – 7.16 (m, 8H), 6.73 (d, 1H, $J = 15.5$ Hz), 6.54 (d, 1H, $J = 15.3$ Hz), 5.46 (s, 0.11H, branched), 5.22 (s, 0.11H, branched), 4.02 (s, 2H), 3.90 (s, 0.22H, branched). Known compound.¹⁶⁷



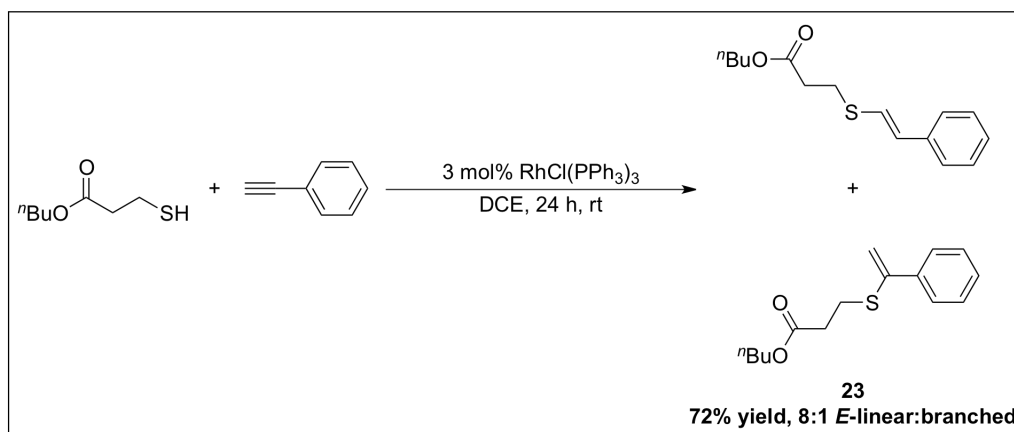
Vinyl sulfide **20**, 4:1 mixture of *E*-linear:branched. ^1H NMR (CDCl_3 , 300 MHz, δ 7.26): δ 7.49 – 7.27 (m, 9H), 7.12 (d, 2H, $J = 8.2$ Hz), 6.72 (d, 1H, $J = 15.5$ Hz), 6.44 (d, 1H, $J = 15.5$ Hz), 5.45 (s, 0.23H, branched), 5.23 (s, 0.23H, branched), 4.01 (s, 2H), 3.88 (s, 0.46H, branched) $^{13}\text{C}\{^1\text{H}\}$ NMR (CDCl_3 , 75 MHz, δ 77.0): δ 131.7, 131.5, 128.8, 128.8 (branched), 128.8 (branched), 128.7, 128.5, 127.4, 127.2, 127.0, 126.3, 125.5, 121.2 (branched), 120.6 (branched), 115.7 (branched), 115.0 (branched), 112.7 (branched), 37.3, 37.1 (branched). HRMS (EI) m/z calcd for $\text{C}_{15}\text{H}_{13}\text{SBr}$: 303.9921; found: 303.9917.



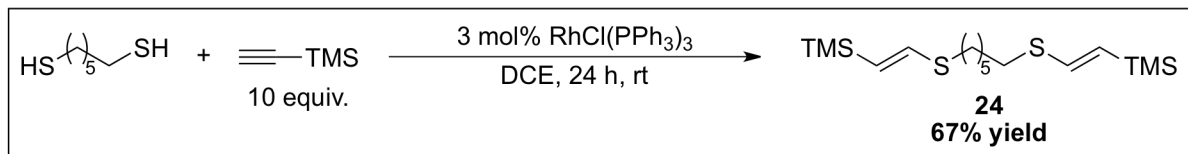
Vinyl sulfide **21**, 4:1 mixture of *E*-linear:branched. ^1H NMR (CDCl_3 , 300 MHz, δ 7.26): δ 7.64 (d, 0.55H, $J = 8.7$ Hz, branched), 7.31 – 7.10 (m, 8.6H), 6.83 (d, 0.6H $J = 8.7$ Hz, branched) 6.79 (d, 2H, $J = 8.7$ Hz), 6.60 (AB q, 2H, $J = 15.5$ Hz), 5.44 (s, 0.28H), 5.21 (s, 0.28H, branched), 3.79 (s, 0.54H, branched), 3.74 (s, 2H), 3.37 (s, 3H), 3.35 (s, 0.99H, branched). Known compound.¹⁴⁴



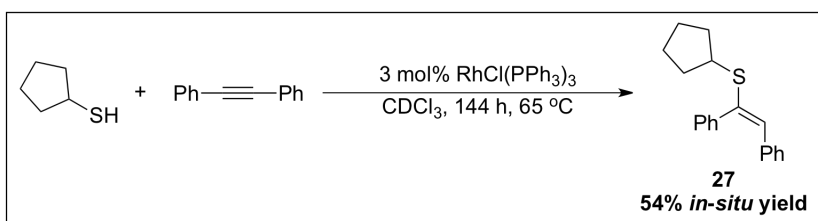
Vinyl sulfide **22**, 8:1 mixture of *E*-linear:branched. ¹H NMR (CDCl₃, 300 MHz, δ 7.26): δ 7.64 (d, 0.55H, *J* = 8.7 Hz, branched), 7.39 – 7.17 (m, 7H), 6.75 (d, 1H, *J* = 15.5 Hz), 6.58 (d, 1H, *J* = 15.5 Hz), 6.34 – 6.32 (m, 1H), 6.27 – 6.26 (m, 1H), 5.50 (s, 0.13H, branched), 5.32 (s, 0.13H, branched), 4.00 (s, 2H), 3.89 (s, 0.26H, branched). Known compound.⁸⁶



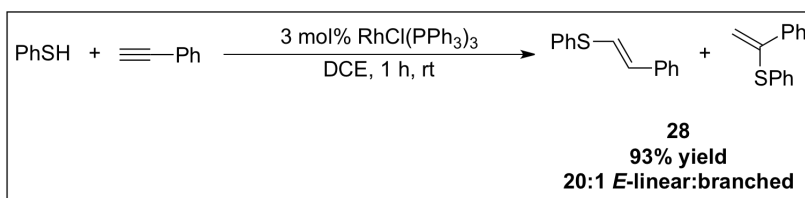
Vinyl sulfide **23**, 8:1 mixture of *E*-linear:branched. ¹H NMR (CDCl₃, 300 MHz, δ 7.26): δ 7.55 – 7.53 (m, 0.35m), 7.37 – 7.17 (m, 6H), 6.69 (d, 1H, *J* = 15.5 Hz), 6.53 (d, 1H, *J* = 15.5 Hz), 5.51 (s, 0.14H, branched), 5.27 (d, 0.14H, branched), 4.11 (t, 2.4H, *J* = 6.4 Hz), 3.07 (t, 2H, *J* = 7.3 Hz), 2.93 (t, 0.35H, *J* = 7.3 Hz, branched), 2.71 (t, 2H, *J* = 7.3 Hz), 2.62 (t, 0.40H, *J* = 7.3 Hz, branched), 1.66 – 1.57 (m, 2.6H), 1.44 – 1.31 (m, 2.4H), 0.93 (t, 4H, *J* = 7.3 Hz). Known compound.⁸⁶



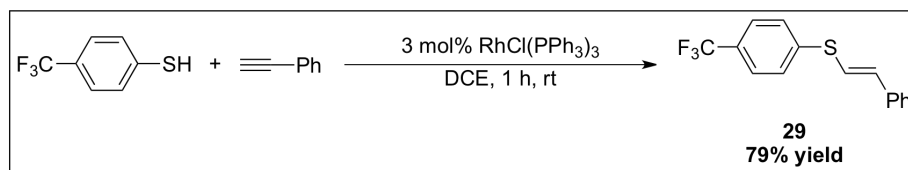
Vinyl sulfide **24**, exclusively the *E*-linear isomer. ^1H NMR (CDCl_3 , 300 MHz, δ 7.26): δ 6.52 (d, 2H, $J = 18.1$ Hz), 5.70 (d, 2H, $J = 18.1$ Hz), 2.73 (t, 4H, $J = 7.3$ Hz), 1.65 (m, 4H), 1.44 (m, 4H), 0.07 (s, 18H). $^{13}\text{C}\{^1\text{H}\}$ NMR (CDCl_3 , 75 MHz, δ 77.0): δ 138.7, 124.6, 31.0, 28.9, 28.5, -1.1. HRMS (APCI) m/z calcd for $\text{C}_{16}\text{H}_{35}\text{S}_2\text{Si}_2$: 347.1719 ($\text{M}+\text{H}$) $^+$; found: 347.1717.



Vinyl sulfide **27**, yield determined *in-situ* with 1,3,5-Trimethoxybenzene as internal standard. Known compound.¹⁴⁴

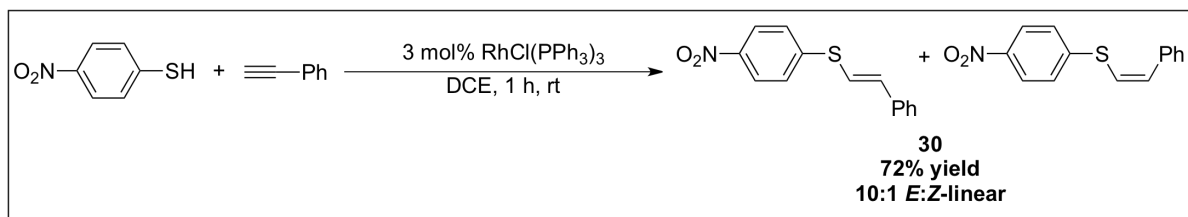


Vinyl sulfide **28**, 20:1 mixture of *E*-linear:branched. ^1H NMR (CD_3CN , 400 MHz, δ 1.94): δ 7.45 – 7.22 (m, 11H), 7.04 (d, 1H, $J = 15.5$ Hz), 6.76 (d, 1H, $J = 15.3$ Hz), 5.75 (s, 0.05H, branched), 5.44 (s, 0.05H, branched). Known compound.¹⁴⁵

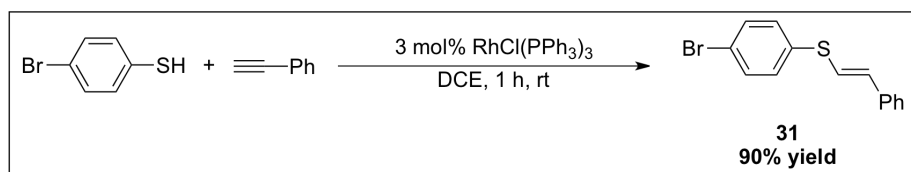


Vinyl sulfide **29**, exclusively the *E*-linear isomer. ^1H NMR (CD_3CN , 400 MHz, δ 1.94): δ 7.64 (d, 2H, $J = 8.3$ Hz), 7.60 (d, 2H, $J = 8.2$ Hz), 7.50 – 7.48 (m, 2H), 7.39 – 7.29 (m, 3H) 7.09 (d, 1H, $J = 15.7$ Hz), 6.96 (d, 1H, $J = 15.4$ Hz). $^{13}\text{C}\{^1\text{H}\}$ NMR (CD_3CN ,

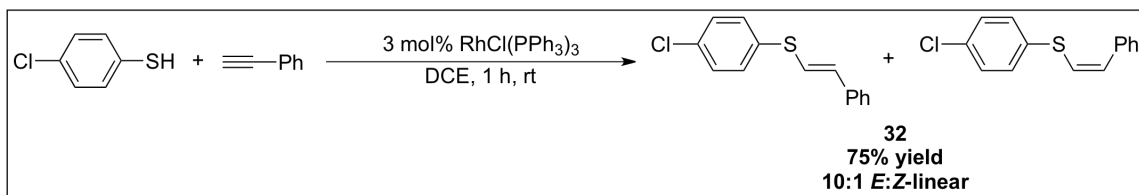
75 MHz, δ 118.26): δ 142.6, 137.1, 136.0, 129.8, 129.4, 129.2, 128.9, 127.4, 126.9 (q, $J = 3.8$ Hz), 121.0, 118.3. $^{19}\text{F}\{^1\text{H}\}$ NMR (CD_3CN , 300 MHz): δ 13.7. HRMS (EI) m/z calcd for $\text{C}_{15}\text{H}_{11}\text{SF}_3$: 280.0534; found: 280.0530.



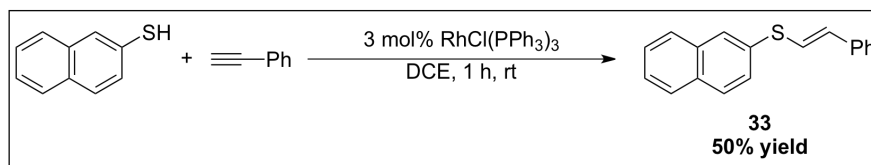
Vinyl sulfide **30**, 10:1 mixture of *E* and *Z*-linear. ^1H NMR (CD_3CN , 400 MHz, δ 1.94): δ 8.19 – 8.14 (m, 4H), 7.72 (d, 1H, $J = 8.8$ Hz), 7.60 (d, 1H, $J = 8.8$ Hz), 7.54 – 7.51 (m, 5H) 7.43 – 7.31 (m, 4H), 7.08 (AB q, 2H, $J = 15.4$ Hz), 6.92 (d, 0.2H, $J = 10.7$ Hz, *Z*-linear), 6.69 (d, 0.2H, $J = 10.7$ Hz, *Z*-linear). Known compound.²³⁹



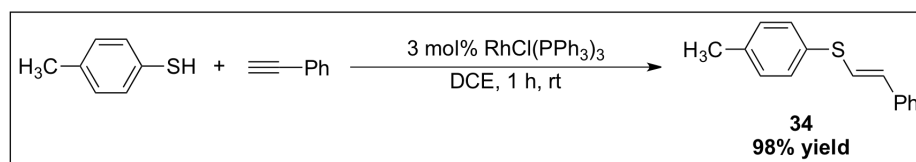
Vinyl sulfide **31**, exclusively the *E*-linear isomer. ^1H NMR (CD_3CN , 400 MHz, δ 1.94): δ 7.52 (d, 2H, $J = 8.5$ Hz), 7.44 – 7.42 (m, 2H), 7.36 – 7.33 (m, 4H), 7.29 – 7.25 (m, 1H), 7.01 (d, 1H, $J = 15.2$ Hz), m, 3H) 6.81 (d, 1H, $J = 15.5$ Hz). Known compound.¹⁴⁷



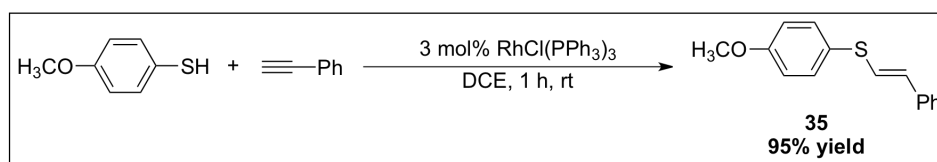
Vinyl sulfide **32**, 10:1 mixture of *E* and *Z*-linear. ^1H NMR (CD_3CN , 400 MHz, δ 1.94): δ 7.50 – 7.25 (m, 12H), 7.01 (d, 1H, $J = 15.5$ Hz), 6.79 (d, 1H, $J = 15.5$ Hz), 6.70 (d, 0.09H, $J = 10.7$ Hz, *Z*-linear), 6.55 (d, 0.09H, $J = 10.7$ Hz, *Z*-linear). Known compound.¹⁴⁷



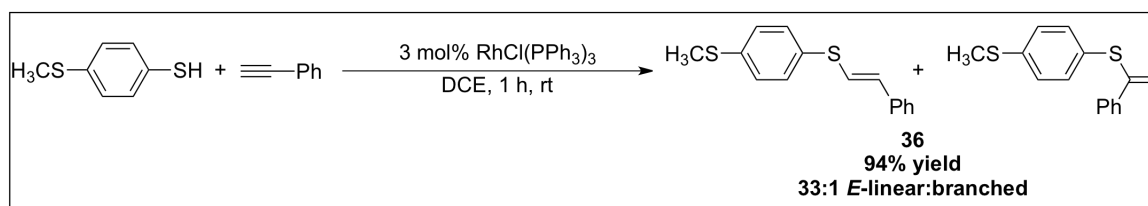
Vinyl sulfide **33**, exclusively the *E*-linear isomer, potentially contaminated with a disulfide or sulfoxide impurity. $^1\text{H NMR}$ (CD_3CN , 400 MHz, δ 1.94): δ 8.06 (br d, 0.4H), 7.99 (br d, 0.2H), 7.93 (br d, 1H), 7.89 – 7.84 (m, 4H), 7.81 – 7.78 (m, 0.5H), 7.67 – 7.65 (dd, 0.5H, $J = 8.7, 2.0$ Hz), 7.59 – 7.55 (m, 0.6H), 7.54 – 7.48 (m, 4H), 7.47 – 7.44 (m, 2H), 7.37 (app t, 2H, $J = 7.5$ Hz), 7.27 (td, 1H, $J = 7.3, 1.2$ Hz), 7.17 (d, 1H, $J = 15.5$ Hz), 6.84 (d, 1H, $J = 15.5$ Hz), 6.73 (s, 0.3H). Known compound.²⁴⁰



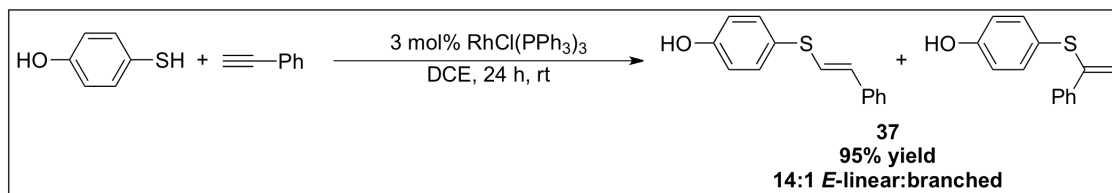
Vinyl sulfide **34**, exclusively the *E*-linear isomer. $^1\text{H NMR}$ (CD_3CN , 400 MHz, δ 1.94): δ 7.41 – 7.20 (m, 10H), 7.01 (d, 1H, $J = 15.6$ Hz), 6.67 (d, 1H, $J = 15.6$ Hz), 2.34 (s, 3H). Known compound.¹⁴⁷



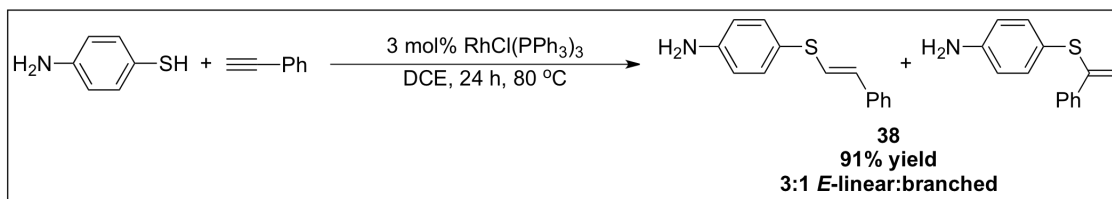
Vinyl sulfide **35**, exclusively the *E*-linear isomer. $^1\text{H NMR}$ (CD_3CN , 400 MHz, δ 1.94): δ 7.42 (d, 2H, $J = 8.9$ Hz), 7.36 – 7.28 (m, 4H), 7.24 – 7.19 (m, 1H), overlapping signals 6.97 (d, 2H, $J = 8.9$ Hz) and 6.96 (d, 1H, $J = 15.5$ Hz), 6.52 (d, 1H, $J = 15.5$ Hz), 3.80 (s, 3H). Known compound.¹⁴⁷



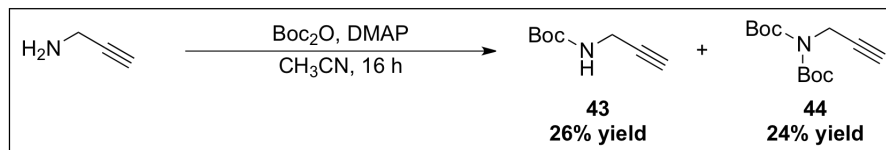
Vinyl sulfide **36**, 33:1 mixture of *E*-linear and branched. ^1H NMR (CD_3CN , 400 MHz, δ 1.94): δ 7.41 – 7.22 (m, 10H), 7.00 (d, 1H, $J = 15.5$ Hz), 6.70 (d, 1H, $J = 15.5$ Hz), 5.69 (s, 0.03H, branched), 5.35 (s, 0.03H, branched), 2.48 (s, 3H). $^{13}\text{C}\{^1\text{H}\}$ NMR (CD_3CN , 100 MHz, δ 118.26): δ 139.1, 137.5, 131.8, 131.6, 131.5, 129.7, 128.5, 127.9, 126.9, 124.5, 15.6. HRMS (EI) m/z calcd for $\text{C}_{15}\text{H}_{14}\text{S}_2$: 258.0537; found: 258.0534.



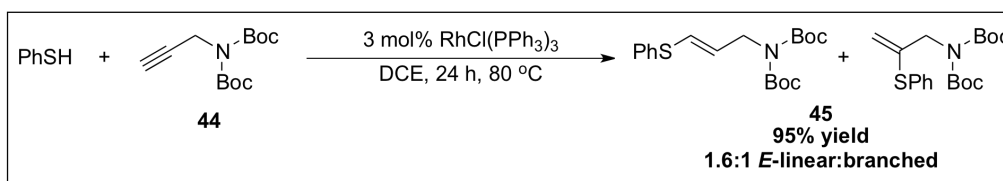
Vinyl sulfide **37**, 14:1 mixture of *E*-linear and branched. ^1H NMR (CD_3CN , 400 MHz, δ 1.94): δ 7.35 – 7.27 (m, 6H), 7.23 – 7.18 (m, 2H), 6.95 (d, 1H, $J = 15.5$ Hz), 6.86 (d, 2H, $J = 8.6$ Hz), 6.47 (d, 1H, $J = 15.5$ Hz), 5.51 (s, 0.07H, branched), 5.00 (s, 0.07H, branched). $^{13}\text{C}\{^1\text{H}\}$ NMR (CD_3CN , 100 MHz, δ 118.26): δ 158.1, 137.7, 134.5, 129.6, 129.1, 128.1, 126.9, 126.7, 123.8, 117.3. HRMS (EI) m/z calcd for $\text{C}_{14}\text{H}_{12}\text{OS}$: 228.0609; found: 228.0610.



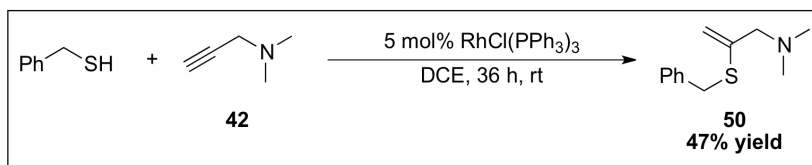
Vinyl sulfide **38**, 3:1 mixture of *E*-linear and branched. ^1H NMR (CD_3CN , 400 MHz, δ 1.94): δ 7.59 – 7.56 (m, 0.9H, branched), 7.35 – 7.16 (m, 10H), 6.92 (d, 1H, $J = 15.5$ Hz), 6.68 (d, 2H, $J = 8.7$ Hz), 6.63 (d, 0.78H, $J = 8.7$ Hz, branched), 6.36 (d, 1H, $J = 15.5$ Hz), 5.43 (s, 0.38H, branched), 4.88 (s, 0.37H, branched), 4.38 (br s, 3H, NH_2). $^{13}\text{C}\{^1\text{H}\}$ NMR (CD_3CN , 100 MHz, δ 118.26): δ 150.9, 149.9, 149.6, 148.5, 143.2, 140.0, 137.9, 136.7, 135.1, 129.6, 129.5, 129.3, 128.2, 127.9, 127.6, 126.5, 119.1, 116.1, 116.0, 111.4. HRMS (ESI) m/z calcd for $\text{C}_{14}\text{H}_{14}\text{NS}$: 228.0847 ($\text{M}+\text{H}$) $^+$; found: 228.0845.



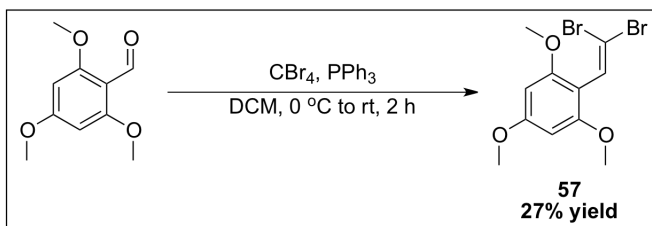
Propargyl amine substrates **43** and **44** were prepared according to a literature procedure.²³⁶ To a solution of propargyl amine (1.2 mL, 18.7 mmol) in 10 mL of CH₃CN was added Boc₂O (10.8 mL, 47 mmol, 2.5 equiv.). The Boc₂O was added by syringe, after allowing the bottle to reach roughly 40 °C in a hot water bath. To this solution was added DMAP (2.2295 g, 18.7 mmol) in one portion, and the mixture was stirred overnight. The mixture was diluted with ethyl acetate (30 mL) and the organic layer separated. The organic layer was then washed with water (10 mL) and brine (10 mL), dried over Na₂SO₄, then filtered and concentrated *in-vacuo*. The crude mixture was then purified by column chromatography with 9:1 hexanes:ethyl acetate as eluent, which was gradually increased to 1:1 hexanes:ethyl acetate. Visualization of the propargyl amines during elution was facilitated by a KMnO₄ stain. This provided **43** in 26% yield and **44** in 24% yield, respectively. Propargyl amine **43**: ¹H NMR (CD₃CN, 400 MHz, δ 1.94): δ 5.56 (br s, 1H, NH), 3.80 – 3.78 (dd, 2H, *J* = 2.4, 5.9 Hz), 2.42 (t, 1H, 2.4 Hz), 1.41 (s, 9H). Propargyl amine **44**: ¹H NMR (CD₃CN, 400 MHz, δ 1.94): δ 4.29 (d, 2H, *J* = 2.4 Hz), 2.45 (t, 1H, *J* = 2.4 Hz), 1.49 (s, 19H). Known compounds.²³⁶



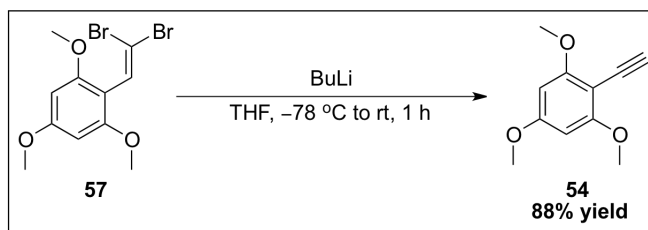
Vinyl sulfide **45**, 1:6:1 mixture of *E*-linear and branched. ¹H NMR (CD₃CN, 400 MHz, δ 1.94): δ 7.55 – 7.52 (m, 0.5H), 7.44 – 7.25 (m, 9H), 6.40 – 6.37 (dt, 1H, *J* = 1.2, 15.1 Hz), 5.87 – 5.83 (dt, 1H, 6.2, 15.0 Hz), 5.32 (t, 0.6H, *J* = 1.4 Hz, branched), 5.15 (t, 0.6H, *J* = 1.4 Hz, branched), 4.26 (t, 1H, *J* = 1.4 Hz, branched), 4.20 – 4.18 (dd, 2H, 1.2, 6.2 Hz), 1.46 (s, 19H), 1.45 (s, 12H branched). ¹³C{¹H} NMR (CD₃CN, 100 MHz, δ 118.26): δ 153.1, 153.0, 141.9, 135.9, 132.9, 130.4, 130.3, 130.2, 130.1, 128.8, 128.5, 127.9, 126.3, 118.3, 116.0, 83.3, 83.2, 50.9, 48.4, 28.2, 28.1. HRMS (ESI) *m/z* calcd for C₁₉H₂₇NO₄NaS: 388.1559 (M+Na)⁺; found: 388.1555.



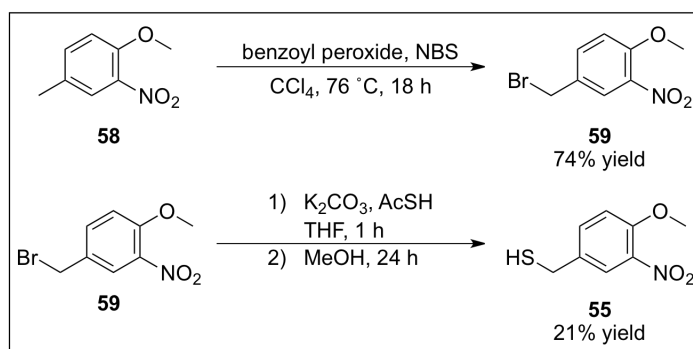
Vinyl sulfide **50**, exclusively the branched isomer. Chromatographic purification of **50** necessitated the use of 3:1 hexanes:ethyl acetate, which was spiked with small amounts of ammonium hydroxide or methanol to facilitate elution. ¹H NMR (CD₃CN, 400 MHz, δ 1.94): δ 7.40 – 7.23 (m, 5H), 5.20 (t, 1H, *J* = 1.2 Hz), 4.88 (br s, 1H), 3.97 (s, 2H), 3.01 (s, 2H), 2.15 (s, 6H). ¹³C{¹H} NMR (CD₃CN, 75 MHz, δ 118.26): δ 145.5, 138.5, 129.7, 129.4, 128.0, 118.3, 108.6, 66.5, 45.1, 36.0. HRMS (ESI) *m/z* calcd for C₁₂H₁₈NS: 208.1160 (M+H)⁺; found: 208.1159.



Dibromoolefin **57** was prepared according to a literature procedure.²²³ To a flame dried round bottom equipped with a magnetic stir bar and serum cap was added 2,4,6-trimethoxybenzaldehyde (5.0214 g, 25.6 mmol, 0.43 M) and 60 mL of DCM. To this was added PPh₃ (13.4897 g, 51.4 mmol, 2 equiv.), which was recrystallized in toluene prior to use. The solution was then cooled to 0 °C and CBr₄ (10.0443 g, 30.3 mmol, 1.2 equiv.) was added in 10 mL of DCM. The clear solution immediately turned an orange-red and was left to stir for 2 hours. The crude mixture was then concentrated *in-vacuo*, dissolved in DCM, and fused to dry SiO₂. The crude dibromoolefin was then purified by column chromatography with 9:1 hexanes:ethyl acetate as eluent, which was gradually increased to 3:1 hexanes:ethyl acetate, providing **57** in 27% yield. ¹H NMR (CD₃CN, 400 MHz, δ 1.94): δ 7.19 (s, 1H), 6.20 (s, 2H), 3.81 (s, 3H), 3.79 (s, 6H). Known compound.²²³

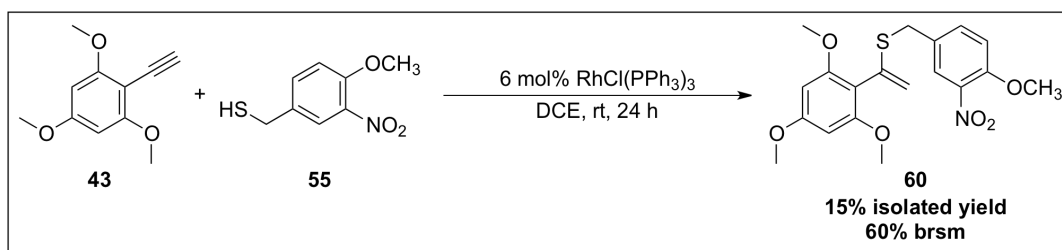


Alkyne **54** was prepared according to a literature procedure.²²³ To a flamed dried round bottom equipped with a magnetic stir bar and a serum cap was added **57** (1.941 g, 5.5 mmol) in 34 mL of THF. The solution was cooled to $-78\text{ }^\circ\text{C}$ and *n*-BuLi was added (4.9 mL, 2.39 M in hexanes, 11.6 mmol, 2.1 equiv.). The solution of *n*-BuLi was titrated against *N*-benzylbenzamide prior to use.²⁴¹ The solution was stirred for 5 minutes at $-78\text{ }^\circ\text{C}$, before being warmed to room temperature and the reaction progress monitored by TLC. The reaction was complete following 1 hour and was then quenched with water. The aqueous layer was extracted with ethyl acetate (3 x 10 mL). The combined organic layers were then washed with brine (1 x 10 mL), and dried over Na_2SO_4 , filtered and concentrated *in-vacuo*. The crude mixture was then purified by column chromatography with 9:1 hexanes:ethyl acetate as eluent, which was gradually increased to 2:1 hexanes:ethyl acetate, providing alkyne **54** in 88% yield. $^1\text{H NMR}$ (CD_3CN , 400 MHz, δ 1.94): δ 6.19 (s, 2H), 3.82 (s, 9H), 3.52 (s, 1H). Known compound.²²³

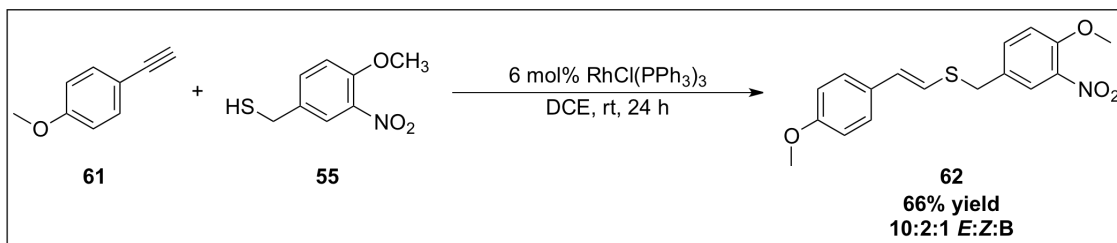


Thiol **55** was prepared from bromide **59** according to a literature procedure.^{223,242} To a flame dried round bottom equipped with a magnetic stir bar and a serum cap was added **58** (5.5 mL, 40 mmol) in 150 mL of CCl_4 . To this was added benzoyl peroxide (1.2935 g, 4 mmol, 75% reagent purity), followed by *N*-bromosuccinimide (8.5124 g, 47.8 mmol, 1.2 equiv.), and the mixture heated to reflux overnight. The following day the mixture was

cooled and diluted with water. The aqueous layer was then extracted with DCM (3 x 30 mL), and the combined organic layers washed with water (1 x 30 mL), brine (1 x 30 mL). The combined organic layers were then dried over Na₂SO₄, filtered and concentrated *in-vacuo*. Crude **59** was fused to SiO₂ and purified by column chromatography with 9:1 hexanes:ethyl acetate, which was gradually increased to 3:1 hexanes:ethyl acetate. The purified sample of **59** was then dissolved in anhydrous THF and K₂CO₃ (1.5221 g, 11 mmol, 2.2 equiv.) was added. To this was added thioacetic acid (0.43 mL, 6.1 mmol, 1.2 equiv.) and the mixture stirred at room temperature for 1 hour. The flask was then charged with MeOH (15 mL) and the solution stirred overnight. The solution was then neutralized with HCl, and the aqueous layer was extracted with CHCl₃ (2 x 10 mL). The combined organic layers were then washed with water (1 x 10 mL) and brine (1 x 10 mL). The organic layers were then dried over Na₂SO₄, filtered and concentrated *in-vacuo*. The crude thiol was then purified by column chromatography with 9:1 hexanes:ethyl acetate as eluent, which was gradually increased to 1:1 hexanes:ethyl acetate, providing **55** in 21% yield. ¹H NMR (CD₃CN, 400 MHz, δ 1.94): δ 7.78 (d, 1H, *J* = 2.1 Hz), 7.57 – 7.55 (dd, 1H, *J* = 2.1, 8.6 Hz), 7.17 (d, 1H, *J* = 8.6 Hz), 3.91 (s, 3H), 3.73 (d, 2H, *J* = 8.1 Hz), 2.16 (t, 1H, *J* = 8.1 Hz). Known compound.²²³



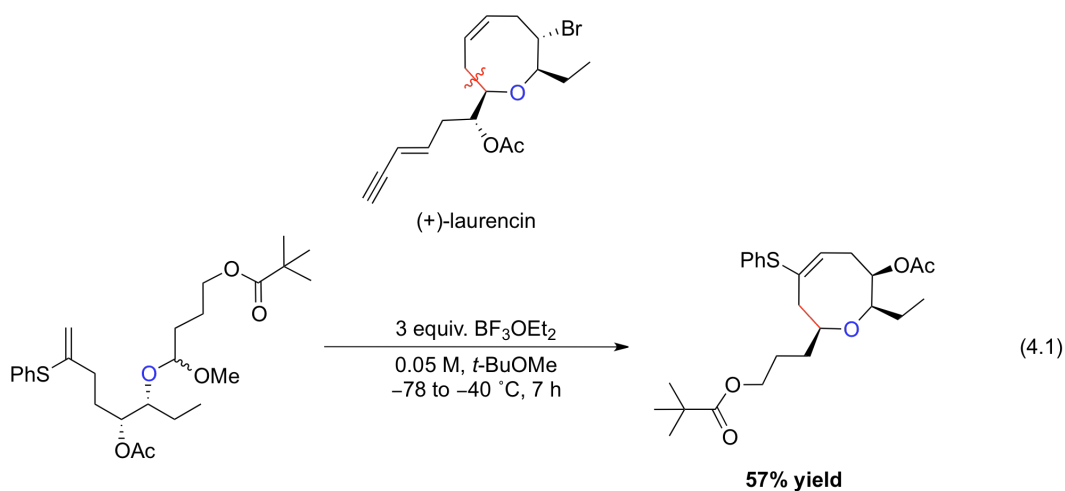
Vinyl sulfide **60**, mixture of branched isomer and an impurity similar to thiol **55**. ¹H NMR (CD₃CN, 400 MHz, δ 1.94): δ 7.76 (d, 1H, *J* = 2.3 Hz), 7.56 – 7.54 (dd, 1H, *J* = 2.3, 8.7 Hz), 7.27 – 7.25 (dd, 1H, *J* = 2.1, 8.6 Hz), 7.22 (d, 1H, 2.2 Hz), 7.17 (d, 1H, *J* = 8.7 Hz), 7.01 (d, 1H, 8.6 Hz), 6.05 (s, 2H), 5.91 (s, 1H, branched), 5.44 (s, 1H, branched), 3.91 (s, 6H), 3.87 (s, 3H), 3.76 (s, 3H), 3.56 (s, 6H), 3.55 (s, 2H).



Vinyl sulfide **62**, mixture of all regioisomers. Representative signals: ^1H NMR (CD_3CN , 400 MHz, δ 1.94): δ 6.65 (d, 1H, $J = 15.6$ Hz), 6.48 (d, 1H, $J = 15.6$ Hz), 6.41 (d, 0.17H, $J = 10.8$ Hz, Z-linear), 6.19 (d, 0.17H, $J = 10.8$ Hz, Z-linear), 5.42 (s, 0.12H, branched), 5.14 (s, 0.12H, branched).

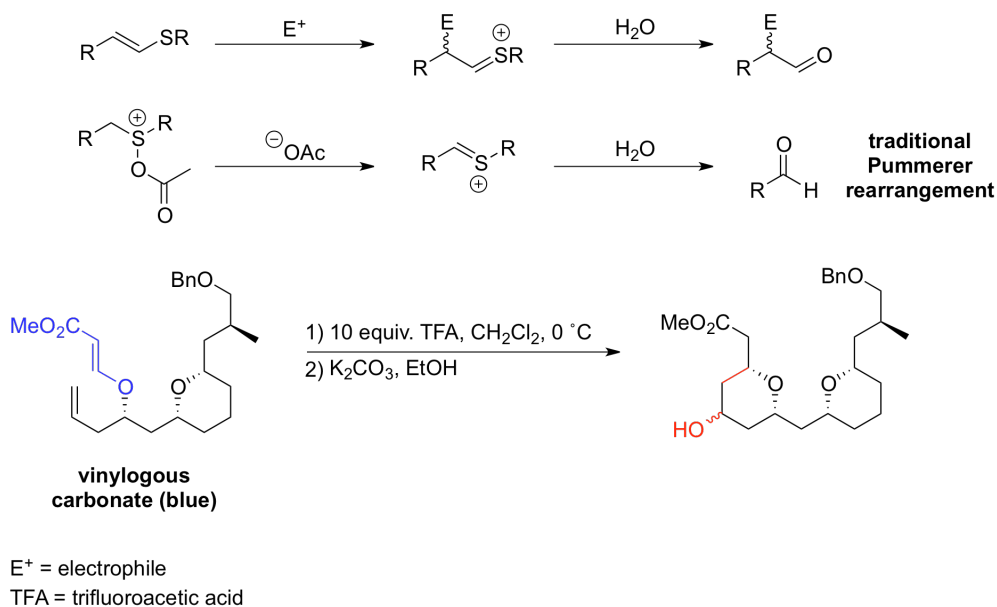
Chapter 4 Applications of Alkyne Hydrothiolation

The success of our alkyne hydrothiolation methodology for the synthesis of aryl and alkyl vinyl sulfides led us to further explore the utility of these intermediates. As vinyl sulfides are equivalent to thioenol ethers, these compounds are capable of reacting with a variety of electrophiles under appropriate conditions. This was exploited in Overman's synthesis of (+)-laurencin, where the branched vinyl sulfide reacted with the oxonium ion formed upon Lewis acid activation of the acetal (Eq. 4.1). The product of this Prins-type cyclization was then elaborated into (+)-laurencin in several steps upon removal of the phenyl sulfide moiety with Raney nickel.²⁴³



Similarly, vinyl sulfides can be directly converted into the respective aldehyde or ketone upon treatment with aqueous acid. This is due to the susceptibility of the thionium ion to hydrolysis, following the protonation of the alkene (Scheme 4.1). This transformation is functionally equivalent to the Pummerer rearrangement discussed in Section 1.3.1; however, oxidation to the corresponding sulfoxide is unnecessary in obtaining the thionium species. We became interested in inducing the formation of this species in the presence of Lewis or Brønsted acids, in order to initiate cascade carbon-carbon bond forming events. Indeed, examples of Brønsted acid activation of vinylogous carbonates are known, and are often accompanied by subsequent Prins-like reactivity of the resulting oxonium ion.²⁴⁴ The use of vinylogous thioesters in related processes is relatively unknown, inspiring us to pursue the use of these functionalities in other processes. To this end, we elected to evaluate the reactivity of vinylogous thioesters within the context of the Nazarov cyclization. The

following sections discuss mechanistic details regarding the electrocyclic nature of the Nazarov reaction, relevant substituent effects, and the use of this process in initiating cascade bond forming events.

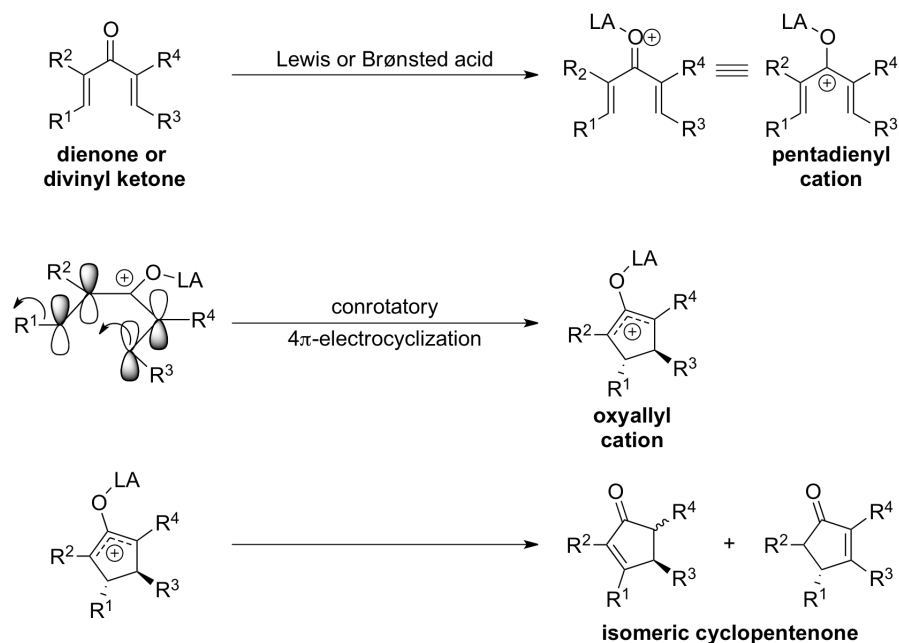


Scheme 4.1

4.1 Divinyl Ketones and the Nazarov Cyclization

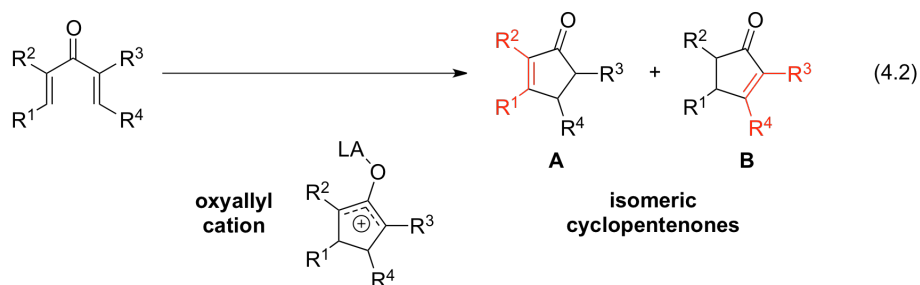
The Nazarov cyclization involves the treatment of dienones with Lewis or Brønsted acid activators, which effectively generate reactive pentadienyl cations. Consequently, these intermediates undergo a conrotatory 4π -electrocyclization to give an oxyallyl cation, which eventually converts into the corresponding cyclopentenone. This process typically occurs by deprotonation proximal to the carbocation, thereby generating the alkene, followed by protonation or tautomerization of the enol or enolate. The electrocyclic nature of this reaction allows for high atom economy and diastereoselectivity, based upon the conservation of orbital symmetry (Scheme 4.2). The full potential of this transformation has only recently been uncovered, and is largely attributable to a greater understanding of substituent effects on the reactivity of the requisite divinyl ketones.²⁴⁵⁻²⁴⁸ Additionally, the ability of the oxyallyl cation to participate in cascade bond forming processes has enabled the use of this cyclization in complex molecules synthesis.²⁴⁹⁻²⁵¹ This synthetic strategy involves the nucleophilic or electrophilic interception of the oxyallyl cation, often leading to a considerable gain in molecular complexity. The following sections highlight substitution-

reactivity patterns, and the discovery of this so-called “interrupted” Nazarov cyclization.



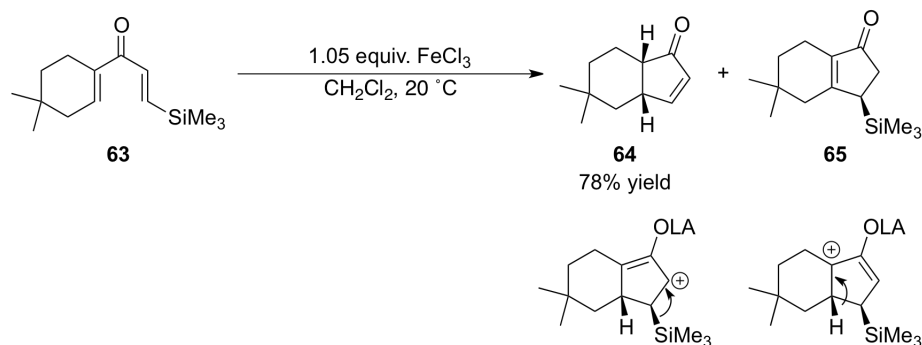
4.1.1 Substituent Effects on the Reactivity of Dienones

A cursory inspection of the intermediates involved in the Nazarov cyclization reveals a number of potential caveats in applying this transformation in complex molecule synthesis. Of particular significance is the lack of control available for the regioselective formation of the cyclopentenone products from unsymmetrical dienones (Eq. 4.2). Differentiation of cyclopentenone **A** from **B** derives from the collapse of the intermediate oxyallyl cation. The electrophilic nature of this intermediate can be biased towards a particular side of the cyclopentyl nucleus by careful selection of carbocation stabilizing functional groups.



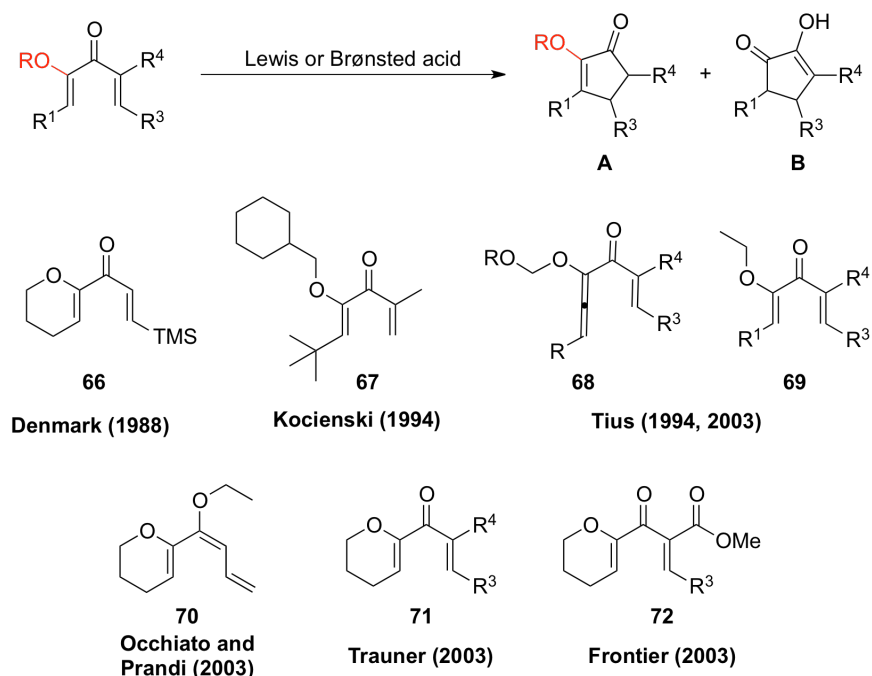
One of the first examples of regioselective elimination involved substitution of R^1 or R^4 with a trialkylsilane, providing hyperconjugative stabilization of the oxyallyl cation intermediate through the β -silyl effect.²⁵²⁻²⁵⁴ The Nazarov cyclization of dienone **63** illustrates

this concept, where exclusive formation of cyclopentenone **64** occurs based upon the directing influence of the trimethylsilyl group (Scheme 4.3).



Scheme 4.3

A separate strategy for biasing the collapse of the oxyallyl cation rests upon the incorporation of electron donating substituents at R² and R³.²⁵⁴ Denmark studied this in conjunction with the trialkylsilane directed Nazarov cyclizations, which involved treating divinyl ketone **66** with a variety of Lewis acids (Scheme 4.4). This substrate appeared to readily undergo reaction with Lewis acids; however, no cyclopentenone products were observed. In an unrelated study, divinyl ketone **67** appeared to undergo the Nazarov cyclization, affording cyclopentenone of type **B**.²⁵⁵ This product is the result of the hydrolysis of the enol ether (**A**), giving the α -diketone, which is drawn as the enol tautomer. Similarly, Tius synthesized α -alkoxy allene substituted divinyl ketones (**68**), which undergo the Nazarov cyclization under mild conditions. Tius later reported the use of divinyl ketones (**69**) in palladium-catalyzed Nazarov cyclizations, where adventitious acid induces formation of cyclopentenones of type **B**. The use of Brønsted acids for initiating this cyclization simply provided the acyclic diketones and not the desired cyclopentenones.^{256, 257}

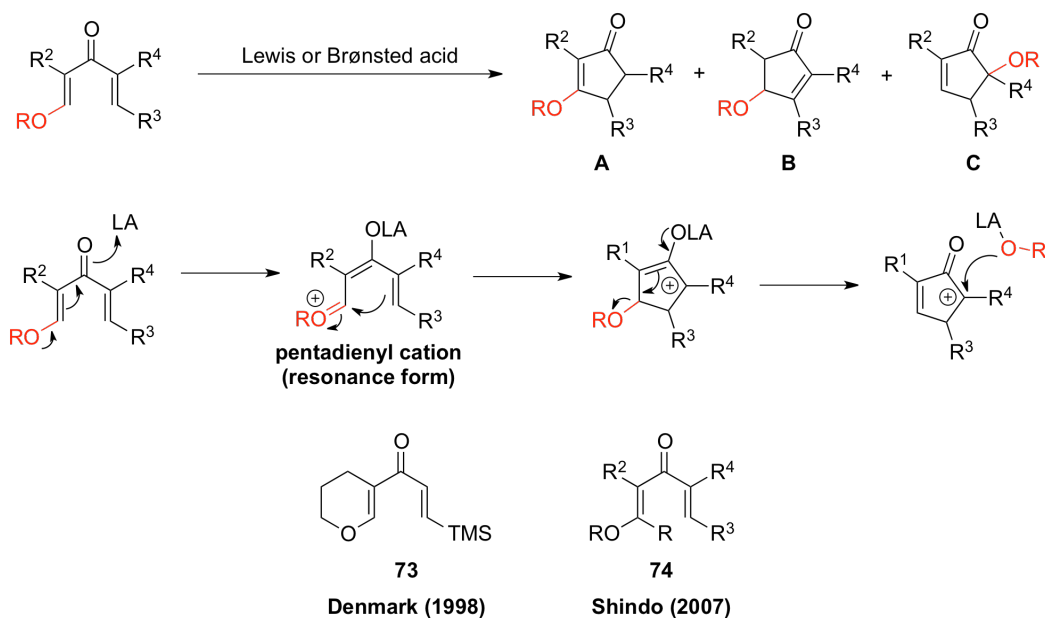


Scheme 4.4

Likewise, several authors reported the use of similar divinyl ketones (**70-72**) in Brønsted and Lewis acid initiated Nazarov cyclizations. Treatment of **70** with Brønsted acids generates the corresponding divinyl ketone, or in select cases, leads directly to the cyclopentenone (**A**).^{245, 258, 259} Divinyl ketones **71** and **72** cyclize with catalytic amounts of Lewis acid, demonstrating the enhanced reactivity of these substrates relative to compounds lacking heteroatom substitution at R². The mild nature of these procedures allow for the isolation of cyclopentenones of type (**A**), where hydrolysis of the enol ether is not observed. Lastly, compound **72** possesses several noteworthy features in allowing for regioselective formation of cyclopentenone (**A**). Substitution of R³ with the methyl ester allows for bidentate chelation of transition metal Lewis acids, effectively locking the substrate in the reactive conformation shown. Additionally, the dihydropyran oxygen serves to enhance the nucleophilicity of the left-hand portion, where the methyl ester at R³ increases the electrophilicity of the right-hand portion. This is believed to “polarize” the divinyl ketone, allowing for facile Nazarov cyclization.^{245, 246}

Conversely, the substitution of R¹ or R⁴ with an electron donating group (EDG) typically reduces the overall rate of reaction, relative to the rate enhancement observed for R²

and R³. A noteworthy exception is the successful cyclization of divinyl ketone **73**, where the analogous substrate (**66**) did not afford any observable cyclopentenone products. The observed reduction in rate for compounds like **73** and **74** is rationalized by the stabilization of the pentadienyl cation by the electron rich vinylogous ester (Scheme 4.5). This form also explains how the rearrangement product (**C**) forms during cyclization, where addition to the oxonium ion generates the oxyallyl cation. This intermediate can then undergo unimolecular elimination (by conjugate base, E1cB) followed by nucleophilic interception of the carbocation giving cyclopentenone (**C**).²⁶⁰ The tertiary α -hydroxyketones afforded through such a rearrangement are synthetically useful molecules present in a variety of agrochemicals.²⁶¹ The use of divinyl ketones (**74**) are also capable of undergoing cyclization with catalytic Lewis or Brønsted acids. However, no cyclization is observed if these substrates lack substitution at R³.



Scheme 4.5

Lastly, substituents in positions R² and R³ may positively influence the conformation of the divinyl ketone, which may lead to an increase in the rate of cyclization. Typically, the U-shaped conformation is preferred if the olefin geometries are consistent with that depicted in Figure 4.1. If R¹ or R⁴ faces towards the center of the divinyl ketone, the less reactive S or W-form may predominate, in order to minimize steric repulsion of these groups. However, the ground state conformation of the divinyl ketone does not exclusively determine whether

cyclization occurs. Upon coordination of a Lewis acid, all forms may fluctuate, thus slowly populating the reactive U-shaped conformation. Nonetheless, substituents that reinforce the adoption of the U-shaped divinyl ketone allow for more facile Nazarov cyclization, and often require less forcing conditions.

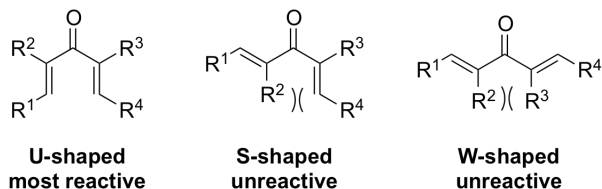
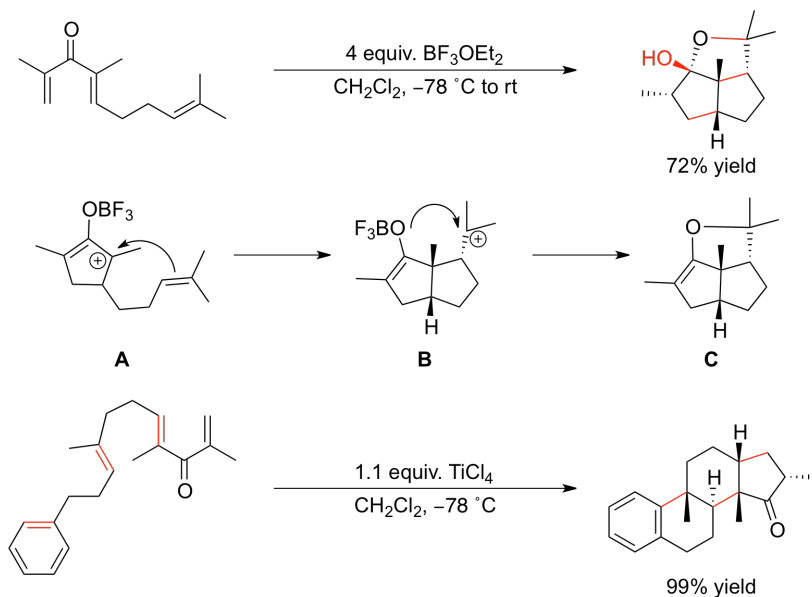


Figure 4.1 Possible Conformations for Substituted Divinyl Ketones

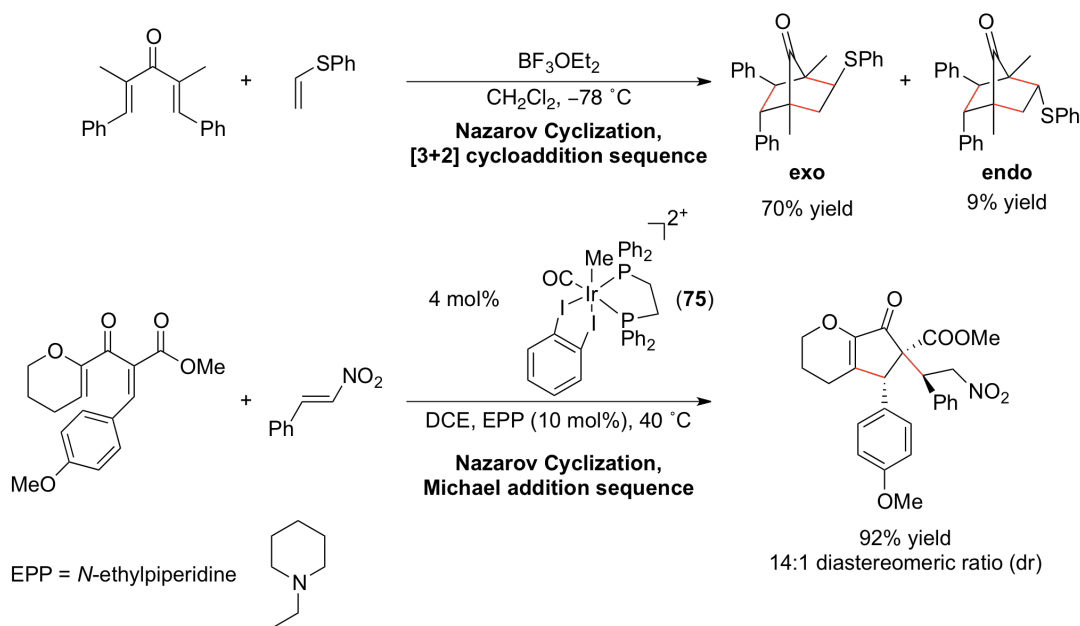
4.1.2 Cascade Processes Involving the Nazarov Cyclization

The ability to intercept the oxyallyl cation with alkene nucleophiles was originally discovered by Frederick West. The example in Scheme 4.6 demonstrates that treatment of the illustrated dienone with an excess of boron trifluoride diethyl etherate (BF_3OEt_2) initiated a cationic cascade. This involves attack of the pendant olefin on the tertiary carbocation, forming intermediate **(B)**, which then undergoes a subsequent enolate *O*-alkylation generating the cyclic enol ether **(C)**. It was reported that the hemiketal formed is a consequence of the acid hydrolysis of **(C)**, which occurs during the reaction workup. Overall, this reaction forms two carbon-carbon bonds, two oxygen-carbon bonds, and 5 stereogenic with excellent diastereoselectivity.²⁴⁷ The similarity of this transformation to the cationic polycyclizations described by Johnson and coworkers²⁶² prompted a further study of nucleophiles capable of intercepting the oxyallyl cation. To this end, the West group reported the use of various arenes in terminating cascade processes initiated by the Nazarov cyclization (Scheme 4.6). This particular reaction required the use of a small excess of titanium tetrachloride, where BF_3OEt_2 failed to provide the tetracyclic product shown below.²⁴⁸ The dramatic increase in molecular complexity afforded by the Nazarov cyclization of acyclic dienones demonstrates the synthetic potential of this reaction in the synthesis of natural products.



Scheme 4.6

Since the initial reports of the interrupted Nazarov cyclization, several cascade processes have been developed that rely on the generation of an oxyallyl cation.²⁶³⁻²⁹³ The previous examples illustrate the nucleophilic capture of this reactive intermediate; however, it is possible to intercept the enol or enolate portion as well. This may function as part of a cycloaddition process, or through reaction with carbonyl electrophiles. As illustrated in Scheme 4.7, vinyl sulfides may serve as electron rich dipolarophiles in [3+2]-cycloadditions with the intermediate oxyallyl cations generated during the Nazarov Cyclization. Furthermore, the second example illustrates the mild nature of catalytic Nazarov cyclizations, where coordination of the electron deficient iridium species (**75**) generates the pentadienyl cation. This coordination is largely facilitated by the neighbouring ester and helps lock the compound in the conformation most conducive to cyclization. For clarity the [3,5-bis(trifluoromethyl)phenyl] borate (BARF) counterions are omitted. The use of *N*-ethylpiperidine serves to generate the requisite enolate necessary for Michael addition to the α , β -unsaturated nitro compound.

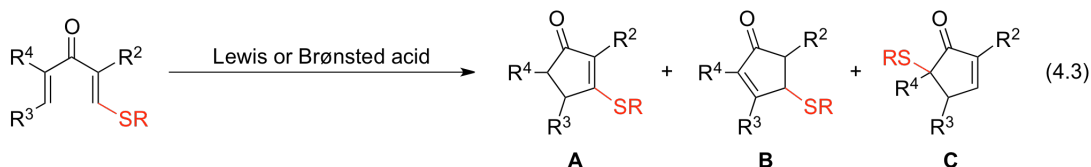


Scheme 4.7

While not exhaustive, the examples above demonstrate the synthetic potential of Nazarov cyclizations in rapidly generating molecular complexity. For this reason, the Nazarov cyclization has undergone resurgence in the literature, particularly in the synthesis of complex natural products.^{249-251, 256, 261, 293-306}

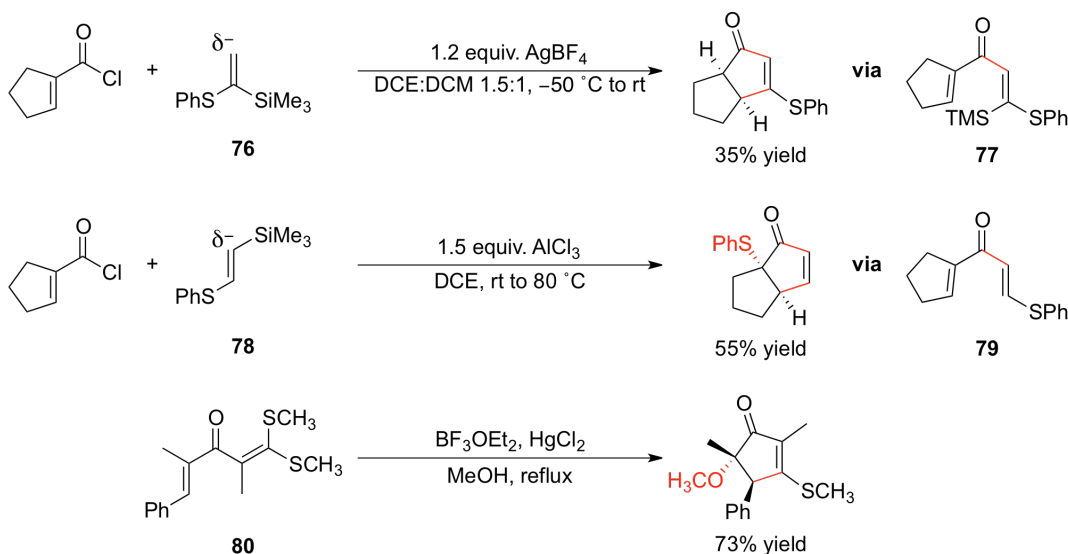
4.2 Vinyl Sulfide Containing Divinyl Ketones

The ability of vinylogous esters to engage in the Nazarov cyclization prompted us to evaluate whether this is possible for the analogous thioesters (Eq. 4.3). The products formed will likely reflect that of the oxygen derivatives, where preference for cyclopentenones (**A**) and (**B**) will depend on substitution at positions R²-R⁴. The formation of cyclopentenone (**C**) is representative of a cyclization-E1cB sequence, where the sulfur species eliminated may intercept the oxyallyl cation.



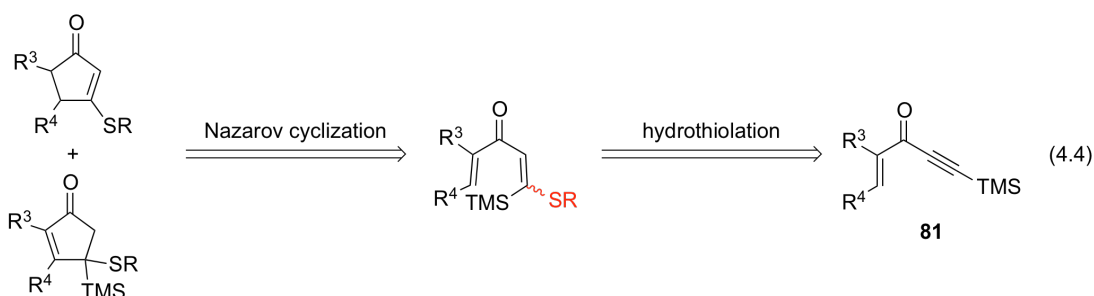
Indeed, limited examples of sulfur substitution at R¹ in divinyl ketones are present within the literature (Scheme 4.8). The majority of examples involve the generation of

vinyllogous thioesters through Friedel-Crafts type substitution of acyl halides, with sulfur-substituted vinyl silanes **76** and **78**.³⁰⁷ These vinyl sulfides are generated through addition of phenylsulfenyl chloride to vinyltrimethylsilane followed by base catalyzed elimination of chloride, forming **76**. Alternatively, **78** was synthesized by UV-irradiation of a mixture of thiophenol and ethynyltrimethylsilane. The complementary reactivity of the branched derivative (**76**) allowed for controlled formation of the indicated cyclopentenone. This is a result of the stabilization afforded by the trimethylsilyl group on the formation of the oxyallyl cation. Interestingly, the regioisomer (**78**) leads to cyclopentenone (type **C**) through cyclization and elimination of thiophenol. This is echoed in the use of the vinyllogous thioketal (**80**), where an analogous process occurs, with the exception that MeOH intercepts the oxyallyl cation generated through cyclization.³⁰⁸ The synthesis of divinyl ketone (**80**) involves the treatment of the corresponding α , β -unsaturated ketone with an enolizable base, followed by addition of carbon disulfide and excess methyl iodide. Based upon the use of toxic mercury (II) salts in the cyclization of (**80**) and the hazardous materials required for the synthesis of this material, we elected to pursue cyclizations similar to **77** and **79**.



The ability of divinyl ketone (**77**) to engage in Nazarov cyclizations as part of one-pot processes inspired us to synthesize similar compounds and evaluate their reactivity with Lewis acids (Eq. 4.4). However, the harsh conditions employed for the synthesis of divinyl ketones **77** and **79** led us to choose an alternate route based upon our hydrothiolation

methodology. Encouraged by the high level of chemoselectivity for alkyne versus alkene hydrothiolation with Wilkinson's catalyst, treatment of **81** could lead to the formation of the requisite divinyl ketones. However, our evaluation of substrate scope for this process identified ynones as challenging substrates for alkyne hydrothiolation, where all vinyl sulfide regioisomers were formed. This is presumably through uncatalyzed conjugate addition processes, prompting us to explore simple base-mediated procedures for the synthesis of sulfur-substituted dienones.



4.2.1 Hydrothiolation Approach to Divinyl Ketones (Substrate Design)

To ensure chemoselectivity in the conjugate addition, we elected to explore substrates where substituents R^3 and R^4 preclude Michael addition to the conjugated enone. Embedding these groups within a heteroaromatic ring satisfies this requirement, guaranteeing exclusive reaction at the ynone (Figure 4.2). These substrates could be synthesized by the addition of bistrimethylsilylacetylene to the corresponding acyl halide, or by a Sonogashira-type cross-coupling process.^{309, 310}

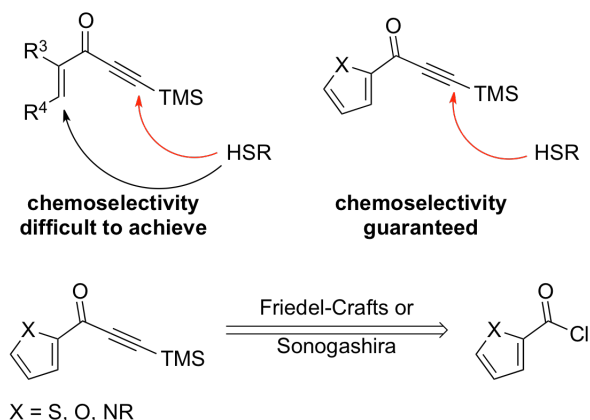
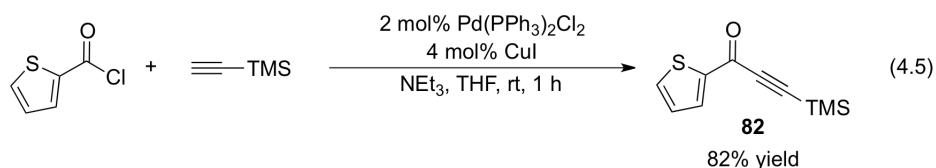
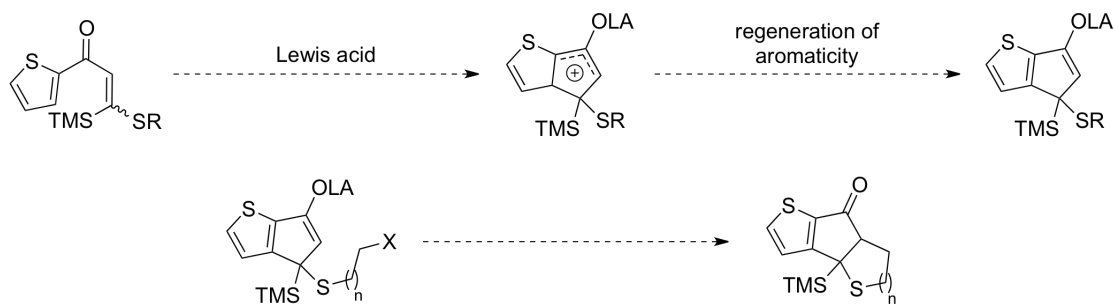


Figure 4.2 Chemoselectivity for Cross-Conjugated Ynones

Gratifyingly, such a cross-coupling methodology exists for the synthesis of heterocyclic substituted ynones.³¹⁰ Additionally, this procedure was adapted into a one-pot process for the preparation of pyrimidines, by addition of amidinium or guanidinium salts to the crude ynone. This inspired us to attempt a similar one-pot procedure for the synthesis of vinylogous thioesters involving the addition of an appropriate sulfur compound. As the coupling between 2-thiophenecarbonyl chloride is known to occur with ethynyltrimethylsilane, we decided that this would be an appropriate starting point (Eq. 4.5).³¹⁰



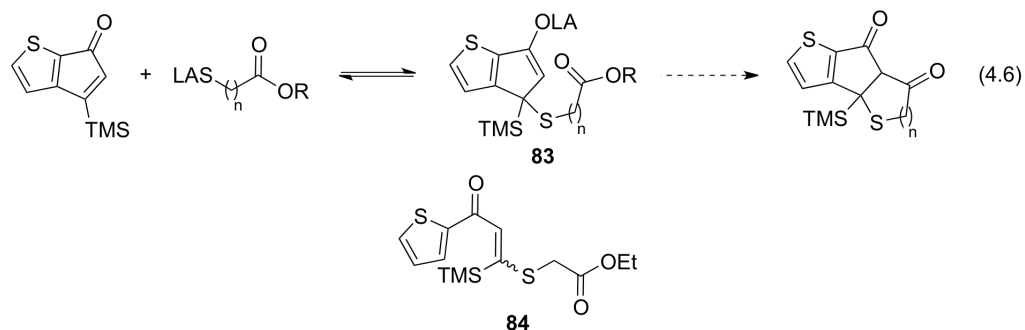
A separate advantage in choosing heterocyclic divinyl ketones derived from ynone (**82**), is the selective collapse of the oxyallyl cation, generating a single cyclopentanone. This relates to the low barrier for regeneration of aromaticity, which will likely be more influential than a β -silyl effect (Scheme 4.9). If regeneration of aromaticity does occur, we hoped that thiols with suitable X groups would induce nucleophilic attack from the incipient enolate, constituting an interrupted Nazarov cyclization.



Scheme 4.9

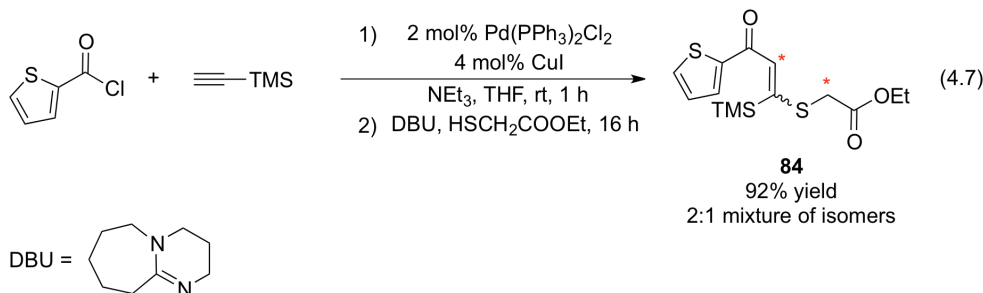
For example, we rationalized that an ester would serve as a suitable electrophile, allowing for an unprecedented interruption of the Nazarov cyclization, involving subsequent Dieckmann condensation. Additionally, the use of a pendant ester could avoid potential complications stemming from elimination of the thiol, as an equilibrium between the enolate (**83**) and free thiol may be established (Eq. 4.6). Upon addition of the thiol to the enone, the tricyclic product could eventually be formed, ideally preventing any further elimination

reactions. This process is known in the literature in contexts separate from electrocyclizations, and has been used to form interesting sulfur heterocycles.³¹¹



4.2.2 Synthesis of **84** and Optimization of Conditions for the Nazarov Cyclization

The decision to explore sulfur-substituted divinyl ketones with pendant esters led us to choose **84** as an initial substrate for the Nazarov cyclization. We hoped that a suitable Lewis acid would induce both cyclization and concomitant Dieckmann condensation to form the tricycle shown in Eq. 4.6. The synthesis of divinyl ketone (**84**) commenced with the aforementioned Sonogashira cross-coupling (Eq. 4.5 and 4.7). Furthermore, it was found that the resulting ynone could be intercepted by the addition of 1,8-diazabicyclo[5.4.0]undec-7-ene (DBU) and ethyl thioglycolate in a one-pot procedure. The ability of ynone to act as Michael-acceptors obviates the need for transition metal catalysts in the synthesis of vinylogous thioester **84**. Using this method, the desired divinyl ketone (**84**) could be produced in 92% yield, as a 2:1 mixture of olefin isomers. Interestingly, when this reaction was stopped after 2 hours, divinyl ketone (**84**) formed as a 14:1 mixture of the *E* and *Z*-linear vinyl sulfide in 93% yield, rather than an equal mixture of olefin isomers. The origin of the observed selectivity is difficult to rationalize, but may result from a thiophene-palladium complex that biases conjugate addition of the thiolate. Alternatively, the acidic amine salts generated during the cross-coupling, or Michael addition, may cause the vinylogous thioesters to isomerize over time. The geometry of the isomerically pure (**84**) was confirmed by a 2-dimensional Nuclear Overhauser Effect Spectroscopy experiment (2-D NOESY). The spectrum indicated a strong correlation between the vinyl C-H resonance and the signal corresponding to the hydrogen atoms adjacent to the ethyl ester (*).

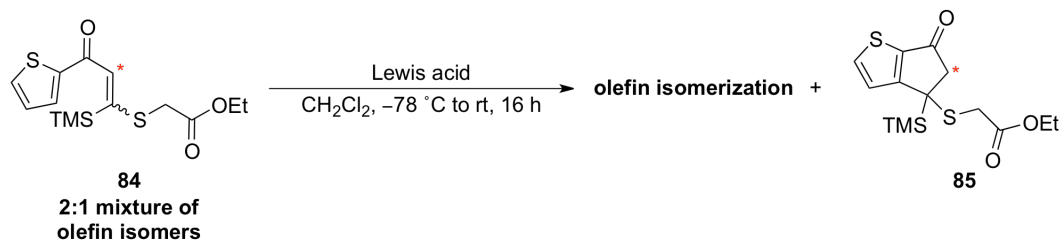


With multigram quantities of **84** in hand, we began to explore the reactivity of this substrate with various Lewis acid activators. We elected to use highly oxophilic Lewis acids such as BF_3OEt_2 or TiCl_4 at cryogenic temperatures, given the recurrence of these conditions in literature examples of the interrupted Nazarov cyclization. Additionally, we elected to use Lewis acids capable of trapping intermediate **83** as the silyl enol ether (Eq. 4.6). This involved treatment of **84** with trimethyl or *tert*-butyldimethylsilyl trifluoromethanesulfonates (TMSOTf, TBSOTf). Ideally, this would prevent elimination of ethyl thioglycolate and allow for reaction of the silyl enol ether with the pendant ester, upon activation of this species with fluoride or alkyl lithium reagents.

In order to assess whether olefin geometry of **84** had any impact on the reactivity of the Nazarov cyclization, we elected to use the 2:1 isomeric mixture illustrated in Eq. 4.7. As polymerization of the oxyallyl cation is a typical side reaction associated with the Nazarov cyclization, we elected to use dilute conditions in order to minimize this process. The initial optimization results are shown in Table 4.1. For simplicity, the reactions were monitored by TLC, concentrated after 16 hours and analyzed by ^1H NMR spectroscopy to determine whether any cyclization had occurred. The formation of **85** would be easily detectable by the disappearance of the vinyl C-H resonance and the emergence of a signal corresponding to the hydrogen atoms adjacent to the ketone (*). The new signal indicative of (**85**) should appear as a second-order doublet with a large J^1 -value ($\sim 15\text{-}18$ Hz), given the diastereotopic relationship of the aforementioned α -hydrogen atoms. Unfortunately, olefin isomerization appeared to be the only reaction evident, causing the original mixture for (**84**) to reach parity, following subjection to the cyclization conditions. The use of TBSOTf appeared to cleanly afford a single olefin isomer; however, this material was not characterized. Conversely, the more reactive TMSOTf provided a complex mixture containing products consistent with olefin isomerization, where **85** or the silyl enol ether was not evident. The conditions

indicated for Table 4.1 were repeated at $-40\text{ }^{\circ}\text{C}$, leading to no appreciable change in reactivity.

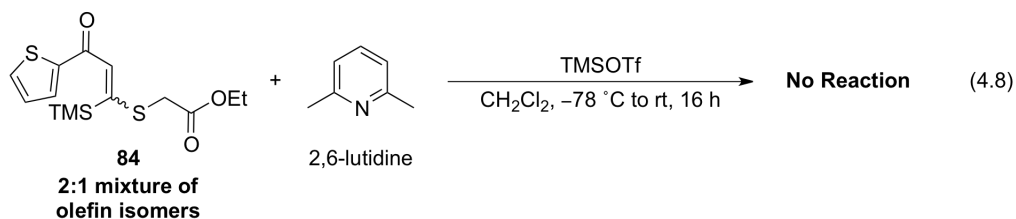
Table 4.1 Reactivity of **84 with Various Lewis Acids (Initial Screening)**



Entry	Lewis Acid ^a	Isomeric Ratio (84) ^b	% Conversion to (86) ^b	Comments
1	BF_3OEt_2	~1:1	< 5	olefin isomerization ^c
2	TiCl_4	~1:1	< 5	olefin isomerization
3	TBSOTf	single isomer	< 5	olefin isomerization
4	TMSOTf	complex mixture	n/a	several byproducts

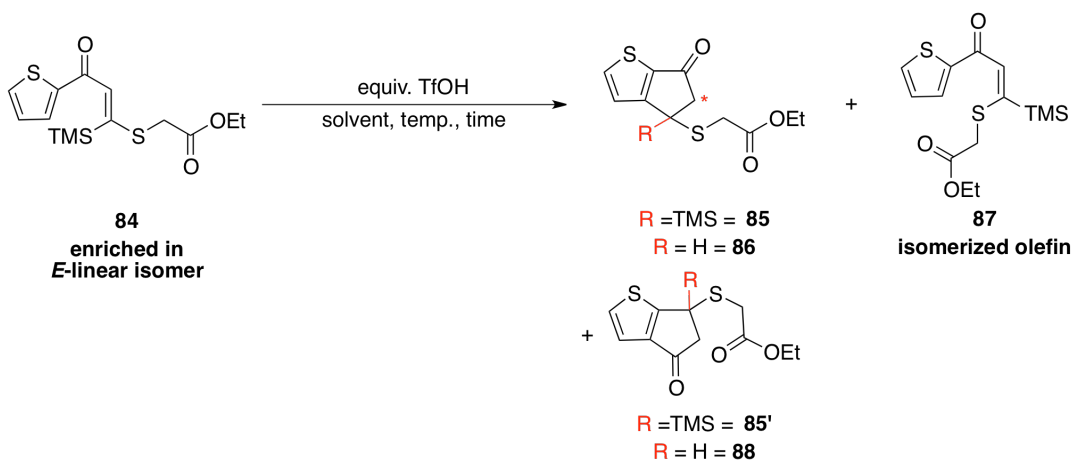
^a 0.3 mmol **84** (0.02 M), 0.3 mmol Lewis acid. ^b Determined by ^1H NMR spectroscopy following treatment with the Lewis acid. ^c 0.6 mmol BF_3OEt_2 .

In spite of olefin isomerization being the predominant process initiated by addition of Lewis acids (Table 4.1), we were interested in further exploring the reactivity of the silyl triflates (TBSOTf and TMSOTf). The complex mixture accompanied by the use of TMSOTf may relate to the formation of adventitious trifluoromethanesulfonic acid (TfOH). The presence of this species could likely result in the hydrolysis of the trimethylsilyl enol ether associated with the formation of **85**. Therefore, a reaction was conducted with TMSOTf in the presence of 2,6-lutidine, in order to effectively scavenge any acid byproducts generated. The presence of a hindered base appeared to halt all reactivity, including olefin isomerization, returning **84** unchanged (Eq. 4.8). The lack of reactivity observed in the presence of a hindered base suggests that TfOH is likely responsible in generating the complex mixture observed in Table 4.1 (entry 4).



With the observation that TfOH may be capable of initiating the Nazarov cyclization, we began to evaluate this Brønsted acid with the *E*-linear divinyl ketone (**84**). We screened a number of solvents, temperatures, and equivalents of triflic acid and evaluated conversion based on ¹H NMR spectroscopy. The spectral analysis was simplified by the use of **84** enriched in the *E*-linear regioisomer. This allowed for ease in integration of resonances corresponding to **84** relative to peaks suggestive of olefin isomerization (**87**), or products consistent with cyclization (**85** or **86**), as reported in Table 4.2.

Table 4.2 Reactivity of **84 with Triflic Acid (TfOH)**



Entry	Equivalents TfOH	Concentration (M)	Solvent	Temperature (°C)	Time (h)	Conversion (%) ^a
1	0.50	0.02	DCM	-78 to rt	16	< 5
2	10	0.02	DCM	-78 to rt	16	20 (86)
3	5	0.2	<i>d</i> ² -DCM	rt	24	> 95 (86) ^b
4	1	0.3	DCE	rt	16	27 (86)
5	5	0.3	DCE	rt	16	68 (86) ^c
6	5	0.02	DCE	rt	16	87 (86)
7	10	0.02	THF	-78 to rt	16	polymerized THF
8	10	0.02	DMF	-78 to rt	16	< 5
9	1	0.02	CH ₃ CN	-78 to rt	16	17 (87)
10	10	0.02	CH ₃ CN	-78 to rt	16	66 (87)
11	20	0.02	CH ₃ CN	-78 to rt	16	72 (87)
12	8	0.02	CH ₃ CN	rt	16	23 (88)
13	15	0.02	CH ₃ CN	rt	16	89 (1:2 85' : 88)
14	20	0.02	CH ₃ CN	rt	3	52 (88) ^d

^a Determined by ¹H NMR, following workup and concentration of the crude reaction mixture.

^b *in-situ* experiment. ^c 50% isolated yield. ^d 28% isolated yield.

Initially, halogenated solvents were investigated, showing only modest reactivity with a large excess of TfOH under dilute conditions (entries 1 and 2). It appeared that protodesilylation occurred prior to, or following cyclization of (**84**) leading us to assign the product formed in entry 2 as **86**. The presence of this compound was accompanied by the appearance of second-order multiplets involving coupling of the methine hydrogen with the diastereotopic methylene hydrogens adjacent to the ketone (*). To this end, an *in-situ*

experiment was performed involving the treatment of a 0.2 M solution (**84**) in CD₂Cl₂ with 5 equivalents of TfOH. The appearance of signals consistent with disubstituted vinyl sulfides was not observed during cyclization, suggesting that protodesilylation likely occurs following the formation of the cyclopentanone (**85**). Furthermore, the addition of 5 equivalents TfOH to a 0.2 M solution of dienone **84** led to complete consumption of starting material (entry 3). Similar reactivity was observed when DCM was replaced with 1,2-Dichloroethane (DCE) as solvent. Again, the use of 5 equivalents TfOH relative to the dienone substrate appeared optimal, providing cyclopentanone (**86**) in 68% conversion (entry 5). Purification of the crude sample by column chromatography resulted in a 50% isolated yield of cyclopentanone **86** (entry 5).

The formation of the desilylated cyclopentanone (**86**) in halogenated solvents prompted us to evaluate the use of solvents capable of undergoing proton exchange with TfOH. We hoped that the use of tetrahydrofuran (THF), dimethylformamide (DMF) or acetonitrile would allow for the isolation of the silylated cyclopentanone (**85**). Not surprisingly, the use of tetrahydrofuran and dimethylformamide led to substantially reduced reactivity (entries 7 and 8). In the case of THF, polymerization of solvent occurred, precluding the isolation of material suitable for ¹H NMR spectroscopic analysis. With DMF, exchange between TfOH and solvent occurs rapidly, where the conjugate acid of DMF appears to lack the strength necessary for inducing cyclization. Likewise, the use of stoichiometric and excess quantities of TfOH in acetonitrile (CH₃CN) led to isomerization of (**84**) at low temperature (entries 9-11). The greater strength of the conjugate acid associated with CH₃CN relative to DMF appears to be sufficient in activating (**84**) towards cyclization. Gratifyingly, when TfOH is added at room temperature to solutions of (**84**) in acetonitrile, the formation of a cyclopentanone product was observed (entries 12-14). Conversely, heating mixtures of **84** and TfOH in acetonitrile appeared to negatively effect conversion and yield, leading to numerous byproducts likely associated with polymerization of **84**. Increasing the amount of TfOH seemed to positively effect conversion, where treatment with 20 equivalents led to 52% conversion following 3 hours. Purification by column chromatography provided an isomeric cyclopentanone (**88**) in 28% isolated yield (entry 14).

Interestingly, the ¹H NMR of the cyclopentanone isolated in entry 14 (Table 4.2) differed slightly from that formed when DCE was used as solvent (entry 5, Table 4.2). In

particular, the thiophene resonances for entry 5 (DCE as solvent) are deshielded to a greater extent than those observed for entry 14 (acetonitrile as solvent). Otherwise, the spectra are nearly identical, and possess very similar coupling patterns that are in agreement with the proposed cyclopentanone product (**86**). The similarity between the spectra suggests that the cyclopentanone products are constitutional isomers; such as compounds **86** and **88**, where either entry 5 or entry 14 may represent the analogous 3-substituted thiophene (**88**). Figure 4.3 illustrates the chemical shift values associated with 2 and 3-substituted thioindanones. Evidently, the C-H bond (**A**) adjacent to the thiophene sulfur atom is consistently downfield from the more distal C-H bond (**B**). The greater deshielding of the C-H bond (**A**) in 2-substituted thioindanones is in agreement with the greater degree of conjugation of the thiophene with the carbonyl. Conversely, the 3-substituted thioindanones do not allow for a contiguous delocalization of the thiophene π -electrons with the adjacent carbonyl.^{312, 313}

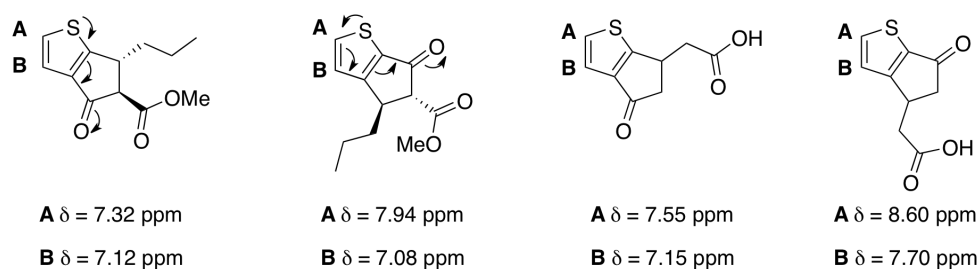


Figure 4.3 ^1H NMR Chemical Shift Values for 2 and 3-Substituted Thiaindanones

Analysis of the ^1H NMR spectra corresponding to the cyclopentanone (**86**) generated upon reaction of **84** with TfOH in DCE and CH_3CN is shown below. The aryl C-H resonances for cyclopentanone (**86**) obtained with DCE as solvent (δ 8.07 and 7.21 ppm) appear further downfield relative to the analogous reaction conducted in CH_3CN (δ 7.57 and 7.09 ppm). The greater extent of deshielding evident for the aryl C-H resonances suggests that the cyclopentanone formed with DCE as solvent is likely the 2-substituted derivative. Conversely, the cyclization conducted in CH_3CN is more consistent with a 3-substituted thiaindanone formed upon rearrangement of the pentadienyl or oxyallyl cation intermediate. Diagnostic signals for (**86**) include the disatereotopic splitting patterns for positions C and E. For the cyclopentanone formed in acetonitrile, coupling of the methine proton (**D'**) with the hydrogens (**C'**) was confirmed by ^1H - ^1H correlated spectroscopy (COSY). Additionally, the

connectivity was established by heteronuclear multiple-bond correlation spectroscopy (HMBC).

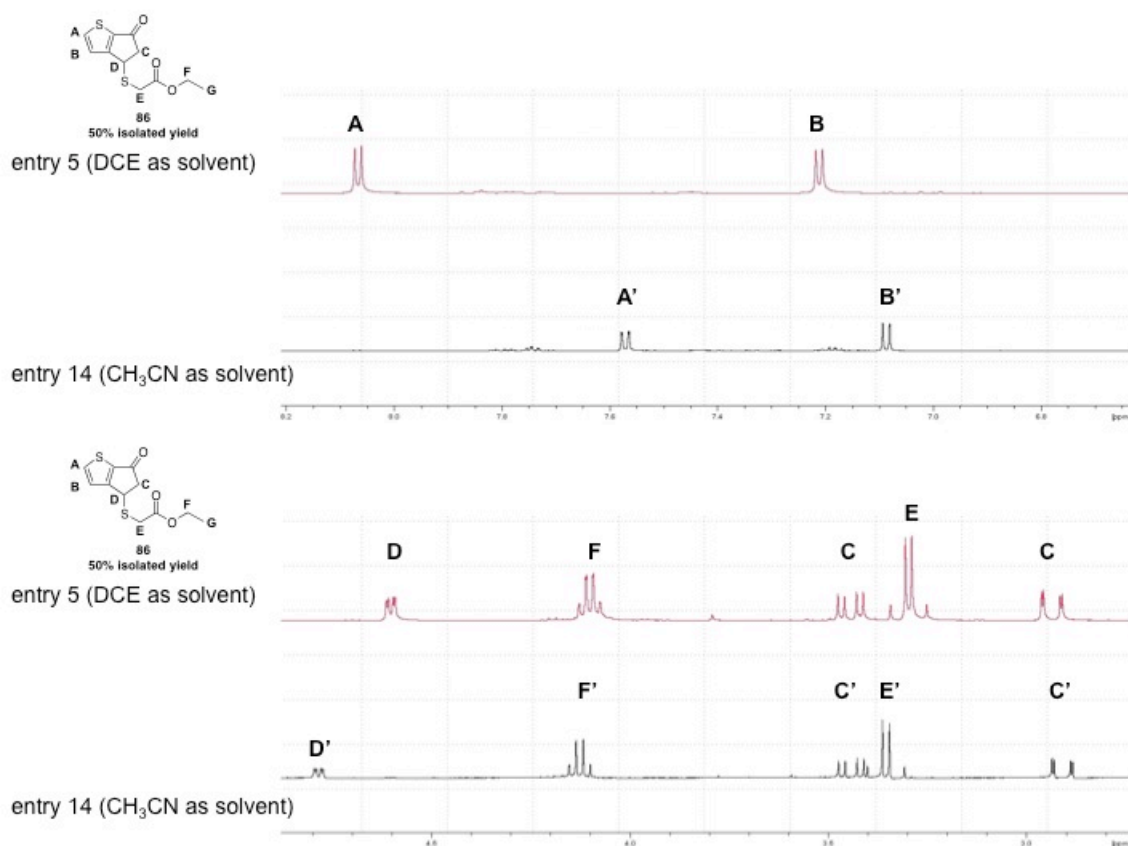
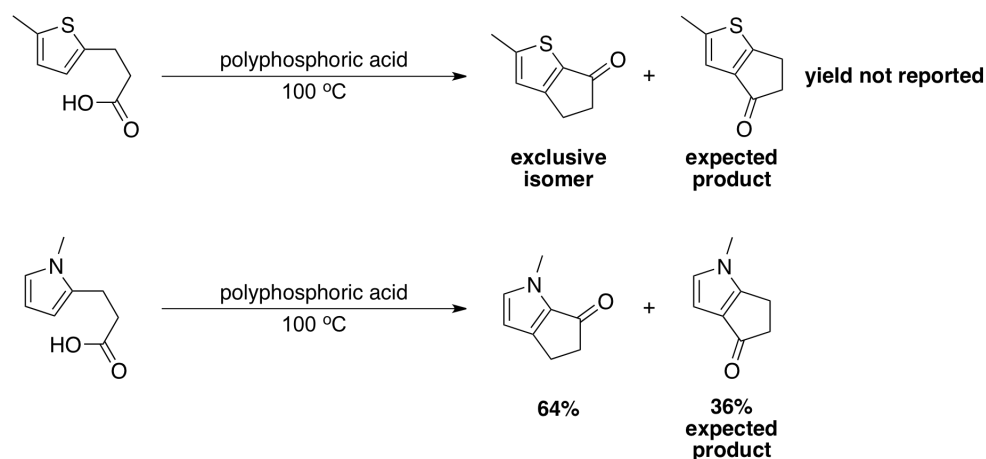


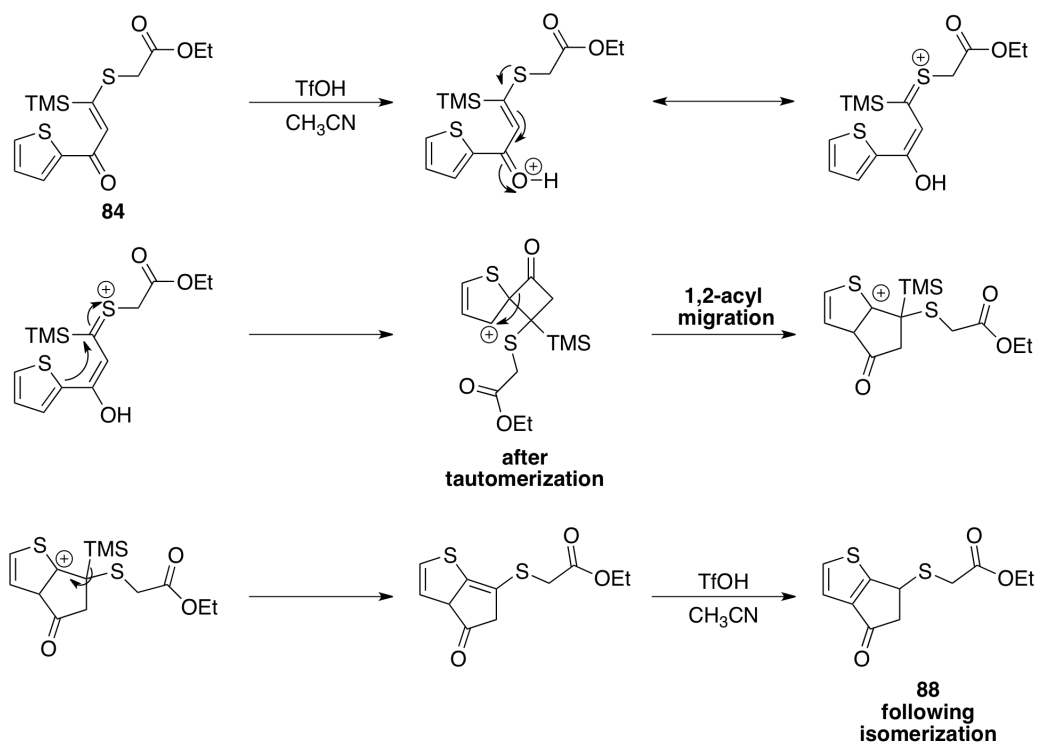
Figure 4.4 ^1H NMR Spectra of the Cyclopentanones Obtained with DCE or CH_3CN

The apparent formation of a 3-substituted thiaindanone from dienone **84** was certainly unexpected. However, literature examples concerning intramolecular Friedel-Crafts acylations with 2 and 3-substituted thiophenes and pyrroles have demonstrated similar rearrangements.³¹⁴ The cyclization of propionic acid derivatives with the aforementioned aromatic heterocycles led to mixtures of the corresponding cyclization products (Scheme 4.10). The cyclization of the thiophene derived propionic acid was shown to exclusively form the 2-substituted thiaindanone, rather than the expected 3-substituted analogue. A similar observation was made for the pyrrole derived propionic acid, where a mixture of the cyclization products was observed, favouring the rearranged product.



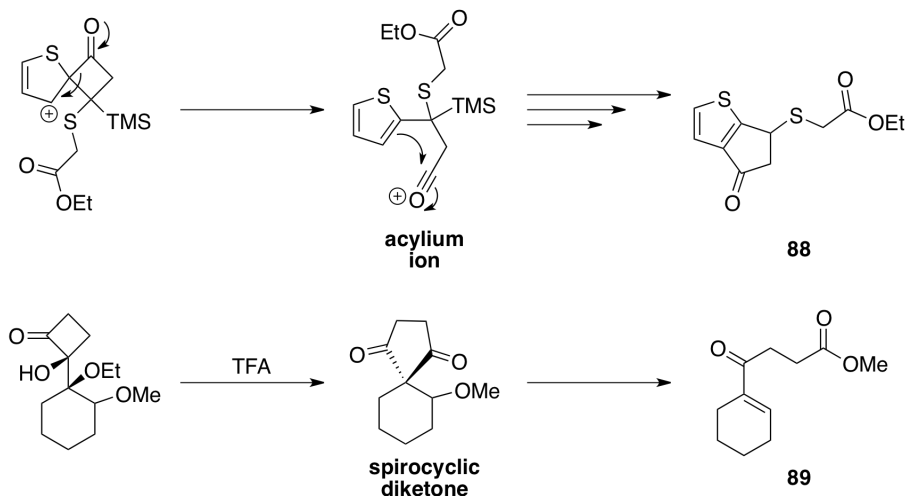
Scheme 4.10

The authors who studied the rearrangement of heteroaromatic propionic acids put forth a mechanistic rationale based upon the formation of spirocyclic intermediates during cyclization. The mechanistic interpretation is based upon the greater propensity of the 2-position of heteroaromatic species to engage in electrophilic addition processes, such as the Friedel-Crafts reaction. Explaining the rearrangement involved in treating dienone **84** with excess TfOH in CH₃CN is slightly more complex. The presence of the acyl group at the 2-position of the thiophene ring should render this position less reactive towards electrophilic addition, relative to the propionic acids shown in Scheme 4.10. Nonetheless, if dienone **84** were to occupy the conformation shown in Scheme 4.11, protonation of the vinylogous thioester would provide the expected pentadienyl cation, which would be in resonance with the corresponding thionium ion. Spirocyclization would then generate a cyclobutanone intermediate, which may subsequently undergo a 1,2-acyl migration providing the rearranged cyclopentanone. Similar 1,2-acyl migrations with concomitant ring expansion have been invoked in pinacol-type rearrangements for the synthesis of spirocyclic diketones.³¹⁵ The migration of the acyl group may be facilitated by stabilization of the carbocation in the 2-position by virtue of the β -trimethylsilane. Restoration of aromaticity can then be accomplished upon elimination of the trimethylsilyl group and subsequent γ -protonation (Scheme 4.11). Alternatively, α -deprotonation of the ketone and tautomerization would also restore aromaticity, which would be followed by proteodesilylation.



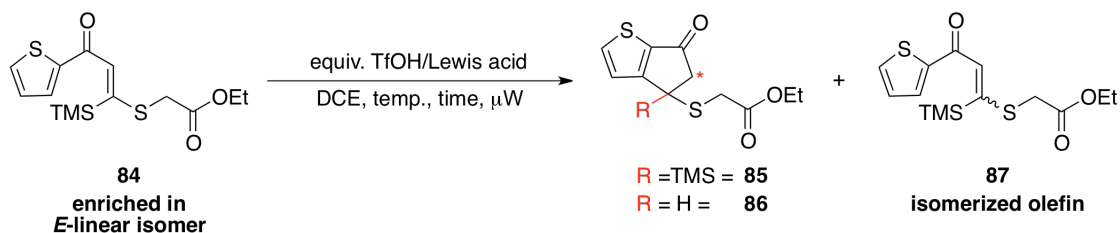
Scheme 4.11

An alternate mechanism for rearrangement to cyclopentanone (**88**) involves a retro Friedel-Crafts acylation whereby a highly reactive acylium ion is formed. A similar mechanism has been proposed for the generation of the γ -ketoester (**89**) from the spirocyclic diketone upon prolonged exposure to acidic media.³¹⁵ The proposed mechanism for the formation of **88** involves the elimination of methanol via the formation of an acylium ion. The formation of this electrophilic species is depicted in Scheme 4.12, which may occur through a common intermediate as the 1,2-acyl migration pathway (Scheme 4.11). The regeneration of the thiophene may then lead to preferential reaction at the 3-position given the steric bulk imparted by the adjacent sulfide and trimethylsilane. Additionally, the carbocation generated by reaction of the 3-position may be electronically favoured via the β -silicon effect, similar to that described in the 1,2-acyl migration.



Scheme 4.12

The interesting solvent dependence on the reactivity of dienone **84** with excess TfOH inspired us to further evaluate the cyclization efficiency upon microwave irradiation. We elected to continue using DCE as solvent, given the absence of rearrangement during cyclization, and the greater temperature range possible relative to DCM. It seemed reasonable that the use of microwave heating would enable either a reduction in the necessary quantity of TfOH, or rate acceleration for the cyclization of dienone **84**. The polarity associated with the pentadienyl and oxyallyl cation intermediates characteristic of the Nazarov cyclization suggest that microwave heating may indeed promote reactivity. To this end, microwave acceleration has been observed for pyrrole-substituted dienones, where numerous byproducts were observed upon prolonged conventional heating.³¹⁶ In our hands, conventional heating also resulted in polymerization or decomposition of starting material, or the resulting cyclopentanone products. The effect of microwave irradiation on the reactivity of **84** with TfOH and various Lewis acids was thus evaluated, and the results are summarized in Table 4.3.

Table 4.3 Reactivity of (84) with Triflic Acid (TfOH) Under Microwave Irradiation

Entry	Equivalents TfOH/Lewis acid	Lewis Acid	Temperature (°C)	Time (h)	Conversion (%) ^b
1	1.2	n/a	80	1	28 (87)
2	1.2	n/a	110	0.5	57 (87)
3	1.2	n/a	110	1	50 (87)
4	5	n/a	80	1	82 (86)
5	5	n/a	80	1.5	82 (86)
6	8	n/a	80	1	82 (86)
7	5	TiCl ₄	80	1	48 (85)
8	5	TBSOTf	80	1	complex mixture
9	5	TMSOTf	80	1	65 (86) ^c

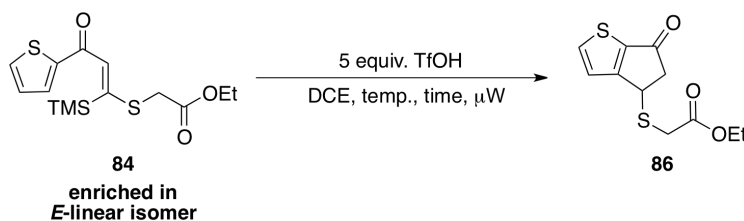
^a Concentration (**84**) was 0.2M. ^b Determined by ¹H NMR, following workup and concentration of the crude reaction mixture. ^c Byproducts present.

The use of microwave heating appeared to greatly accelerate the reactivity of (**84**) with TfOH, leading to high conversions after irradiation for one hour. However, excess TfOH is still required in order to obtain useful conversions, where olefin isomerization predominates with 1.2 equivalents of Brønsted acid (entries 1 to 3). Extending the reaction time beyond one hour does not appear to have an appreciable effect on conversion, as does increasing the amount of TfOH beyond 5 equivalents (entries 4 to 6). Given the ability of microwave irradiation in accelerating the Nazarov cyclization of **84** with Brønsted acids, we decided to reevaluate the Lewis acids initially screened. Of these, TiCl₄ appeared to facilitate cyclization to **85**; whereas, the silyl triflates provided complex mixtures of products. Again, this is likely due to adventitious triflic acid, which may be the substance responsible for the observed reactivity. It was hoped that the use of Lewis acids under these conditions would promote the Nazarov cyclization/Dieckmann condensation cascade sequence. However, no tricyclic products of this nature were detected in the ¹H NMR spectra for entries 7 to 9. The use of Brønsted acids does not appear to facilitate the Dieckmann condensation, which is

likely due to equilibration between the keto and enol forms of **86**. Additionally, the reactivity of the enol form of **86** coupled with the reduced electrophilicity of ester functionalities, likely impedes the Dieckmann condensation, favouring tautomerization.

Undaunted, we sought to finalize the conditions for the Nazarov cyclization of **84** under microwave irradiation. A slight increase in the isolated yield for **86** was observed upon four-fold dilution (entry 1 versus 2). Furthermore, the addition of trifluoromethanesulfonic anhydride (Tf₂O) as dehydrating agent appeared to slightly improve the yield with a concentration of 0.2 M **84** (entry 2 versus 3). Lastly, as microwave heating using conventional microwave ovens typically involves a ramp time in achieving the desired temperature, we decided to test whether variable temperature programs would affect the observed yield.³¹⁷ To this end, **84** was heated at 80, 100, and 120 °C at 10 minute intervals, to assess whether this may facilitate the Nazarov cyclization, or the subsequent Dieckmann condensation (entries 4 and 5). This proved less effective than heating at 80 °C for 1 hour (entries 1 and 2). As the yield of the Nazarov cyclization did not appreciably increase upon dilution or treatment with Tf₂O, it was decided that heating **84** at 80 °C for 1 hour in the presence of 5 equivalents TfOH was optimal for the production of **86** (entry 2). The discrepancy between the isolated yields, and the conversions observed by ¹H NMR spectroscopy suggest that **86** may be unstable towards chromatographic purification.

Table 4.4 Final Screening of Conditions for Cyclization of 84

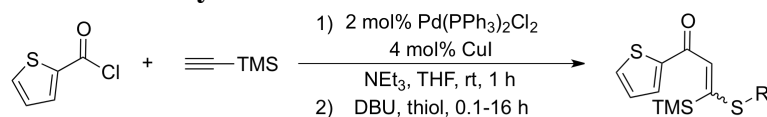


Entry ^a	Concentration (M)	Temperature (°C)	Time	Isolated Yield (%)
1	0.05	80	1	56
2	0.2	80	1	51
3	0.2	80	1	55 ^b
4	0.05	variable ^c	0.5	39
5	0.2	variable ^c	0.5	28

^a 0.6 mmol (**84**), 3.0 mmol TfOH. ^b 0.15 mmol Tf₂O added. ^c The microwave was programmed to increase the temperature from 80 to 100 to 120 °C at 10 minute intervals.

4.2.3 Analysis of Sulfide Substitution on the Nazarov Cyclization

With the conditions optimized for the cyclization of **84**, we elected to evaluate the reactivity of a variety of sulfur-substituted dienones. The synthesis of these compounds was readily accomplished using the Sonogashira-type cross-coupling/Michael addition sequence mentioned for the preparation of **84**. It was found that a diverse array of alkyl and aryl thiols were tolerated under these conditions, often providing quantitative amounts of the dienone. In situations where reduced yields were evident, small amounts of products correlating to desilylation were observed. A number of these dienones were obtained with excellent selectivity for the *E*-linear vinyl sulfide, which was determined by 2-D NOESY experiments. For aliphatic thiols, a correlation between the vinylic signal and the methylene resonances proximal to the sulfur could be identified. For dienones **92** and **93** an additional correlation could be detected between the vinyl and thiophene C-H resonances, suggesting that the dienones may partially exist as the S-shaped conformer at room temperature. For aryl substituted vinylogous thioesters, the hydrogens in the *ortho* or *meta*-positions (in relation to sulfur) demonstrated clear correlations with the vinylic signal.

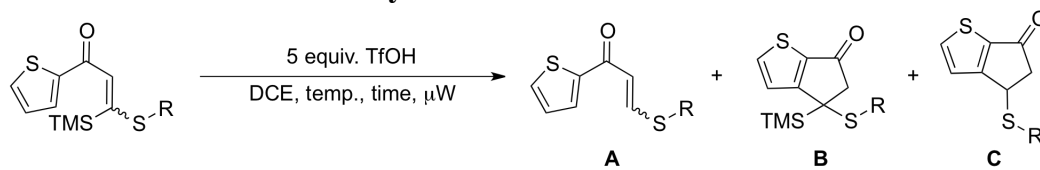
Table 4.5 Synthesis of Sulfur-Substituted Dienones

Entry ^a	Dienone	Thiol	Isomeric Ratio	Isolated Yield (%)
1	90	HS-Ph	6:1 ^b	95
2	91	HS-CH ₂ -CH ₂ -C(=O)OEt	5:1 ^c	79
3	92	HS-C ₆ H ₅	only <i>E</i> -linear ^b	95
4	93	HS-C ₆ H ₄ -	only <i>E</i> -linear ^b	95
5	94	HS-C ₆ H ₄ -OMe	10:1 ^c	95
6	95	HS-C ₆ H ₄ -Br	only one isomer ^c	72

^a 1.3 mmol 2-thiophenecarbonyl chloride (0.2 M), 1.3 mmol ethynyltrimethylsilane, 1.3 mmol NEt₃, 0.03 mmol Pd(PPh₃)₂Cl₂, 0.07 mmol CuI, 1.06 mmol DBU, 1.06 mmol thiol. ^b Major isomer determined to be the *E*-linear by 2-D NOESY. ^c Major isomer not determined.

As we were interested in how sulfur-substitution would impact the reactivity of the vinylogous thioester towards Nazarov cyclization, we subjected the various dienones to the optimized conditions studied earlier (Table 4.4). In general, it seemed that all dienones studied demonstrated reduced reactivity toward the Nazarov cyclization with TfOH. Of the substrates examined, only **91** appeared to undergo the Nazarov cyclization to give (**C**) in 67% conversion, along with unreacted starting material. Dienone **90** underwent olefin isomerization and protodesilylation yielding an 11:1 ratio of *E* and *Z*-linear isomers in 20% isolated yield (Table 4.6). The use of aryl substituted vinylogous thioesters (**92** to **95**) demonstrated similar reactivity in comparison to **84** (entries 2-6). The use of dienone **92** yielded a mixture of starting material and *E*-linear vinylogous thioester (**A**) in 48% yield (entry 3). Extending the reaction time appeared to mainly facilitate decomposition; however, *E*-linear olefin and small amounts of products consistent with the Nazarov cyclization were present in the ¹H NMR spectrum (entry 4). The absence of the *Z*-linear vinylogous thioester suggests that phenyl substitution may hinder olefin isomerization.

Table 4.6 Nazarov Cyclizations of Sulfur-Substituted Dienones



Entry ^a	Dienone	R	Reaction Conditions	Conversion (%)	Isolated Yield (%)	Product
1	90		1	n/a	20	A ^a
2	91		1 ^b	67	n/a	C
3	92		1	n/a	48	A ^c
4	92		1 ^d	decomposition	n/a	A:C (2:1)
5	93		2	n/a	26	A ^e
6	94		1	87	n/a	A:C (1:1) ^e
7	95		1	84	n/a	n/a ^e

Condition 1: 0.2 M dienone, 5 equivalents TfOH, 80 °C μ W, 1 h. Condition 2: 0.2 M dienone, 5 equivalents TfOH, 80 to 100 to 120 °C (10 minute intervals) μ W. ^a 11:1 *E*:*Z* linear. ^b Stir period of 1.5 hours. ^c 1.7:1 ratio *E*-linear isomer (A) to starting dienone (**92**). ^d Stir period of 2 hours. ^e Unidentified byproducts present.

The use of electron releasing *para*-substituents seemed to enhance reactivity, but consequently led to the formation of several byproducts. The use of electron withdrawing groups in the *para*-position also enhanced the reactivity relative to dienone **92**. Interestingly, the use of dienone **95** provided a species that seemed consistent with addition of a second equivalent of thiol (Figure 4.5).

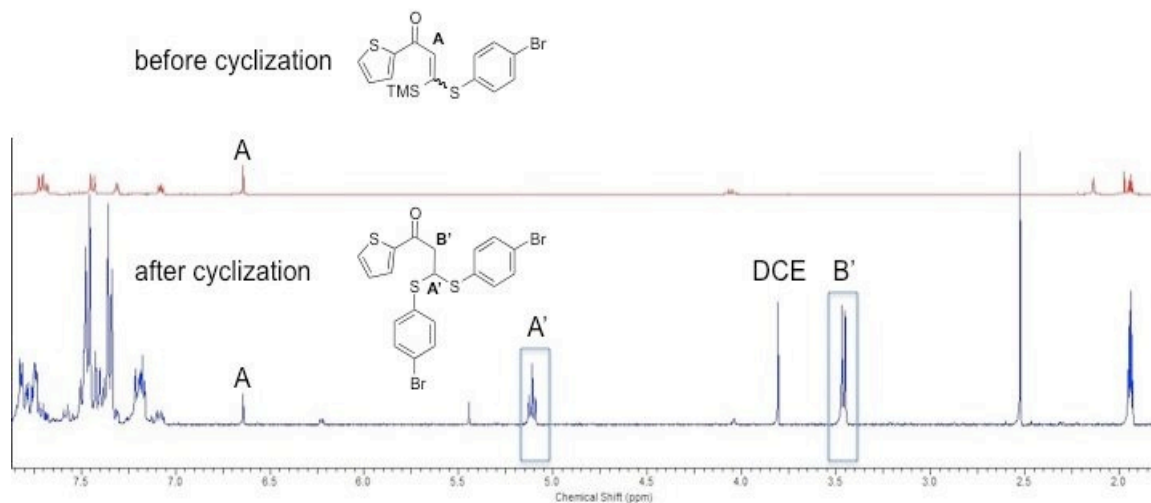
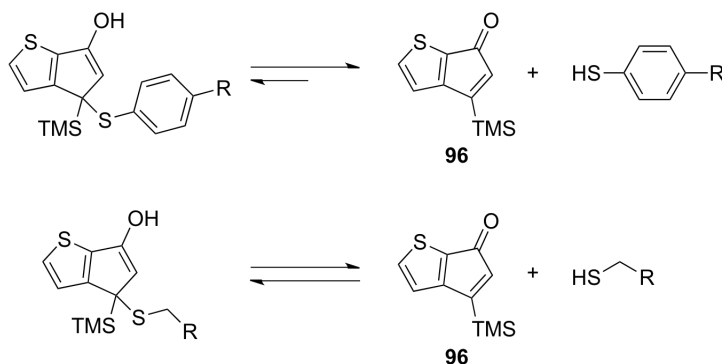


Figure 4.5 ^1H NMR Spectra of Dienone (**92**) Before and After Cyclization

The differences in reactivity observed for alkyl and aryl substituted vinylogous thioesters is likely a consequence of the delocalization of the sulfur lone pair electrons. It could be expected that the use of aryl sulfide substituted dienones (**92** to **95**) would lead to lower reactivity with Brønsted and Lewis acids. This is reflected in the degree of olefin isomerization observed for dienone **90**, where the initial 6:1 *E* and *Z*-linear vinylogous thioesters became enriched in the *E*-linear following reaction with TfOH. The treatment of dienone **92** with TfOH simply returned unreacted starting material with an equal amount of the *E*-linear vinylogous thioester formed following protodesilylation. As dienone **92** was isolated exclusively as the *E*-linear isomer, the absence of the corresponding *Z*-linear species following treatment with TfOH suggests these species may react less productively with Brønsted acids. The use of electron releasing groups in the *para*-position helped increase reactivity generating small amounts of products consistent with Nazarov cyclization (**C**); however, numerous byproducts were formed. This suggests that a fine balance exists between the electronic contribution of the sulfur, and the ability of the sulfide to be eliminated following cyclization. To this end, the *para*-bromo substituted dienone (**95**) demonstrated the formation of a product that may relate to the addition of a second equivalent of thiol to the original dienone (Figure 4.5). Similar products were observed to a lesser extent for the other aryl substituted vinylogous thioesters examined. The formation of this product can be explained by the elimination of the thiol following cyclization as depicted in Scheme 4.9. The equilibrium for this process will likely favour the formation of **96** given the better

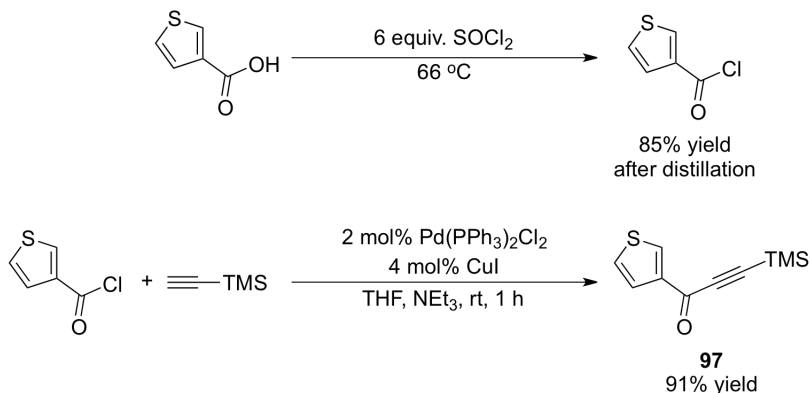
leaving group ability of aryl relative to alkyl thiols. Furthermore, the formation of **96** may lead to dimeric or polymeric compounds as a consequence of the antiaromatic character (Scheme 4.13). This has been observed for cyclopentadienones, where Diels-Alder dimerization occurred immediately following acid hydrolysis of the corresponding ketal.³¹⁸



Scheme 4.13

4.2.4 Investigation of 3-Substituted Thiophene Dienones

The greater reactivity of the 2-position in electrophilic addition reactions of thiophene prompted us to evaluate 3-substituted dienones.^{319, 320} The preparation of these compounds proved lower yielding relative to the 2-substituted dienones, as the silyl-protected vinylogous thioesters appeared to undergo protodesilylation more readily. Given the difficulty in isolating the silyl protected vinylogous thioesters, we conducted the Michael addition and the Nazarov cyclization as a one-pot procedure with the trimethylsilylone (**97**). Treatment of 3-thiophenecarboxylic acid with excess SOCl_2 at reflux gave the corresponding acyl halide in 85% yield following Kugelrohr distillation. The acyl halide underwent smooth Sonogashira-type cross-coupling with ethynyltrimethylsilane providing **97** in 91% isolated yield following chromatographic purification (Scheme 4.14).



Scheme 4.14

The treatment of ynone **97** with DBU and ethylthioglycolate followed by addition of TfOH and microwave irradiation (80 °C, 1 hour) provided a cyclopentanone consistent with **88**. The similarity of the expected 3-substituted thiaindanone with that previously observed for the cyclization of dienone **84** in CH₃CN provides additional support for our initial prediction. By conducting the Michael addition and the Nazarov cyclization in one-pot, it became apparent that 2.5 equivalents of TfOH was sufficient for initiating cyclization, relative to the 5 equivalents typically required for useful conversions of dienone **84** to cyclopentanone **86**. The addition of less than 2.5 equivalents of TfOH or longer reaction times simply led to lower conversion to the cyclopentanones. The substitution of ethylthioglycolate with benzylmercaptan, thiophenol or 4-methylthiophenol in the one-pot Michael addition Nazarov cyclization proved less successful. Not surprisingly, a common side reaction during the Michael addition was alkylated thiol, where the thiolate underwent nucleophilic substitution with solvent (DCE). Additionally, the formation of a mixture of cyclopentanones was observed in all cases. Increasing the temperature from 80 to 100 to 120 °C for 10 minute intervals seemed to increase the conversion to cyclopentanone **88**. Interestingly, the variable temperature program seems to afford a greater amount of the expected 3-substituted thiaindanone (**88**), relative to the other cyclopentanone formed during cyclization.

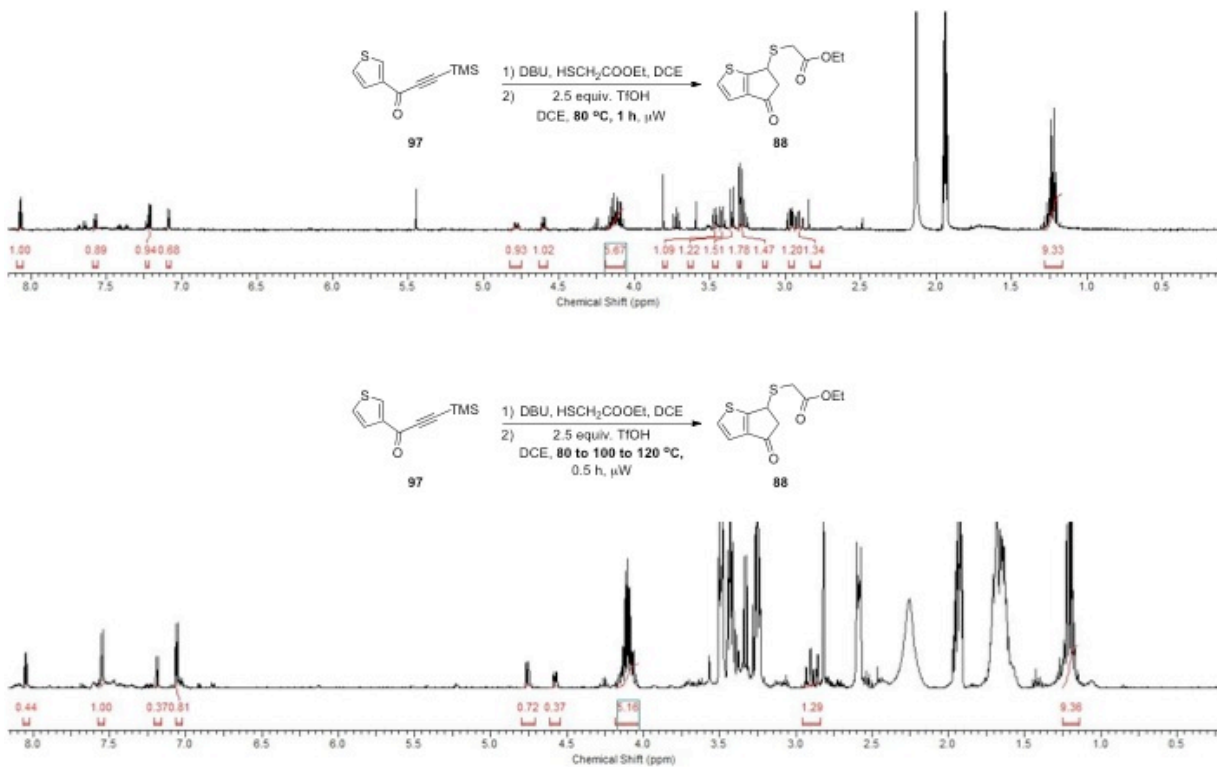
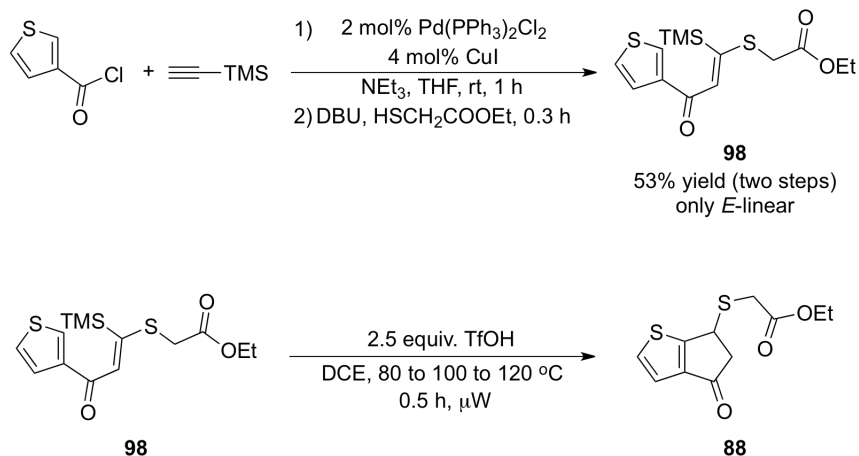


Figure 4.6 Crude ¹H NMR Analysis for the Synthesis of Cyclopentanone 98

In order to better assess the cyclopentanone formed in addition to (**88**) we synthesized dienone **98** in an attempt to isolate sufficient material for further characterization. To this end, our one-pot synthesis of vinylogous thioesters provided dienone **98** in 53% isolated yield, with exclusive selectivity for the *E*-linear regioisomer. Treatment of dienone **98** with 2.5 equivalents of TfOH and subjection to the variable microwave heating program allowed for the isolation of the mixture of cyclopentanones in very low yield.



Scheme 4.15

The comparison of the previously synthesized thiaindanones with the mixture obtained during cyclization of (**98**) is shown in Figure 4.7 and 4.8. As can be seen, the mixture obtained upon cyclization of the 3-substituted dienone matches that previously obtained with the analogous 2-substituted derivatives.

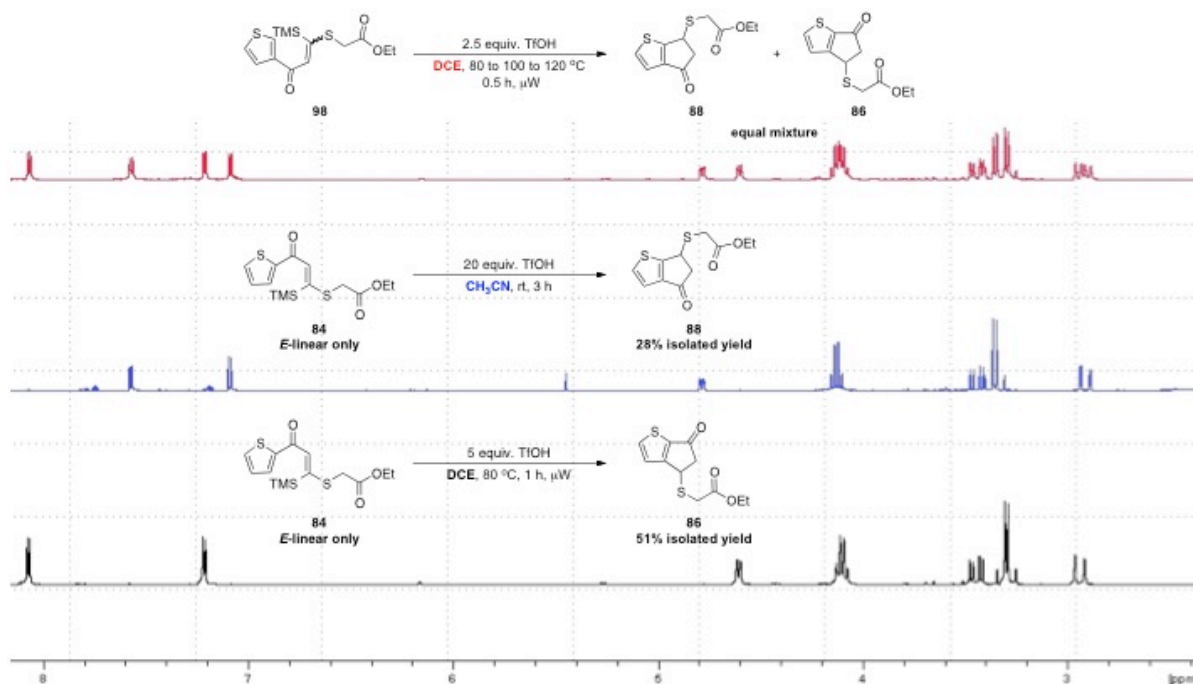


Figure 4.7 Product Comparison for the Cyclization of 3 and 2-Substituted Dienones

Comparative analysis of the second-order multiplets in the ^1H NMR spectra further exemplifies the similarity of the cyclopentanones (Figure 4.8). The apparent mirroring of signals originally identified for the cyclizations performed in CH_3CN and DCE with dienone **84** is also present in the mixture obtained with dienone **98**. This strongly suggests that the mixture of cyclopentanones formed upon cyclization of **98** consists of both the expected product (**88**) and the 2-substituted thiandane (**86**).

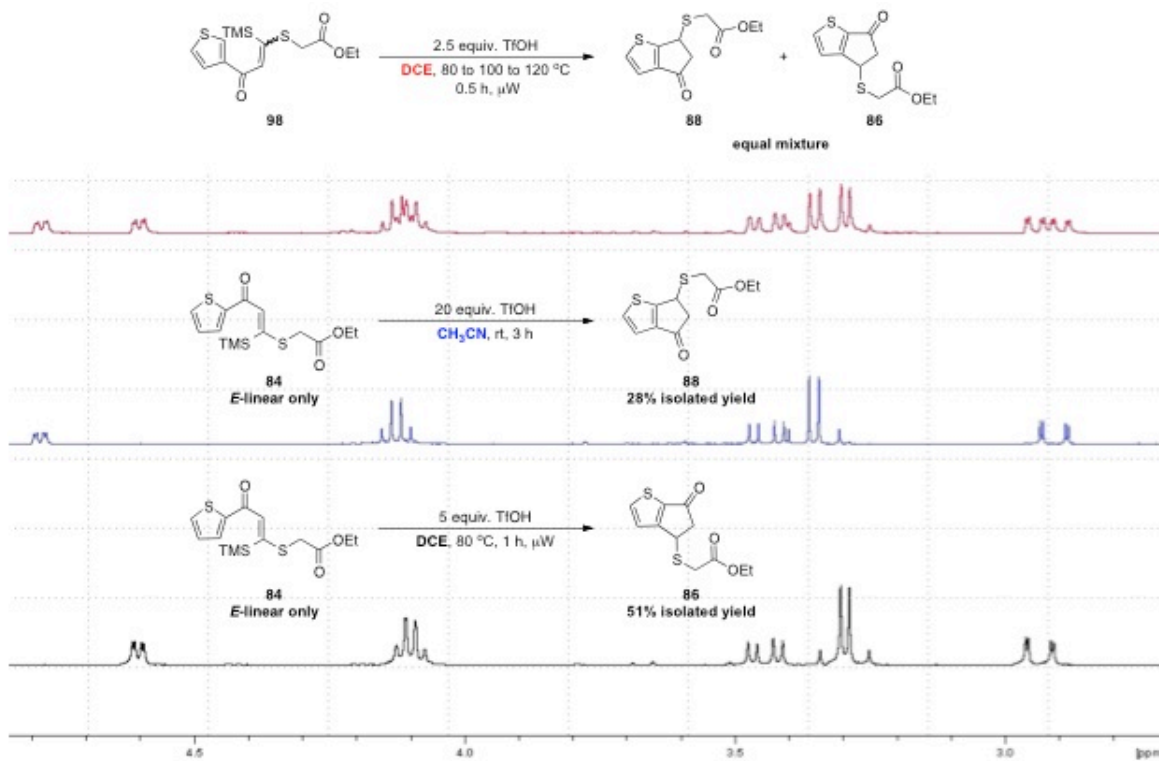
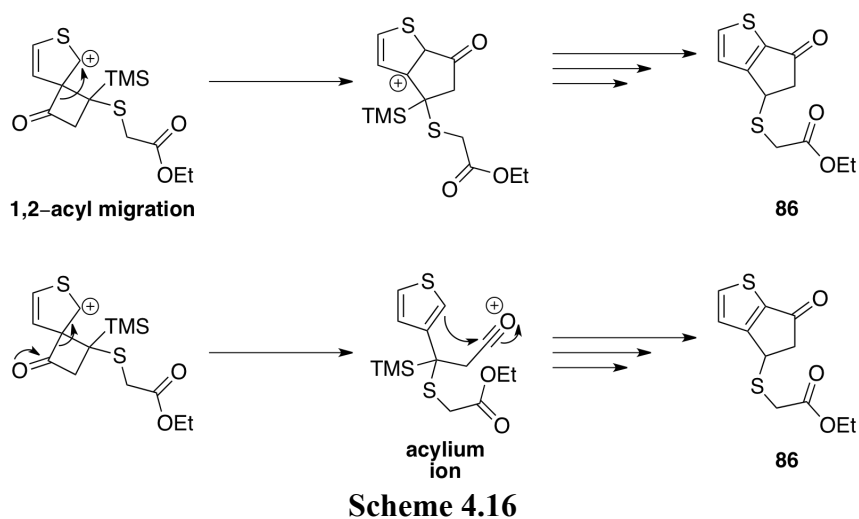


Figure 4.8 Similarity of Products Obtained by Cyclization of Dienone (98**) and (**84**)**

A mechanistic rationale for rearrangement for the formation of **86** from a 3-substituted dienone is expected to be similar to that originally proposed in Scheme 4.11 and 4.12. The formation of a spirocyclic cyclobutanone would be predicted to be less favourable with a 3-substituted dienone, given the deactivating effect of the acyl group and the tendency for the 2-position to engage in electrophilic addition. Nonetheless, if the spirocyclic intermediate forms, the 1,2-acyl migration would provide a highly stabilized carbocation due to delocalization through the thiophene ring, and the presence of the β -trimethylsilane. Additionally, formation of the acylium ion would be expected to readily undergo

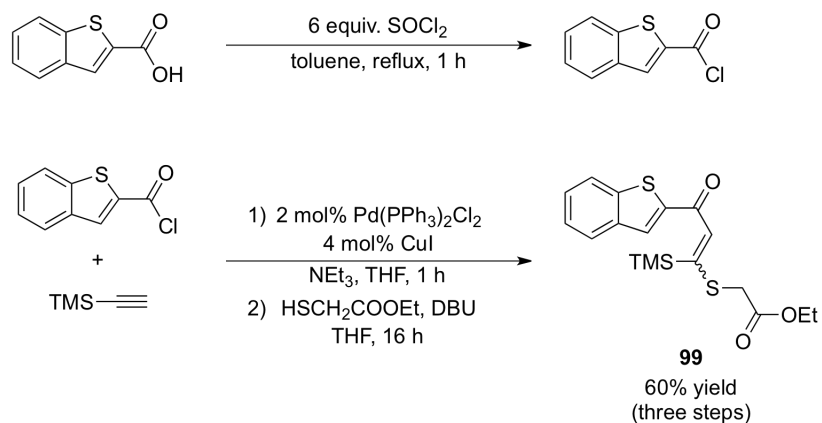
electrophilic addition given the accessibility of the 2-position (Scheme 4.16).



4.2.5 Investigation of Benzothiophene Containing Dienones

The ability of dienone **84** and **98** to undergo Nazarov cyclization with strong Brønsted acids led us to explore the use of benzannulated derivatives. It was anticipated that benzothiophene substituted dienones would undergo cyclization more readily, as the barrier to interrupting aromaticity is lower than the analogous thiophene.

Dienone **99** was synthesized using our one-pot cross-coupling Michael addition sequence starting from thianaphene-2-carboxylic acid. As the carbonyl chloride is not available commercially, the acid was heated in the presence of thionyl chloride, followed by evaporation of the volatiles. The acyl halide formed *in-situ* was then carried forward without purification. The subjection of this species to the conditions for the cross-coupling Michael addition sequence resulted in dienone **99** with a small amount of an unknown impurity (60% combined yield).



Scheme 4.17 Synthesis of Benzothiophene Dienone **99**

The contaminant could be partially separated from dienone **99**, leading to a sample enriched in this species (12% isolated yield). The ^1H NMR spectrum of this impurity contained peaks consistent with the formation of a cyclopentanone product. Figure 4.9 shows the ^1H - ^1H correlation spectrum (COSY), which illustrates the expected coupling between the hydrogen atoms at positions **A** and **C**. Additionally, the characteristic pattern for diastereotopic methylene hydrogens is present for **C** as highlighted in Figure 4.9. The coupling patterns observed for **A** and **C** is also consistent with that identified during the characterization of the 2 and 3-substituted thiophene cyclopentanones **86** and **88**.

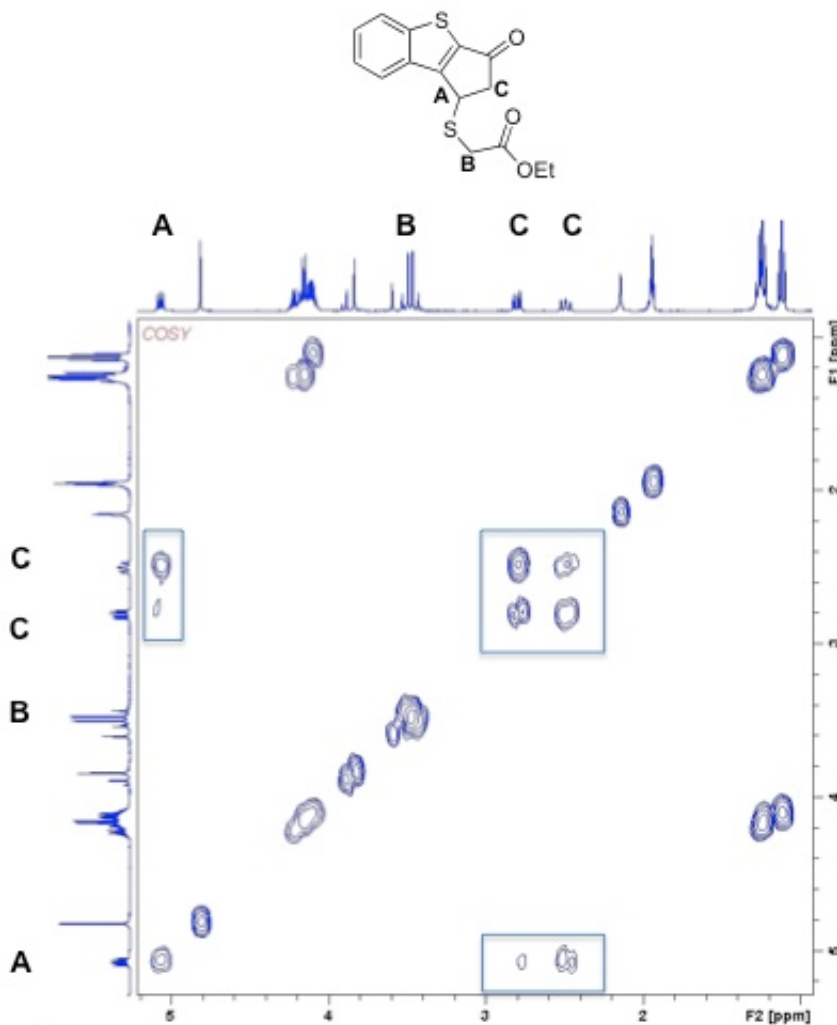
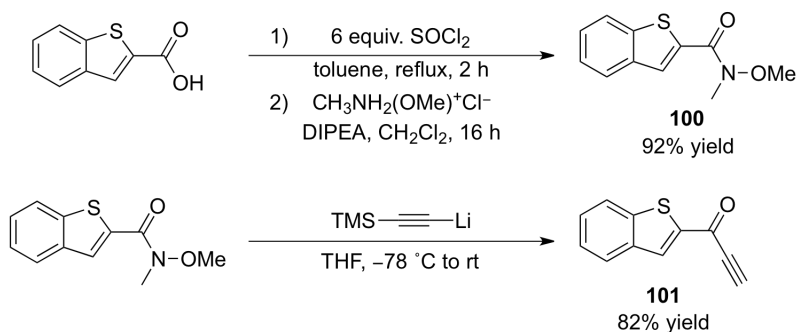


Figure 4.9 ^1H - ^1H Correlation Spectrum (COSY) for Dienone (**99**) Contaminant

The formation of the tricyclic cyclopentanone during the synthesis of dienone **99** was unexpected. The use of thionyl chloride in forming the acyl halide and the reduction of $\text{Pd}(\text{PPh}_3)_2\text{Cl}_2$ to $\text{Pd}(0)$ during the Sonogashira cross-coupling may generate quantities of HCl . However, the adventitious acid should have been scavenged by the hindered nitrogenous bases used in the cross-coupling. The corresponding conjugate acids formed during the Michael addition would not be expected to effectively induce Nazarov cyclization, but may play a role in facilitating the reactivity. This suggests that trace amounts of electrophilic palladium or copper complexes may be responsible for the observed reactivity. The sample consisting primarily of dienone **99** was treated with one equivalent of TfOH , and a variety of Lewis acids including: TiCl_4 , BF_3OEt_2 , AlEtCl_2 , and SiCl_4 . With the exception of SiCl_4 , starting material was consumed in all cases. Unfortunately, only BF_3OEt_2 and AlEtCl_2

seemed to produce compounds that resembled a cyclopentanone product, where the remaining Lewis and Brønsted acids caused decomposition to complex mixtures. However, the ^1H NMR spectra for cyclizations of **99** with BF_2OEt_2 and AlEtCl_2 did not contain peaks resembling those shown in Figure 4.5. Additionally, the ^1H NMR spectra did not contain resonances indicating the formation of the Dieckmann adduct. These results were puzzling, as the one-pot synthesis of dienone **99** contained a cyclopentanone that clearly resembled that produced following the Nazarov cyclization of **84** or **98** with TfOH .

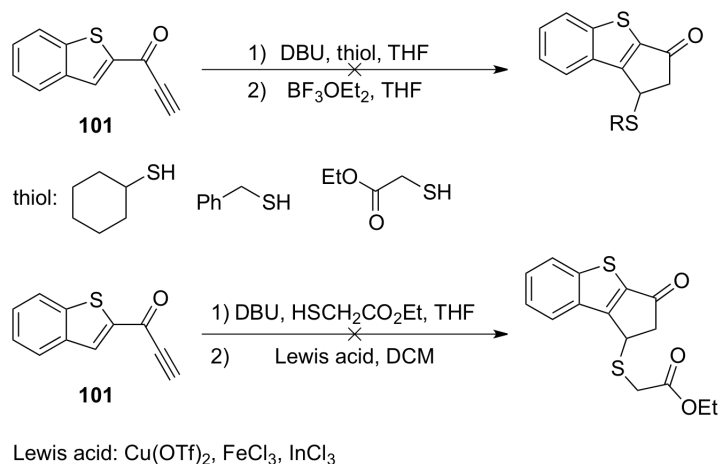
Overall, the benzothiophene substituted dienone **99** appeared significantly more reactive than the analogous 2-substituted thiophene derivative. The observed reactivity prompted us to explore an alternative route for the synthesis of dienone **99**, in order to assess whether trace amounts of transition metals were indeed the culprit behind the formation of the cyclopentanone. We decided to prepare **99** using the more conventional Weinreb ketone synthesis, starting with thianaphene-2-carboxylic acid.³²¹ To this end, the acid was treated with an excess of SOCl_2 followed by evaporation of the volatiles, yielding the crude acyl halide (Scheme 4.18). Subsequently, excess *N,O*-dimethylhydroxylamine hydrochloride was added in conjunction with *N,N*-diisopropylethylamine (DIPEA) providing the corresponding Weinreb amide (**100**) in 92% isolated yield. The addition of lithium trimethylsilylacetylide to the Weinreb amide provided the terminal ynone (**101**) after acidic workup. We had hoped to form the trimethylsilyl-protected ynone; however, the dilute acidic conditions required for collapse of the tetrahedral intermediate apparently led to protodesilylation.



Scheme 4.18

We then investigated the addition of various thiols to **101**, where Nazarov cyclization was attempted as a one-pot procedure, following thio-Michael addition. The thiols examined were cyclohexylmercaptan, benzylmercaptan, and ethylthioglycolate. The addition of a two-

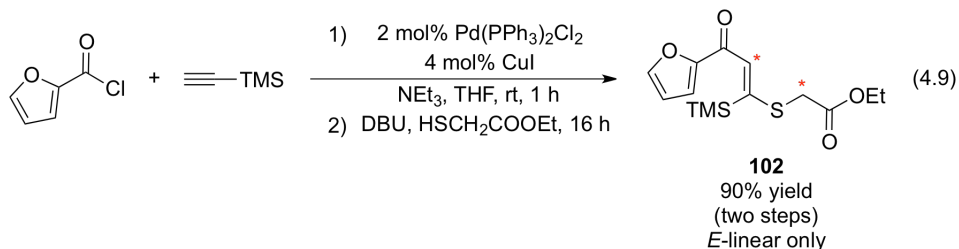
fold excess of BF_3OEt_2 to any of the *in-situ* generated vinylogous thioesters did not produce any of the desired cyclopentanone product. Similarly, the vinylogous thioester formed upon addition of ethylthioglycolate to **101** was extracted from the crude reaction mixture to remove residual DBU. The crude material was then treated with a variety of Lewis acids yielding an equimolar mixture of the vinylogous thioester in all cases. The lack of reactivity observed for the disubstituted vinylogous thioesters formed in Scheme 4.19 suggests that the trimethylsilane is required for cyclization, due to the stabilization of the intermediate oxyallyl cation.



Scheme 4.19

4.2.6 Investigation of Other Heteroaromatic Substituted Dienones

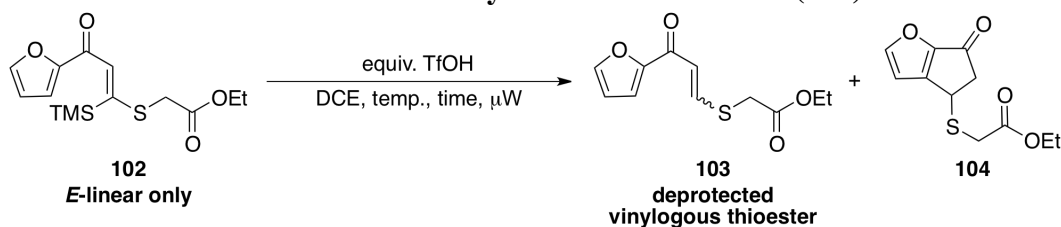
The unexpected formation of a cyclopentanone product during the synthesis of dienone **99** prompted us to investigate other heteroaromatic dienones. Initially we tested the analogous furan derivatives of dienone **84**. To this end, our one-pot protocol for the synthesis of vinylogous thioesters was used to synthesize the 2-substituted furan containing dienone (**102**) in 90% isolated yield (Eq. 4.9). Using this method, dienone **102** was formed exclusively as the *E*-linear vinylogous thioester as determined by 2-D NOESY spectroscopy.



The Nazarov cyclization of dienone (**102**) at various temperatures and equivalents of TfOH was then examined in order to assess the reactivity of this substrate. The optimized conditions for **84** proved less successful in initiating the Nazarov cyclization. Microwave irradiation of **102** for 1 hour at 80 °C in the presence of 5 equivalents of TfOH resulted in 66% conversion to a mixture of the deprotected vinylogous thioester (**103**) and the cyclopentanone (**104**). The observation that microwave power output may affect the reactivity of azide cycloaddition reactions led us to use a fixed power setting.³²² The use of a continuous output of 30 watts during microwave irradiation resulted in a slight increase in conversion; however, a greater proportion of **103** was formed (entry 2). The use of fewer equivalents TfOH, lower temperature, and extended reaction times also provided a greater proportion of the deprotected vinylogous thioester (**103**) with varying degrees of olefin isomerization (entries 3-6). Similarly, increasing the temperature also appeared to yield a greater proportion of **103** regardless of the amount of TfOH, where decomposition occurred upon heating the mixture above 130 °C.

The lower reactivity observed for **102** relative to **84** may relate to the barrier in disrupting the aromaticity of the heterocycle. However, quantitative data concerning the degree of aromatic stabilization energies (ASE) or resonance energies (RE) seem to vary in the ranking of 5-membered aromatic heterocycles. In general, it appears that thiophene and pyrrole are interchangeably ranked as the heterocycle with the greatest aromatic character; whereas, furan possesses the least aromatic character. The ASE values for pyrrole, thiophene, and furan are 20.57, 18.57, and 14.77 kcal/mol, respectively, indicating that pyrrole possesses the greatest aromatic character.³²³ Conversely, the resonance energy for thiophene, pyrrole and furan is 43.0, 34.8, and 27.2 kcal/mol, respectively.³²⁴ This illustrates the variance in quantitatively describing the degree of aromaticity for common heteroaromatic compounds. If the rate of Nazarov cyclization depended largely on the energy required in interrupting aromaticity, then dienone **102** would be predicted to cyclize more readily than the analogous thiophene derivative (**84**). Instead, subjection of dienone **102** to the conditions optimized for the thiophene derivative causes significant protodesilylation, likely preventing further reaction to the corresponding cyclopentanone.

Table 4.7 Nazarov Cyclizations of Dienone (102)

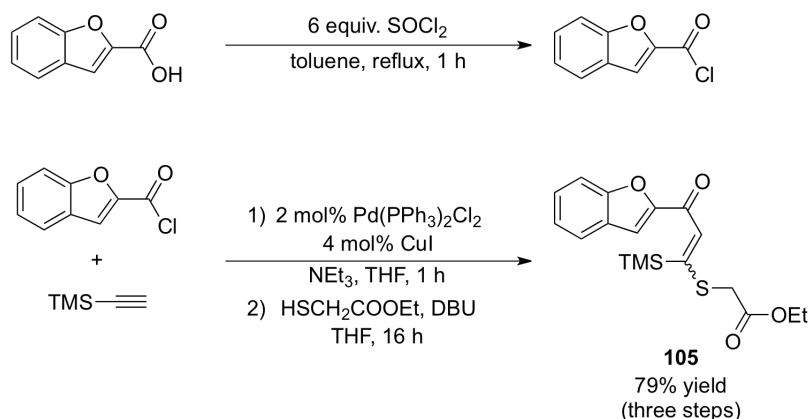


Entry ^a	Equivalents TfOH	Temperature (°C)	Time (h)	Conversion (%) ^b
1	5	80	1	66 (103 ^c : 104 1:2)
2 ^d	5	80	1	73 (103 ^c : 104 1:1)
3	2.5	80	1	22 (103 ^c : 104 8:1)
4	5	65	1	36 (103 ^e : 104 3:1)
5	5	80	2	95 (103 ^f : 104 2:1)
6	5	80	3	> 95 (103 ^f : 104 2.5:1)
7	5	85	1	90 (103 ^g : 104 1.5:1)
8	5	90	1	> 95 (103 ^f : 104 2.5:1)
9	2.5	110	1	32 (103) 2:1 <i>E:Z</i>
10	5	110	1	> 95 (103) 3:1 <i>E:Z</i>
11	1.2	130	0.25	> 95 (103) 2:1 <i>E:Z</i>
		110	0.75	
12	1	130	0.5	decomposition
13	1	180	2	decomposition

^a 0.2 mmol (0.2 M, **102**), 1.0 mmol TfOH. ^b Based on ¹H NMR. ^c 2:1 *E:Z*.

^d 30 W fixed power. ^e 6:1 *E:Z*. ^f 4:1 *E:Z*. ^g 3:1 *E:Z*.

The unexpected reactivity observed for benzothiophene dienone (**99**) led us to explore the reactivity of the analogous benzofuran derivatives. The preparation of this compound was accomplished in a similar manner, beginning with benzofuran-2-carboxylic acid. Treatment of benzofuran-2-carboxylic acid with excess SOCl₂ in refluxing toluene provided the acid chloride following evaporation of the volatiles. The Sonogashira-type cross-coupling generated the ynone *in-situ*, which was reacted with ethylthioglycolate in the presence of DBU.



Scheme 4.20

Similar to the benzothiophene example, a mixture of the expected dienone (**105**) and a byproduct resembling the corresponding cyclopentanone were isolated in a combined yield of 79%. The ^1H NMR spectra of the cyclopentanone byproduct for the benzothiophene and benzofuran compounds are depicted in Figure 4.7. The 3J coupling values for the methine signal (**A**) were determined to be 8.2 and 4.4 Hz. The diastereotopic protons labeled (**C**) possessed identical 3J coupling values, along with a strong 2J coupling (13.7 Hz).

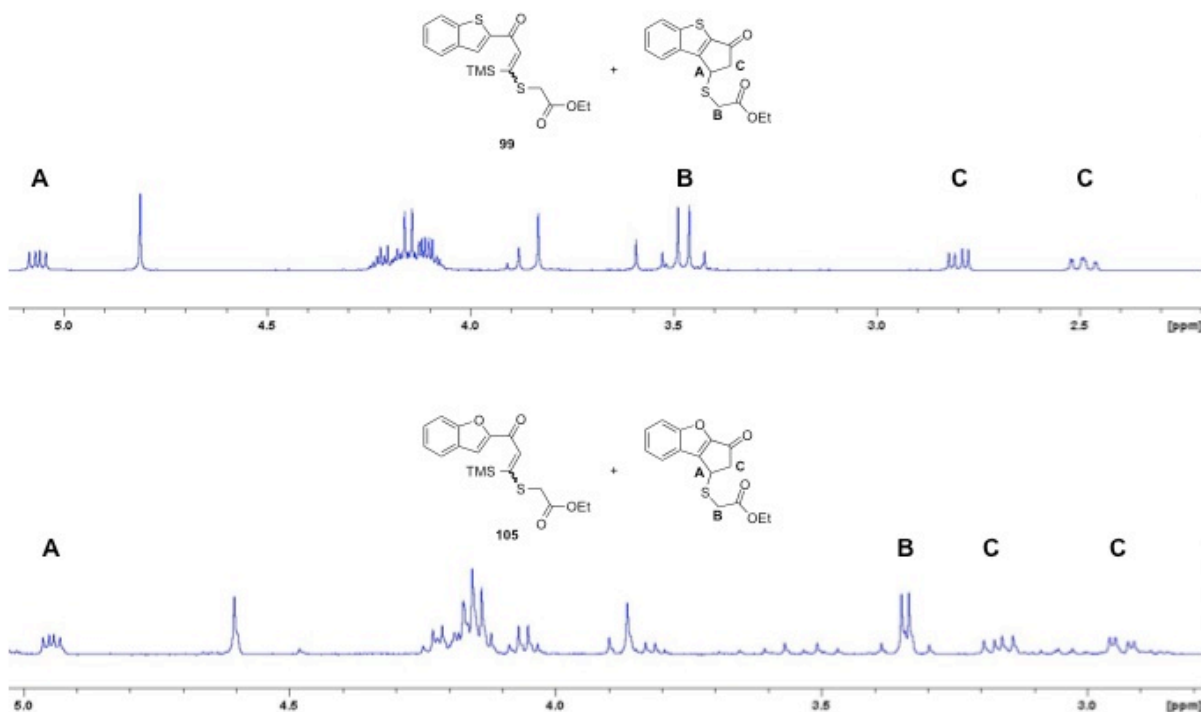
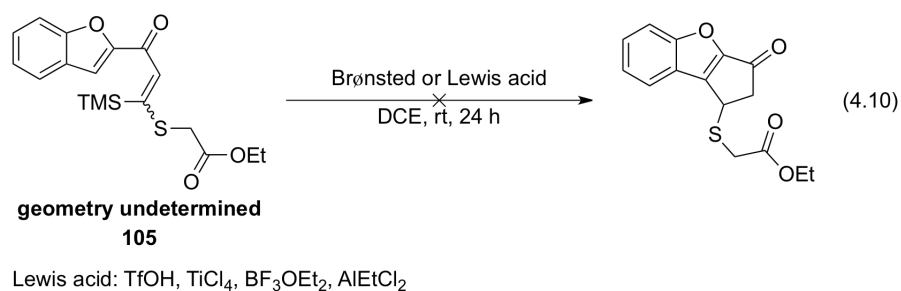
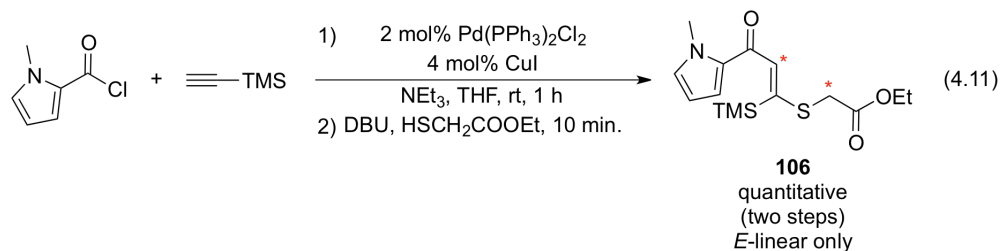


Figure 4.10 Comparison of Dienone 105 to 99

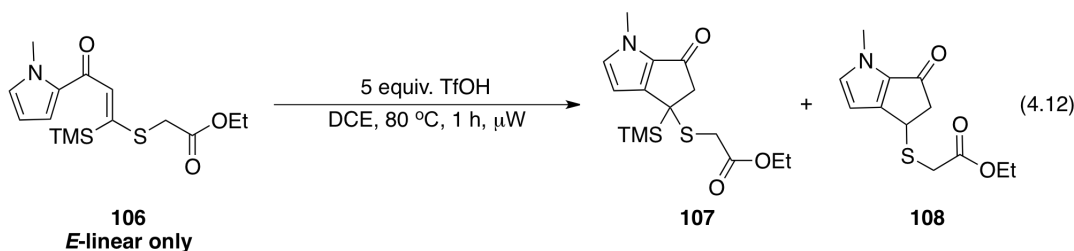
Subjection of dienone **105** to stoichiometric quantities of TfOH seemed to lead only to decomposition and not to an increase in the cyclopentanone product (Figure 4.7). Additionally, treatment with TiCl_4 , BF_3OEt_2 led to decomposition; whereas, AlEtCl_2 appeared to generate the cyclopentanone in 14% conversion. The cyclization of the benzannulated derivatives of dienone **84** and **102** likely require additional optimization as the conditions screened thus far have either led to decomposition or recovery of unreacted starting material. However, studies involving the benzothiophene dienone derived from ynone (**101**) have revealed that the silyl-protected dienones appear to be more reactive, despite the steric bulk of this group.



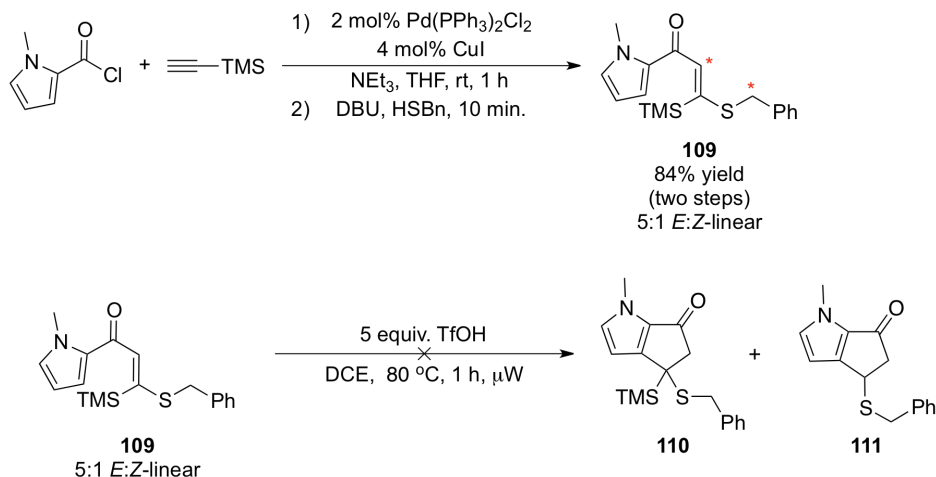
Lastly, we decided to evaluate the 2-substituted pyrrole dienone (**106**) to establish whether any trends exist between the various heteroaromatic species. As mentioned earlier, the ranking of furan, thiophene, and pyrrole in terms of increasing aromatic character suggests that the pyrrole derivatives should react more slowly relative to dienone **84**. However, thiophene and pyrrole are often interchangeably ranked as the heteroaromatic compound possessing the greatest degree of aromatic character. Regardless, dienone **106** was synthesized employing our one-pot methodology for the formation of vinylogous thioesters (Eq. 4.11). To this end, *N*-methylpyrrole-2-carbonyl chloride underwent smooth coupling with ethynyltrimethylsilane. The ynone was then intercepted with ethylthioglycolate providing dienone **106** in quantitative yield with exclusive selectivity for the *E*-linear isomer, as determined by a 2-D NOESY experiment. The correlation between the vinylic signal and the pyrrole C-H resonances was also detected, suggesting that dienone **106** partially exists as the S-shaped conformer at room temperature.



Dienone **106** was then reacted with 5 equivalents of TfOH at 80 °C for 1 hour, under microwave irradiation, yielding a mixture of cyclopentanones **107** and **108** in a 4:1 ratio (95% conversion). The high conversion to cyclopentanones **107** and **108** suggests that the pyrrole-substituted dienones are more reactive than the corresponding thiophene analogues (Eq. 4.12). Additionally, the silane remains intact following cyclization, whereas the thiophene substrates appeared to undergo protodesilylation.



Encouraged by the reactivity of dienone **106** we elected to study a derivative that proved relatively inert to the conditions optimized for dienone **84**. The benzylthiol derivative (**109**) was synthesized in 84% isolated yield as a 5:1 mixture of *E*:*Z*-linear isomers using our one-pot procedure for the synthesis of vinylogous thioesters. The major isomer was determined to be the *E*-linear based upon the observed correlation of the signals (*) in a 2-D NOESY experiment. Similar to dienone **106**, a correlation between the vinylic signal and the pyrrole C-H resonance was identified, suggesting that **109** partially exists as the S-shaped conformer at room temperature. The submission of **109** to the optimized conditions for the Nazarov cyclization led to consumption of starting material, generating a complex mixture. Unfortunately, no cyclopentanone products correlating to **110** or **111** could be identified, as with the formation of desilylated starting material.



Scheme 4.21

4.3 Conclusions

The cyclization of vinylogous thioesters appears to depend largely on the substitution about sulfur. A representation of a possible energy coordinate diagram is shown in Figure 4.11. The first intermediate during the Nazarov cyclization is the pentadienyl cation (**A**), which forms readily with electron rich dienones such as the vinylogous thioesters examined. The energetic barrier (**B**) in reaching the oxyallyl cation (**C**) is expected to be larger than protonation of the ketone oxygen, as the aromaticity of the heterocycle is disrupted. The barrier to cyclization (**B**) appears to be increased when the R-group bound to sulfur is aliphatic. The electron releasing nature of the sulfide in these substrates should correspondingly stabilize the pentadienyl cation (**A**); thereby, increasing the energy necessary in reaching intermediate (**C**).

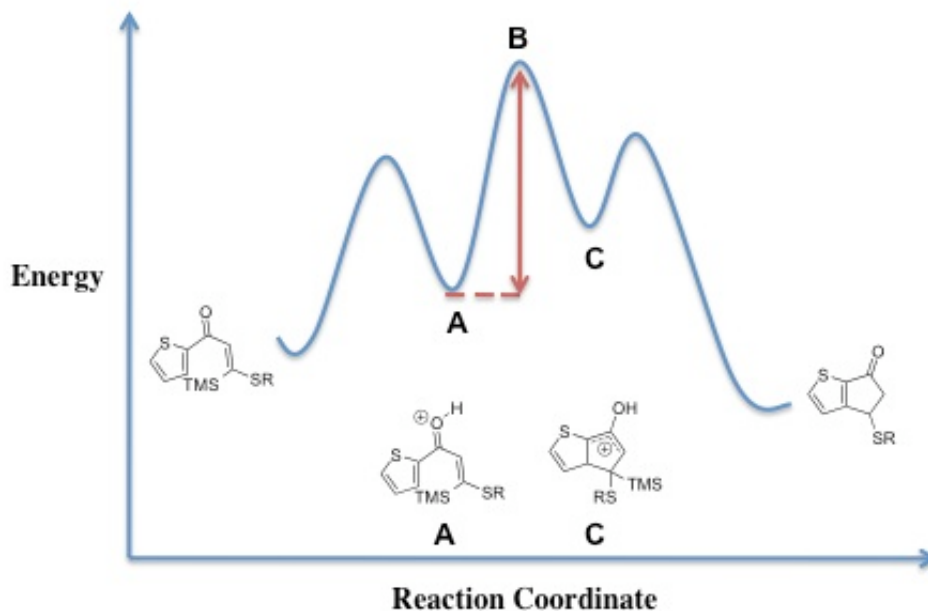


Figure 4.11 Reaction Coordinate Diagram for Cyclization of Vinylogous Thioesters

Indeed, olefin isomerization appears to predominate when these substrates are treated with Brønsted acids. A notable exception is dienone **84**, where the sulfur is α to the electron withdrawing ethyl ester. The presence of this group may facilitate cyclization by destabilizing the pentadienyl cation (**A**). The lower reactivity of dienone **91**, in which the sulfur is now β to the ethyl ester, lends support to this assumption. When the R-group is an aryl substituent (phenyl, anisole) the electron releasing nature of the sulfide will be less than that of the aliphatic derivatives. Therefore, the pentadienyl cation (**A**) will be less stable relative to when R is an alkyl group. The barrier to cyclization (**B**) should then be lower for substrates derived from aryl thiols. Unfortunately, the use of vinylogous thioesters of this nature appeared to decompose during cyclization, or following the formation of the product cyclopentanone via elimination of the free thiol. It seems that a fine balance exists regarding the electronic contribution of the sulfide to the stability of the pentadienyl cation, where electron withdrawing groups tend to favour cyclization from intermediate (**A**) to (**C**). However, the particular electron withdrawing group employed must not facilitate elimination of the sulfide following cyclization. Thus far, the use of ethylthioglycolate substituted vinylogous thioesters **84**, **98**, **99**, **102**, **105** and **106** appear to satisfy this criteria.

The aromaticity of the heterocycle appended to the dienone will also affect the

energetic barrier for the formation of the oxyallyl cation (**C**). The use of thiophene (**84**, **98**), furan (**102**) and pyrrole (**106**) substituted dienones illustrated that the pyrrole and thiophene substrates undergo cyclization most readily; whereas, furan is much less reactive under the optimized conditions. Benzannulated derivatives of the thiophene (**99**) and furan (**105**) derivatives appeared to undergo cyclization during the preparation of these substrates. An alternative route to **99** was explored in order to assess whether trace acid, or an electrophilic palladium or copper species, was responsible for the observed reactivity. A Weinreb ketone synthesis facilitated the formation of the desilylated derivative of **99**, which failed to cyclize under a variety of conditions. Therefore, the trimethylsilane may greatly aid in the formation of the oxyallyl cation intermediate. However, isolation and reaction of the silylated dienones **99** and **105** with various Brønsted and Lewis acids failed to provide the desired cyclopentanones, primarily leading to decomposition instead. Further optimization of these systems is necessary, as well as an investigation of the indole analogue of dienone **106**.

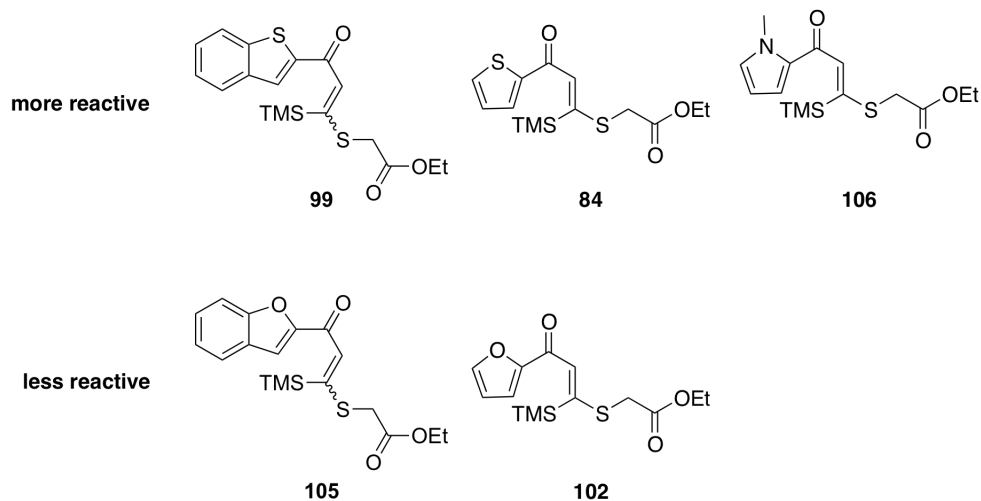


Figure 4.12 Reactivity of Various Heteroaromatic Vinylogous Thioesters

The formation of 3-substituted cyclopentanones from the 2-substituted dienones, and vice-versa, was unexpected. The observation of similar rearrangements during the intramolecular Friedel-Craft acylations of heteroaromatic propionic acids suggests that a similar spirocyclic intermediate is operable in our systems.³¹⁵ Additionally, the mechanism speculated for rearrangement suggests that an intramolecular Friedel-Crafts acylation pathway may compete with the Nazarov cyclization for the dienones investigated in this thesis. The competition between Nazarov and intramolecular Friedel-Crafts cyclizations has

been previously suggested with similar heteroaromatic containing dienones that lack sulfur-substitution.^{313, 325} Exploring the mechanism behind the rearrangements observed in our system will ideally shed light on the determinants for whether the Friedel-Crafts process or Nazarov cyclization occurs.

4.4 Experimental

4.4.1 General Procedures

Manipulation of organometallic compounds was performed using standard Schlenk techniques under an atmosphere of dry nitrogen or in a nitrogen-filled Vacuum Atmospheres drybox ($O_2 < 2$ ppm). NMR spectra were recorded on Bruker Avance 300 or Bruker Avance 400 spectrometers. 1H and ^{13}C NMR spectra are reported in parts per million and were referenced to residual solvent: $CD_3CN = 1.94$ 1H NMR, 118.26 for ^{13}C NMR, for $CDCl_3 = 7.26$ 1H NMR, 77.0 for ^{13}C NMR, for $CD_2Cl_2 = 5.32$ for 1H NMR, 53.8 for ^{13}C NMR. Coupling constant values were extracted assuming first-order coupling. The multiplicities are abbreviated as follows: s = singlet, d = doublet, t = triplet, q = quartet, m = multiplet, br = broad signal, dd = doublet of doublets, dt = doublet of triplets, td = triplet of doublets, AB t = second-order triplet, AB dd = second order doublet of doublets, AB q = second order quartet. The chemical shift value for second order quartets (AB q) were reported based upon the solution to the equation $(1-3) = (2-4) = [(\Delta\nu)^2 + J^2]^{1/2}$ where J = coupling constant (Hz) and $\Delta\nu$ = chemical shift difference (Hz) = unknown value, and (1-3) or (2-4) represents left to right numbering of the individual peaks related to the multiplet (Hz). The value for $\Delta\nu$ was then subtracted or added to the middle of the coupling pattern and converted to ppm based upon spectrometer frequency. All spectra were obtained at 25 °C. Mass spectra were recorded on a Kratos MS-50 mass spectrometer.

4.4.2 Materials and Methods

THF, CH_2Cl_2 , and toluene were dried by passage through solvent purification columns.²³⁷ Acetonitrile was distilled over CaH_2 prior to use, or purchased from Aldrich as anhydrous grade and stored in a Sure Seal bottle. 1,2-Dichloroethane and $CDCl_3$ were distilled over P_2O_5 and degassed prior to use. Unless specifically mentioned, all organic reagents were obtained from commercial sources and used without further purification.

Transition metal reagents such as $\text{Pd}(\text{PPh}_3)_2\text{Cl}_2$ and CuI were purchased from Strem Chemicals and taken directly into an inert atmosphere glovebox without further purification.

4.4.3 General Experimental Procedures

Dienone Synthesis

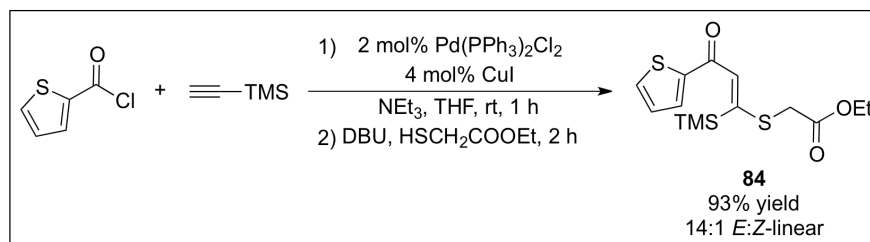
In an inert atmosphere glovebox, $\text{Pd}(\text{PPh}_3)_2\text{Cl}_2$ (82.6 mg, 0.12 mmol) was added to a round bottom flask equipped with a magnetic stir bar. To this was added CuI (43.4 mg, 0.23 mmol), the flask was then sealed with a serum cap and removed from the glovebox. Under a dynamic flow of N_2 , 30 mL of THF was added and the solution was vigorously sparged for 5 minutes. To the pale yellow heterogenous mixture was added NEt_3 (0.82 mL, 5.9 mmol). Following addition of NEt_3 the solution became homogenous and turned a dark red colour. To this was then added the acyl halide (5.9 mmol), which was typically accompanied by the evolution of gas (HCl), and a colour change to a light orange. Lastly, the ethynyltrimethylsilane (5.9 mmol) was added causing the solution to turn a black-grey colour. The mixture was then stirred for 1 hour, where the colour would sometimes return to a light orange-red, and the appearance of $[\text{HNEt}_3]^+\text{Cl}^-$ or a separate precipitate was evident. The ynone formed during this process was carried directly to the next step without further purification. Therefore, DBU (0.93 mL, 6.2 mmol) was added causing the precipitation of various amine salts, and was followed by the addition of the thiol (6.2 mmol). A TLC was taken immediately following addition of thiol and was compared to an aliquot of the mixture prior to the Michael addition step. Consumption of the alkyne typically occurred immediately; otherwise, the mixture was stirred overnight. Once the reaction was judged to be complete, the mixture was concentrated *in-vacuo* and purified by column chromatography using gradient elution. This involved an initial eluent of 9:1 hexanes:ethyl acetate and ended with 4:1 or 3:1 hexanes:ethyl acetate. The 3-substituted dienones sometimes require pre-treatment of the SiO_2 gel with a 10% solution of NEt_3 in hexanes or 9:1 hexanes:ethyl acetate, in order to prevent protodesilylation during chromatography.

Nazarov Cyclization

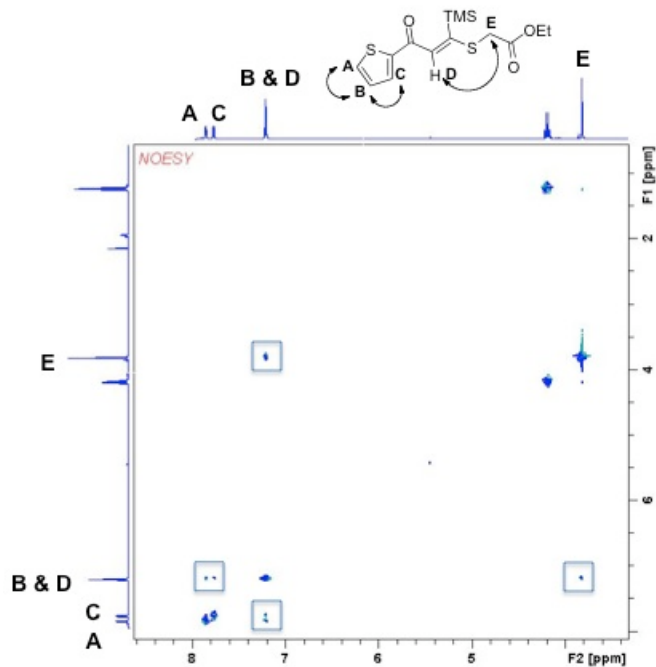
To a standard 2-5 mL microwave vial equipped with a magnetic stir bar (purchased from Biotage) was added (0.62 mmol) dienone (weighed by difference). To this was added

3.1 mL of 1,2-Dichloroethane. The microwave vial was then mechanically sealed with a cap (purchased from biotage) and stirred under N₂. To the solution was added TfOH (3.1 mmol), which was accompanied by a colour change from a yellow-orange solution to a dark red. The tube was then placed within a Biotage Initiator 2.0 single cavity microwave reactor and heated to 80 °C with a maximum power output of 400 W. The solution was programmed for a stir period of 1 hour. The microwave vial was then mechanically opened and the reaction quenched with saturated Na₂CO₃ (5 mL). The aqueous layer was then back extracted with CH₂Cl₂ (3 x 10 mL). The combined organic layers were then washed with successively with Na₂CO₃ (10 mL), distilled H₂O (10 mL), and brine (10 mL). The organic layer was then dried over Na₂SO₄, filtered and concentrated *in-vacuo*. The crude mixture was then purified by column chromatography using gradient elution. This involved an initial eluent of 9:1 hexanes:ethyl acetate and ended with 4:1 or 2:1 hexanes:ethyl acetate. When conversion is reported, the crude mixture was simply dried further by high vacuum, taken up in CD₃CN and the reaction progress evaluated by ¹H NMR.

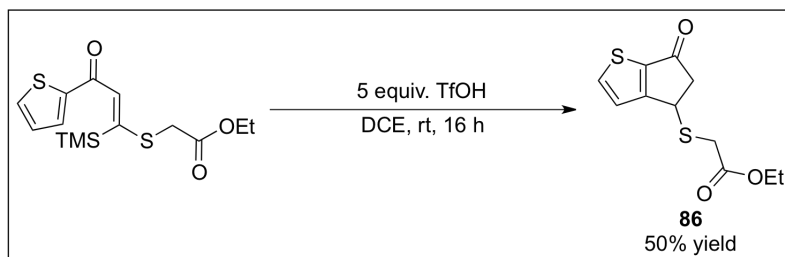
4.4.4 Analytical Data for Dienones and Cyclopentanones



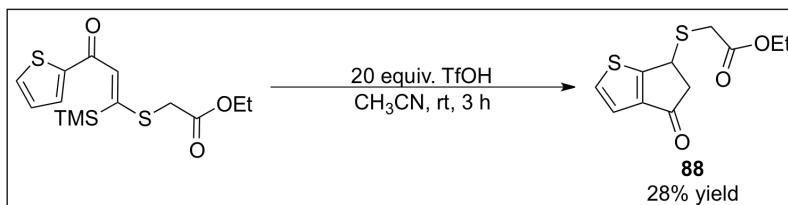
Dienone **84**, 14:1 mixture of *E*:*Z*-linear isomers. ¹H NMR (CD₃CN, 400 MHz, δ 1.94): δ 7.85 (d, 1H, *J* = 3.9 Hz), 7.77 (d, 1H, *J* = 3.9 Hz), 7.22 – 7.20 (m, 2H), 4.19 (q, 2H, *J* = 7.1 Hz), 3.85 (s, 0.14H, *Z*-linear isomer), 3.82 (s, 2H), 1.23 (t, 3H, *J* = 7.1 Hz), 0.29 (s, 9H). ¹³C {¹H} NMR (d₃-acetonitrile, 100 MHz, 298 K): δ 179.9, 169.5, 165.8, 146.7, 134.9, 132.9, 129.6, 124.4, 62.7, 35.8, 14.5, -0.3. HRMS (ESI) *m/z* calcd for C₁₄H₂₀O₃NaSi₂: 351.0521 (M+Na)⁺; found: 351.0527. As B and D overlap with one another, it is difficult to distinguish whether **84** partially exists as the S-shaped conformer. The spectrum depicted below has **84** represented as the S-shaped conformer simply for ease in visualizing the correlations indicated.



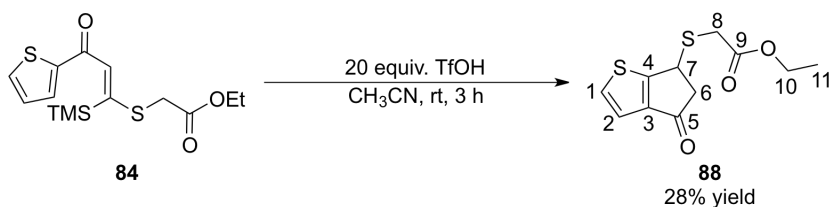
2D-NOESY



Cyclopentanone **86**. ^1H NMR (CD_3CN , 400 MHz, δ 1.94): δ 8.07 (d, 1H, $J = 4.9$ Hz), 7.21 (d, 1H, $J = 4.9$ Hz), 4.61 – 4.59 (AB dd, 1H, $J = 6.7, 2.1$ Hz), 4.10 (q, 2H, $J = 7.1$ Hz), 3.47 – 3.42 (AB dd, 1H, $J = 18.8, 6.7$ Hz), 3.32 – 3.28 (AB q, 2H, $J = 15.1$ Hz), 2.96 – 2.91 (AB dd, 1H, $J = 18.8, 2.1$ Hz), 1.22 (t, 3H, $J = 7.1$ Hz). ^{13}C $\{^1\text{H}\}$ NMR (d_3 -acetonitrile, 100MHz, 298K): δ 194.7, 171.0 (two signals), 168.6, 142.3, 125.0, 118.3, 62.2, 50.9, 39.9, 33.5, 14.4. HRMS (ESI) m/z calcd for $\text{C}_{11}\text{H}_{12}\text{O}_3\text{NaS}_2$: 279.0126 ($\text{M}+\text{Na}$) $^+$; found: 279.0124.

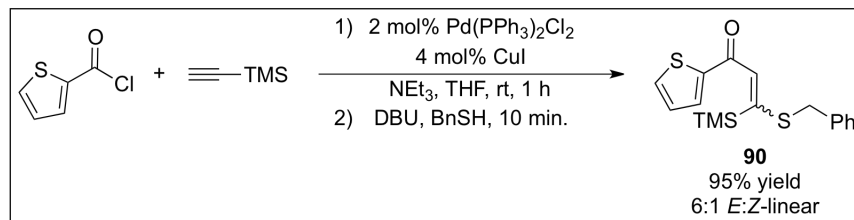


Cyclopentanone **88**. ^1H NMR (CD_3CN , 400 MHz, δ 1.94): δ 7.57 (dd, 1H, $J = 5.1, 0.7$ Hz), 7.09 (d, 1H, $J = 5.1$ Hz), 4.79 – 4.78 (AB dd, 1H, $J = 6.7, 2.2$ Hz), 4.13 (q, 2H, $J = 7.1$ Hz), 3.47 – 3.42 (AB dd, 1H, $J = 18.8, 6.8$ Hz), 3.37 – 3.33 (AB q, 2H, $J = 15.1$ Hz), 2.93 – 2.89 (AB dd, 1H, $J = 18.8, 2.3$ Hz), 1.23 (t, 3H, $J = 7.1$ Hz). ^{13}C $\{^1\text{H}\}$ NMR (d_3 -acetonitrile, 100MHz, 298K): δ 195.5, 171.4 (two signals), 148.1, 134.9, 120.2, 62.8, 51.7, 40.9, 34.2, 14.8. HRMS (ESI) m/z calcd for $\text{C}_{11}\text{H}_{13}\text{O}_3\text{S}_2$: 257.0306 ($\text{M}+\text{H}^+$); found: 257.0308. Summary of the 2-D NMR data obtained for the cyclopentanone product formed during cyclization in CH_3CN .

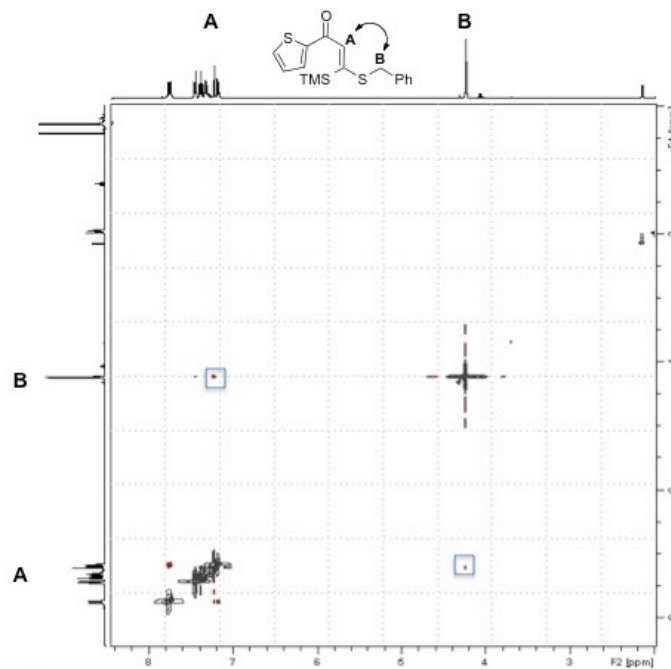


	Carbon	C-1	C-2	C-3	C-4	C-5	C-6	C-7	C-8	C-9	C-10	C-11
Proton	(ppm)	134.9	120.2	148.1	171.3	195.2	51.7	40.9	34.2	171.4	62.8	14.8
H-1	7.57	bonded	α	β	β							
H-2	7.09	α	bonded	α	β							
H-6	3.44 2.91				β β	α α	bonded	α α				
H-7	4.78			β	α	β	α	bonded	β			
H-8	3.35							β	bonded	α		
H-10	4.13									β	bonded	α
H-11	1.23										α	bonded

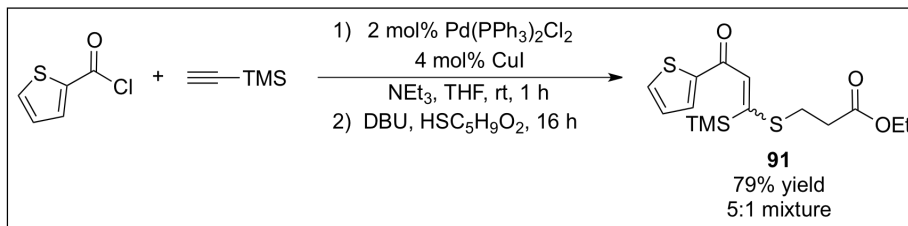
^a Recorded at 400 MHz. ^b Assignments based on COSY, HSQC and HMBC. ^c α refers to 2J coupling, β refers to 3J coupling, bonded refers to 1J coupling based upon HSQC assignments.



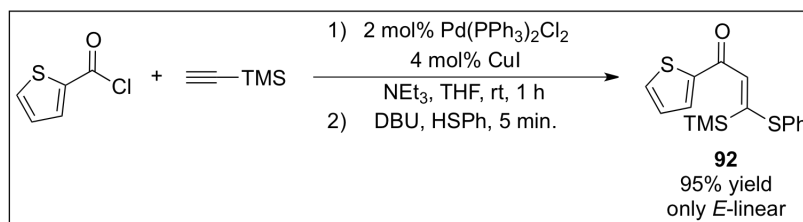
Dienone **90**, 6:1 mixture of *E*:*Z*-linear isomers. ¹H NMR (CD₃CN, 400 MHz, δ 1.94): δ 7.77 – 7.76 (AB dd, 1H, *J* = 3.9, 1.0 Hz), 7.75 – 7.74 (AB dd, 1H, 4.9, 1.0 Hz), 7.46 – 7.29 (m, 6H), 7.22 (s, 1H), 7.19 – 7.17 (AB dd, 1H, *J* = 4.9, 3.9 Hz), 4.23 (s, 2H), 4.22 (s, 0.3H *Z*-linear isomer), 0.42 (s, 1.5 H, *Z*-linear isomer), 0.27 (s, 9H). ¹³C {¹H} NMR (d₃-acetonitrile, 100MHz, 298K): δ 179.8, 168.1, 146.8, 136.6, 134.6, 134.5, 132.7, 132.3, 130.2, 130.0, 129.8, 129.6, 129.5 (two peaks), 128.5, 128.4, 125.7, 124.0, 39.6, 38.1, 0.5, –0.2. HRMS (ESI) *m/z* calcd for C₁₇H₂₁OSi₂: 333.0803 (M+H)⁺; found: 333.0811.



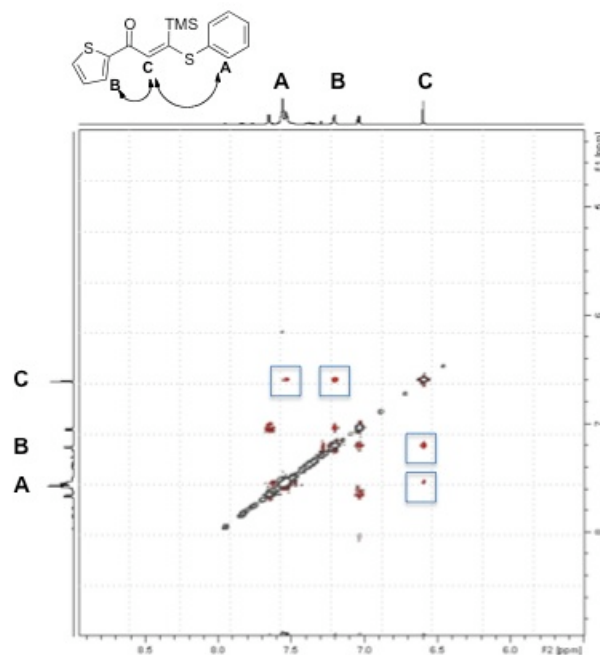
2D-NOESY



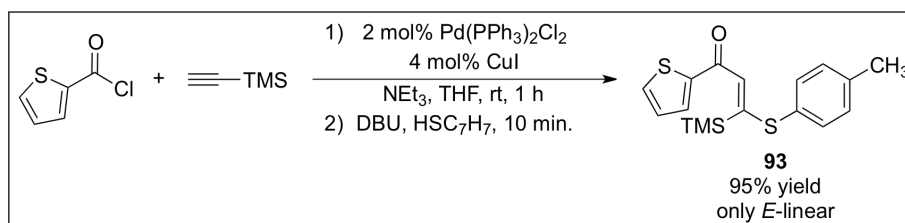
Dienone **91**, 5:1 mixture of *E*:*Z*-linear isomers. ¹H NMR (CD₃CN, 400 MHz, δ 1.94): δ 7.88 – 7.87 (AB dd, 1H, *J* = 3.8, 1.0 Hz), 7.76 – 7.75 (AB dd, 1H, 5.0, 1.0 Hz), 7.21 – 7.19 (AB dd, 1H, *J* = 5.0, 3.8), 7.14 (s, 1H), 4.14 (q, 2H, *J* = 7.1 Hz), 3.22 (t, 2H, *J* = 7.2 Hz), 2.71 (t, 2H, *J* = 7.2 Hz), 2.57 (t, 0.44H, *J* = 7.2 Hz, *Z*-linear isomer), 1.23 (t, 3H, *J* = 7.1 Hz), 0.38 (s, 1.8H, *Z*-linear isomer), 0.27 (s, 9H). ¹³C {¹H} NMR (d₃-acetonitrile, 100MHz, 298K): δ 179.9, 172.3, 167.4, 146.9, 134.6, 134.5, 132.8, 132.3, 129.5 (two signals), 126.2, 123.5, 61.6, 61.5, 34.7, 32.9, 29.8, 27.9, 14.5 (two signals), 0.5, –0.2. HRMS (ESI) *m/z* calcd for C₁₅H₂₂O₃NaSiS₂: 365.0677 (M+Na)⁺; found: 365.0678.



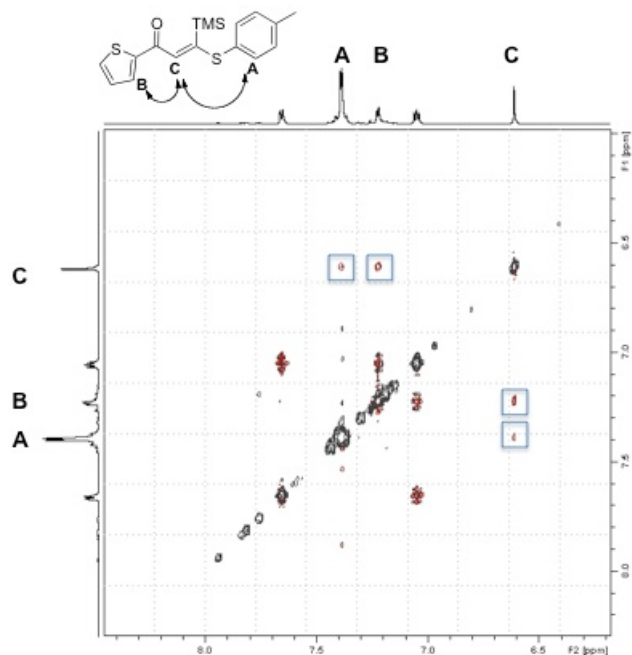
Dienone **92**, only *E*-linear isomer. ¹H NMR (CD₃CN, 300 MHz, δ 1.94): δ 7.65 – 7.64 (AB dd, 1H, *J* = 5.0, 1.1 Hz), 7.57 – 7.52 (m, 5H), 7.21 – 7.20 (AB dd, 1H, *J* = 3.8, 1.1 Hz), 7.04 – 7.03 (AB dd, 1H, *J* = 5.0, 3.8 Hz), 6.60 (s, 1H), 0.35 (s, 9H). ¹³C {¹H} NMR (d₃-acetonitrile, 75MHz, 298K): δ 179.8, 169.2, 146.5, 136.2, 134.6, 132.2, 131.2, 131.1, 129.5, 125.4, –0.3. HRMS (ESI) *m/z* calcd for C₁₆H₁₉OSiS₂: 319.0647 (M+H)⁺; found: 319.0648.



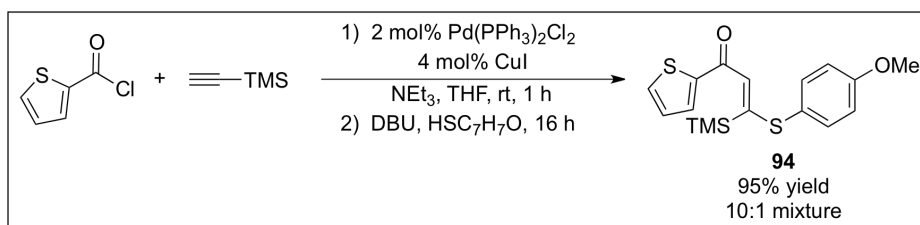
2D-NOESY



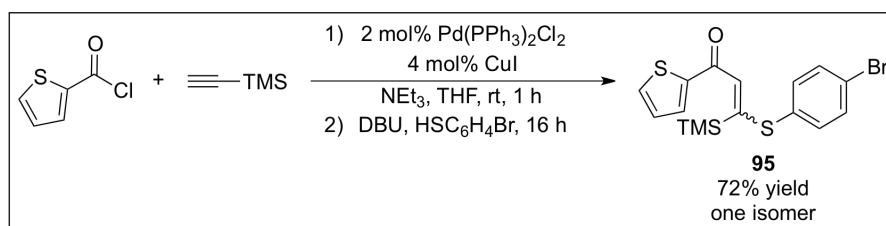
Dienone **93**, only *E*-linear isomer. ^1H NMR (CD_3CN , 400 MHz, δ 1.94): δ 7.66 – 7.65 (AB dd, 1H, $J = 5.0, 1.0$ Hz), 7.40 – 7.38 (AB q, 4H, $J = 8.5$ Hz), 7.23 – 7.22 (AB dd, 1H, $J = 3.8, 1.0$ Hz), 7.06 – 7.05 (AB dd, 1H, $J = 5.0, 3.8$ Hz), 6.6 (s, 1H), 2.42 (s, 3H), 0.34 (s, 9H). ^{13}C $\{^1\text{H}\}$ NMR (d_3 -acetonitrile, 100MHz, 298K): δ 179.8, 169.7, 146.6, 141.6, 136.1, 134.5, 132.2, 131.9, 129.5, 127.6, 125.2, 21.4, -0.3 . HRMS (ESI) m/z calcd for $\text{C}_{17}\text{H}_{21}\text{OSi}_2$: 333.0803 ($\text{M}+\text{H}^+$); found: 333.0805.



2D-NOESY

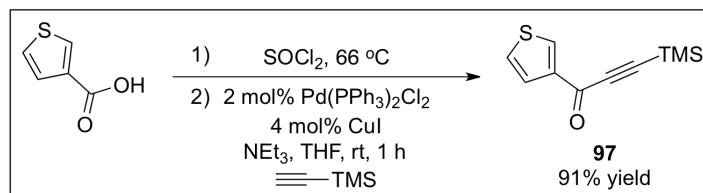


Dienone **94**, 10:1 mixture of *E:Z*-linear isomers. ^1H NMR (CD_3CN , 400 MHz, δ 1.94): δ 7.67 – 7.66 (AB dd, 1H, $J = 5.0, 1.1$ Hz), 7.43 (d, 2H, 8.9 Hz), 7.26 – 7.25 (AB dd, 1H, $J = 3.8, 1.1$ Hz), 7.10 (d, 2H, $J = 8.9$ Hz), 7.07 – 7.06 (AB dd, 1H, $J = 5.0, 3.8$ Hz), 6.61 (s, 1H), 3.86 (s, 3H), 3.84 (s, 0.33H, other olefin isomer), 0.34 (s, 9H), 0.01 (s, 0.51H, other olefin isomer).

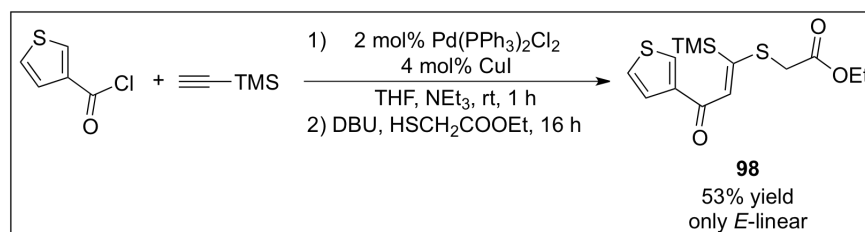


Dienone **95**, only one olefin isomer, geometry not determined. ^1H NMR (CD_3CN , 400

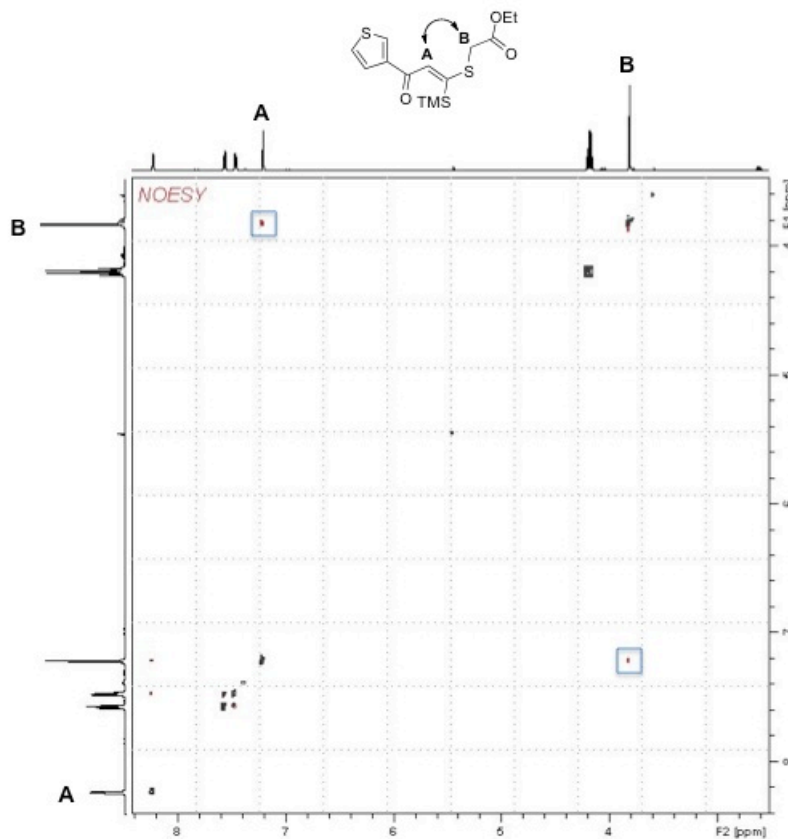
MHz, δ 1.94): δ 7.71 (d, 2H, $J = 8.6$ Hz), 7.69 – 7.68 (AB dd, 1H, $J = 5.0, 1.1$ Hz), 7.44 (d, 2H, $J = 8.6$ Hz), 7.32 – 7.31 (AB dd, 1H, $J = 3.8, 1.1$ Hz), 7.09 – 7.07 (AB dd, 1H, $J = 5.0, 3.8$ Hz), 6.64 (s, 1H), 0.34 (s, 9H).



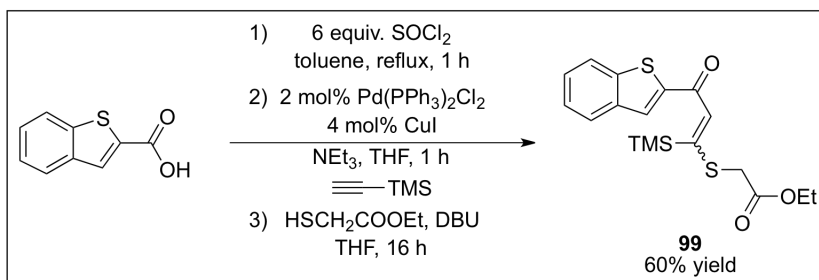
Alkyne **97**. In a flame dried round bottom equipped with a magnetic stir bar and a drying tube was added the above carboxylic acid (1.763 g, 13.8 mmol). To this was added SOCl_2 (6 mL, 82.5 mmol, 6 equiv.) and the mixture refluxed for 1 hour. The mixture appeared to become homogenous and was subsequently concentrated by high vacuum. The low melting solid was then purified by kugelrohr distillation, and subjected to the general conditions for the Sonogashira-type cross-coupling, providing the ynone in 91% yield, following chromatography. ^1H NMR (CD_3CN , 400 MHz, δ 1.94): δ 8.41 – 8.40 (AB dd, 1H, $J = 2.9, 1.2$ Hz), 7.56 – 7.54 (AB dd, 1H, $J = 5.1, 1.2$ Hz), 7.49 – 7.48 (AB dd, 1H, $J = 5.1, 2.9$ Hz), 0.30 (s, 9H).



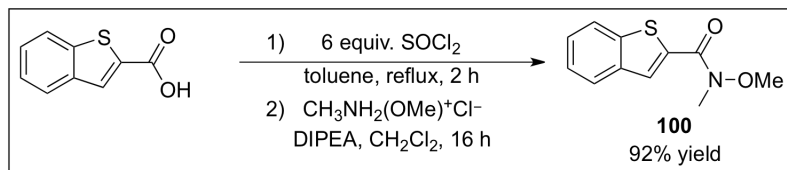
Dienone **98**, only *E*-linear isomer. ^1H NMR (CD_3CN , 400 MHz, δ 1.94): δ 8.23 – 8.22 (AB dd, 1H, $J = 2.8, 1.2$ Hz), 7.57 – 7.56 (AB dd, 1H, $J = 5.1, 1.2$ Hz), 7.47 – 7.46 (AB dd, 1H, $J = 5.1, 2.8$ Hz), 7.21 (s, 1H), 4.19 (q, 2H, $J = 7.1$ Hz), 3.82 (s, 2H), 1.22 (t, 3H, $J = 7.1$ Hz), 0.29 (s, 9H). ^{13}C $\{^1\text{H}\}$ NMR (d_3 -acetonitrile, 100MHz, 298K): δ 181.3, 169.6, 165.2, 144.1, 133.2, 128.1, 128.0, 125.7, 62.6, 35.7, 14.4, -0.3 . HRMS (ESI) m/z calcd for $\text{C}_{14}\text{H}_{20}\text{O}_3\text{S}_2\text{Si}$: 329.0701 ($\text{M}+\text{H}$) $^+$; found: 329.0706.



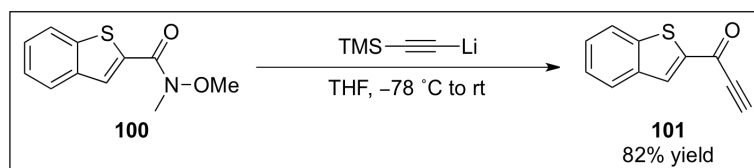
2D-NOESY



Dienone **99**, mixture of olefin isomers, contaminated with small amount of the corresponding cyclopentanone. The acyl halide was prepared in a similar manner to the procedure described for the preparation of alkyne **97**. As the carboxylic acid was insoluble in neat SOCl_2 , toluene was added and the mixture heated to reflux for 1 hour. The crude acyl halide was concentrated by high vacuum, rinsed with anhydrous THF and concentrated several more times prior to the one-pot cross-coupling Michael addition sequence. ^1H NMR (CD_3CN , 400 MHz, δ 1.94): δ 8.17 (s, 1H), 8.00 (m, 2H), 7.57 – 7.45 (m, 3H), 7.34 (s, 1H), 4.22 (q, 3H, $J = 7.1$ Hz), 3.88 (s, 5H), 1.26 (t, 3H, $J = 7.1$ Hz), 0.32 (s, 9H).

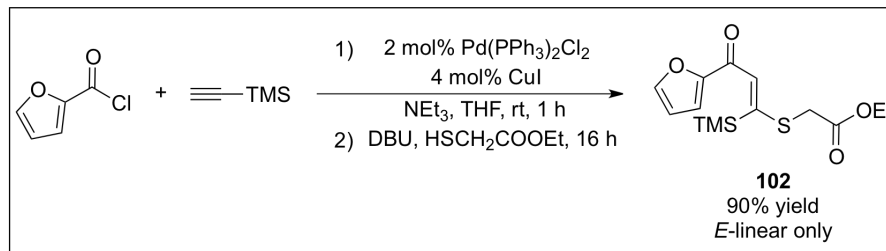


Weinreb amide **100**. In a flame dried round bottom equipped with a magnetic stir bar and a serum cap was added the carboxylic acid (0.5021 g, 2.8 mmol) in 2 mL of toluene. To this was added SOCl_2 (1.2 mL, 16.5 mmol, 6 equiv.) and the mixture refluxed for 2 hours. The mixture was then concentrated by high vacuum and the crude acyl halide rinsed with anhydrous CH_2Cl_2 and concentrated again. The crude acyl halide was dissolved in 14 mL of DCM and the amine salt (0.4408 g, 4.5 mmol, 1.5 equiv.) added in one portion. To this was added diisopropylethylamine (1.5 mL, 8.6 mmol, 2.8 equiv.) and the mixture stirred at room temperature overnight. The mixture was then poured into 0.5 M HCl and the aqueous layer extracted with DCM (3 x 10 mL). The combined organic layers were then washed with 0.5 M NaOH (10 mL) and brined (10 mL). The organic layers were then dried over Na_2SO_4 , filtered and concentrated *in-vacuo* providing **100** in 92% yield. ^1H NMR (CD_3CN , 400 MHz, δ 1.94): δ 8.17 (s, 1H), 7.97 – 7.92 (m, 2H), 7.51 – 7.41 (m, 2H), 3.82 (s, 3H), 3.35 (s, 3H).

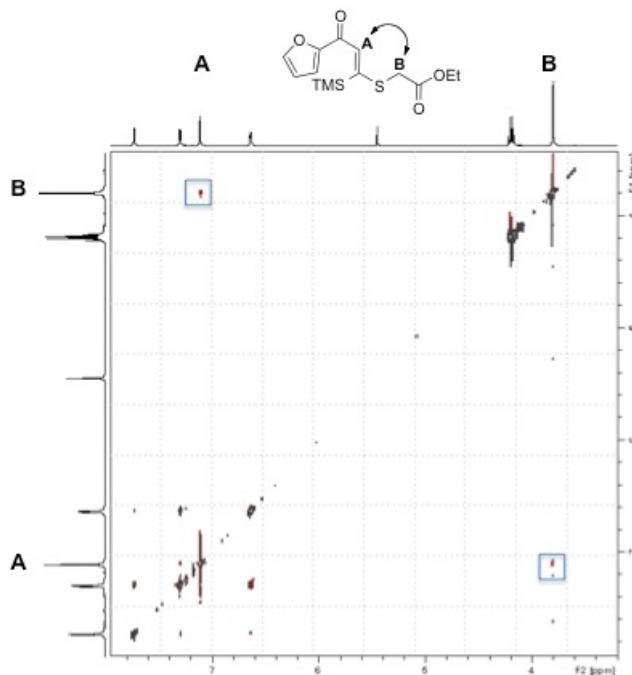


Ynone **101**. To a flame dried round bottom equipped with a magnetic stir bar and a serum cap was added ethynyltrimethylsilane (0.44 mL, 3.1 mmol) in 10 mL of THF. The flask was cooled to -78°C and *n*-BuLi added (2.3 mL, 1.35 M in hexanes, 1.0 equiv.) over a period of 2 minutes. The solution of *n*-BuLi was titrated against *N*-benzylbenzamide prior to use.²⁴¹ The flask was allowed to warm to room temperature and then cooled back to -78°C . In a separate flame dried round bottom, Weinreb amide **100** was dissolved in 5 mL of THF. The solution of lithium trimethylsilylacetylide was then transferred by cannula to the solution of **100**, which was cooled to -78°C . The flask formerly containing lithium trimethylsilylacetylide was rinsed twice with THF (2 mL portions). The mixture was allowed to warm to room temperature and quenched with 0.5 M HCl (10 mL), which turned the red solution a yellow colour upon shaking within a separatory funnel. The aqueous layer was

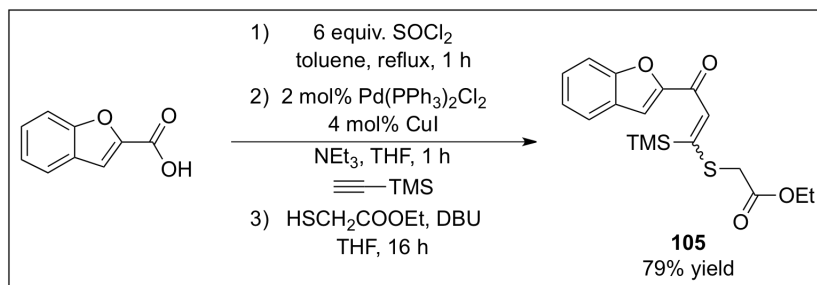
extracted with diethyl ether (3 x 10 mL) and the combined organic layers washed with 0.5 M NaOH (10 mL) and brine (10 mL). The organic layer was then dried over Na₂SO₄, filtered and concentrated *in-vacuo*, providing ynone **101** in 82% yield. ¹H NMR (CD₃CN, 400 MHz, δ 1.94): δ 8.38 (br s, 1H), 8.05 (d, 1H, *J* = 8.3 Hz), 7.98 (d, 1H, *J* = 8.0 Hz), 7.58 – 7.50 (td, 2H, *J* = 8.3, 8.0, 1.3 Hz), 3.97 (s, 1H).



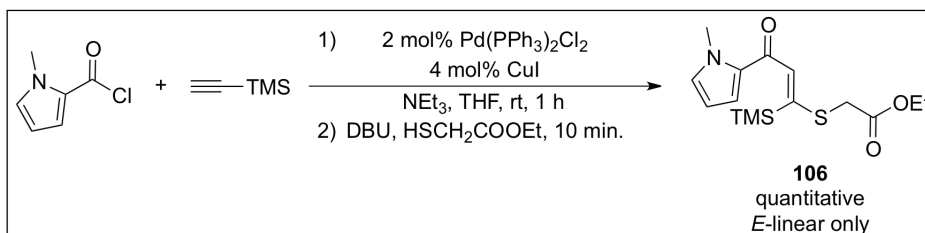
Dienone **96**, only *E*-linear isomer. ¹H NMR (CD₃CN, 400 MHz, δ 1.94): δ 7.73 – 7.72 (AB dd, 1H, *J* = 1.7, 0.6 Hz), 7.30 – 7.29 (AB dd, 1H, *J* = 3.6, 0.6 Hz), 7.11 (s, 1H), 6.64 – 6.63 (AB dd, 1H, *J* = 3.6, 1.7 Hz), 4.19 (q, 2H, *J* = 7.1 Hz), 3.80 (s, 2H), 1.24 (t, 3H, *J* = 7.1 Hz), 0.29 (s, 9H). ¹³C {¹H} NMR (d₃-acetonitrile, 100MHz, 298K): δ 175.4, 169.4, 165.7, 148.1, 142.9, 124.1, 113.4, 62.6, 35.8, 14.4, -0.3. HRMS (ESI) *m/z* calcd for C₁₄H₂₀O₄NaSiS: 335.0749 (M+Na)⁺; found: 335.0745.



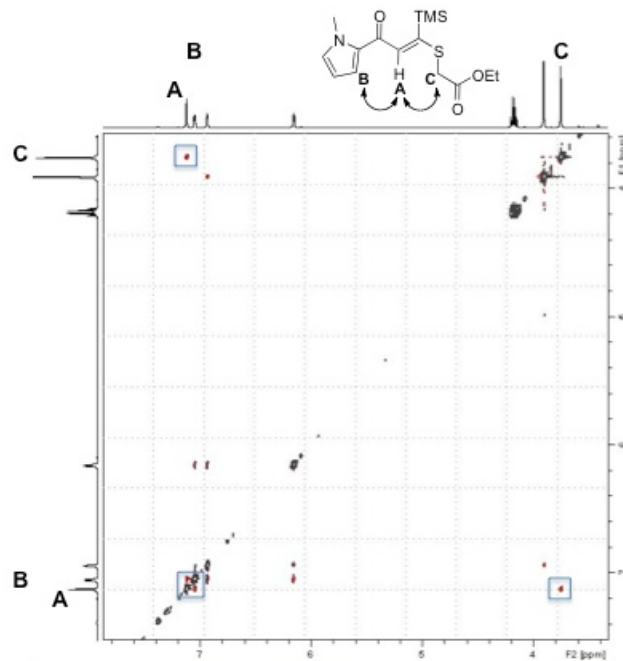
2D-NOESY



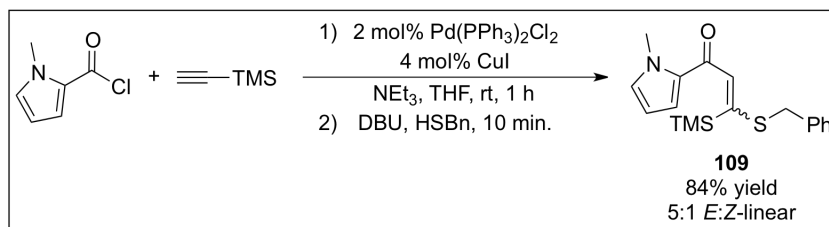
Dienone **105**, mixture of isomers, contaminated with the corresponding cyclopentanone. The preparation of **105** was analogous to that described for the benzothiophene analogue. ¹H NMR (CD₃CN, 400 MHz, δ 1.94): δ 7.80 (d, 0.5H, *J* = 7.6 Hz), 7.69 – 7.60 (m, 2.4H), 7.55 – 7.52 (m, 1.9H), 7.38 – 7.26 (m, 3.8H), 7.07 (d, 1H, *J* = 0.8 Hz), 6.82 (d, 0.2H, *J* = 0.8 Hz), 4.96 – 4.94 (AB dd, 0.9H, *J* = 8.2, 4.5 Hz, cyclopentanone), 4.60 (s, 0.9H), 4.25 – 4.12 (m, 5.7H), 4.06 (q, 1.0H, *J* = 7.2 Hz), 3.86 (s, 0.8H), 3.36 – 3.32 (AB q, 1.9H, *J* = 15.1 Hz, cyclopentanone), 3.18 – 3.15 (AB dd, 0.9H, *J* = 13.7, 8.2 Hz), 2.95 – 2.92 (AB dd, 0.9H, *J* = 13.7, 4.3 Hz, cyclopentanone), 1.28 – 1.19 (m, 9.7H), 0.32 (s, 3.5H), –0.07 (s, 10.1H).



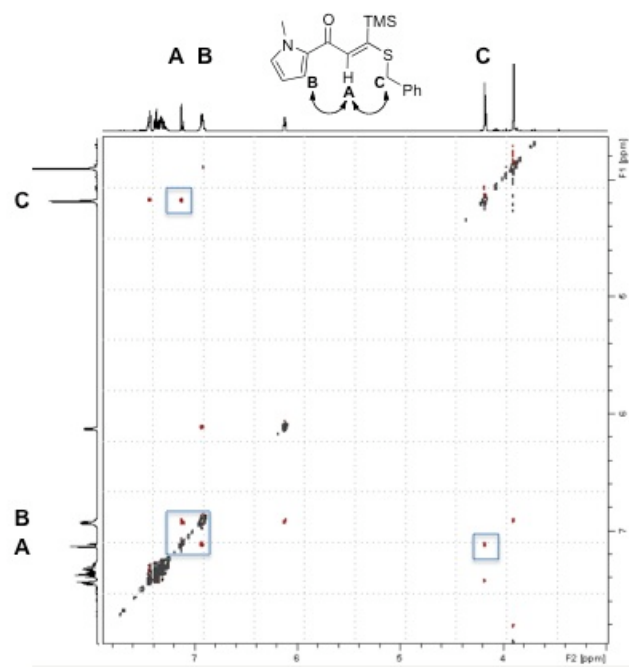
Dienone **106**, only *E*-linear isomer. ¹H NMR (CD₃CN, 400 MHz, δ 1.94): δ 7.12 (s, 1H), 7.05 – 7.04 (AB dd, 1H, *J* = 4.1, 1.6 Hz), 6.94 (AB t, 1H, *J* = 1.8-2.1 Hz), 6.16 – 6.15 (AB dd, 1H, *J* = 4.1, 2.6 Hz), 4.18 (q, 2H, *J* = 7.2 Hz), 3.91 (s, 3H), 3.75 (s, 2H), 1.23 (t, 3H, *J* = 7.2 Hz), 0.28 (s, 9H). ¹³C {¹H} NMR (d₃-acetonitrile, 100MHz, 298K): δ 178.4, 169.8, 160.3, 132.6, 132.5, 127.0, 119.7, 108.9, 62.6, 37.9, 35.5, 14.4, 0.1. HRMS (ESI) *m/z* calcd for C₁₅H₂₃NO₃SSi: 326.1246 (M+H)⁺; found: 326.1236.



2D-NOESY



Dienone **109**, 5:1 mixture of *E*:*Z*-linear isomers. ^1H NMR (CD_3CN , 400 MHz, δ 1.94): δ 7.45 – 7.27 (m, 7H), 7.12 (s, 1H), 7.10 (s, 0.2H, *Z*-linear isomer), 6.94 – 6.89 (m, 2H), 6.12 – 6.11 (AB dd, 1H, $J = 4.1, 2.5$ Hz), 4.17 (s, 2H), 4.16 (s, 0.5H, *Z*-linear isomer), 3.90 (s, 0.9H, *Z*-linear isomer), 3.89 (s, 3H), 0.39 (s, 2H, *Z*-linear isomer), 0.27 (s, 9H). ^{13}C $\{^1\text{H}\}$ NMR (d_3 -acetonitrile, 100MHz, 298K): δ 178.5, 162.6, 137.0, 132.5, 132.3, 132.1, 130.1, 129.9, 129.7, 129.5, 128.6, 128.4, 128.2, 126.6, 119.3, 118.9, 108.8, 108.7, 39.4, 37.9, 37.8, 0.5, 0.18. HRMS (ESI) m/z calcd for $\text{C}_{18}\text{H}_{23}\text{NOSSi}$: 330.1348 ($\text{M}+\text{H}$) $^+$; found: 330.1348.



2D-NOESY

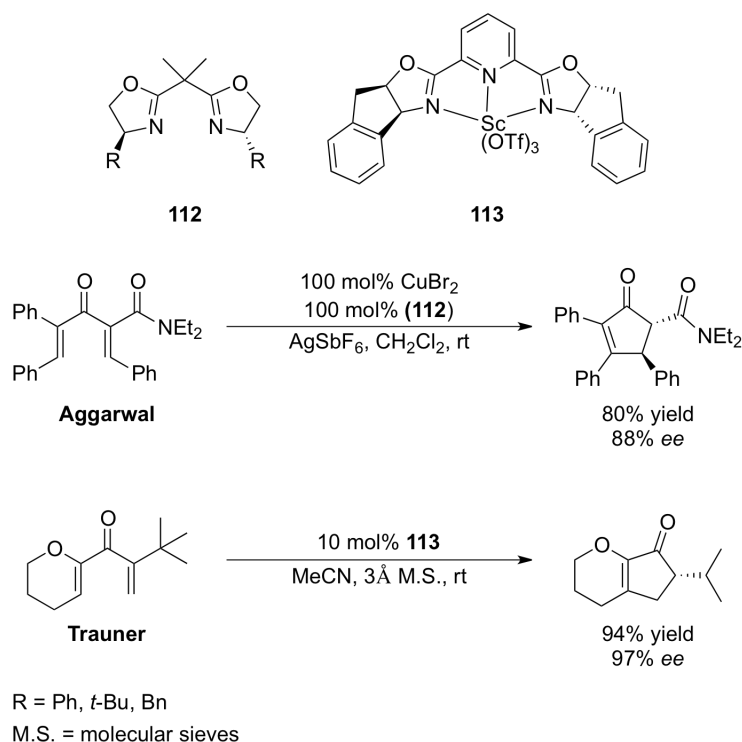
Chapter 5 Development of Novel Scorpionate-Type Proligands

Our interest in the Nazarov cyclization of β -heteroatom substituted dienones prompted us to explore the development of transition metal complexes capable of catalyzing this transformation. In particular, we were interested in designing asymmetric metal complexes in an attempt to render the 4π electrocyclization enantioselective. The term torquoselective describes the bias of rotation about the π -bonds in forming enantiomerically enriched cyclopentenones.^{326, 327} As the Nazarov cyclization is conrotatory in nature, the aforementioned rotational bias is either clockwise or counterclockwise about the termini involved in the formation of the σ -bond. The lack of chelating functionalities in electrocyclic processes has largely precluded the development of asymmetric variants involving the use of chiral Lewis or Brønsted acids. Gratifyingly, dienones are capable of binding these species to variable extents, allowing for asymmetric induction with the use of appropriate chiral reagents. This chapter serves to illustrate our development of novel scorpionate-type proligands that we hope to apply to catalytic asymmetric Nazarov cyclizations and other transformations, including olefin aziridination. Few examples of asymmetric Nazarov cyclizations and olefin aziridinations are known in the literature, and are restricted to select substrates. A common theme present in these reports is the use of bisoxazoline ligands in conjunction with scandium or copper (II) salts. The following chapter details the design, synthesis and evaluation of novel bisoxazoline proligands and how scorpionate-type analogues may allow for novel reactivity in processes such as the Nazarov cyclization and olefin aziridination.

5.1 Catalytic Asymmetric Nazarov Cyclizations and Olefin Aziridinations

The first example of a catalytic asymmetric Nazarov cyclization was reported by Aggarwal, followed shortly thereafter by Trauner.^{328, 329} These reports detailed the use of bidentate and tridentate bisoxazoline complexes containing scandium or copper (II). The use of copper (II) salts was normally accompanied with silver hexafluoroantimonate, presumably to generate cationic complexes by halide abstraction.³²⁸ Of the substrates examined, dienones containing Lewis basic functionalities were required for bidentate coordination of the bisoxazoline complexes. The substrates investigated by Aggarwal contained α -esters and α -

amides, while Trauner utilized 2-oxo-substituted dienones capable of binding to the Lewis acidic catalysts. The enantioselectivities obtained in these methods widely varied depending on the alkyl or aryl substituents on the dienone (Scheme 5.1). Additionally, the use of bidentate ligands of the type (**112**) typically required the use of stoichiometric quantities of an *in-situ* generated copper (II) catalyst.³²⁸ Trauner demonstrated that the use of indanyl pybox ligands could provide greater than 90% enantiomeric excesses for substrates with bulky alkyl groups adjacent to the ketone. Furthermore, scandium complex **113** proved capable of catalyzing the Nazarov cyclization at relatively low loadings of 10 mol% at room temperature or 0 °C.³²⁹ As only select substrates were examined, the development of Lewis acid catalysts capable of asymmetric Nazarov cyclizations across a broad range of dienones has still not been accomplished.



Scheme 5.1

A similar scenario exists for the catalytic asymmetric aziridination of olefins, where bisoxazoline ligands of the type (**113**) are effective for activated alkenes.³³⁰⁻³³² In addition to these bisoxazoline scaffolds, Jacobsen reported the use of salen-type proligands (**114**) that demonstrate equal effectiveness for chromenes.³³³ However, these complexes are not

effective in generating similar reactivity and enantioselectivities for unactivated olefins, such as cyclooctene. To this end, Trofimenko and Perez have developed copper-homoscorpionate complexes (**115**), which demonstrate considerable reactivity with unactivated olefins (Figure 5.1).³³⁴ The scorpionate ligands used were similar to the trispyrazolylborates that we demonstrated as effective in the catalytic synthesis of branched vinyl sulfides, discussed in chapters 2 and 3. However, as these ligands are not asymmetric, only racemic mixtures of the corresponding aziridines are obtained.

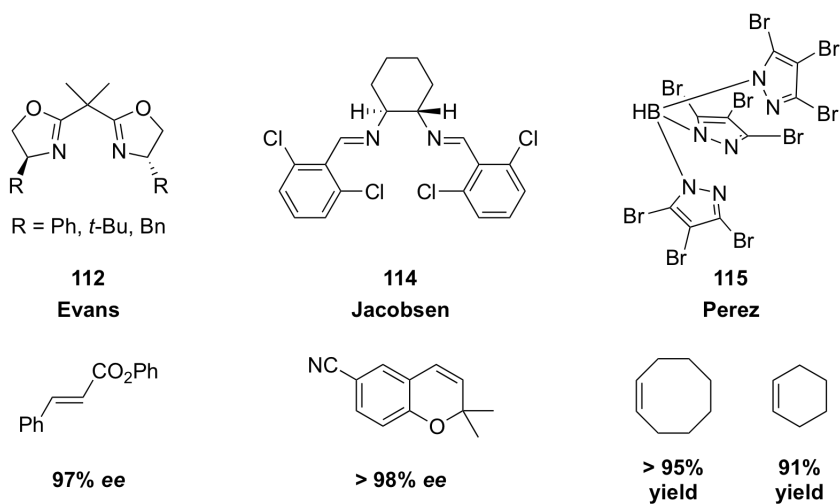


Figure 5.1 Proligands for Asymmetric Aziridination

Given our success in the use of rhodium (I) scorpionate complexes ($\text{RhTp}^*(\text{PPh}_3)_2$) in catalytic alkyne hydrothiolation, we became interested in synthesizing chiral analogues of this ligand class. Scorpionate ligands where the pyrazolyl heterocycles are substituted by bisoxazolines have been prepared previously, but use of these proligands in asymmetric transformations is notably absent.³³⁵⁻³³⁷ The use of chiral pyrazolylborates proligands is also known; however, complexes of these compounds place the chiral information at appreciable distances from the metal center.³³⁸ This is opposite for bisoxazoline proligands, where the chiral information is proximal to the metal center and can lead to high enantiomeric excesses, dependent on substrate binding. Indeed, the use of enantiopure pyrazolylborates in copper-catalyzed cyclopropanations have shown lower enantiomeric excesses in comparison to the Evans bisoxazoline copper complexes. With this in mind, we decided to explore bisoxazoline proligands with various appendages (scorpionate tails) capable of tridentate binding. These so-called sidearm-substituted bisoxazolines should be capable of flexible tridentate

binding.³³⁹⁻³⁴² Additionally, the use of anionic “tails” may effectively mimic the electron rich properties of the pyrazolylborates, thus allowing for the stabilization of high oxidation state transition metals. This chapter details our synthesis of various sidearm-substituted bisoxazolines and preliminary results concerning the coordination chemistry of these proligands.

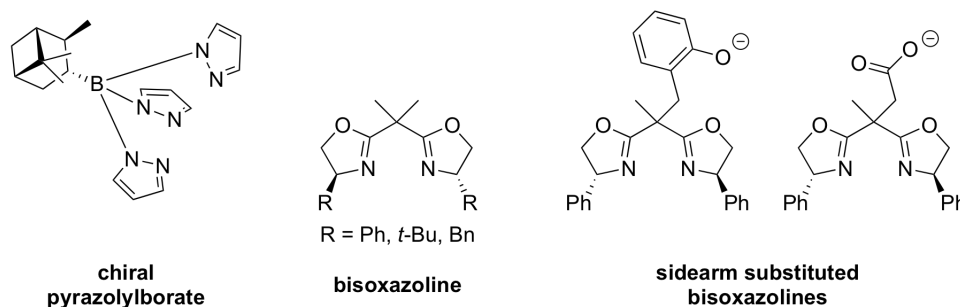
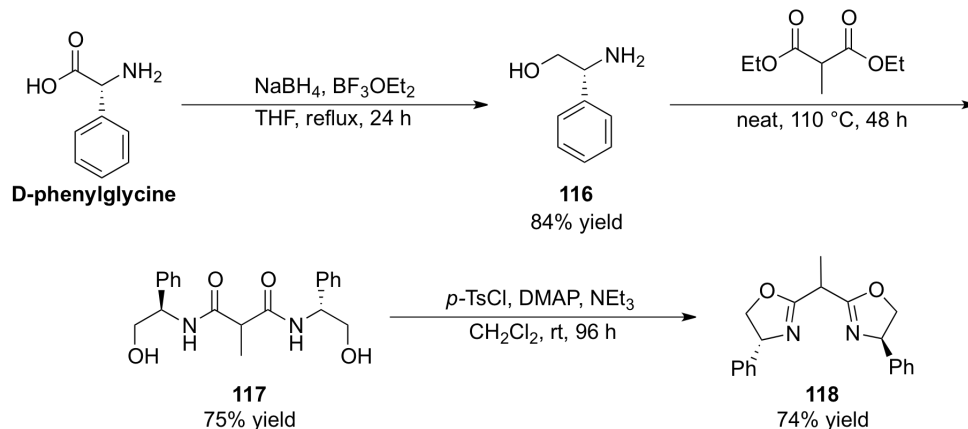


Figure 5.2 Design of Sidearm-Substituted Bisoxazoline Proligands

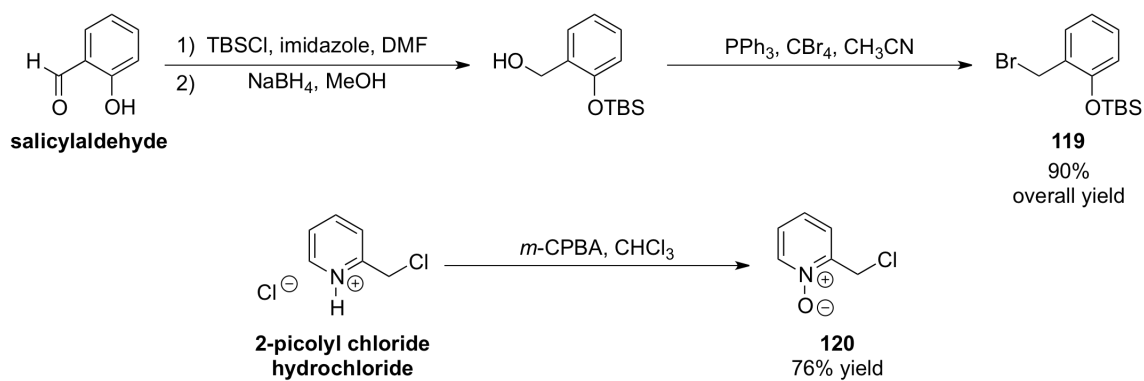
5.2 Synthesis of Sidearm-Substituted Bisoxazolines

The first target en route to the synthesis of sidearm-substituted bisoxazolines is the methylbisoxazoline **118** shown in Scheme 5.2. Deprotonation of this species with an appropriate base will allow for the attachment of various sidearms, through nucleophilic substitution reactions with the corresponding alkyl halide. The synthesis of **118** commenced with the borane reduction of D-phenylglycine to D-phenylglycinol **116** (84% yield). This material was subsequently condensed with diethyl methylmalonate generating the bisamide (**117**) in 75% yield. The synthesis of **118** was then completed upon tosylation of the primary alcohols followed by intramolecular displacement by the amide oxygens (74%). Given the lengthy reaction times for the second and third steps, we attempted to use more electrophilic malonate derivatives including bithioesters. However, these compounds proved difficult to isolate on large scale, and were abandoned in favour of the more traditional approach depicted in Scheme 5.2.



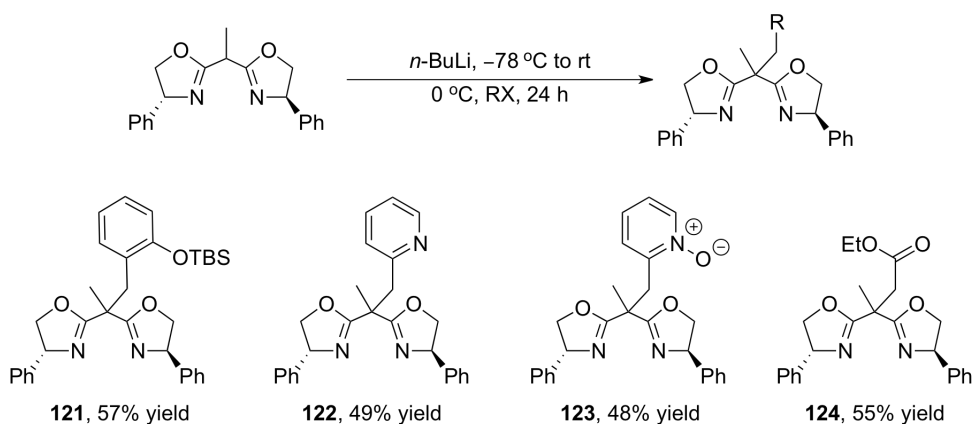
Scheme 5.2

The methylbisoxazoline **118** was selected as deprotonation of this species should readily occur, providing the corresponding tertiary anion. Interception of anionic (**118**) could then be accomplished with a variety of electrophiles, allowing for the divergent synthesis of several sidearm-substituted bisoxazolines from a common intermediate. To this end, the alkyl bromide (**119**) was synthesized from salicylaldehyde by first protecting the free phenol as the *tert*-butyldimethylsilyl ether (TBS). This was deemed necessary as the formation of a quinone methide may occur under the basic conditions required for alkylation of methylbisoxazoline (**118**). The reduction of the aldehyde and subsequent Appel-type bromination provided alkylating agent (**119**) in 90% overall yield (Scheme 5.3). Similarly, 2-picolyl chloride hydrochloride was oxidized with *meta*-chloroperoxybenzoic acid (*m*-CPBA) to the corresponding *N*-oxide (**120**). The free base of 2-picolyl chloride was also isolated by extraction of the hydrochloride salt, and used in conjunction with the alkyl bromide (**119**), and the *N*-oxide (**120**).



Scheme 5.3

Equipped with the three alkylating agents, we were ready to begin our initial studies of the alkylation of methylbisoxazoline (**118**). To this end, treating **118** with 1.1 equivalents of *n*-butyllithium at low temperatures readily generated the corresponding tertiary anion (Scheme 5.4). This solution was allowed to warm to room temperature, then cooled to 0 °C prior to the addition of the alkylating agent. Alex Sun, a Ph.D student with Dr. Jennifer Love, also successfully coupled the haloester with the methylbisoxazoline anion using sodium hydride as base, affording the sidearm-substituted bisoxazoline **124**. In general all alkylations occurred in relatively good yield, and could be scaled to give gram quantities of the sidearm-substituted bisoxazolines.³⁴³



Scheme 5.4

The final steps necessary in accessing the anionic sidearm-substituted bisoxazolines involved the desilylation of **121** and the saponification of **124**. This involved treating **121** with *tert*-butylammonium fluoride (TBAF) followed by acidic workup and chromatography (Scheme 5.5). Alternatively, treating **124** with sodium hydroxide allowed for the formation of the carboxylate **126**.

modes of ligand **125** in anionic form is represented below. We hypothesized that if κ^3 binding was possible, asymmetric catalytic processes involving anionic proligands **125** and **126** may exhibit similar catalytic activity to that of the achiral complexes studied by Perez (**115**). Additionally, we were concerned that complexes involving κ^2 binding may be prone to the formation of dimeric and oligomeric metal species via bridging of the carboxylate or phenolate ions (Figure 5.3).

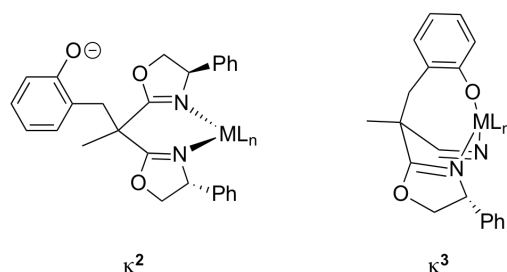


Figure 5.3 κ^2 and κ^3 Binding Modes

Investigation of the different binding modes (κ^2 or κ^3) concerning the sidearm-substituted bisoxazoline complexes was difficult to assess by ^1H NMR spectroscopy, especially with copper (I) and (II) salts. Attempts at crystallizing these coordination complexes yielded a variety of foams, emulsions, and oils, which suggested that the anionic tail of **125** may lead to the formation of oligomeric species. The use of the neutral phenol with $\text{Cu}(\text{OTf})_2$ yielded crystals that were sufficient to establish the connectivity of the complex. Unfortunately, the solid-state structural data was not of suitable quality to determine bond lengths and angles. A representation is shown in Figure 5.4, where a tetrahedral homoleptic copper (II) complex was evident, where two molecules of ligand **125** were bound. For clarity, the trifluoromethanesulfonate counterions, and the bisoxazoline phenyl groups are omitted.

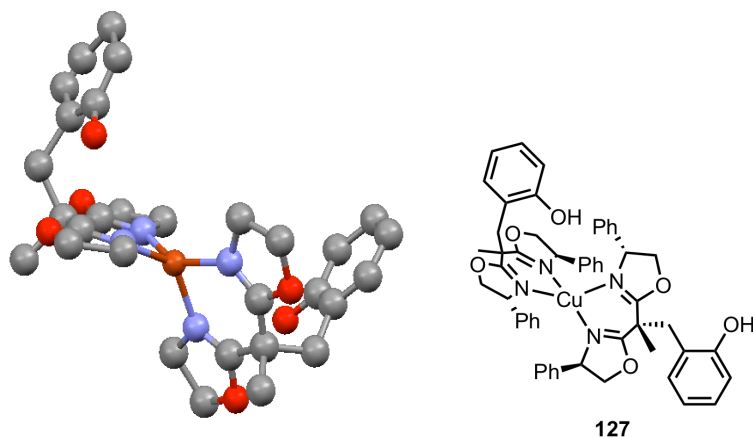


Figure 5.4 Solid-State Structural Representation for Complex 127

Encouraged by the successful coordination of a neutral proligand to copper (II) we decided to explore the coordination of pyridine-substituted bisoxazoline (**122**) and the corresponding *N*-oxide analogue (**123**). We were particularly interested in coordinating these ligands to various copper and iron salts, as complexes involving these metals are prevalent in catalytic Nazarov cyclizations.^{259, 344} With this in mind we studied the complexation of several metal salts including: copper, nickel, palladium, cobalt, rhodium, ruthenium, and iron (II) and (III). Additionally, silver salts were added to complexes containing $[\text{Re}(\text{CO})_4\text{Cl}]_2$ and various copper salts, as a means of forcing κ^3 binding.

Gratifyingly, crystallization of a coordination compound involving proligand **122** and FeCl_2 was successful, and the Oakridge Thermal Elipsoid Plot is demonstrated below. Similar to the homoleptic copper complex, the iron (II) complex was found to exist in κ^2 form in the solid state. The geometry of the complex was distorted tetrahedral, given the rigid binding pocket characteristic of the bidentate bisoxazoline ligands, where the N4-Fe2-N5 bond angle was determined to be 86.7° (ORTEP numbering). Additionally, the angle for the Cl3-Fe2-Cl4 bond was determined to be 115.5° , which is expanded beyond the expected angle of 109° . The pyridine sidearm faces towards the iron (II) center, suggesting that tridentate binding may be fluxional in solution, or could be adapted upon treatment with a halide abstraction reagent (Figure 5.5). However, initial attempts at promoting κ^3 binding by the addition of silver salts have thus far been unsuccessful.

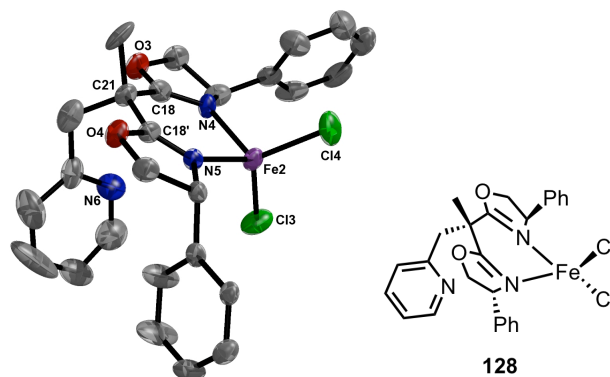


Figure 5.5 ORTEP for Complex 128

Similarly, the formation of complexes involving proligand **122** and the *N*-oxide analogue (**123**) were successfully coordinated to the metal salt $[\text{Re}(\text{CO})_4\text{Cl}]_2$. The ORTEP diagram of the pyridine substituted bisoxazoline is shown below. The geometry of the complex is distorted octahedral, with a N1-Re-N2 (ORTEP numbering) bond angle of 82.97° , similar to that observed for the iron (II) complex. Again, the pyridine sidearm faces the rhenium center opposite the chloride ligand, suggesting that tridentate binding may be adopted under the appropriate conditions (Figure 5.6).

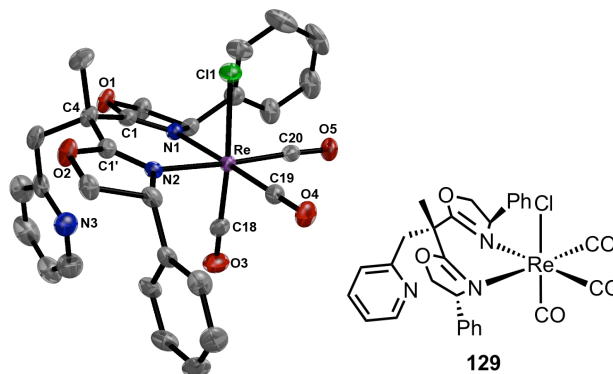


Figure 5.6 ORTEP for Complex 129

The bisoxazoline containing the pyridine *N*-oxide sidearm was successfully coordinated to $[\text{Re}(\text{CO})_4\text{Cl}]_2$, the ORTEP diagram for this complex is shown below. The rigid binding of the bisoxazoline results in a N1-Re-N2 bond angle of 80.92° , which is slightly contracted from that observed for the pyridine substituted complex (82.97°). The geometry of the complex is distorted octahedral, and the *N*-oxide functionality is bent slightly away from the chlorine ligand in the apical position, which is positioned opposite relative to the pyridine

substituted bisoxazolines in complexes (**128**) and (**129**).

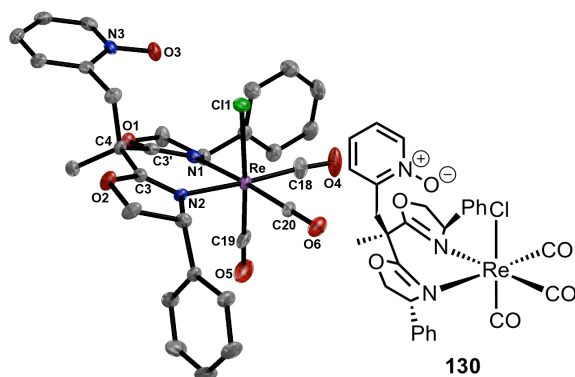
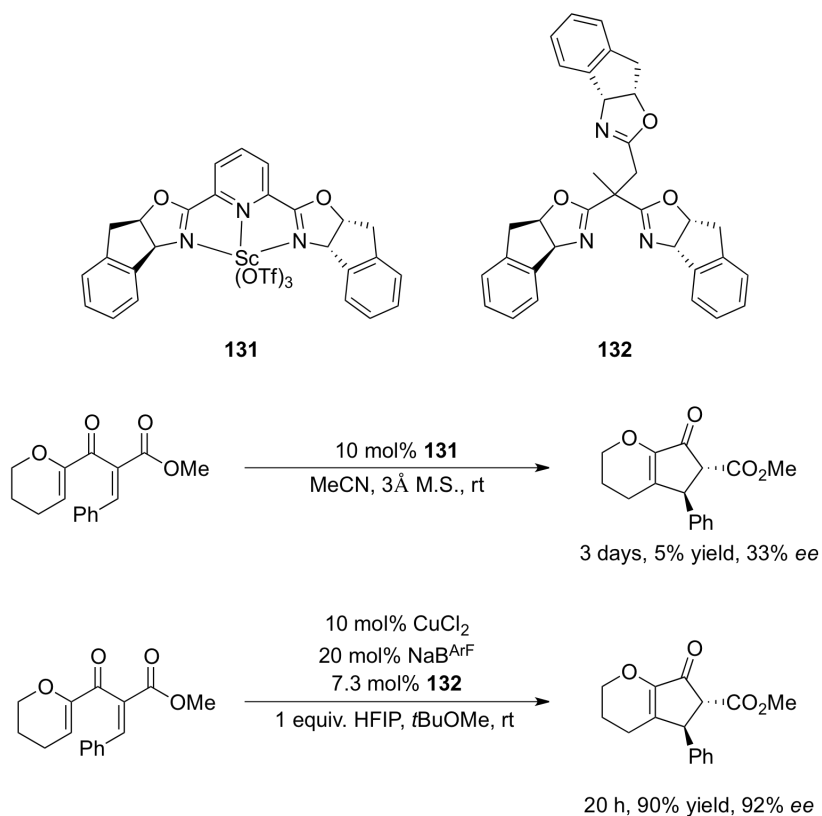


Figure 5.7 ORTEP for Complex (**130**)

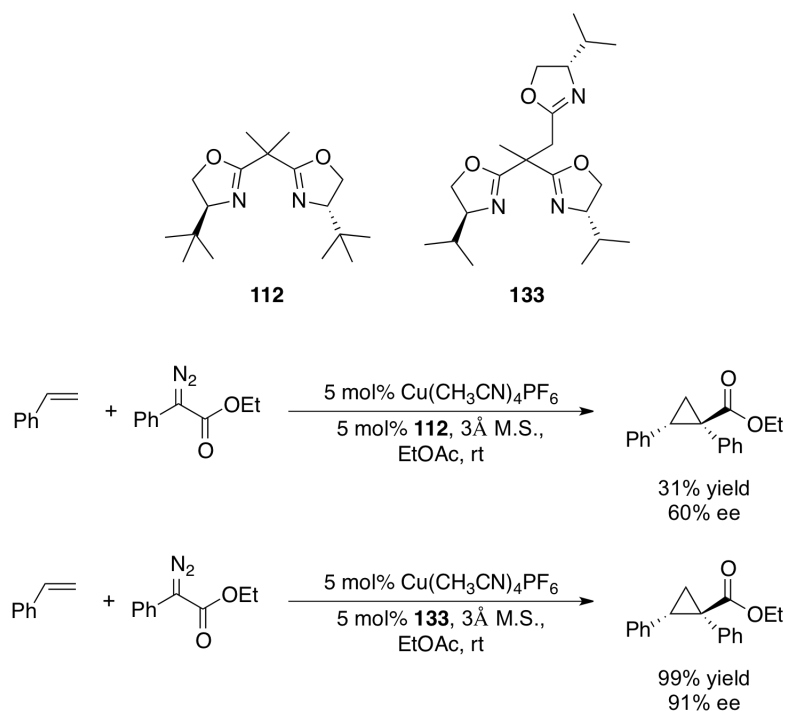
5.4 Conclusions

The successful synthesis and coordination of a series of sidearm-substituted bisoxazoline proligands lends promise to the implementation of these molecules in asymmetric catalysis. During, and shortly following the development of these complexes, reports in the literature emerged regarding similar complexes in processes such as the Nazarov cyclization and the cyclopropanation of olefins. The Tang group recently reported that the indanyl trisoxazoline **132** outperformed the more rigid pybox analogue (**131**) in catalytic asymmetric Nazarov cyclizations (Scheme 5.6).³⁴⁵ This is rather surprising given the success of complex **131** in catalyzing the Nazarov cyclizations of less polarized dienones as shown in Scheme 5.1. Interestingly, when the sidearm of proligand **132** is simply replaced with a hydrogen atom, the enantioselectivity obtained is still greater than that for pybox complex (**131**).³⁴⁵ This result suggests that the sidearm may play a significant role in conformationally orienting the activated dienone for torquoselective cyclization. Furthermore, replacing the sidearm substituent with its respective enantiomer led to an appreciable decrease in yield and enantiomeric excess. The reduction in selectivity suggests that the sidearm substituent may interact with the bound dienone, and not in coordinating to the copper center. The solid-state structural data obtained for our sidearm-substituted bisoxazolines is consistent with this, where the sidearm appears to rest near the metal, and could potentially influence rotation of a bound dienone.



Scheme 5.6

Similarly, a recent report detailed the superior enantioselectivities obtainable with trisoxazolines (**133**) relative to the traditional bisoxazoline proligands (**112**) in asymmetric cyclopropanation.³⁴⁶ The use of disubstituted diazoesters was possible, yielding quaternary carbon stereocenters, and trisubstituted cyclopropanes with high enantio- and diastereoselectivities. Additionally, *para*-substituted styrenes, conjugated alkenes, and electron rich enol ethers were suitable substrates with the *in-situ* generated trisoxazoline-copper complex. In general, high enantiomeric excesses ranging from 82-95% were achievable under the optimized conditions; however, no details were provided regarding whether other sidearms could achieve similar results. Interestingly, methylbisoxazolines derived from L-valine also outperformed proligand **112** (Scheme 5.7).³⁴⁶



Scheme 5.7

The ability of sidearm-substituted bis- and trisoxazolines to provide superior results relative to the traditional box and pybox proligands demonstrates the relevance in exploring this ligand family. This may aid in expanding upon catalytic asymmetric processes for the synthesis of useful synthetic building blocks including cyclopropanes, aziridines, and cyclopentenones. We plan to expand upon the sidearm-substituted bisoxazolines reported here, in an effort to develop asymmetric iron complexes capable of catalyzing the Nazarov cyclization. This will involve synthesizing analogues to proligands **122**, **125** and **126** containing amino acids other than phenylglycine. Furthermore, various sidearms including amide, nitro, and *para*-substituted phenols will be examined, in order to assess the electronic and steric influence of these groups on catalysis.

5.5 Experimental

5.5.1 General Procedures

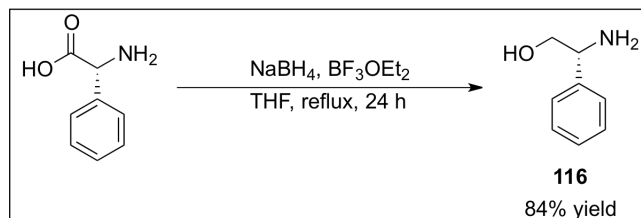
Manipulation of organometallic compounds was performed using standard Schlenk techniques under an atmosphere of dry nitrogen or in a nitrogen-filled Vacuum Atmospheres drybox ($\text{O}_2 < 2$ ppm). NMR spectra were recorded on Bruker Avance 300 or Bruker Avance

400 spectrometers. ^1H and ^{13}C NMR spectra are reported in parts per million and were referenced to residual solvent: $\text{CDCl}_3 = 7.26$ ^1H NMR, 77.0 for ^{13}C NMR, for $\text{CD}_2\text{Cl}_2 = 5.32$ ^1H NMR, 53.8 for ^{13}C NMR, d^6 DMSO = 2.50 ^1H NMR, 39.4 for ^{13}C NMR. Coupling constant values were extracted assuming first-order coupling. The multiplicities are abbreviated as follows: s = singlet, d = doublet, t = triplet, q = quartet, m = multiplet, br = broad signal, dd = doublet of doublets, ddd = doublet of doublet of doublets, dt = doublet of triplets, app. d = apparent doublet, app. t = apparent triplet, AB d = second order doublet, AB t = second order triplet, AB q = second order quartet. Abbreviations for ^{13}C NMR (APT) include C, CH, CH_2 , CH_3 which correspond to quaternary, methine, methylene, and methyl substitution respectively, where APT = attached proton test. The chemical shift value for second order quartets and (AB q) were reported based upon the solution to the equation $(1-3) = (2-4) = [(\Delta\nu)^2 + J^2]^{1/2}$ where J = coupling constant (Hz) and $\Delta\nu$ = chemical shift difference (Hz) = unknown value, and (1-3) or (2-4) represents left to right numbering of the individual peaks related to the multiplet (Hz). The value for $\Delta\nu$ was then subtracted or added to the middle of the coupling pattern and converted to ppm based upon spectrometer frequency. All spectra were obtained at 25 °C. Mass spectra were recorded on a Kratos MS-50 mass spectrometer. IR spectra for solid compounds were obtained using a Thermo Scientific Nicolet 6700 FT-IR spectrometer equipped with the diamond Attenuated Total Reflectance. All liquid samples were analyzed as thin films from solutions in dichloromethane on KCl plates and were recorded with a Thermo Nicolet 4700 FT-IR spectrometer. UV analysis was done with a Varian Cary 5000 UV spectrophotometer using HPLC grade CHCl_3 .

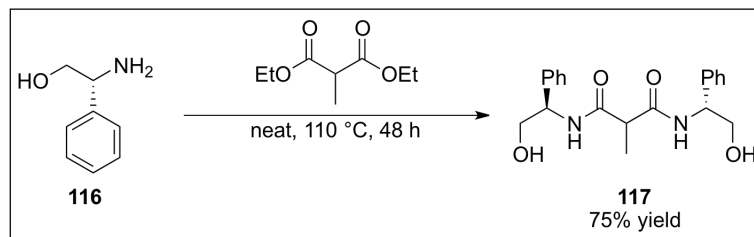
5.5.2 Materials and Methods

Dichloromethane and THF were purified, and degassed, via passage through solvent purification columns.²³⁷ All other reagents and solvents were obtained from commercial sources and used as received, with the exception of DMF, which was vacuum distilled over activated molecular sieves and kept in a schlenk tube under N_2 . An authentic sample of $[\text{Re}(\text{CO})_4\text{Cl}]_2$ was generously donated by Dr. Alan Storr, and FeCl_2 (anhydrous) was by the Mehrkhodavandhi lab. Sidearm-substituted bisoxazolines **124** and **126** were synthesized by Alex Sun.

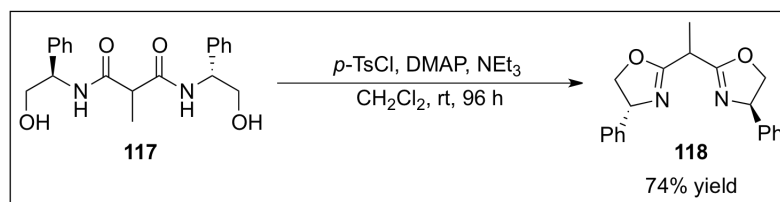
5.5.3 Analytical Data



The following procedure is adapted from Organic Syntheses.³⁴⁷ To a flame dried 3 necked round bottom equipped with two gas inlets, a serum cap and a large stir bar was added NaBH₄ (9.961 g, 263 mmol, 2 equiv.). To this was added 200 mL of anhydrous THF and the round bottom was equipped with an addition funnel equipped with a serum cap. The addition funnel was charged with BF₃OEt₂ (67 mL, 74.743 g, 527 mmol, 4 equiv.) under a stream of N₂ and the solution added slowly over a 20 minute period. Gas evolution was noted during the addition, but no significant exotherm was detected. The resulting slurry was left to stir for an additional 20 minutes before the *R*-phenylglycine was added. The addition funnel was replaced by a serum cap and then *R*-phenylglycine (20.186 g, 134 mmol, 0.67 M) was added in portions over a 20 minute period to prevent any significant exotherm. Vigorous gas evolution occurred during the addition of the *R*-phenylglycine. Once the addition of *R*-phenylglycine was complete the round bottom was fitted with a reflux condenser and the flask heated to reflux for 24 h. Following the reflux period the mixture was cooled to room temperature and then to 0 °C and the solution was quenched with MeOH (wash grade). Vigorous gas evolution was monitored by an external bubbler and the quench was judged to be complete once gas evolution was considerably low or absent. The clear solution was then concentrated *in-vacuo*. The crude mixture (white pasty oil) was then dissolved in 400 mL of aqueous 20 % NaOH and stirred till a slight green colour persisted. The mixture was then extracted with CH₂Cl₂ (3 x 200 mL), a considerable emulsion develops and can be alleviated by the addition of solid NaCl or a brine solution. The combined organic layers were dried with brine and then Na₂SO₄, filtered and concentrated to give *R*-phenylglycinol (**116**, 84 % yield), which was used without further purification.

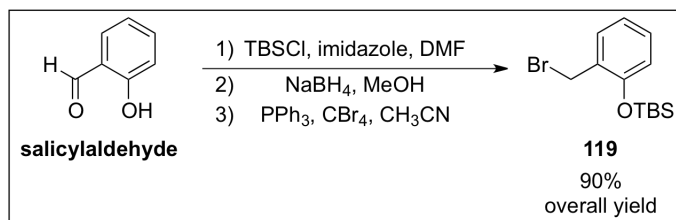


R-phenylglycinol (11.429 g, 83 mmol, 2 equiv.) was added to a ground glass Erlenmeyer flask, which was equipped with a magnetic stir bar. To this was added diethylmethylmalonate (7.2 mL, 7.294 g, 42 mmol) and the mixture heated to 110 °C for 48 hours under a N₂ atmosphere. Following the stir period, the yellow oil had become a caked orange solid, which was dissolved in hot ethanol. This homogenous solution was concentrated to near dryness, giving a white pasty oil. To this was added CHCl₃ and the mixture was stirred for approximately 30 minutes in which a large amount of white solid precipitated. This solid was vacuum-filtered and washed with cold CHCl₃ giving diamide **117** (75% yield). The duration of the reaction can sometimes improve the yield; however, repetitive crystallization of the product from the mother liquor gives additional material as well. The ¹H NMR spectrum was consistent with that reported in the literature, and diamide **117** was carried directly to the next step without additional purification.³⁴⁸



A flame dried 3 necked round bottomed flask equipped with two gas inlets, a magnetic stir bar, and a stopper was cooled under N₂. To this was added diamide **117** (4.730 g, 13 mmol, 0.11 M) and 46 mL of CH₂Cl₂. To this was added NEt₃ (12 mL, 8.712 g, 86 mmol, 6.5 equiv.) and DMAP (0.178 g, 1 mmol, 11 mol %). The cake like solid was stirred vigorously and a solution of *p*-TsCl was added in one 28 mL (CH₂Cl₂) portion (5.603 g, 29 mmol, 2.2 equiv.). The flask having contained *p*-TsCl was rinsed with one 10 mL portion of CH₂Cl₂ and added to the solution. The mixture was then diluted to a final concentration of 0.11 M with respect to the diamide (122 mL CH₂Cl₂). The solid completely dissolved upon addition of *p*-TsCl and a new white precipitate formed slowly while stirring for 96 hours

under a static N₂ atmosphere. Following the stir period the crude mixture was poured into 60 mL 25 mM HCl. The layers were separated and then the aqueous layer back extracted with ethyl acetate (2 x 30 mL). The combined organic layers were washed once with saturated sodium carbonate (25 mL) and brine (25 mL), then dried over Na₂SO₄ filtered and concentrated *in-vacuo*. The mixture was purified by SiO₂ chromatography where the SiO₂ was pretreated with a 10 % NEt₃ solution in hexanes. The compound was eluted by a gradient of 2:1 hexanes:ethyl acetate slowly changed to 1:1 hexanes:ethyl acetate, where 1 % NEt₃ was used as a coeluent. Following purification, bisoxazoline (**118**) was isolated in 74 % yield. The ¹H and ¹³C NMR spectra were consistent with that reported in the literature.³⁴⁸

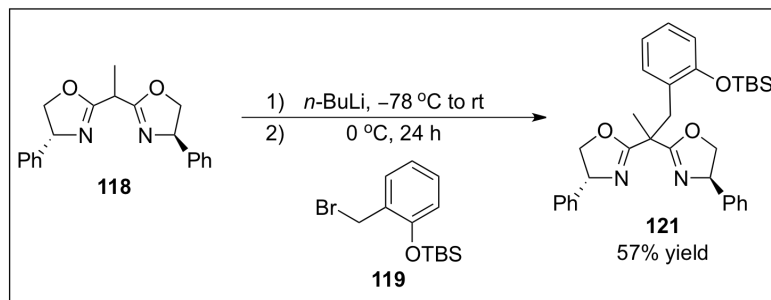


To a flame dried round bottomed flask, equipped with a magnetic stir bar and a serum cap was added salicylaldehyde (4.2 mL, 4.872 g, 40 mmol). To this was added 5 mL of DMF (2 mL/g alcohol) by syringe, which was previously distilled over 4Å molecular sieves. Subsequently, imidazole (6.811 g, 100 mmol, 2.5 equiv.) and TBDMSCl (7.257 g, 48 mmol, 1.2 equiv.) were added in one portion, followed by an additional 5 mL of DMF (total volume DMF = 10 mL). The solution was a slight yellow, which later turned to deep orange as the reaction progressed. The mixture stirred at ambient temperature for 72 h under a static atmosphere of N₂. The reaction was quenched by pouring the contents of the round bottom flask into distilled water (10 mL), which was extracted with petroleum ether (light fraction, 3 x 10 mL). The combined organic layers were then washed with 10 % HCl (2 x 15 mL), followed by distilled water (15 mL per wash) until the solution tested neutral by litmus. The combined organic extracts were then dried over MgSO₄, filtered, and concentrated *in-vacuo*. This yielded the TBS-protected salicylaldehyde (88 %, ca. 95 % purity based on ¹H NMR spectroscopy). The product was carried on to the next step without purification, the data for the crude product matched literature data.³⁴⁹

The 2-(*t*-butyldimethylsiloxy)benzyl alcohol (9.609 g, 41 mmol, 0.34 M) was dissolved in a small amount of anhydrous MeOH. This solution was then transferred to a

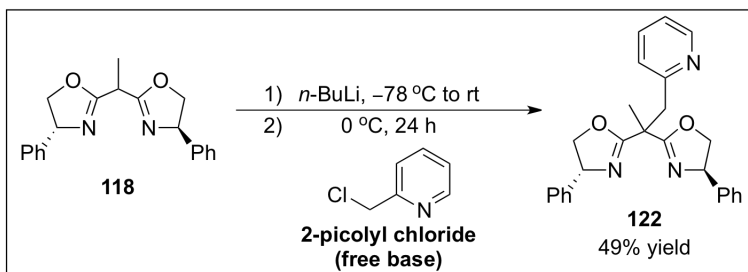
flame dried round bottom equipped with a stir bar and a septa. The mixture was stirred under N₂ and MeOH was added to give a total volume of 100 mL. To this was added NaBH₄ (2.309 g, 61 mmol, 1.5 equiv.) in one portion with rinsing MeOH (20 mL). A considerable amount of heat was generated upon addition of NaBH₄ and necessitated the use of an ice-water bath to cool the reaction flask. The mixture was allowed to warm to room temperature once the bubbling had subsided, and was allowed to stir for 4 hours under a static atmosphere of N₂. Once the reaction was judged complete by TLC, the reaction was quenched by the addition of brine (50 mL). The solution was then concentrated *in-vacuo* and washed with ether (3 x 20 mL). The organic layer was separated and the remaining aqueous layer was extracted another three times with ether (3 x 10 mL). The combined organic fractions were then washed twice with 10 % HCl (2 x 20 mL) and twice with distilled water (2 x 20 mL). The organic extracts were then dried over MgSO₄, filtered, and concentrated *in-vacuo* to afford the crude alcohol (91 %, ca. 95 % purity based on ¹H NMR spectroscopy). The crude product was directly taken to the next step without further purification. The crude product matched literature data.³⁴⁹

The crude alcohol (7.937 g, 33 mmol, 0.24 M) was dissolved in 40 mL of HPLC grade acetonitrile and stirred under N₂ in a flame dried round bottom equipped with a septa. The solution was then diluted with another 60 mL of acetonitrile and cooled to 0 °C via an ice-water bath. To this solution was added CBr₄ (13.291 g, 40 mmol, 1.2 equiv.) in 20 mL of acetonitrile. Following this PPh₃ was added (10.588 g, 40 mmol, 1.2 equiv.) in another 20 mL of acetonitrile (total volume = 140 mL). The solution was then allowed to warm to room temperature overnight and stirred under a static atmosphere of N₂. Following the stir period the solution turned a slight brown, when the solution was originally clear. The solution was then concentrated *in-vacuo* and added to a fritted funnel filled with a layer of SiO₂ (bottom) and a layer of celite (top). The filter pad contained a small excess of hexanes to precipitate any triphenylphosphine oxide prior to reaching the silica layer. The material was then eluted with hexanes with a small amount of DCM to ensure solubility of the desired product. This provided the alkyl bromide **119** (90 % yield from salicaldehyde, slightly contaminated with CH₂Cl₂). The ¹H NMR matched literature data.³⁴⁹



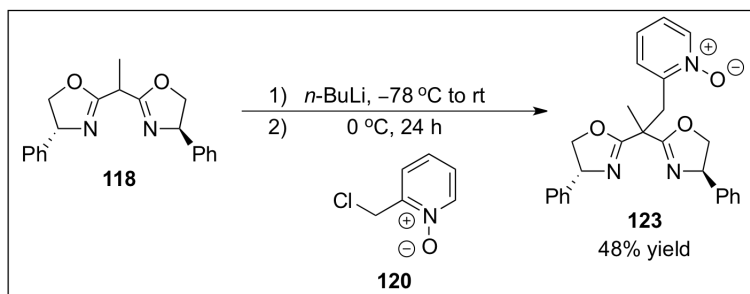
To a flame dried round bottom was added methylbisoaxazoline **118** (0.343 g, 1 mmol) as a 0.2 M solution in anhydrous THF (5 mL). The mixture was stirred under N₂ and cooled to -78 °C. To this was added *n*-BuLi (0.75 mL, 1.58 M, 1.2 mmol, 1.2 equiv.) over a 5 minute period. The solution of *n*-BuLi was titrated against N-benzylbenzamide prior to use.²⁴¹ The addition of *n*-BuLi to the solution of methylbisoaxazoline produced a red colour, where the initial solution is colourless or slightly yellow. The solution was then warmed to 0 °C with a ice-water bath, this sometimes can induce a colour change from red to green, depending on the scale of the reaction. The solution was stirred for 30 minutes at 0 °C, following this, bromide **119** was added (0.328 g, 1.1 mmol, 1.1 equiv.) as a 0.5 M solution in anhydrous THF (2.2 mL). The solution turned from a red colour to a yellow upon the addition of the alkylating agent. The mixture was then left to stir overnight under N₂ at room temperature. The reaction was quenched with brine (3 mL) and the aqueous layer extracted with ethyl acetate (3 x 10 mL). The combined organic layers were then dried over Na₂SO₄, filtered and concentrated *in-vacuo*. The crude product was purified by column chromatography using 1:1 hexanes:ethyl acetate, providing the sidearm-substituted bisoxazoline (**121**) in 57 % yield. ¹H NMR (CD₂Cl₂, 400 MHz): δ 7.35 – 7.28 (m, 10H), 7.22 – 7.13 (m, 4H), 6.89 – 6.87 (d, 2H, 7.7 Hz), 5.25 – 5.24 (dd, 1H, J = 10.1, 8.4 Hz), 5.19 – 5.17 (dd, 1H, J = 10.1, 7.7 Hz), 4.74 – 4.68 (ddd, 2H, 10.1, 8.4, 4.1 Hz), 4.16 – 4.12 (AB q, 2H, J = 8.3, 7.6 Hz), 3.51 – 3.48 (AB q, 2H, J = 16.3 Hz), 1.51 (s, 3H), 1.04 (s, 9H), 0.26 (app. d, 6H, J = 6.6 Hz). ¹³C{APT} NMR (CD₂Cl₂, 100 MHz): δ 169.6 (2 peaks, C), 155.0 (C), 143.2 (two peaks, C), 132.1 (CH), 128.9 (two peaks, CH), 128.1 (CH), 127.7 (two peaks, CH), 127.1 (two peaks, CH), 121.2 (CH), 119.2 (CH), 75.5 (CH₂), 70.0 (two peaks, CH), 44.7 (C), 35.0 (CH₂), 26.1 (CH₃), 21.0 (CH₃), 18.6 (C), -3.9 (two peaks, CH₃). Abundance of peaks in the ¹H and ¹³C NMR may be attributable to hindered rotation or distortions in the pseudo C₂-symmetry. HRMS (ESI) m/z calcd for [C₃₃H₄₀N₂O₃Si+Na]⁺: 563.2706; found: 563.2704. IR (thin film): 3030, 3062, 2930,

2897, 2858, 1652, 1600, 1581, 1492, 1472, 1453.



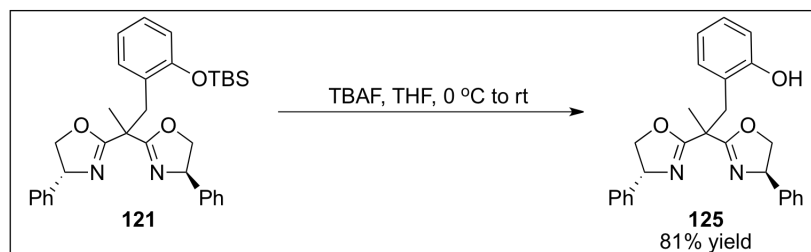
To a flame dried round bottom, equipped with a magnetic stir bar and a serum cap, was added **118** (0.995 g, 3 mmol) as a 0.12 M solution in anhydrous THF (26 mL). The solution was cooled to $-78\text{ }^{\circ}\text{C}$ and then 1.9 mL *n*-buLi was added over a 5 minute period (1.98 M, 3.8 mmol, 1.3 equiv.). The solution of *n*-buLi was titrated against *N*-benzylbenzamide prior to use.²⁴¹ The addition of *n*-buLi turned the solution from colourless/yellow to a reddish colour. The flask was then warmed to room temperature, stirred for 5 minutes, then cooled back to $-78\text{ }^{\circ}\text{C}$ and picolyl chloride was added as a solution in 13 mL THF (0.512 g, 4 mmol, 0.3 M). The picolyl chloride was prepared from picolyl chloride hydrogen chloride salt by the method of Gan *et. al.* and distilled before use.³⁵⁰ The solution was left to stir overnight under N_2 . The reaction was quenched with brine (15 mL) and extracted with ethyl acetate (3 x 10 mL). The combined organic layers were then dried over Na_2SO_4 , filtered and concentrated *in-vacuo*. The crude product was purified by column chromatography with an eluent of 1% MeOH in DCM, which was gradually increased to 5% or 10% MeOH. The column was flushed with MeOH, which eluted the sidearm-substituted bisoxazoline (**122**) in 49 % yield. ^1H NMR (CD_2Cl_2 , 400 MHz): δ 8.54 (app. d, 1H, 4.0 Hz), 7.59 (td, 1H, 7.7, 1.8 Hz), 7.35 – 7.16 (m, 13H), 5.22 – 5.21 (dd, 1H, $J = 10.0, 8.5$ Hz), 5.16 – 5.15 (dd, 1H, 10.1, 7.7 Hz), 4.69 (AB ddd, $J = 10.0, 8.4, 1.6$ Hz), 4.14 (app. dt, 2H, $J = 8.3, 7.9$ Hz), 3.59 – 3.57 (AB q, 2H, $J = 15.6$ Hz), 1.61 (s, 3H). $^{13}\text{C}\{\text{APT}\}$ NMR (CD_2Cl_2 , 100 MHz): δ 169.3 (C, two peaks), 157.9 (C), 149.5 (CH), 143.0 (C, two peaks), 136.3 (CH), 129.0 (CH, two peaks), 127.8 (CH, two peaks), 127.2 (CH, two peaks), 125.2 (CH), 122.0 (CH), 75.7 (CH_2 , two peaks), 70.0 (CH, two peaks), 44.3 (CH_2), 43.6 (C), 21.7 (CH_3). Abundance of peaks in the ^1H and ^{13}C NMR may be attributable to hindered rotation or distortions in the pseudo C_2 -symmetry. HRMS (ESI) m/z calcd for $[\text{C}_{26}\text{H}_{25}\text{N}_3\text{O}_2+\text{H}]^+$:

412.2025; found: 412.2032. IR (thin film): 30611.1, 2984.7, 2898.5, 1653.2, 1589.3, 1569.5, 1493.8, 1473.5, 1454.5, 1435.3.

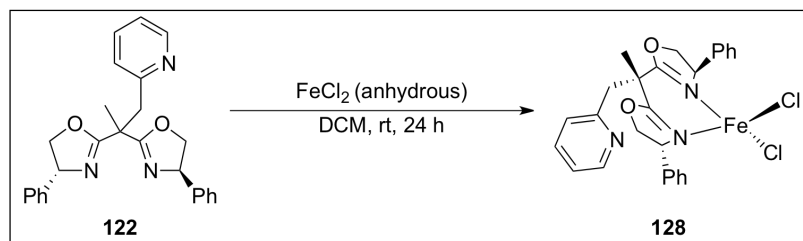


To a flame dried round bottom, equipped with a magnetic stir bar and a serum cap, was added **118** (1.926 g, 6 mmol) as a 0.13 M solution in anhydrous THF (46 mL). The solution was cooled to $-78\text{ }^{\circ}\text{C}$ and *n*-buLi was added over a 5 minute period (5.2 mL, 1.78 M, 9.3 mmol, 1.5 equiv.). The solution of *n*-buLi was titrated against *N*-benzylbenzamide prior to use.²⁴¹ The solution turned from colourless/yellow, to a reddish colour. The solution was allowed to warm to room temperature, stirred for 5 to 10 minutes and cooled to $-78\text{ }^{\circ}\text{C}$. The picolyl chloride N-oxide (**120**) was prepared from picolyl chloride hydrogen chloride salt by the method of Yoo *et. al.*³⁵¹ The N-oxide was then added, in wide excess, as a solution in THF to the mixture and the flask was allowed to warm to room temperature and stir overnight under N_2 . The reaction was quenched with brine (25 mL) and extracted with ethyl acetate (3 x 20 mL). The combined organics were dried over Na_2SO_4 , filtered and concentrated *in-vacuo*. The crude product was purified by column chromatography 1% MeOH in DCM, which was increased to 5 or 10% MeOH in DCM, providing **123** in 48 % isolated yield. ^1H NMR (CD_2Cl_2 , 400 MHz): δ 8.54 (app. d, 1H, $J = 4.0$ Hz), 7.59 (td, 1H, $J = 7.7, 1.8$ Hz), 7.35 – 7.16 (m, 13H), 5.22 – 5.21 (dd, 1H, $J = 10.0, 8.5$ Hz), 5.16 – 5.15 (dd, 1H, $J = 10.1, 7.7$ Hz), 4.69 (AB ddd, $J = 10.0, 8.4, 1.6$ Hz), 4.14 (app. dt, 2H, $J = 8.3, 7.9$ Hz), 3.59 – 3.57 (AB q, 2H, $J = 15.6$ Hz), 1.61 (s, 3H). $^{13}\text{C}\{\text{APT}\}$ NMR (CD_2Cl_2 , 100 MHz): δ 168.7 (C, two peaks), 148.5 (C), 143.0 (C, two peaks), 139.6 (CH), 133.8 (CH), 130.4 (CH), 130.0 (CH), 128.9 (CH, three peaks), 128.8 (CH), 127.8 (CH), 127.2 (CH), 127.1 (CH), 125.4 (CH), 125.2 (CH), 124.6 (CH), 124.3 (CH), 124.2 (CH), 124.1 (CH, two peaks), 123.5 (CH), 75.9 (CH_2 , two peaks), 70.1 (CH_2), 69.9 (CH_2), 67.2 (CH_2), 67.0 (CH_2), 61.5 (CH_2 or C), 43.6 (C), 35.9 (CH_2), 22.1 (CH_3). Abundance of peaks in the ^1H and ^{13}C NMR

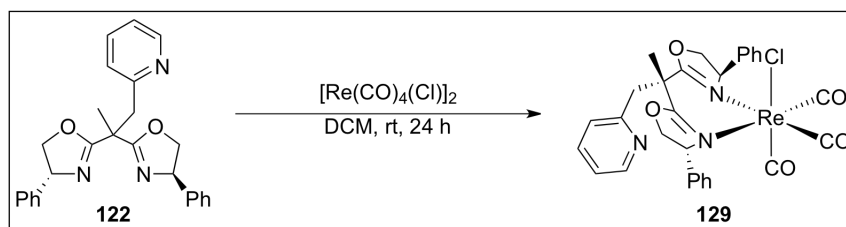
may be attributable to hindered rotation or distortions in the pseudo C_2 -symmetry. HRMS (ESI) m/z calcd for $[C_{26}H_{25}N_3O_3+H]^+$: 428.1974; found: 428.1964. IR (thin film): 3396.4, 2958.4, 1731.0, 1654.8, 1492.6, 1436.5, 1352.3, 1243.5.



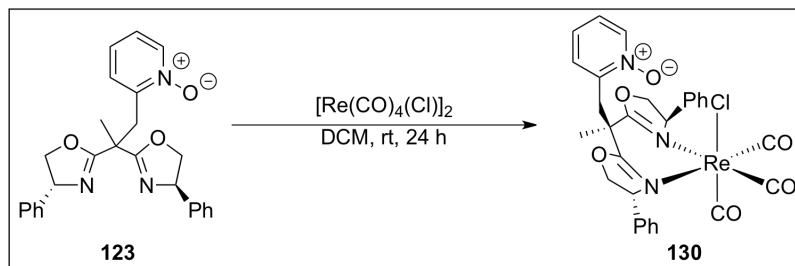
To a flame dried round bottom, equipped with a magnetic stir bar and a serum cap, was added **121** (0.195 g, 0.36 mmol) as a 0.18 M solution in anhydrous THF (2 mL). The mixture was cooled to 0 °C, to this was added 1.5 mL of tetrabutylammonium fluoride (TBAF, 1.0 M in THF, 1.5 mmol, 4 equiv.). The solution turned from a colourless/yellow to a brown and was stirred for 5 minutes at 0 °C and then warmed to room temperature and stirred under N_2 for an additional 5 hours. The reaction was quenched with a saturated ammonium chloride solution (1 mL) and the aqueous layer extracted with ethyl acetate (3 x 10 mL). The combined organics were then washed with brine (10 mL), dried over $MgSO_4$, filtered, and concentrated *in-vacuo*. The crude mixture was purified by column chromatography with an eluent of 4:1 hexanes:ethyl acetate which was gradually increased to 1:1 hexanes:ethyl acetate. This gave phenol **125** in 81% isolated yield. 1H NMR ($CDCl_3$, 400 MHz): δ 11.05 (s, 1H), 7.36 – 7.29 (m, 9H), 7.12 – 7.10 (m, 4H), 6.89 (app. d, 1H, $J = 7.1$ Hz), 6.80 (app. t, 1H, $J = 6.4$ Hz), 5.31 – 5.30 (dd, 1H, $J = 9.9, 9.0$ Hz), 5.25 – 5.23 (dd, 1H, 10.1, 8.2 Hz), 4.72 – 4.66 (m, 2H), 4.16 (t, 2H, 8.2 Hz), 3.48 (AB d, 1H, $J = 14.2$ Hz), 3.25 (AB d, 1H, $J = 14.2$ Hz), 1.74 (s, 3H). $^{13}C\{^1H\}$ NMR ($CDCl_3$, 100 MHz): δ 170.8, 170.2, 156.2, 141.5, 141.3, 133.0, 128.7 (three peaks), 127.8, 127.7, 126.7, 126.4, 123.7, 119.4, 119.2, 75.9, 75.6, 44.8, 38.1, 22.2. Abundance of peaks in the 1H and ^{13}C NMR may be attributable to hindered rotation or distortions in the pseudo C_2 -symmetry. HRMS (ESI) m/z calcd for $[C_{27}H_{26}N_2O_3+Na]^+$: 449.1841; found: 449.1832.



In a N_2 atmosphere glovebox, a solution of proligand **122** was prepared with a concentration of 0.24 M in DCM. 500 μL (0.0502 g, 0.12 mmol) of this solution was then transferred to a 20 mL vial containing 0.0172 g of FeCl_2 (0.14 mmol, 1.1 equiv). The light yellow solution was stirred for 24 hrs until the solution became homogenous. The mixture was then passed through a pipette filled with celite and eluted with a small amount of DCM, then the celite pad was washed with hexanes to layer the solution. This yielded colourless prisms suitable for X-ray analysis. HRMS (ESI) m/z calcd for $[\text{C}_{26}\text{H}_{25}\text{N}_3\text{O}_2^{35}\text{Cl}^{56}\text{Fe} - \text{Cl}]^+$: 502.0985; found: 502.0988.



In a N_2 atmosphere glovebox, a solution of proligand **122** was prepared with a concentration of 0.24 M in DCM. 500 μL (0.0502 g, 0.1 mmol) of this solution was then transferred to a 20 mL vial containing 0.0418 g of $[\text{Re}(\text{CO})_4\text{Cl}]_2$ (0.063 mmol, 0.6 equiv). The pasty orange solution was stirred for 24 hrs upon which the colour changed to a clear deep orange. The homogenous solution was then passed through a pipette filled with celite and eluted with a small amount of DCM, then the celite pad was washed with hexanes to layer the solution. This yielded colourless plates suitable for X-ray analysis. HRMS (ESI) m/z calcd for $[\text{C}_{29}\text{H}_{25}\text{N}_3\text{O}_5^{185}\text{Re} - \text{Cl}]^+$: 680.1324; found: 680.1314.



In a N_2 atmosphere glovebox, a solution of proligand **123** was prepared with a concentration of 0.23 M in DCM. 500 μ L (0.0492 g, 0.1 mmol) of this solution was then transferred to a 20 mL vial containing 0.0396 g of $[Re(CO)_4Cl]_2$ (0.059 mmol, 0.6 equiv). The pasty orange solution was stirred for 24 hrs upon which the colour changed to a clear deep orange. The homogenous solution was then passed through a pipette filled with celite and eluted with a small amount of DCM, then the celite pad was washed with hexanes to layer the solution. This yielded colourless crystals suitable for X-ray analysis. 1H NMR (CD_2Cl_2 , 400 MHz): δ 8.33 (app. d, 1H, 6.4 Hz), 7.44 – 7.21 (m, 13H, 7.7), 6.73 (app. d, 2H, $J = 7.1$ Hz), 5.34 (app. t, 1H, $J = 10.2, 9.6$ Hz), 5.44 – 5.42 (dd, 1H, $J = 10.4, 6.4$ Hz), 4.93 – 4.91 (dd, 1H, $J = 10.4, 8.4$ Hz), 4.87 – 4.86 (dd, 1H, $J = 10.6, 8.8$ Hz), 4.32 – 4.31 (dd, 1H, $J = 8.3, 6.5$ Hz), 4.08 (d, 1H, $J = 14.5$ Hz), 3.98 (t, 1H, $J = 8.9$ Hz), 3.43 (d, 1H, $J = 14.5$ Hz), 2.14 (s, 3H). $^{13}C\{APT\}$ NMR (CD_2Cl_2 , 100 MHz): δ 172.9 (C), 171.3 (C), 147.0 (C), 140.3 (CH), 139.2 (C), 139.0 (C), 129.0 (CH), 128.9 (CH), 128.6 (CH), 128.3 (CH), 127.9 (CH), 126.0 (CH), 125.8 (CH), 77.6 (CH), 76.6 (CH_2), 76.2 (CH_2), 76.0 (CH), 44.9 (C), 41.5 (CH_2), 27.8 (CH_3). Abundance of peaks in the 1H and ^{13}C NMR may be attributable to hindered rotation or distortions in the pseudo C_2 -symmetry. HRMS (ESI) m/z calcd for $[C_{29}H_{25}N_3O_6^{185}Re - Cl]^+$: 696.1273; found: 696.1265. IR (neat solid): 3034.8, 2921.9, 2853.0, 2014.2, 1877.7, 1646.8, 1442.4, 1234.0. UV-vis ($CHCl_3$): 229.0, 290.0 nm.

Chapter 6 Conclusions and Future Work

6.1 Conclusions

The development of novel catalytic methods for the formation of carbon-sulfur bonds is important in the discovery and synthesis of valuable chemotherapeutics. Cross-coupling technologies have facilitated the identification of biologically active molecules, and enabled the large-scale synthesis of active pharmaceutical ingredients.¹⁴¹ These methods are best suited for the synthesis of aryl sulfides, where preparation of vinyl sulfides is often limited by the availability of the vinyl halide precursors. The discovery of vinyl sulfones as promising treatments for malaria, African sleeping sickness, and Chagas disease illustrates the importance of developing new methods towards vinyl sulfides.^{8, 12, 35} To this end, the use of alkyne hydrothiolation has not been applied to the synthesis of biologically active molecules containing vinyl sulfides and their oxidized derivatives (sulfoxides and sulfones). The development and application of our alkyne hydrothiolation methodology employing either $\text{RhTp}^*(\text{PPh}_3)_2$ or Wilkinson's catalyst demonstrates considerable promise in the synthesis of vinyl sulfone containing chemotherapeutics.^{144, 146} Furthermore, alkyne hydrothiolation with either rhodium (I) catalyst represents the first reports capable of tolerating less reactive alkyl thiols. This is significant, as investigation of structure activity relationships (SAR) involving K777 have demonstrated that benzyl sulfones possess greater biological activity than the analogous phenyl substituted derivatives.¹² Our development of a catalytic alkyne hydrothiolation using Wilkinson's catalyst is ideally suited towards further evaluation of SAR pertaining to vinyl sulfone cysteine proteases. This is made possible by the tolerance of this method towards a broad range of aryl and alkyl thiols. During the development of this process, we discovered interesting directing group influences involving substrates such as propargyl amines, and aryl ethers. The presence of a propargyl heteroatom seems to increase the proportion of the branched vinyl sulfide, rather than the desired *E*-linear isomer. Gratifyingly, the hydrothiolation of alkynes derived from boc-protected α -amino acids provided exclusive selectivity for the *E*-linear vinyl sulfide, constituting a formal synthesis of K777. We encountered similar difficulties in the attempted synthesis of ON 01910.Na, a promising cancer chemotherapeutic. The aryl alkyne required for this synthesis possesses two *ortho*-methoxy groups, which seem to influence the regioselectivity of the alkyne

hydrothiolation in favour of the branched regioisomer. This observation was supported by the use of aryl alkynes lacking *ortho*-methoxy groups, which yielded greater proportions of the expected *E*-linear isomer.

The diverse reactivity of sulfur containing molecules prompted us to evaluate the use of alkyne hydrothiolation in synthetic transformations involving the Nazarov cyclization. To this end, heteroaromatic dienones with β -sulfide substituents were evaluated in the Nazarov cyclization. The use of microwave irradiation largely accelerated this reaction, allowing for the isolation of the corresponding cyclopentanones in reasonable yield. The Nazarov cyclizations of these vinylogous thioesters appeared to be highly sensitive to sulfur substitution. Limited substrates were tolerated under the optimized conditions, where elimination of the sulfide following cyclization, or polymerization of the starting dienone represented competing reactions. The use of more reactive 3-substituted thiophenes tolerated a more diverse array of substitution about the vinylogous thioester. However, attempts at developing a one-pot Michael addition, Nazarov cyclization were unsuccessful, as alkylation of the thiol significantly lowered yields. Rearrangement of the 2 or 3-substituted thiophene dienones suggest that multiple pathways exist for the formation of the thiaindanone products.

The use of furan and pyrrole substituted dienones demonstrated opposite reactivity under the optimized conditions for 2-substituted thiophenes. The former proved inert to the optimized conditions, while the latter likely cyclized to an appreciable extent prior to microwave irradiation. Interestingly, use of benzothiophene substituted vinylogous thioesters demonstrated remarkable reactivity in the Nazarov cyclization. The desired cyclopentanone formed during the synthesis of the dienone, following the Sonogashira-type cross-coupling, Michael addition sequence. Analogously, benzofuran containing vinylogous thioesters also seemed to form the desired cyclopentanone during the synthesis of the starting material. This was largely unexpected, as the furan derivatives demonstrated little to no reactivity during the Nazarov cyclization.

Lastly, several sidearm-substituted bisoxazoline proligands were developed in order to explore catalytic asymmetric Nazarov cyclizations, or olefin aziridinations. The successful coordination of these compounds to a variety of transition metals shows promise for the development of chiral Lewis acids capable of initiating the Nazarov cyclization. The literature precedent that sidearms capable of flexible binding with transition metals,

outperform more traditional rigid chelating ligands characteristic of the pybox family. The question of whether this sidearm effect is based upon coordination of the group or by it simply occupying a portion of the chiral space about the transition metal is still unanswered.

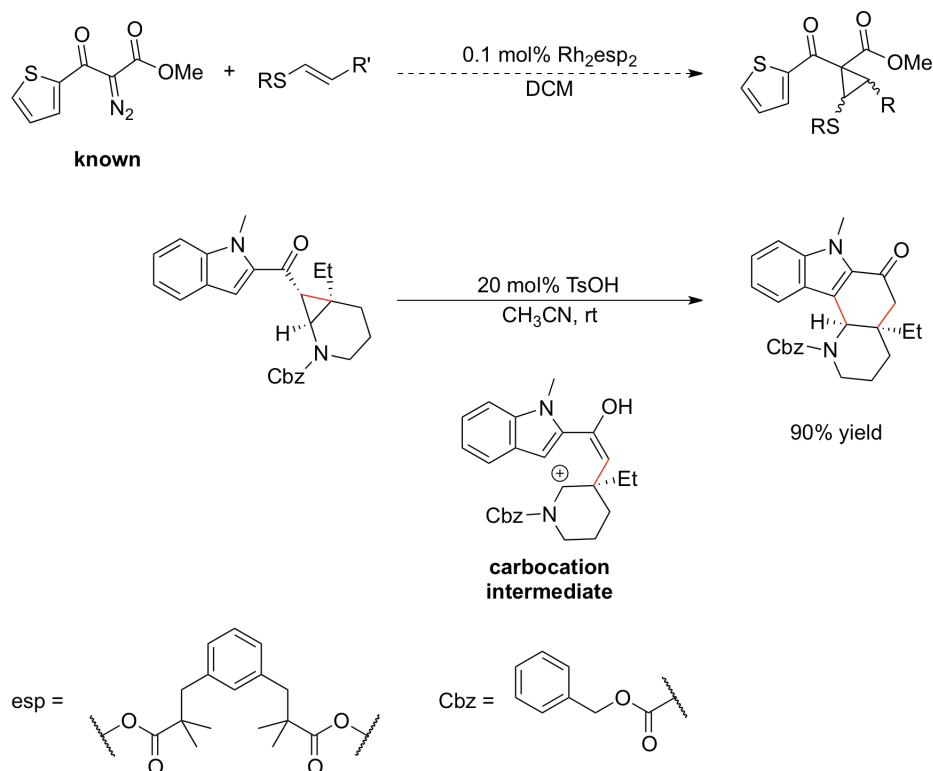
6.2 Future Work

The aforementioned ability of heteroatom substituents in dictating the regioselectivity of alkyne hydrothiolation poses problems to the synthesis of medicinally active molecules containing *E*-linear vinyl sulfones. A potential solution to this problem would be in the synthesis of rhodium (I) precatalysts capable of stronger binding with the alkyne π -system. A simplified approach towards this could involve the preparation of rhodium (I) catalysts with bulky phosphine ligands, where steric clashing may deter chelation of the heteroatom to the metal center. The development of such complexes is certainly necessary in improving the selectivity observed in the synthesis of the vinyl sulfide intermediate en route to the synthesis of ON 01910.Na. Additionally, a more thorough evaluation of nitrogen and oxygen protecting groups may lead to an optimum balance of the steric and electronic influence these heteroatoms may have on alkyne hydrothiolation. Overcoming the challenges presented by these substrates will prove invaluable in the synthesis of K777 and ON 01910.Na, as well as the synthesis of analogues for evaluation of structure activity relationships. Furthermore, more active precatalysts may allow for the reduction of catalyst loadings, allowing for preparation of these important molecules on larger scale. The suspension of these catalysts on solid supports may also prove amenable to large-scale synthesis, by simplifying purification of the vinyl sulfide, and allowing for catalyst recyclability.

The Nazarov cyclization of sulfur-substituted dienones likely could be improved upon cyclopropanation of the vinylogous thioesters. The use of these substrates allows for the synthesis of heteroaromatic-substituted cyclohexanones, and is referred to as the homo-Nazarov cyclization. The synthesis of the necessary substrates could be achieved with the known α -diazo esters, where cyclopropanation with alkyl or aryl vinyl sulfides provides the requisite starting materials. The α -diazo esters are known to undergo cyclopropanation with various styrenes using the conditions in Scheme 6.1.³⁵² Given the electron rich nature of vinyl sulfides relative to styrenes, cyclopropanation of these compounds should proceed readily. This approach would take advantage of the numerous vinyl sulfides synthesized via our

alkyne hydrothiolation methodology with Wilkinson's catalyst. Additionally, heteroatom substitution of the cyclopropane is known to accelerate the homo-Nazarov cyclization by stabilization of the carbocation generated by ring-opening of the strained three-membered ring.³⁵³ The synthesis of the sulfur-substituted cyclopropanes could also serve as a testing ground for asymmetric cyclopropanations using the complexes discussed in chapter 5. Furthermore, the presence of the α -keto ester functionality may allow for the evaluation of our sidearm-substituted bisoxazoline proligands in catalytic asymmetric homo-Nazarov cyclizations.

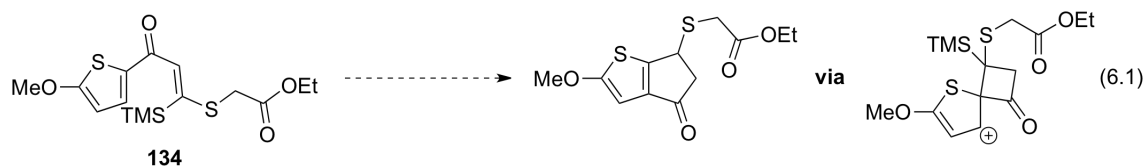
The heteroaromatic-substituted vinylogous thioesters synthesized in chapter 4 may be converted into their respective cyclopropanes upon treatment with a suitable reagent. This could involve treating the vinylogous thioesters with nucleophilic sulfur ylides (Corey-Chaykovsky), or electrophilic diazoesters in the presence of catalytic amounts of copper salts. The reaction of aromatic vinylogous esters (chromones) with a combination of TMSOTf and $\text{Cu}(\text{OTf})_2$ provides the corresponding cyclopropanes in good yields.³⁵⁴ Extending these conditions to the heteroaromatic-substituted vinylogous thioesters may provide access to similar cyclopropanes as those shown in Scheme 6.1. Investigation of the homo-Nazarov cyclization of these compounds will likely provide access to structurally diverse heteroaromatic cyclohexanones.



Scheme 6.1

Lastly, mechanistic investigations regarding the observed rearrangements during cyclization of the 2 and 3-substituted dienones warrant further investigation. As the current evidence is largely circumstantial, further spectroscopic evaluation of the cyclopentanone products generated in DCE and CH_3CN , at ambient temperature and under microwave irradiation, is necessary. In particular, an Incredible Natural Abundance Double Quantum Transfer (INADEQUATE) experiment could help unambiguously assign the ^{13}C -connectivities for the ketone with the adjacent thiophene resonances. By ^{13}C labeling the carbonyl carbon, analysis of the 2J and 3J couplings could also provide unambiguous evidence regarding the connectivity. Furthermore, treatment of dienones like (**134**) with TfOH in DCE using conventional or microwave heating may facilitate rearrangement to the 3-substituted derivative, as the methoxy group may stabilize the carbocation formed upon spirocyclization. Similarly, if the rearrangement occurs via a spirocyclic intermediate capable of forming carbocations, or acylium ions, the use of external trapping agents may intercept these species. The trapping agent could also be appended to the sulfur atom, provided that the substituent does not interfere during reaction with Lewis or Brønsted acids. If products

corresponding to inter- or intramolecular trapping can be isolated, this would provide evidence for a Friedel-Crafts type pathway during the cyclization of the dienones investigated.



References

- (1) Li, Y.; Murakami, Y.; Katsumura, S. *Tetrahedron Lett.* **2006**, *47*, 787-789.
- (2) Starckenmann, C.; Le Calve, B.; Niclass, Y.; Cayeux, I.; Beccucci, S.; Troccaz, M. *J. Agr. Food. Chem.* **2008**, *56*, 9575-9580.
- (3) Rochat, S.; de Saint Laumer, J.; Chaintreau, A. *J. Chromatogr. A.* **2007**, *1147*, 85-94.
- (4) Holm, R.; Kennepohl, P.; Solomon, E. *Chem. Rev.* **1996**, *96*, 2239-2314.
- (5) Hughes, J.; Tregova, A.; Tomsett, A.; Jones, M.; Cosstick, R.; Collin, H. *Phytochemistry* **2005**, *66*, 187-194.
- (6) White, R. *Science* **1975**, *189*, 810-811.
- (7) Wennig, R.; Schneider, S.; Meys, F. *J. Chromatogr. B.* **2010**, *878*, 1433-1436.
- (8) Jaishankar, P.; Hartsell, E.; Zhao, D.; Doyle, P.; McKerrow, J.; Renslo, A. *Bioorg. Med. Chem. Lett.* **2008**, *18*, 624-628.
- (9) Chen, Y.; Lira, R.; Hansell, E.; McKerrow, J.; Roush, W. *Med. Chem. Lett.* **2008**, *18*, 5860-3.
- (10) Scheidt, K.; Roush, W.; McKerrow, J.; Selzer, P.; Hansell, E.; Rosenthal, P. *Bioorg. Med. Chem.* **1998**, *6*, 2477-2494.
- (11) Vicik, R.; Busemann, M.; Baumann, K.; Schirmeister, T. *Curr. Top. Med. Chem.* **2006**, *6*, 331-353.
- (12) Roush, W.; Gwaltney, S.; Cheng, J.; Scheidt, K.; McKerrow, J.; Hansell, E. *J. Am. Chem. Soc.* **1998**, *120*, 10994-10995.
- (13) Kerr, I.; Lee, J.; Farady, C.; Marion, R.; Rickert, M.; Sajid, M.; Pandey, K.; Caffrey, C.; Legac, J.; Hansell, E.; McKerrow, J.; Craik, C.; Rosenthal, P.; Brinen, L. *J. Biol. Chem.* **2009**, *284*, 25697-25703.
- (14) Palmer, J.; Rasnick, D.; Klaus, J.; Bromme, D. *J. Med. Chem.* **1995**, *38*, 3193-3196.
- (15) McGrath, M.; Eakin, A.; Engel, J.; McKerrow, J.; Craik, C.; Fletterick, R. *J. Mol. Biol.* **1995**, *247*, 251-9.
- (16) Santos, M.; Moreira, R. *Mini-Rev. Med. Chem.* **2007**, *7*, 1040-1050.
- (17) Caffrey, C.; Hansell, E.; Lucas, K.; Brinen, L.; Alvarez Hernandez, A.; Cheng, J.; Gwaltney, S.; Roush, W.; Stierhof, Y.; Bogoyo, M.; Steverding, D.; McKerrow, J. *Mol. Biochem. Parasit.* **2001**, *118*, 61-73.
- (18) Leslie, M. *Science* **2011**, *333*, 933-935.
- (19) Bentley, R. *J. Ind. Microbiol. Biot.* **2009**, *36*, 775-786.
- (20) Skold, O. *Drug Resist. Update* **2000**, *3*, 155-160.
- (21) Wainwright, M.; Kristiansen, J. *Dyes Pigments* **2011**, *88*, 231-234.
- (22) Thunnissen, A.; Dijkstra, B. *Nat. Struct. Biol.* **1996**, *3*, 218-221.
- (23) Macheboeuf, P.; Fischer, D.; Brown, T.; Zervosen, A.; Luxen, A.; Joris, B.; Dessen, A.; Schofield, C. *Nat. Chem. Biol.* **2007**, *3*, 565-569.
- (24) Salzmann, T.; Ratcliffe, R.; Christensen, B.; Bouffard, F. *J. Am. Chem. Soc.* **1980**, *102*, 6161-6163.
- (25) Woodward, R.; Heusler, K.; Gosteli, J.; Naegeli, P.; Oppolzer, W.; Ramage, R.; Ranganats, S.; Vorbrugg, H. *J. Am. Chem. Soc.* **1966**, *88*, 852-853.
- (26) Harrison, C.; Bratcher, D. *Pediatr. Rev.* **2008**, *29*, 264-273.
- (27) Viaene, E.; Chanteux, H.; Servais, H.; Mingeot-Leclercq, M.; Tulkens, P. *Antimicrob. Agents Chemother.* **2002**, *46*, 2327-32.
- (28) Perry, C.; Markham, A. *Drugs* **1999**, *57*, 805-843.

- (29) Lee, W.; McDonough, M. A.; Kotra, L. P.; Li, Z. H.; Silvaggi, N. R.; Takeda, Y.; Kelly, J. A.; Mobashery, S. *Proc. Natl. Acad. Sci. U. S. A.* **2001**, *98*, 1427-1431.
- (30) Silverman, R. B. In *The Organic Chemistry of Drug Design and Drug Action*; Elsevier Academic Press: 2004; Vol. 2, pp 617.
- (31) Palermo, C.; Joyce, J. *Trends Pharmacol. Sci.* **2008**, *29*, 22-28.
- (32) Li, Z.; Chen, X.; Davidson, E.; Zwang, O.; Mendis, C.; Ring, C.; Roush, W.; Fegley, G.; Li, R.; Rosenthal, P. *Chem. Biol.* **1994**, *1*, 31-7.
- (33) Robichaud, J.; Oballa, R.; Prasit, P.; Falguyret, J.; Percival, M.; Wesolowski, G.; Rodan, S.; Kimmel, D.; Johnson, C.; Bryant, C.; Venkatraman, S.; Setti, E.; Mendonca, R.; Palmer, J. *J. Med. Chem.* **2003**, *46*, 3709-3727.
- (34) Gauthier, J.; Chauret, N.; Cromlish, W.; Desmarais, S.; Duong, L.; Falguyret, J.; Kimmel, D.; Lamontagne, S.; Leger, S.; LeRiche, T.; Li, C.; Masse, F.; Mckay, D.; Nicoll-Griffith, D.; Oballa, R.; Palmer, J.; Percival, M.; Riendeau, D.; Robichaud, J.; Rodan, G.; Rodan, S.; Seto, C.; Therien, M.; Truong, V.; Venuti, M.; Wesolowski, G.; Young, R.; Zamboni, R.; Black, W. *Bioorg. Med. Chem. Lett.* **2008**, *18*, 923-928.
- (35) Rosenthal, P.; Olson, J.; Lee, G.; Palmer, J.; Klaus, J.; Rasnick, D. *Antimicrob. Agents Chemother.* **1996**, *40*, 1600-3.
- (36) Liu, S.; Hanzlik, R. *J. Med. Chem.* **1992**, *35*, 1067-1075.
- (37) Reddick, J.; Cheng, J.; Roush, W. *Org. Lett.* **2003**, *5*, 1967-1970.
- (38) Ettari, R.; Nizi, E.; Di Francesco, M.; Dude, M.; Pradel, G.; Vičák, R.; Schirmeister, T.; Micale, N.; Grasso, S.; Zappalà, M. *J. Med. Chem.* **2008**, *51*, 988-996.
- (39) Meadows, D.; Sanchez, T.; Neamati, N.; North, T.; Gervay-Hague, J. *Bioorg. Med. Chem.* **2007**, *15*, 1127-1137.
- (40) Chahrour, O.; Abdalla, A.; Lam, F.; Midgley, C.; Wang, S. *Bioorg. Med. Chem. Lett.* **2011**, *21*, 3066-9.
- (41) Patick, A.; Binford, S.; Brothers, M.; Jackson, R.; Ford, C.; Diem, M.; Maldonado, F.; Dragovich, P.; Zhou, R.; Prins, T.; Fuhrman, S.; Meador, J.; Zalman, L.; Matthews, D.; Worland, S. *Antimicrob. Agents Chemother.* **1999**, *43*, 2444-2450.
- (42) Schöffski, P. *Oncologist* **2009**, *14*, 559-70.
- (43) Bickart, P.; Carson, F.; Jacobus, J.; Miller, E.; Mislou, K. *J. Am. Chem. Soc.* **1968**, *90*, 4869-4876.
- (44) Evans, D.; Andrews, G.; Sims, C. *J. Am. Chem. Soc.* **1971**, *93*, 4956-4957.
- (45) Pummerer, R. *Ber.* **1910**, *43*, 1401-1412.
- (46) Pummerer, R. *Ber.* **1909**, *42*, 2275-2282.
- (47) Bonjoch, J.; Catena, J.; Valls, N. *J. Org. Chem.* **1996**, *61*, 7106-7115.
- (48) Julia, M.; Paris, J. *Tetrahedron Lett.* **1973**, *14*, 4833-4836.
- (49) Baudin, J.; Hareau, G.; Julia, S.; Ruel, O. *Tetrahedron Lett.* **1991**, *32*, 1175-1178.
- (50) Blakemore, P.; Cole, W.; Kociński, P. *Synlett* **1998**, 26-28.
- (51) Chan, T.; Fong, S.; Li, Y.; Man, T.; Poon, C. *J. Chem. Soc., Chem. Commun.* **1994**, 1771-1772.
- (52) Corey, E. J.; Chaykovsky, M. *J. Am. Chem. Soc.* **1962**, *84*, 867-868.
- (53) Corey, E. J.; Chaykovsky, M. *J. Am. Chem. Soc.* **1965**, *87*, 1353-1364.
- (54) Aggarwal, V.; Alonso, E.; Bae, I.; Hynd, G.; Lydon, K.; Palmer, M.; Patel, M.; Porcelloni, M.; Richardson, J.; Stenson, R.; Studley, J.; Vasse, J.; Winn, C. *J. Am. Chem. Soc.* **2003**, *125*, 10926-10940.

- (55) Aggarwal, V.; Fang, G.; Kokotos, C.; Richardson, J.; Unthank, M. *Tetrahedron* **2006**, *62*, 11297-11303.
- (56) Smith, A.; Kim, D. *Org. Lett.* **2005**, *7*, 3247-3250.
- (57) Schreiber, S.; Satake, K. *J. Am. Chem. Soc.* **1984**, *106*, 4186-4188.
- (58) Padwa, A.; Heidelbaugh, T.; Kuethe, J. *J. Org. Chem.* **2000**, *65*, 2368-2378.
- (59) Ghosh, A.; Gong, G. *Org. Lett.* **2007**, *9*, 1437-40.
- (60) Kozak, J.; Dake, G. *Angew. Chem. Int. Ed.* **2008**, *47*, 4221-3.
- (61) Berkowitz, B.; Sachs, G. *Mol. Interv.* **2002**, *2*, 6-11.
- (62) Bolinger, J.; Lindsley, C. *Curr. Top. Med. Chem.* **2007**, *7*, 1643-1643.
- (63) Morita, N.; Krause, N. *Angew. Chem. Int. Ed.* **2006**, *45*, 1897-1899.
- (64) Brouwer, C.; Rahatryan, R.; He, C. *Synlett* **2007**, 1785-1789.
- (65) Correa, A.; Carril, M.; Bolm, C. *Angew. Chem. Int. Ed.* **2008**, *47*, 2880-2883.
- (66) Fernández-Rodríguez, M.; Shen, Q.; Hartwig, J. F. *J. Am. Chem. Soc.* **2006**, *128*, 2180-2181.
- (67) Kim, G.; Chu-Moyer, M.; Danishefsky, S. J.; Schulte, G. K. *J. Am. Chem. Soc.* **1993**, *115*, 30-39.
- (68) Moreau, X.; Campagne, J. *J. Org. Chem.* **2003**, *68*, 5346-5350.
- (69) Namyslo, J. C.; Stanitzek, C. *Synthesis-Stuttgart* **2006**, 3367-3369.
- (70) Kondo, T.; Mitsudo, T. *Chem. Rev.* **2000**, *100*, 3205-3220.
- (71) Beletskaya, I.; Moberg, C. *Chem. Rev.* **1999**, *99*, 3435-3462.
- (72) Ley, S. V.; Thomas, A. W. *Angew. Chem. Int. Ed.* **2003**, *42*, 5400-5449.
- (73) Prim, D.; Campagne, J. M.; Joseph, D.; Andrioletti, B. *Tetrahedron* **2002**, *58*, 2041-2075.
- (74) Kuniyasu, H.; Kambe, N. *Chem. Lett.* **2006**, *35*, 1320-1325.
- (75) Beletskaya, I. P.; Ananikov, V. P. *Eur. J. Org. Chem.* **2007**, *2007*, 3431-3444.
- (76) Beletskaya, I. P.; Ananikov, V. P. *Pure Appl. Chem.* **2007**, *79*, 1041-1056.
- (77) Arisawa, M.; Yamaguchi, M. *Pure Appl. Chem.* **2008**, *80*, 993-1003.
- (78) Soederberg, B. *Coordin. Chem. Rev.* **2008**, *252*, 57-133.
- (79) Hartwig, J. F. *Acc. Chem. Res.* **2008**, *41*, 1534-1544.
- (80) Ullmann, F.; Bielecki, J. *Ber.* **1901**, *34*, 2174-2185.
- (81) Ullmann, F. *Ber.* **1903**, *36*, 2382-2384.
- (82) Ullmann, F. *Ber.* **1904**, *37*, 853-854.
- (83) Savarin, C.; Srogl, J.; Liebeskind, L. S. *Org. Lett.* **2002**, *4*, 4309-4312.
- (84) Kwong, F. Y.; Buchwald, S. L. *Org. Lett.* **2002**, *4*, 3517-3520.
- (85) Bates, C. G.; Gujadhur, R. K.; Venkataraman, D. *Org. Lett.* **2002**, *4*, 2803-2806.
- (86) Bates, C. G.; Saejueng, P.; Doherty, M. Q.; Venkataraman, D. *Org. Lett.* **2004**, *6*, 5005-5008.
- (87) Sawada, N.; Itoh, T.; Yasuda, N. *Tetrahedron Lett.* **2006**, *47*, 6595-6597.
- (88) Enguehard-Gueiffier, C.; Thery, I.; Gueiffier, A.; Buchwald, S. L. *Tetrahedron* **2006**, *62*, 6042-6049.
- (89) Krafft, E. A.; Pinard, E.; Thomas, A. W. *Tetrahedron Lett.* **2006**, *47*, 5355-5357.
- (90) Evindar, G.; Batey, R. A. *J. Org. Chem.* **2006**, *71*, 1802-1808.
- (91) Zhu, W.; Ma, D. *J. Org. Chem.* **2005**, *70*, 2696-2700.
- (92) Zhang, H.; Cao, W.; Ma, D. L. *Syn. Commun.* **2007**, *37*, 25-35.
- (93) Guo, S.; Yuan, Y. *Syn. Commun.* **2008**, *38*, 2722-2730.
- (94) Kabir, M. S.; Van Linn, M.; Monte, A.; Cook, J. M. *Org. Lett.* **2008**, *10*, 3363-3366.

- (95) Bagley, M. C.; Dix, M. C.; Fusillo, V. *Tetrahedron Lett.* **2009**, *50*, 3661-3664.
- (96) Prasad, D.; Naidu, A. B.; Sekar, G. *Tetrahedron Lett.* **2009**, *50*, 1411-1415.
- (97) Luo, P.; Wang, F.; Li, J.; Tang, R.; Zhong, P. *Synthesis-Stuttgart* **2009**, 921-928.
- (98) Haldón, E.; Álvarez, E.; Nicasio, M. C.; Pérez, P. *Organometallics* **2009**, *28*, 3815-3821.
- (99) Evano, G.; Blanchard, N.; Toumi, M. *Chem. Rev.* **2008**, *108*, 3054-3131.
- (100) Palomo, C.; Oiarbide, M.; Lopez, R.; Gomez-Bengoa, E. *Tetrahedron Lett.* **2000**, *41*, 1283-1286.
- (101) Baranano, D.; Hartwig, J. F. *J. Am. Chem. Soc.* **1995**, *117*, 2937-2938.
- (102) Louie, J.; Hartwig, J. F. *J. Am. Chem. Soc.* **1995**, *117*, 11598-11599.
- (103) Hartwig, J. F. *Acc. Chem. Res.* **1998**, *31*, 852-860.
- (104) Mann, G.; Baranano, D.; Hartwig, J. F.; Rheingold, A. L.; Guzei, I. A. *J. Am. Chem. Soc.* **1998**, *120*, 9205-9219.
- (105) Hartwig, J. F. *Inorg. Chem.* **2007**, *46*, 1936-1947.
- (106) Hartwig, J. F. *Nature* **2008**, *455*, 314-322.
- (107) Fernández-Rodríguez, M.; Hartwig, J. F. *J. Org. Chem.* **2009**, *74*, 1663-1672.
- (108) Alvaro, E.; Hartwig, J. F. *J. Am. Chem. Soc.* **2009**, *131*, 7858-7868.
- (109) Kosugi, M.; Shimizu, T.; Migita, T. *Chem. Lett.* **1978**, 13-14.
- (110) Migita, T.; Shimizu, T.; Asami, Y.; Shiobara, J.; Kato, Y.; Kosugi, M. *Bull. Chem. Soc. Jpn.* **1980**, *53*, 1385-1389.
- (111) Murahashi, S.; Yamamura, M.; Yanagisawa, K.; Mita, N.; Kondo, K. *J. Org. Chem.* **1979**, *44*, 2408-2417.
- (112) Kosugi, M.; Ogata, T.; Terada, M.; Sano, H.; Migita, T. *Bull. Chem. Soc. Jpn.* **1985**, *58*, 3657-3658.
- (113) Carpita, A.; Rossi, R.; Scamuzzi, B. *Tetrahedron Lett.* **1989**, *30*, 2699-2702.
- (114) Ciattini, P.G.; Morera, E.; Ortar, G. *Tetrahedron Lett.* **1995**, *36*, 4133-4136.
- (115) Ishiyama, T.; Mori, M.; Suzuki, A.; Miyaura, N. *J. Organomet. Chem.* **1996**, *525*, 225-231.
- (116) Zheng, N.; McWilliams, J. C.; Fleitz, F. J.; Armstrong, J. D.; Volante, R. P. *J. Org. Chem.* **1998**, *63*, 9606-9607.
- (117) Li, G. Y.; Zheng, G.; Noonan, A. F. *J. Org. Chem.* **2001**, *66*, 8677-8681.
- (118) Li, G. Y. *Angew. Chem. Int. Ed.* **2001**, *40*, 1513-1516.
- (119) Schopfer, U.; Schlapbach, A. *Tetrahedron* **2001**, *57*, 3069-3073.
- (120) Savarin, C.; Srogl, J.; Liebeskind, L. S. *Org. Lett.* **2000**, *3*, 91-93.
- (121) Li, G. Y. *J. Org. Chem.* **2002**, *67*, 3643-3650.
- (122) Cacchi, S.; Fabrizi, G.; Goggiamani, A.; Parisi, L. M. *Org. Lett.* **2002**, *4*, 4719-4721.
- (123) Lengar, A.; Kappe, C. O. *Org. Lett.* **2004**, *6*, 771-774.
- (124) Bandgar, B. P.; Bettigeri, S. V.; Phopase, J. *Org. Lett.* **2004**, *6*, 2105-2108.
- (125) Itoh, T.; Mase, T. *Org. Lett.* **2004**, *6*, 4587-4590.
- (126) Mispelaere-Canivet, C.; Spindler, J. F.; Perrio, S.; Beslin, P. *Tetrahedron* **2005**, *61*, 5253-5259.
- (127) Moreau, X.; Campagne, J. M.; Meyer, G.; Jutand, A. *Eur. J. Org. Chem.* **2005**, 3749-3760.
- (128) Kreis, M.; Brase, S. *Adv. Synth. Catal.* **2005**, *347*, 313-319.
- (129) Ranu, B. C.; Chattopadhyay, K.; Banerjee, S. *J. Org. Chem.* **2005**, *71*, 423-425.
- (130) Fukuzawa, S.; Tanihara, D.; Kikuchi, S. *Synlett* **2006**, 2145-2147.

- (131) Willis, M. C.; Taylor, D.; Gillmore, A. T. *Tetrahedron* **2006**, *62*, 11513-11520.
- (132) Maitro, G.; Vogel, S.; Prestat, G.; Madec, D.; Poli, G. *Org. Lett.* **2006**, *8*, 5951-5954.
- (133) Cai, L.; Cuevas, J.; Peng, Y.; Pike, V. W. *Tetrahedron Lett.* **2006**, *47*, 4449-4452.
- (134) Maitro, G.; Vogel, S.; Sadaoui, M.; Prestat, G.; Madec, D.; Poli, G. *Org. Lett.* **2007**, *9*, 5493-5496.
- (135) Lee, J.; Lee, P. H. *J. Org. Chem.* **2008**, *73*, 7413-7416.
- (136) Dahl, T.; Tornøe, C.; Bang-Andersen, B.; Nielsen, P.; Jørgensen, M. *Angew. Chem. Int. Ed.* **2008**, *47*, 1726-1728.
- (137) Norris, T.; Leeman, K. *Org. Process Res. Dev.* **2008**, *12*, 869-876.
- (138) Duan, Z.; Ranjit, S.; Zhang, P.; Liu, X. *Chem. Eur. J.* **2009**, *15*, 3666-3669.
- (139) Sayah, M.; Organ, M. G. *Chem. Eur. J.* **2011**, *17*, 11719-11722.
- (140) Bang-Andersen, B.; Ruhland, T.; Jørgensen, M.; Smith, G.; Frederiksen, K.; Jensen, K. G.; Zhong, H.; Nielsen, S. M.; Hogg, S.; Mørk, A.; Stensbøl, T. *J. Med. Chem.* **2011**, *54*, 3206-3221.
- (141) de Koning, P.; Murtagh, L.; Lawson, J. P.; Vonder Embse, R.; Kunda, S. A.; Kong, W. *Org. Proc. Res. Dev.* **2011**, *15*, 1046-1051.
- (142) Field, L. D.; Messerle, B. A.; Vuong, K. Q.; Turner, P. *Dalton Trans.* **2009**, 3599-3614.
- (143) Burling, S.; Field, L. D.; Messerle, B. A.; Vuong, K. Q.; Turner, P. *Dalton Trans.* **2003**, 4181-4191.
- (144) Cao, C. S.; Fraser, L. R.; Love, J. A. *J. Am. Chem. Soc.* **2005**, *127*, 17614-17615.
- (145) Ogawa, A.; Ikeda, T.; Kimura, K.; Hirao, T. *J. Am. Chem. Soc.* **1999**, *121*, 5108-5114.
- (146) Shoai, S.; Bichler, P.; Kang, B.; Buckley, H.; Love, J. A. *Organometallics* **2007**, *26*, 5778-5781.
- (147) Sridhar, R.; Surendra, K.; Krishnaveni, N. S.; Srinivas, Rao, K.R. *Synlett* **2006**, *20*, 3495-3497.
- (148) Benson, S. W. *Chem. Rev.* **1978**, *78*, 23-35.
- (149) Truce, W. E.; Simms, J. A. *J. Am. Chem. Soc.* **1956**, *78*, 2756-2759.
- (150) Truce, W. E.; Simms, J. A.; Boudakian, M. M. *J. Am. Chem. Soc.* **1956**, *78*, 695-696.
- (151) Wang, Z.; Tang, R.; Luo, P.; Deng, C.; Zhong, P.; Li, J. *Tetrahedron* **2008**, *64*, 10670-10675.
- (152) Zou, K. B.; Yin, X. H.; Liu, W. Q.; Qiu, R. H.; Li, R. X.; Shao, L. L.; Li, Y. H.; Xu, X. H.; Yang, R. H. *Syn. Commun.* **2009**, *39*, 2464-2471.
- (153) Cintas, P. *Synlett* **1995**, 1087-1096.
- (154) Nair, V.; Ros, S.; Jayan, C. N.; Pillai, B. S. *Tetrahedron* **2004**, *60*, 1959-1982.
- (155) Peppe, C.; de Castro, L.; Mello, M.; do, R. B. *Synlett* **2008**, 1165-1170.
- (156) Yadav, J. S.; Reddy, B. V. S.; Raju, A.; Ravindar, K.; Baishya, G. *Chem. Lett.* **2007**, *36*, 1474-1475.
- (157) Watanabe, S.; Mori, E.; Nagai, H.; Iwamura, T.; Iwama, T.; Kataoka, T. *J. Org. Chem.* **2000**, *65*, 8893-8898.
- (158) Manarin, F.; Roehrs, J. A.; Prigol, M.; Alves, D.; Nogueira, C. W.; Zeni, G. *Tetrahedron Lett.* **2007**, *48*, 4805-4808.
- (159) Schneider, C. C.; Godoi, B.; Prigol, M.; Nogueira, C. W.; Zeni, G. *Organometallics* **2007**, *26*, 4252-4256.
- (160) Bhadra, S.; Ranu, B. C. *Can. J. Chem.* **2009**, *87*, 1605-1609.

- (161) Kuniyasu, H.; Ogawa, A.; Sato, K.; Ryu, I.; Kambe, N.; Sonoda, N. *J. Am. Chem. Soc.* **1992**, *114*, 5902-5903.
- (162) Ogawa, A.; Takeba, M.; Kawakami, J.; Ryu, I.; Kambe, N.; Sonoda, N. *J. Am. Chem. Soc.* **1995**, *117*, 7564-7565.
- (163) Han, L.; Zhang, C.; Yazawa, H.; Shimada, S. *J. Am. Chem. Soc.* **2004**, *126*, 5080-5081.
- (164) Ananikov, V.; Malyshev, D.A. Beletskaya, I.P.; Aleksandrov, G.G.; Eremenko, I.L. *Adv. Synth. Catal.* **2005**, *347*, 1993-2001.
- (165) Ananikov, V. P.; Orlov, N. V.; Beletskaya, I. P.; Khrustalev, V. N.; Antipin, M. Y.; Timofeeva, T. V. *J. Am. Chem. Soc.* **2007**, *129*, 7252-7253.
- (166) Ananikov, V. P.; Orlov, N. V.; Beletskaya, I. P. *Organometallics* **2006**, *25*, 1970-1977.
- (167) Yatsumonji, Y.; Okada, O.; Tsubouchi, A.; Takeda, T. *Tetrahedron* **2006**, *62*, 9981-9987.
- (168) Malyshev, D. A.; Scott, N. M.; Marion, N.; Stevens, E. D.; Ananikov, V. P.; Beletskaya, I. P.; Nolan, S. P. *Organometallics* **2006**, *25*, 4462-4470.
- (169) Ananikov, V.; Zalesskiy, S.; Orlov, N.; Beletskaya, I. P. *Russ. Chem. Bull.* **2006**, *55*, 2109-2113.
- (170) Hua, R.; Takeda, H.; Onozawa, S.; Abe, Y.; Tanaka, M. *Org. Lett.* **2006**, *9*, 263-266.
- (171) Ananikov, V. P.; Orlov, N. V.; Kabeshov, M. A.; Beletskaya, I. P.; Starikova, Z. A. *Organometallics* **2008**, *27*, 4056-4061.
- (172) Silveira, C. C.; Santos, P.; Mendes, S. R.; Braga, A. L. *J. Organomet. Chem.* **2008**, *693*, 3787-3790.
- (173) Kuniyasu, H.; Ogawa, A.; Miyazaki, S.; Ryu, I.; Kambe, N.; Sonoda, N. *J. Am. Chem. Soc.* **1991**, *113*, 9796-9803.
- (174) Ishiyama, T.; Nishijima, K.; Miyaura, N.; Suzuki, A. *J. Am. Chem. Soc.* **1993**, *115*, 7219-7225.
- (175) Baekvall, J.; Ericsson, A. *J. Org. Chem.* **1994**, *59*, 5850-5851.
- (176) Ogawa, A.; Kawakami, J.; Sonoda, N.; Hirao, T. *J. Org. Chem.* **1996**, *61*, 4161-4163.
- (177) Ogawa, A.; Kuniyasu, H.; Sonoda, N.; Hirao, T. *J. Org. Chem.* **1997**, *62*, 8361-8365.
- (178) Xiao, W.; Vasapollo, G.; Alper, H. *J. Org. Chem.* **1998**, *63*, 2609-2612.
- (179) Xiao, W.; Vasapollo, G.; Alper, H. *J. Org. Chem.* **1999**, *64*, 2080-2084.
- (180) Han, L.; Tanaka, M. *Chem. Commun.* **1999**, 395-402.
- (181) Xiao, W.; Alper, H. *J. Org. Chem.* **1999**, *64*, 9646-9652.
- (182) Xiao, W.; Vasapollo, G.; Alper, H. *J. Org. Chem.* **2000**, *65*, 4138-4144.
- (183) Xiao, W.; Alper, H. *J. Org. Chem.* **2001**, *66*, 6229-6233.
- (184) Sugoh, K.; Kuniyasu, H.; Kurosawa, H. *Chem. Lett.* **2002**, 106-107.
- (185) Ananikov, V. P.; Kabeshov, M. A.; Beletskaya, I. P. *Dokl. Chem.* **2003**, *390*, 112-114.
- (186) Ananikov, V.; Beletskaya, I. P. *Russ. Chem. Bull.* **2004**, *53*, 561-565.
- (187) Ananikov, V. P.; Kabeshov, M. A.; Beletskaya, I. P. *Synlett* **2005**, 1015-1017.
- (188) Gonzales, J. M.; Musaev, D. G.; Morokuma, K. *Organometallics* **2005**, *24*, 4908-4914.
- (189) Kamiya, I.; Kawakami, J.; Yano, S.; Nomoto, A.; Ogawa, A. *Organometallics* **2006**, *25*, 3562-3564.
- (190) Kuniyasu, H.; Kato, T.; Asano, S.; Ye, J. H.; Ohmori, T.; Morita, M.; Hiralke, H.; Fujiwara, S.; Terao, J.; Kurosawa, H.; Kambe, N. *Tetrahedron Lett.* **2006**, *47*, 1141-1144.
- (191) Cai, M.; Wang, Y.; Hao, W. *Green Chem.* **2007**, *9*, 1180-1184.
- (192) Lee, Y. T.; Choi, S. Y.; Chung, Y. K. *Tetrahedron Lett.* **2007**, *48*, 5673-5677.

- (193) Kodama, S.; Nishinaka, E.; Nomoto, A.; Sonoda, M.; Ogawa, A. *Tetrahedron Lett.* **2007**, *48*, 6312-6317.
- (194) Ananikov, V.; Gayduk, K.; Beletskaya, I.; Khrustalev, V.; Antipin, M. *Chem. Eur. J.* **2008**, *14*, 2420-2434.
- (195) Wang, M.; Cheng, L.; Wu, Z. *Dalton Trans.* **2008**, 3879-3888.
- (196) Yamashita, F.; Kuniyasu, H.; Terao, J.; Kambe, N. *Org. Lett.* **2008**, *10*, 101-104.
- (197) Ananikov, V. P.; Gayduk, K. A.; Beletskaya, I. P.; Khrustalev, V. N.; Antipin, M. Y. *Ber.* **2009**, *2009*, 1149-1161.
- (198) Minami, Y.; Kuniyasu, H.; Miyafuji, K.; Kambe, N. *Chem. Commun.* **2009**, 3080-3082.
- (199) Ogawa, A.; Kawakami, J.; Mihara, M.; Ikeda, T.; Sonoda, N.; Hirao, T. *J. Am. Chem. Soc.* **1997**, *119*, 12380-12381.
- (200) Sugoh, K.; Kuniyasu, H.; Sugae, T.; Ohtaka, A.; Takai, Y.; Tanaka, A.; Machino, C.; Kambe, N.; Kurosawa, H. *J. Am. Chem. Soc.* **2001**, *123*, 5108-5109.
- (201) Ohtaka, A.; Kuniyasu, H.; Kinomoto, M.; Kurosawa, H. *J. Am. Chem. Soc.* **2002**, *124*, 14324-14325.
- (202) Kawakami, J.; Mihara, M.; Kamiya, I.; Takeba, M.; Ogawa, A.; Sonoda, N. *Tetrahedron* **2003**, *59*, 3521-3526.
- (203) Hirai, T.; Kuniyasu, H.; Kambe, N. *Tetrahedron Lett.* **2005**, *46*, 117-119.
- (204) Hirai, T.; Kuniyasu, H.; Asano, S.; Terao, J.; Kambe, N. *Synlett* **2005**, 1161-1163.
- (205) Kuniyasu, H.; Yamashita, F.; Hirai, T.; Ye, J.; Fujiwara, S.; Kambe, N. *Organometallics* **2005**, *25*, 566-570.
- (206) Kajitani, M.; Kamiya, I.; Nomoto, A.; Kihara, N.; Ogawa, A. *Tetrahedron* **2006**, *62*, 6355-6360.
- (207) Kuniyasu, H.; Yamashita, F.; Terao, J.; Kambe, N. *Angew. Chem. Int. Ed.* **2007**, *46*, 5929-5933.
- (208) Bonnington, K. J.; Jennings, M. C.; Puddephatt, R. J. *Organometallics* **2008**, *27*, 6521-6530.
- (209) Kuniyasu, H.; Takekawa, K.; Yamashita, F.; Miyafuji, K.; Asano, S.; Takai, Y.; Ohtaka, A.; Tanaka, A.; Sugoh, K.; Kurosawa, H.; Kambe, N. *Organometallics* **2008**, *27*, 4788-4802.
- (210) Nakata, N.; Yamamoto, S.; Hashima, W.; Ishii, A. *Chem. Lett.* **2009**, *38*, 400-401.
- (211) Kawakami, J.; Takeba, M.; Kamiya, I.; Sonoda, N.; Ogawa, A. *Tetrahedron* **2003**, *59*, 6559-6567.
- (212) Misumi, Y.; Seino, H.; Mizobe, Y. *J. Organomet. Chem.* **2006**, *691*, 3157-3164.
- (213) Fraser, L. R.; Bird, J.; Wu, Q.; Cao, C.; Patrick, B. O.; Love, J. A. *Organometallics* **2007**, *26*, 5602-5611.
- (214) Sabarre, A.; Love, J. *Org. Lett.* **2008**, *10*, 3941-3944.
- (215) Yang, J.; Sabarre, A.; Fraser, L. R.; Patrick, B. O.; Love, J. A. *J. Org. Chem.* **2009**, *74*, 182-187.
- (216) Ghosh, C. K.; Graham, W. *J. Am. Chem. Soc.* **1987**, *109*, 4726-4727.
- (217) Xiao, W.; Alper, H. *J. Org. Chem.* **2005**, *70*, 1802-1807.
- (218) Haraguchi, K.; Matsui, H.; Takami, S.; Tanaka, H. *J. Org. Chem.* **2009**, *74*, 2616-2619.
- (219) Demaude, T.; Knerr, L.; Pasau, P. *J. Comb. Chem.* **2004**, *6*, 768-775.
- (220) Pearson, W. H.; Mi, Y.; Lee, I. Y.; Stoy, P. *J. Am. Chem. Soc.* **2001**, *123*, 6724-6725.
- (221) Pearson, W. H.; Lee, I. Y.; Mi, Y.; Stoy, P. *J. Org. Chem.* **2004**, *69*, 9109-9122.

- (222) Holmes, J. M.; Albert, A. L.; Gravel, M. *J. Org. Chem.* **2009**, *74*, 6406-6409.
- (223) Reddy, M.; Venkatapuram, P.; Mallireddigari, M. R.; Pallela, V. R.; Cosenza, S. C.; Robell, K. A.; Akula, B.; Hoffman, B. S.; Reddy, E. P. *J. Med. Chem.* **2011**, *54*, 6254-6276.
- (224) Shoai, S. Ph. D., UBC Vancouver, 2010.
- (225) Moxham, G. L.; Brayshaw, S. K.; Weller, A. S. *Dalton Trans.* **2007**, 1759-1761.
- (226) Wang, J.; Tong, X.; Xie, X.; Zhang, Z. *Org. Lett.* **2010**, *12*, 5370-5373.
- (227) Allen, D. P.; Crudden, C. M.; Calhoun, L. A.; Wang, R. Y. *J. Organomet. Chem.* **2004**, *689*, 3203-3209.
- (228) Tanaka, K.; Ajiki, K. *Org. Lett.* **2005**, *7*, 1537-1539.
- (229) Singer, H.; Wilkinson, G. *J. Chem. Soc., A.* **1968**, 849-853.
- (230) Carlton, L.; Read, G. *J. Chem. Soc., Perkin Trans.* **1978**, 1631-1633.
- (231) Higuchi, Y.; Atobe, S.; Tanaka, M.; Kamiya, I.; Yamamoto, T.; Nomoto, A.; Sonoda, M.; Ogawa, A. *Organometallics* **2011**, *30*, 4539-4543.
- (232) Bordwell, F. G.; Zhang, X.; Satish, A. V.; Cheng, J. *J. Am. Chem. Soc.* **1994**, *116*, 6605-6610.
- (233) Beare, K. D.; Coote, M. L. *J. Phys. Chem. A.* **2004**, *108*, 7211-7221.
- (234) Ananikov, V. P.; Kabeshov, M. A.; Beletskaya, I. P.; Khrustalev, V. N.; Antipin, M. Y. *Organometallics* **2005**, *24*, 1275-1283.
- (235) Weiss, C. J.; Marks, T. J. *J. Am. Chem. Soc.* **2010**, *132*, 10533-10546.
- (236) Sasmal, P. K.; Chandrasekhar, A.; Sridhar, S.; Iqbal, J. *Tetrahedron* **2008**, *64*, 11074-11080.
- (237) Pangborn, A. B.; Giardello, M. A.; Grubbs, R. H.; Rosen, R. K.; Timmers, F. J. *Organometallics* **1996**, *15*, 1518-1520.
- (238) Benati, L.; Capella, L.; Montevicchi, P. C.; Spagnolo, P. *J. Org. Chem.* **1994**, *59*, 2818-2823.
- (239) Chu, C.; Tu, Z.; Wu, P.; Wang, C.; Liu, J.; Kuo, C.; Shin, Y.; Yao, C. *Tetrahedron* **2009**, *65*, 3878-3885.
- (240) Zheng, Y.; Xingfen, D.; Weiliang, B. *Tetrahedron Lett.* **2006**, *47*, 1217-1220.
- (241) Burchat, A. F.; Chong, J. M.; Nielsen, N. *J. Organomet. Chem.* **1997**, *542*, 281-283.
- (242) Han, C.; Balakumar, R. *Tetrahedron Lett.* **2006**, *47*, 8255-8258.
- (243) Bratz, M.; Bullock, W. H.; Overman, L. E.; Takemoto, T. *J. Am. Chem. Soc.* **1995**, *117*, 5958-5966.
- (244) Kwon, M. S.; Woo, S. K.; Na, S. W.; Lee, E. *Angew. Chem. Int. Ed.* **2008**, *47*, 1733-1735.
- (245) He, W.; Sun, X. F.; Frontier, A. J. *J. Am. Chem. Soc.* **2003**, *125*, 14278-14279.
- (246) He, W.; Herrick, I. R.; Atesin, T. A.; Caruana, P. A.; Kellenberger, C. A.; Frontier, A. J. *J. Am. Chem. Soc.* **2008**, *130*, 1003-1011.
- (247) Bender, J. A.; Blize, A. E.; Browder, C. C.; Giese, S.; West, F. G. *J. Org. Chem.* **1998**, *63*, 2430-2431.
- (248) Bender, J. A.; Arif, A. M.; West, F. G. *J. Am. Chem. Soc.* **1999**, *121*, 7443-7444.
- (249) De Simone, F.; Gertsch, J.; Waser, J. *Angew. Chem. Int. Ed.* **2010**, *49*, 5767-5770.
- (250) Malona, J. A.; Cariou, K.; Frontier, A. J. *J. Am. Chem. Soc.* **2009**, *131*, 7560-7561.
- (251) He, W.; Huang, J.; Sun, X.; Frontier, A. J. *J. Am. Chem. Soc.* **2007**, *129*, 498-499.
- (252) Denmark, S. E.; Hite, G. A. *Helv. Chim. Acta.* **1988**, *71*, 195-208.
- (253) Denmark, S. E.; Jones, T. K. *J. Am. Chem. Soc.* **1982**, *104*, 2642-2645.

- (254) Denmark, S. E.; Habermas, K. L.; Hite, G. A. *Helv. Chim. Acta.* **1988**, *71*, 168-194.
- (255) Casson, S.; Kocienski, P. *J. Chem. Soc., Perkin Trans.* **1994**, 1187-1191.
- (256) Tius, M. A.; Kwok, C. K.; Gu, X. Q.; Zhao, C. W. *Synthetic Commun.* **1994**, *24*, 871-885.
- (257) Bee, C.; Leclerc, E.; Tius, M. A. *Org. Lett.* **2003**, *5*, 4927-4930.
- (258) Occhiato, E. G.; Prandi, C.; Ferrali, A.; Guarna, A.; Venturello, P. *J. Org. Chem.* **2003**, *68*, 9728-9741.
- (259) Liang, G. X.; Gradl, S. N.; Trauner, D. *Org. Lett.* **2003**, *5*, 4931-4934.
- (260) Shindo, M.; Yaji, K.; Kita, T.; Shishido, K. *Synlett* **2007**, 1096-1100.
- (261) Yaji, K.; Shindo, M. *Tetrahedron* **2010**, *66*, 9808-9813.
- (262) Johnson, W. S.; Bunes, L. A. *J. Am. Chem. Soc.* **1976**, *98*, 5597-5602.
- (263) Marx, V. M.; LeFort, F. M.; Burnell, D. J. *Adv. Synth. Catal.* **2011**, *353*, 64-68.
- (264) Giese, S.; Kastrup, L.; Stiens, D.; West, F. G. *Angew. Chem. Int. Ed.* **2000**, *39*, 1970-1973.
- (265) Browder, C. C.; Marmsater, F. P.; West, F. G. *Can. J. Chem.* **2004**, *82*, 375-385.
- (266) Grant, T. N.; Rieder, C. J.; West, F. G. *Chem. Commun.* **2009**, 5676-5688.
- (267) Harmata, M. *Chem. Commun.* **2010**, *46*, 8886-8903.
- (268) Liu, L.; Wei, L.; Lu, Y.; Zhang, J. *Chem. Eur. J.* **2010**, *16*, 11813-11817.
- (269) Nakanishi, W.; West, F. G. *Curr. Opin. Drug Disc.* **2009**, *12*, 732-751.
- (270) Leitich, J.; Heise, I.; Rust, J.; Schaffner, K. *Eur. J. Org. Chem.* **2001**, *2001*, 2719-2726.
- (271) Huang, J.; Frontier, A. J. *J. Am. Chem. Soc.* **2007**, *129*, 8060-8061.
- (272) Janka, M.; He, W.; Haedicke, I. E.; Fronczek, F. R.; Frontier, A. J.; Eisenberg, R. *J. Am. Chem. Soc.* **2006**, *128*, 5312-5313.
- (273) Marx, V. M.; Burnell, D. J. *J. Am. Chem. Soc.* **2010**, *132*, 1685-1689.
- (274) Song, D.; Rostami, A.; West, F. G. *J. Am. Chem. Soc.* **2007**, *129*, 12019-12022.
- (275) Wang, Y.; Arif, A. M.; West, F. G. *J. Am. Chem. Soc.* **1999**, *121*, 876-877.
- (276) Browder, C. C.; Marmsäter, F. P.; West, F. G. *Org. Lett.* **2001**, *3*, 3033-3035.
- (277) Grant, T. N.; West, F. G. *Org. Lett.* **2007**, *9*, 3789-3792.
- (278) Marx, V. M.; Burnell, D. J. *Org. Lett.* **2009**, *11*, 1229-1231.
- (279) Rostami, A.; Wang, Y.; Arif, A. M.; McDonald, R.; West, F. G. *Org. Lett.* **2007**, *9*, 703-706.
- (280) Scadeng, O.; Ferguson, M. J.; West, F. G. *Org. Lett.* **2011**, *13*, 114-117.
- (281) Wang, Y.; Schill, B. D.; Arif, A. M.; West, F. G. *Org. Lett.* **2003**, *5*, 2747-2750.
- (282) Kawatsura, M.; Kajita, K.; Hayase, S.; Itoh, T. *Synlett* **2010**, 1243-1246.
- (283) Frontier, A. J.; Collison, C. *Tetrahedron* **2005**, *61*, 7577-7606.
- (284) Giese, S.; West, F. G. *Tetrahedron* **2000**, *56*, 10221-10228.
- (285) Cui, H.; Dong, K.; Nie, J.; Zheng, Y.; Ma, J. *Tetrahedron Lett.* **2010**, *51*, 2374-2377.
- (286) Giese, S.; West, F. G. *Tetrahedron Lett.* **1998**, *39*, 8393-8396.
- (287) Mahmoud, B.; West, F. G. *Tetrahedron Lett.* **2007**, *48*, 5091-5094.
- (288) Marx, V. M.; Cameron, T. S.; Burnell, D. J. *Tetrahedron Lett.* **2009**, *50*, 7213-7216.
- (289) Sai, K.; O'Connor, M.; Klumpp, D. A. *Tetrahedron Lett.* **2011**, *52*, 2195-2198.
- (290) White, T. D.; West, F. G. *Tetrahedron Lett.* **2005**, *46*, 5629-5632.
- (291) Kerr, D. J.; White, J. M.; Flynn, B. L. *J. Org. Chem.* **2010**, *75*, 7073-7084.
- (292) Lin, G.; Yang, C.; Liu, R. *J. Org. Chem.* **2007**, *72*, 6753-6757.
- (293) Yungai, A.; West, F. G. *Tetrahedron Lett.* **2004**, *45*, 5445-5448.
- (294) Miller, A. K.; Trauner, D. *Angew. Chem. Int. Ed.* **2003**, *42*, 549-552.

- (295) Gao, S.; Wang, Q.; Chen, C. *J. Am. Chem. Soc.* **2009**, *131*, 1410-1412.
- (296) Cheney, D. L.; Paquette, L. A. *J. Org. Chem.* **1989**, *54*, 3334-3347.
- (297) Singh, R.; Panda, G. *Org. Biomol. Chem.* **2011**, *9*, 4782-4790.
- (298) Cai, Z.; Harmata, M. *Org. Lett.* **2010**, *12*, 5668-5670.
- (299) Churruca, F.; Foustieris, M.; Ishikawa, Y.; von, W. R.; Hounsou, C.; Surrey, T.; Giannis, A. *Org. Lett.* **2010**, *12*, 2096-2099.
- (300) Lazarski, K. E.; Hu, D. X.; Stern, C. L.; Thomson, R. J. *Org. Lett.* **2010**, *12*, 3010-3013.
- (301) Li, W. D.; Duo, W. G.; Zhuang, C. H. *Org. Lett.* **2011**, *13*, 3538-3541.
- (302) De Simone, F.; Waser, J. *Synlett* **2011**, 589-593.
- (303) Fernandez-Mateos, A.; Herrero Teijon, P.; Pascual Coca, G.; Rubio Gonzalez, R.; Simmonds, M. *Tetrahedron* **2010**, *66*, 7257-7261.
- (304) Nakagawa, D.; Miyashita, M.; Tanino, K. *Tetrahedron Lett.* **2010**, *51*, 2771-2773.
- (305) Yaji, K.; Shindo, M. *Tetrahedron Lett.* **2010**, *51*, 5469-5472.
- (306) Occhiato, E. G.; Prandi, C.; Ferrali, A.; Guarna, A. *J. Org. Chem.* **2005**, *70*, 4542-4545.
- (307) Magnus, P.; Quagliato, D. *J. Org. Chem.* **1985**, *50*, 1621-1626.
- (308) Asokan, C. V.; Bhattacharji, S.; Ila, H.; Junjappa, H. *Synthesis-Stuttgart* **1988**, 281-283.
- (309) Bichler, P.; Chalifoux, W. A.; Eisler, S.; Shi Shun, A.; Chernick, E. T.; Tykwinski, R. *Org. Lett.* **2009**, *11*, 519-522.
- (310) Karpov, A. S.; Müller, T. *Org. Lett.* **2003**, *5*, 3451-3454.
- (311) Confalone, P. N.; Baggiolini, E.; Hennessy, B.; Pizzolato, G.; Uskokovic, M. R. *J. Org. Chem.* **1981**, *46*, 4923-4927.
- (312) Malona, J. A.; Colbourne, J. M.; Frontier, A. J. *Org. Lett.* **2006**, *8*, 5661-5664.
- (313) Jilale, A.; Netchitaïlo, P.; Decroix, B.; Vegh, D. *J. Heterocycl. Chem.* **1993**, *30*, 881-885.
- (314) Palmer, M. H.; Leitch, D. S.; Greenhalgh, C. W. *Tetrahedron* **1978**, *34*, 1015-1021.
- (315) Pottie, I. R.; Crane, S. N.; Gosse, A. L.; Miller, D. O.; Burnell, D. J. *Can. J. Chem.* **2010**, *88*, 1118-1124.
- (316) Bachu, P.; Akiyama, T. *Bioorg. Med. Chem. Lett.* **2009**, *19*, 3764-3766.
- (317) Baar, M. R.; Falcone, D.; Gordon, C. *J. Chem. Educ.* **2009**, *87*, 84-86.
- (318) Garbisch, E. W.; Sprecher, R. F. *J. Am. Chem. Soc.* **1969**, *91*, 6785-6800.
- (319) Zou, Y.; Peng, B.; Liu, B.; Li, Y.; He, Y.; Zhou, K.; Pan, C. *J. Appl. Polym. Sci.* **2010**, *115*, 1480-1488.
- (320) Clementi, S.; Linda, P.; Marino, G. *J. Chem. Soc., B.* **1971**, 79-82.
- (321) Nahm, S.; Weinreb, S. M. *Tetrahedron Lett.* **1981**, *22*, 3815-3818.
- (322) Alterman, M.; Hallberg, A. *J. Org. Chem.* **2000**, *65*, 7984-7989.
- (323) Cyrański, M. K.; Krygowski, T. M.; Katritzky, A. R.; Schleyer, P. v. R. *J. Org. Chem.* **2002**, *67*, 1333-1338.
- (324) Neuvonen, H.; Fülöp, F.; Neuvonen, K.; Koch, A.; Kleinpeter, E. *J. Phys. Org. Chem.* **2008**, *21*, 173-184.
- (325) Vaidya, T.; Manbeck, G. F.; Chen, S.; Frontier, A. J.; Eisenberg, R. *J. Am. Chem. Soc.* **2011**, *133*, 3300-3303.
- (326) Buda, A. B.; Wang, Y.; Houk, K. N. *J. Org. Chem.* **1989**, *54*, 2264-2266.
- (327) Denmark, S. E.; Wallace, M. A.; Walker, C. B. *J. Org. Chem.* **1990**, *55*, 5543-5545.
- (328) Aggarwal, V. K.; Beffield, A. J. *Org. Lett.* **2003**, *5*, 5075-5078.

- (329) Liang, G.; Trauner, D. *J. Am. Chem. Soc.* **2004**, *126*, 9544-9545.
- (330) Evans, D. A.; Faul, M. M.; Bilodeau, M. T. *J. Org. Chem.* **1991**, *56*, 6744-6746.
- (331) Evans, D. A.; Faul, M. M.; Bilodeau, M. T.; Anderson, B. A.; Barnes, D. M. *J. Am. Chem. Soc.* **1993**, *115*, 5328-5329.
- (332) Evans, D. A.; Bilodeau, M. T.; Faul, M. M. *J. Am. Chem. Soc.* **1994**, *116*, 2742-2753.
- (333) Li, Z.; Conser, K. R.; Jacobsen, E. N. *J. Am. Chem. Soc.* **1993**, *115*, 5326-5327.
- (334) Mairena, M. A.; Mar Díaz-Requejo, M.; Belderraín, T.; Nicasio, M. C.; Trofimenko, S.; Pérez, P. *Organometallics* **2003**, *23*, 253-256.
- (335) Dunne, J. F.; Su, J.; Ellern, A.; Sadow, A. D. *Organometallics* **2008**, *27*, 2399-2401.
- (336) Ho, H.; Dunne, J. F.; Ellern, A.; Sadow, A. D. *Organometallics* **2010**, *29*, 4105-4114.
- (337) Pawlikowski, A. V.; Ellern, A.; Sadow, A. D. *Inorg. Chem.* **2009**, *48*, 8020-8029.
- (338) Bailey, P. J.; Pinho, P.; Parsons, S. *Inorg. Chem.* **2003**, *42*, 8872-8877.
- (339) Bellemin-Laponnaz, S.; Gade, L. H. *Angew. Chem. Int. Ed.* **2002**, *41*, 3473-3475.
- (340) Foltz, C.; Stecker, B.; Marconi, G.; Bellemin-Laponnaz, S.; Wadepohl, H.; Gade, L. H. *Chem. Commun.* **2005**.
- (341) Ward, B. D.; Bellemin-Laponnaz, S.; Gade, L. H. *Angew. Chem. Int. Ed.* **2005**, *44*, 1668-1671.
- (342) Seitz, M.; Capacchione, C.; Bellemin-Laponnaz, S.; Wadepohl, H.; Ward, B. D.; Gade, L. H. *Dalton Trans.* **2006**, 193-202.
- (343) Bichler, P.; Sun, A. D.; Patrick, B. O.; Love, J. A. *Inorg. Chim. Acta.* **2009**, *362*, 4546-4552.
- (344) Aggarwal, V. K.; Beffield, A. J. *Org. Lett.* **2003**, *5*, 5075-5078.
- (345) Cao, P.; Deng, C.; Zhou, Y.; Sun, X.; Zheng, J.; Xie, Z.; Tang, Y. *Angew. Chem. Int. Ed.* **2010**, *49*, 4463-4466.
- (346) Xu, Z.; Zhu, S.; Sun, X.; Tang, Y.; Dai, L. *Chem. Commun.* **2007**, 1960-1962.
- (347) Tschantz, M. A.; Burgess, L. E.; Meyers, A. I. *Organic Syntheses* **1996**, *73*, 221.
- (348) Bourguignon, J.; Bremberg, U.; Dupas, G.; Hallman, K.; Hagberg, L.; Hortala, L.; Levacher, V.; Lutsenko, S.; Macedo, E.; Moberg, C.; Queguiner, G.; Rahm, F. *Tetrahedron* **2003**, *59*, 9583-9589.
- (349) Heslin, J. C.; Moody, C. J. *J. Chem. Soc., Perkin Trans. 1.* **1988**, 1417-1423.
- (350) Gan, X.; Binyamin, I.; Rapko, B. M.; Fox, J.; Duesler, E. N.; Paine, R. T. *Inorg. Chem.* **2004**, *43*, 2443-2448.
- (351) Yoo, M.; Jeong, B.; Lee, J.; Park, H.; Jew, S. *Org. Lett.* **2005**, *7*, 1129-1131.
- (352) Phun, L. H.; Patil, D. V.; Cavitt, M. A.; France, S. *Org. Lett.* **2011**, *13*, 1952-1955.
- (353) De Simone, F.; Waser, J. *Synlett* **2011**, 589-593.
- (354) Rotzoll, S.; Appel, B.; Langer, P. *Tetrahedron Lett.* **2005**, *46*, 4057-4059.

Appendix A: X-ray Data for Chapter Five.

General Considerations

All crystals were mounted on a glass fiber and measurements recorded on a Bruker X8 APEX II diffractometer with graphite monochromated Mo-K α radiation. The temperature during collection was -100 °C and the distance between the crystal sample and detector varied from 36.00 to 50.00 mm. The data collected was integrated using the Bruker SAINT software package and the solid-state structure solved by direct methods.

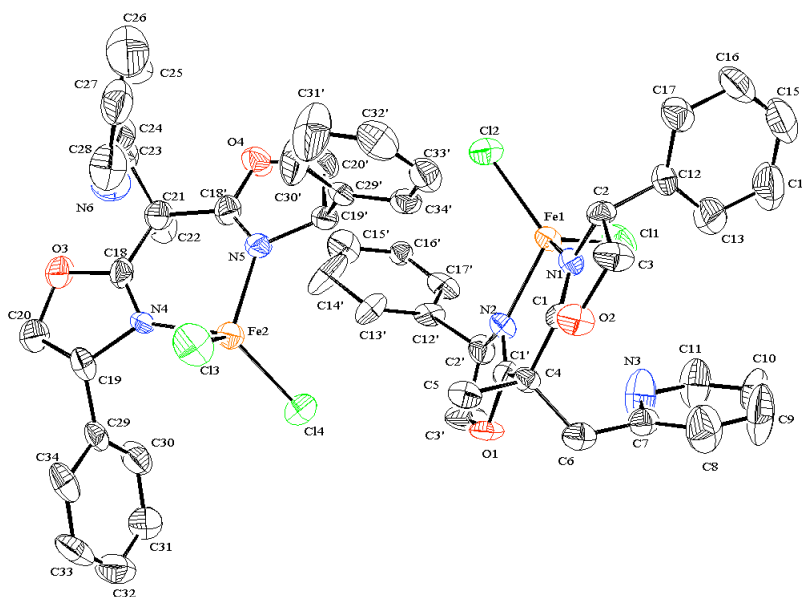


Figure A.1 Original ORTEP Diagram of Complex 128

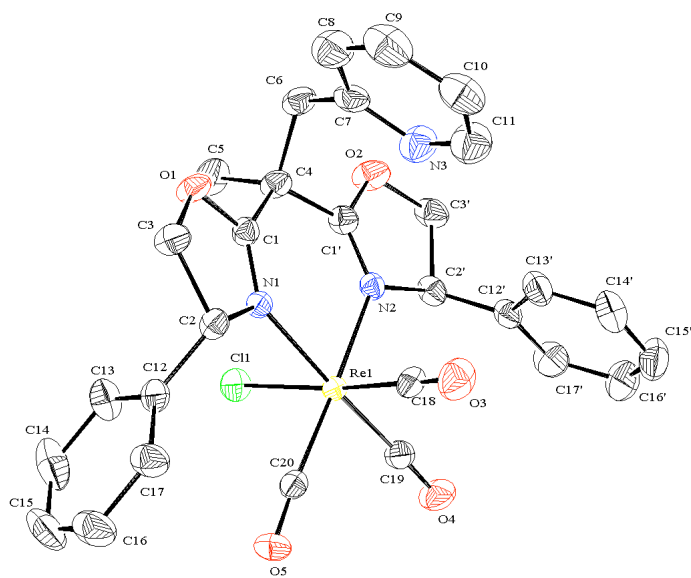


Figure A.2 Original ORTEP Diagram of Complex 129

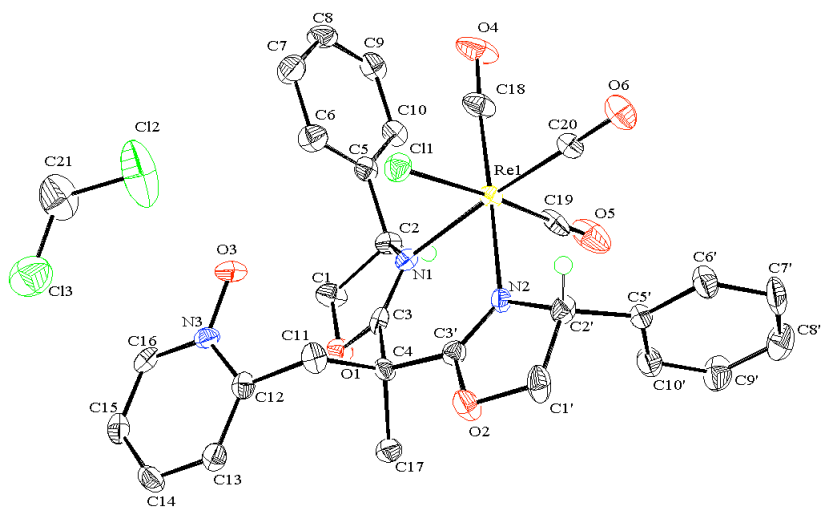


Figure A.3 Original ORTEP Diagram of Complex 130

Table A.1: Selected Crystallographic Parameters for Compounds 128-130

Compound	128	129	130
Dataset ID	jl057	jl054	jl061
Empirical formula	C ₅₃ H ₅₂ N ₆ O ₄ Fe ₂ Cl ₆	C ₂₉ H ₂₅ N ₃ O ₅ ReCl	C ₂₉ H ₂₅ N ₃ O ₆ ReCl ₃
Formula weight (g/ mol)	1161.41	717.17	818.10
$\lambda/\text{\AA}$	0.71073	0.71073	0.71073
Crystal system	orthorhombic	orthorhombic	orthorhombic
Space group	<i>P</i> 2 ₁ 2 ₁ 2 ₁ (#19)	<i>P</i> 2 ₁ 2 ₁ 2 ₁ (#19)	<i>P</i> 2 ₁ 2 ₁ 2 ₁ (#19)
<i>a</i> / \AA	9.2586(13)	10.5991(11)	10.4938(15)
<i>b</i> / \AA	14.4048(19)	14.5686(14)	11.1197(16)
<i>c</i> / \AA	40.801(5)	17.1386(18)	24.986(4)
$\alpha/^\circ$	90.0	90.0	90.0
$\beta/^\circ$	90.0	90.0	90.0
$\gamma/^\circ$	90.0	90.0	90.0
<i>V</i> / \AA^3	5441.5(13)	2646.4(5)	2915.5(7)
<i>Z</i>	4	4	4
<i>D</i> _c / g cm ⁻³	1.418	1.800	1.864
μ/cm^{-1}	8.78	47.38	44.93
<i>F</i> (000)	2392.00	1408.00	1608.00
Crystal size/ mm ³	0.12 x 0.32 x 0.44	0.03 x 0.12 x 0.24	0.32 x 0.40 x 0.50
$\theta_{\text{max}}/^\circ$	25.6	28.0	28.2
Reflections collected	36166	30216	32918
Independent reflections [<i>R</i> (int)]	9886 [0.024]	6369 [0.035]	7077 [0.036]
Max. and Min. transmisson	0.900, 0.738	0.867, 0.590	0.237, 0.166
Goodness-of-fit on <i>F</i> ²	1.21	1.04	1.09
<i>R</i> [<i>I</i> > 2 σ (<i>I</i>)]	<i>R</i> 1 = 0.067, w <i>R</i> 2 = 0.141	<i>R</i> 1 = 0.019, w <i>R</i> 2 = 0.040	<i>R</i> 1 = 0.025, w <i>R</i> 2 = 0.055
<i>R</i> (all data)	<i>R</i> 1 = 0.0877, w <i>R</i> 2 = 0.1958	<i>R</i> 1 = 0.022, w <i>R</i> 2 = 0.041	<i>R</i> 1 = 0.027, w <i>R</i> 2 = 0.056
Largest diff. peak and hole (e ⁻ / \AA^3)	0.747 and -0.524	0.85 and -0.39	1.21 and -1.25